ABSTRACT

Title of Dissertation:	EXPLORING RECENT DIRECTIONS IN INTEGRATED ASSESSMENT MODELING RESEARCH: IMPLICATIONS FOR SCENARIO ANALYSES OF CLIMATE CHANGE MITIGATION AND IMPACTS USING THE GCAM MODEL
	Silvia Regina Santos da Silva, Doctor of Philosophy, 2021
Dissertation directed by:	Professor Fernando R. Miralles-Wilhelm, CMNS-Earth System Science Interdisciplinary Center

Integrated assessment models (IAMs) are essential analytical tools in climate change science. There is wide recognition of the need of credible IAM scenarios for guidance on developing climate change mitigation and adaptation measures. This dissertation employs the Global Change Analysis Model (GCAM), a state-of-the-art IAM, in three studies that develop meaningful scenario analyses of climate change mitigation and impacts to address key gaps in the contemporary IAM research. The first study deals with the challenge of reconciling mitigation strategies consistent with the Paris Agreement climate goals with constraints on energy-water-land (EWL) resources. The study highlights the fact that mitigation strategies can have unintended repercussions for the EWL sectors, which can undermine their overall effectiveness. In Latin American countries used as case studies, increased water demands for crop and biomass

irrigation and for electricity generation stand out as potential trade-offs resulting from climate mitigation policies. The second study demonstrates that scenarios that explore the consequences of climate change impacts on renewable energy for the electric power sector need to adopt a comprehensive modeling approach that accounts for climate change impacts in all renewables. Using such an approach, the findings from this study show that climate impacts on renewables can result in additional capital investment requirements in Latin America. Conversely, accounting for climate impacts only on hydropower – a primary focus of previous studies – can significantly underestimate investment estimates, particularly in scenarios with high intermittent renewable deployment. The last study demonstrates that GCAM projections of solar photovoltaics and wind onshore electricity generation can be largely affected by methodological uncertainties in the computation of global renewable energy potentials – used to produce resource cost-supply curves that are key input assumptions to IAMs. Consequently, the role of these renewables in the modeled long-term scenarios can be under- or overestimated with potential implications for decision-making on energy planning, climate change mitigation and on the adaptation efforts to climate impacts on these renewables. The three studies encompass questions that have received little or no attention by the IAM community, and contribute with relevant approaches and insights that offer improvements relative to prior analyses. Importantly, these results help to enhance the value of GCAM scenarios to decision-making and identify research opportunities that might help improve GCAM as well as other IAM projections.

EXPLORING RECENT DIRECTIONS IN INTEGRATED ASSESSMENT MODELING RESEARCH: IMPLICATIONS FOR SCENARIO ANALYSES OF CLIMATE CHANGE MITIGATION AND IMPACTS USING THE GCAM MODEL

by

Silvia Regina Santos da Silva

Dissertation submitted to the Faculty of the Graduate School of the
University of Maryland, College Park, in partial fulfillment
of the requirements for the degree of
Doctor of Philosophy
2021

Advisory Committee:
Professor Fernando R. Miralles-Wilhelm, Chair/Advisor
Dr. Mohamad Hejazi
Professor Xin-Zhong Liang
Professor Raghu Murtugudde
Assistant Research Professor Thomas B. Wild
Professor Kuishuang Feng, Dean's Representative

© Copyright by
Silvia Regina Santos da Silva
2021

Dedication

My dissertation is dedicated to my parents, Onofre Eduardo da Silva and Acidilea Santos da Silva, and to my brother, Nelson Santos da Silva, for their support and for having taken care of me the best way they could in light of the many difficulties we have faced. Sadly, my father has passed away a long time ago, but he certainly would have been very proud of my accomplishments.

Acknowledgements

The PhD degree from the University of Maryland is a significant accomplishment for me and I am indebted to many individuals who helped me in achieving it.

First, I would like to express my gratitude to my advisor Dr. Fernando Miralles-Wilhelm for the opportunity of joining the “integrated assessment modeling world”, in which I have learned significantly. I also would like to thank him for the continued support, guidance, and patience throughout the time we have worked together.

I also owe my highest gratitude to Dr. Mohamad Hejazi for hosting my stay as a fellow at JGCRI/PNNL and for his invaluable contributions to the direction of my research. Over the past few years, he has given me the opportunity to work on interesting and challenging research initiatives. Without his expertise, guidance and constant voice of encouragement this dissertation would not have been possible. I also thank him for his supportive words during some difficult moments I have passed on my personal life last year.

I must express my sincere gratitude and thanks to numerous members of the JGCRI for their help, advice, discussion, direction, and friendship. These people include (but are not limited to): Dr. Thomas Wild, Dr. Gokul Iyer, Mr. Matthew Binsted, Dr. Zarrar Khan, Mrs. Paulette Land and Dr. Leon Clarke.

I would also like to thank all the faculty members of the Department of Atmospheric and Oceanic Science, in special the ones that I took courses with, who shared their valuable expertise, challenged me and showed that every day is an opportunity of constant learning and growing in the atmospheric sciences field. I am

also grateful to the entire AOSC Department staff, in particular to Jeff Henrikson and Tammy Hendershot, who were always very helpful. Additionally, I would like to thank Dr. Flavio Iturbide-Sanchez (NOAA/NESDIS), who I had the privilege to work with during my M.Sc. studies, for his constant motivation and belief in my potential.

My deepest thanks and gratitude are extended to my family and friends. To my mother Acidilea and my brother Nelson, who I miss very much, for having tolerated my many and long moments of absence. I really do not know how to thank you enough for the love and support you have unconditionally given me throughout my life. Thank you very much!!!

Table of Contents

List of Tables

List of Figures

List of Abbreviations and Acronyms

AFOLU	Agriculture, Forestry and Other Land Uses
AGMIP	Agricultural Model Inter-comparison Project
AR5	Fifth Assessment Report
BAU	Business-as-usual
BIOCCS	Bioenergy coupled with CCS
CCS	Carbon Capture and Storage
CMIP5	Coupled Model Intercomparison Project phase 5
CSP	Concentrating Solar Power
DSSAT	Decision Support System for Agrotechnology Transfer
EWL	Energy-water-land
EJ	Exajoule
FFI	Fossil Fuel and Industrial
GCAM	Global Change Analysis Model
GCM	General Circulation Model
GDP	Gross Domestic Product
GHG	Greenhouse Gas
GHM	Global Hydrological Model
GWPs	Global Warming Potentials
IAM	Integrated Assessment Model
INDC	Intended Nationally Determined Contribution
IPCC	Intergovernmental Panel on Climate Change
ISIMIP	Inter-Sectoral Impact Model Intercomparison Project
JGCRI	Joint Global Change Research Institute
LAC	Latin America and the Caribbean
LTSs	Long-term Strategies
LUC	Land Use and Land Cover
NASA	National Aeronautics and Space
NCAR	National Center for Atmospheric Research
NCEP	National Centers for Environmental Prediction
NDC	Nationally Determined Contribution
PV	Photovoltaics
RCP	Representative Concentration Pathway
RE	Renewable Energy
SCM	Simple Climate Model
SDGs	Sustainable Development Goals
SRES	IPCC Special Report on Emissions Scenarios
SSP	Shared Socioeconomic Pathway
STC	Standard Test Conditions
TPES	Total Primary Energy Supply
UNFCCC	United Nations Framework Convention on Climate Change

Chapter 1: Introduction

1.1 Overview of Integrated Assessment Models

Integrated assessment models (IAMs) can be defined as analytical tools that describe the most relevant interactions between environmental, social and economic factors that determine future climate change and the effectiveness of climate policy to derive policy-relevant insights (van Vuuren et al. 2011a). Their strengths lie on their representation of multiple systems in a single, integrated computational platform, their focus on interactions, and on the fact that they allow global-scale simulations that span the end of the 21st century at very low computational costs. The latter is achieved with simplifications and parameterized modeling approaches that capture the most relevant processes, but at the expense of less detailed representations of the modeled systems compared to sector- or process-specific models. IAMs are particularly useful to explore how the future might evolve under a particular set of conditions, how the system might change under the influence of external factors, and to understand uncertainties under a wide range of possible futures (Calvin et al. 2019).

IAMs produce long-term quantitative scenarios based on a number of input assumptions such as population and economic growth, resource supplies, technology costs, technological change and mitigation policy. Typical IAM outputs include energy and land-use transitions and emissions trajectories with decision-making based on economics (e.g., prices affecting competition among individual choices). A

fundamental characteristic is that IAMs tend to minimize the aggregate economic costs of achieving mitigation (Clarke et al. 2014).

IAMs have been of utmost importance by producing socioeconomic scenarios – e.g., the Shared Socioeconomic Pathways (SSPs) (Riahi et al. 2017)) – and greenhouse gas emissions scenarios – e.g., the Representative Concentration Pathways (RCPs) (van Vuuren et al. 2011b) – that are the backbone of the current climate change research. For example, greenhouse gas emissions scenarios are required as input to the state-of-the-art General Circulation Models (GCMs) that provide projections of the future climate. In addition, IAM scenarios have played a central role in the assessment of mitigation pathways in the Intergovernmental Panel on Climate Change (IPCC) Fifth Assessment Report (AR5) (Clarke et al. 2014).

Over time, IAMs have been required to address questions of larger complexity due to concerns about climate change impacts, and to increasing awareness on challenges related to simultaneous changes in multiple sectors and to the important linkages between mitigation and adaptation (Fisher-Vanden and Weyant 2020). Figure 1.1, taken from Fisher-Vanden and Weyant 2020, highlights many of the key recent needs in IAM development. According to these authors, current IAM frameworks need to include greater physical system detail (that can consider, for example, climate information from earth system models), feedbacks between component models, and finer resolution (spatial, temporal, and sectoral) to be more useful to decision-making on mitigation and adaptation policy. This work also highlights the increased demand for country-level analyses of mitigation strategies after the 2015 Paris Agreement and for information on 'nonclimate change–related metrics' (e.g., air quality, water

availability and quality, food security) motivated by the United Nations Sustainable Development Goals.

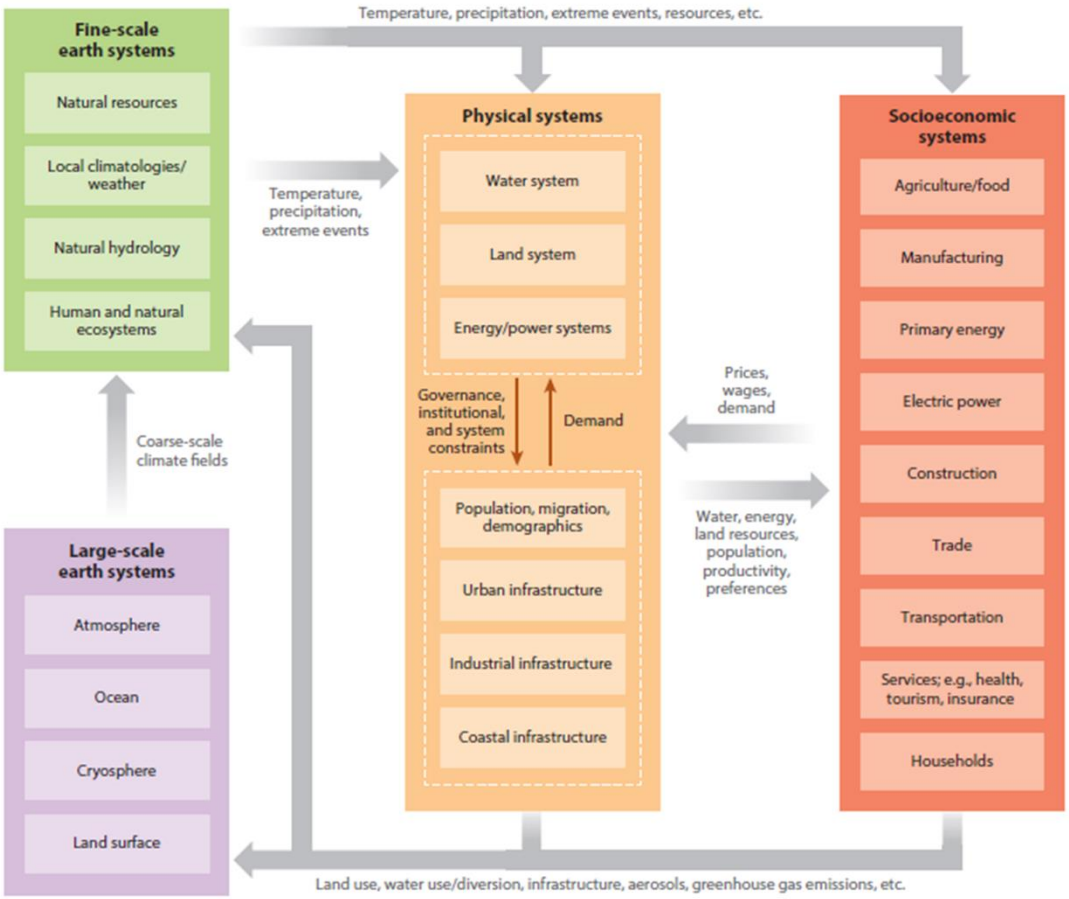

Figure 1.1 Key components of an integrated system within a contemporary integrated assessment framework. Source: Fisher-Vanden and Weyant 2020.

1.1.1 The Global Change Analysis Model (GCAM)

A prominent model within the IAM community is the Global Change Analysis Model (GCAM), formerly known as Global Change Assessment Model. GCAM has contributed significantly to the climate science by producing the RCP4.5 (Thomson et al. 2011) and the SSP4 storyline (Calvin et al. 2017).

GCAM is a global IAM that simulates the evolution of five key systems (socioeconomics, energy, agriculture and land, water and climate) and their interactions over time. The core modeling framework couples: (1) a technology-detailed energy model with representations of supplies and demands; (2) a land and agricultural submodule that provides projections of commodity supply and prices as well as land use and cover changes; (3) a water module that tracks demands in six major sectors, and represents supplies based on global estimates of current and future water availability from three main sources – renewable water, non-renewable groundwater, and desalinated water – for all major river basins of the world; and (4) the reduced-complexity climate model Hector (Hartin et al. 2015).

The driver of demands within the model is the human system, i.e., population and gross domestic product (GDP) growth assumptions, upon which the future evolution of energy, water and land sectors depend. On top of socioeconomics, a range of mitigation policies, climate impact inputs, technology choices, among other assumptions can be added within the scenarios set-up. Given limits imposed by its inputs (costs, technological progress, efficiencies, availability of resources, etc.), GCAM iteratively searches for the set of prices that equilibrates supplies and demands in all sectors. This process aims at finding a solution that minimizes costs or maximizes profits (in the case of the land sector). However, decision-making in GCAM relies on a logit formulation, a statistically-based representation of competition among multiple options (Clarke and Edmonds 1993), in which preference among competing objects depend on their costs or expected profit rates (Calvin et al. 2019). As a result, the largest shares of markets are allocated to the least-cost or most profitable options, but the other

higher-priced or less profitable options also gain some market share. This avoids that the single best choice captures the entire market, which is unrealistic. Further details on GCAM will be provided throughout this dissertation.

1.2 Rationale of the dissertation and research questions

GCAM has a long tradition of contributions focusing on the analysis of long-term energy system transformation pathways needed for climate change mitigation such as those analyzed in the IPCC AR5. In line with the recent development trends highlighted by Fisher-Vanden and Weyant 2020, GCAM has evolved in complexity to also investigate questions related to climate change impacts, notably on energy demand (Clarke et al. 2018), energy supply – hydropower (Turner et al. 2017), water supply (Graham et al. 2020a; Graham et al. 2020b; Khan et al. 2020) and agriculture (Kyle et al. 2014); and to the cross-sectoral energy-water-land 'nexus' research (Khan et al. 2020; Santos Da Silva et al. 2019).

This dissertation contributes to these recent research efforts by examining questions relevant within the present scope of IAM research but virtually unexplored by prior studies. This study focuses on questions pertaining to climate change mitigation and impacts that can (1) enhance the value of GCAM scenarios to decision-making, and (2) identify opportunities for improvements in GCAM projections. Specifically, this dissertation uses GCAM to target angles and approaches that provide new perspectives to traditional analyses (Chapters 2 and 3), and highlight unexplored sources of uncertainties that open new research directions (Chapter 4). Although the three studies are distinctive in their own scope and approach, they are tied into one another through the analysis of climate change mitigation and impacts.

The first analysis (Chapter 2) addresses one of the recent research questions IAMs are being employed to answer, i.e., how further knowledge concerning the interdependencies across sectors can contribute to decision-making in climate change mitigation. Specifically, this study deals with the challenge of reconciling mitigation strategies consistent with the Nationally Determined Contributions (NDCs) (major components of the Paris Agreement) with constraints on the energy-water-land (EWL) resources in Latin America. The relationship between NDCs and EWL resource systems had not been addressed by previous studies examining NDCs implications. Results show that the implementation of mitigation strategies might result in critical country-level trade-offs within the EWL nexus systems domain. The key research question addressed in the study is: ***What type of implications might be triggered by NDC mitigation strategies in line with the climate goals of the Paris Agreement on the EWL nexus resource systems in Latin America?***

The second study (Chapter 3) shares the same long-term mitigation goal (2^{o}C) as in Chapter 2, but the modeling approach is enhanced to account for climate change impacts on all renewables. Climate impacts accounted for in this study include effects on solar and wind energy that have been largely absent from the IAM literature. Using this improved modeling capability, the analysis is the first to investigate key consequences of climate impacts on renewables for the Latin American power-system and the implications for capital investment requirements in the electricity sector. The analysis is framed on contrasting implications resulting from distinct IAM modeling approaches: the representation of climate impacts on all renewables versus impacts only on hydropower – a major focus of prior IAM studies. Specific research questions

to be addressed are: ***What are the implications of climate impacts on renewables on the electricity sector in Latin America in terms of electricity generation and capital investment requirements? How do these implications change under alternative energy technology pathways and modeling approaches?***

Chapter 4 builds on recently published methods outlined in Chapter 3 that incorporate climate impacts on solar and wind sources in IAMs, i.e., the computation of solar and wind technical potentials that are used to produce resource-cost supply curves (curves that map the relationship between the availability of the renewable resource and energy production costs). The analysis is the first to demonstrate how GCAM projections can be largely under or overestimated due to the uncertain methodological assumptions on the computation of these renewable potentials. These results have large implications for the entire IAM community because the resource cost-supply curves produced from solar and wind technical potentials are important input assumptions to many IAMs. Research questions addressed in this analysis are: ***What are the implication of key parametric uncertainties in the computation of renewable energy potentials for GCAM solar and wind electricity production? Which parameters drive the largest changes? What are the potential implications for decision-making on climate change mitigation and impacts?***

1.3 Dissertation Structure

This dissertation is structured as follows. Chapter 1 provides a broad overview of integrated assessment models (IAMs) and GCAM, and describes the research questions and rationale behind this dissertation. Chapters 2–4 describe each of the three studies that answer the posed research questions. Chapters 2 and 3 use the Latin

America and Caribbean (LAC) region as a case-study region although similar analyses can be extended to other regions. Chapter 4 has a global scope, but could be used as a basis for follow-on regional studies. The findings of Chapters 2 and 3 are published in peer-reviewed journals, *Plos One* (Santos Da Silva et al. 2019) and *Nature Communications* (Santos da Silva et al. 2021), respectively. Chapter 4 is in preparation for submissions to a journal. Relevant supplementary materials from published Chapters are provided in Appendices. The dissertation is closed by some concluding remarks, a summary of the overall findings and suggested directions for future work.

Chapter 2: The Paris pledges and the energy-water-land nexus in Latin America: exploring implications of greenhouse gas emission reductions (Santos Da Silva et al. 2019)

2.1 Abstract

In the 2015 Paris Agreement, nations worldwide pledged emissions reductions (Nationally Determined Contributions - NDCs) to avert the threat of climate change, and agreed to periodically review these pledges to strengthen their level of ambition. Previous studies have analyzed NDCs largely in terms of their implied contribution to limit global warming, their implications on the energy sector or on mitigation costs. Nevertheless, a gap in the literature exists regarding the understanding of implications of the NDCs on countries' energy-water-land nexus resource systems. This chapter explores this angle within the regional context of Latin America by employing the Global Change Assessment Model, a state-of-the-art integrated assessment model capable of representing key system-wide interactions among nexus sectors and mitigation policies. By focusing on Brazil, Mexico, Argentina and Colombia, potential implications on national-level water demands are stressed depending on countries' strategies to enforce energy-related emissions reductions and their interplays with the land sector. Despite the differential implications of the Paris pledges on each country, increased water demands for crop and biomass irrigation and for electricity generation stand out as potential trade-offs that may emerge under the NDC policy. Hence, this study underscores the need of considering a nexus resource planning framework in the forthcoming NDCs updating cycles as a mean to contribute toward sustainable development.

2.2 Introduction

The "Nexus Approach" was defined by Hoff 2011 as a conceptual paradigm to tackle the inherent linkages among the energy, water, food and land sectors. This novel concept has helped to identify critical barriers to a more efficient governance across sectors in light of the escalating human demands and climate change.

Particularly in Latin America, interest in nexus issues has been motivated by some key domestic characteristics: great dependence on the water supply (abundant in total, albeit with large spatial and temporal heterogeneities) that can transfer climate change impacts to several sectors, importance of agriculture to local economies (whose expansion has been historically based on excessive exploitation of natural resources), and lower adaptive capacity to climate change compared to developed economies.

Given the multitude of nexus interconnections occurring in a wide range of temporal and spatial scales, a growing body of literature has recognized that governance of nexus resources should evolve from the current view centered on only one or two of these sectors toward an integrated nexus approach of planning and management. Such paradigm aims at ensuring economic and resource efficiency, avoiding unintended competition for nexus resources, and capturing vulnerabilities across the three systems (Bazilian et al. 2011; Howells et al. 2013; Miralles-Wilhelm 2016).

While general awareness of nexus issues has increased throughout this decade, a major societal concern has been how to overcome the challenge of significantly curbing anthropogenic GHG emissions by the end of the 21st century. In this sense, the 2015 Paris Climate Agreement brought the United Nations Framework Convention on

Climate Change (UNFCCC) member states to put forward actions to keep global warming well below 2°C above pre-industrial levels and to pursue further efforts toward a 1.5°C increase limit (United Nations 2015a). To this end, the UNFCCC members have submitted their "Intended Nationally Determined Contributions" (INDCs), in which Parties voluntarily expressed their post-2020 emissions reduction targets. A key aspect of the agreement is the inclusion of a framework for the regular updating of the Nationally Determined Contributions (NDCs) (official INDCs designation after ratification of the agreement) every 5 years to strengthen their level of ambition.

Within this context, Latin America is globally relevant due to: the large share of land-sector emissions (the region accounted for about 20% of global net emissions from Agriculture, Forestry and Other Land Uses (AFOLU) in 2014; (FAO 2018a)); as well as the prospects of growing energy-related emissions in the forthcoming decades (van Ruijven et al. 2016). Among the major regional economies, Brazil's NDC states the commitment to reduce all GHG emissions by 37% in 2025 and 43% in 2030 relative to 2005 levels. Mexico has committed to a reduction of 22% in all GHGs below a business-as-usual (BAU) scenario for the year 2030. Likewise, Argentina has committed to a target of 18% reduction in all GHGs below BAU for 2030 whereas Colombia announced a 20% reduction in all GHGs below BAU for 2030. Regarding the forestry sector, Brazil and Mexico intend to adopt measures to conserve and reforest ecosystems and to reach a rate of zero illegal deforestation by 2030. Along similar lines, Colombia's NDC indicates a commitment to reduce deforestation and to preserve important natural ecosystems whereas Argentina is planning actions related to the

promotion of sustainable forest management. It is worth mentioning that Brazil, which explains the bulk of the regional AFOLU emissions trend, has shown progress by cutting deforestation in the Legal Amazon by 75% between 2004 and 2017 (PRODES-INPE 2018).

In light of the Latin American NDCs, the understanding of how these pledges can affect the interdependencies among nexus systems is essential to inform coherent policy-making. This study explores potential implications of the Paris pledges on the nexus sectors in Argentina, Brazil, Colombia and Mexico. The analysis is carried out within the framework of the Global Change Assessment Model (GCAM) (Wise et al. 2009), a state-of-the-art integrated assessment model (IAM), which accounts for the physical, economic and social domains as well as cross-sectoral interactions.

Previous studies have assessed NDCs largely from the point of view of their collective contribution to limit global warming (Fawcett et al. 2015; Rogelj et al. 2016), in terms of their implications on the energy sector (Postic et al. 2017) or on mitigation costs (Hof et al. 2017; Iyer et al. 2015b). At the same time, the nexus literature has evolved from a conceptual framework (Ringler et al. 2013) to the recent development and use of analytical approaches to assess and analyze interactions. A recent literature review (Albrecht et al. 2018) identified that quantitative methods to address nexus issues are still limited (less than one third of the literature assessed), revealing a critical need for the development and application of appropriate quantitative methods and tools that can support the integrated decision-making. Recognizing that few tools have capabilities to address nexus linkages while allowing the explicit modeling of the Paris pledges, this study relies on a robust self-consistent integrated framework to produce

insights unexplored in previous works that assessed NDCs. That is, this study explores national level implications of NDCs in the major Latin American economies within a nexus perspective that seeks to highlight the inseparable links between sectors while drawing attention to the emergence of potential macro-scale trade-offs among systems. Bearing in mind the close links between the nexus concept and the 2030 Agenda for Sustainable Development (United Nations 2015b), in which climate action, energy, water and food securities are pivotal elements, it is therefore becoming clear that nexus trade-offs can undermine the full attainment of the Sustainable Development Goals (SDGs).

2.3 Scenario analysis

2.3.1 GCAM model

Here, a general description of the essential aspects of GCAM v4.3 relevant for the purposes of the present study is provided. A more comprehensive description of the model is available on the GCAM documentation (https://jgcri.github.io/gcam-doc/v4.3/toc.html).

Along the socioeconomics system, population and labor productivity assumptions are used to derive GDP in each region, which, in turn, drive the regional economic activity, as well as a large chain of interconnected processes and demand responses in the other systems. Within a market equilibrium economic framework, GCAM represents the global economy by disaggregating the world in 32 geopolitical regions. Latin America and the Caribbean region (henceforward LAC), in particular, is

represented as seven distinct regions: Argentina, Brazil, Central America and Caribbean, Colombia, Mexico, South America Northern, and South America Southern.

As a long-term model, GCAM operates in 5-year time steps until 2100. The base year for the model is 2010 based on calibration to the historical period, which requires multiple datasets (listed in the GCAM documentation) to cover the different sectors. GCAM is a dynamic-recursive model, which means that decisions in any period depend only upon information about that period, but the consequences of such decisions (resource depletion, capital stock build-up, etc.) influence decisions in the following periods. GCAM solves each period sequentially through the establishment of market-clearing prices for all existing markets (energy, agriculture, land, GHG emissions). This means that, for each model period, an iterative scheme ensures convergence to final equilibrium prices such that supplies and demands are equal in all markets.

The energy system structure in GCAM contains representations of the energy supply and demand sectors for each region, also considering the trading of primary resources (coal, natural gas, oil and biomass) among regions. The model simulates the temporal evolution of the energy system from the extraction of primary energy resources (oil, natural gas, coal, bioenergy, uranium, hydropower, geothermal, solar, and wind energy) until the transformation processes (e.g., liquid fuel refineries and power generation) that produce the final energy carriers (refined liquids, gas, coal, commercial bioenergy, hydrogen, and electricity) required by the end-use sectors (buildings, industry, and transport). GCAM utilizes a comprehensive technology database encompassing different energy supply and conversion technology options,

and includes assumptions on technological progress. These technologies compete for a share of energy markets based on cost differences among competing options (more details on this aspect will be provided in Chapter 3).

The agriculture and land-use system provides projections of agricultural supply (crops, livestock, forest products, and bioenergy), prices, and changes in land use and cover, taking into consideration the trading of primary agricultural and forest goods. In this component, each of the 32 geopolitical regions can be disaggregated into up to 18 agro-ecological zones resulting in 283 agriculture and land use regions. Within each of these 283 subregions, land is categorized into twelve types based on cover and use (e.g., forestlands, shrublands, grasslands, croplands, etc.). Land allocation within any geopolitical region depends on the relative profitability of all possible land uses within each of the 283 land-use regions (Kyle et al. 2014). Land used for any purpose competes economically with croplands, commercial forests, pastures, and all lands not involved in commodity production, with the exception of tundra, deserts, and urban lands (assumed constant over time). The profitability of any land used for commercial production is derived from the price (value) of the commodity produced, the costs of production, and the yield (Kyle et al. 2014). GCAM models the production of twelve crop categories based on exogenously specified yields that are crop-specific but vary depending on the subregion.

Bioenergy production in GCAM derives from: (1) various types of second-generation cellulosic crops (e.g., switchgrass, miscanthus, willow, jatropha, and eucalyptus), (2) residues from forestry and agriculture, (3) municipal solid waste, and (4) traditional bioenergy. Conventional or first-generation biofuel crops such as corn,

sugars, oil crops are grown as part of food production. In this case, the biomass liquids subsector within the energy module includes a number of transforming technologies for biofuels production from these food crops. Note that, throughout this analysis, the terms “purpose-grown” and “dedicated” bioenergy feedstocks are used to refer to the second-generation cellulosic bioenergy crops.

The physical atmosphere, oceans and climate are represented in GCAM by the Hector Earth System model (Hartin et al. 2015), which is a reduced-form global climate carbon-cycle model (or simple climate model – SCM). As a SCM, Hector was developed to represent only the most important large-scale earth system processes so that to significantly reduce computational costs relative to the most complex Earth-System Models. Although it can be used as a stand-alone model, Hector is fully integrated within the computational GCAM platform. This coupling allows Hector to track emissions of 24 GHGs and short-lived species generated by the energy, agriculture and land systems and to calculate future GHG concentrations in each modeling scenario. From GHG concentrations and short-lived climate forcers, Hector can then derive global mean radiative forcing, which is converted to global mean temperature and other variables.

The GCAM water module estimates water demands (water withdrawals and consumption) in six sectors: agriculture (irrigation), livestock, primary energy extraction and processing, electricity generation, industrial (manufacturing), and municipal (domestic). Details concerning each sector are available in the literature (Hejazi et al. 2014a; Hejazi et al. 2014b). Agricultural water demands in GCAM depend on crop production (noting that this is divided in rainfed and irrigated

production), the share of crop production in irrigated lands in each of the 283 subregions, irrigation efficiency and crop type (12 categories of crops plus biomass). The estimates of water demands for biomass include a number of second-generation biomass crops, but crops such as corn, sugar and oil palm used for biofuel production are not included since their water demands are quantified in the irrigation category. The water demand estimates for the livestock sector accounts for drinking water requirements for five animal commodities (beef, dairy, sheep & goats, pigs, and poultry), and for the water used in the animal production. In the electricity sector, the water usage depend on the type of cooling system. Cooling technologies represented in the model are: once-through cooling systems (responsible for the largest withdrawal volumes in the GCAM energy sector); recirculating cooling systems, and dry cooling systems (associated with the lowest water use). Domestic water demands are driven by population, per capita GDP, and technological change while the water demanded by the manufacturing sector depends on the total industrial output. Lastly, demands for the primary energy sector hinge on the fuel production, and accounts for coal, oil (conventional and unconventional), natural gas, and uranium.

2.3.2 Reference and NDC scenarios

In this model-based scenario approach, focus is placed on contrasting relevant sectoral outcomes of three scenarios through 2050: the reference scenario and two policy (NDC) scenarios.

The reference scenario is based upon BAU assumptions about key drivers (e.g., population, economic growth and technological evolution), and assumes that no new mitigation actions are implemented beyond 2010. The socioeconomics assumptions are

consistent with the "Middle of the Road" SSP 2 (Riahi et al. 2017). The reference scenario is characterized by population and GDP growth of 26% and 167%, respectively, in LAC from 2010 to 2050.

For the two NDC scenarios, the GHG mitigation targets are consistent with the countries' emissions levels provided in their official NDC submissions (UNFCCC 2019). This set of scenarios share the same general assumptions. Nevertheless, they differ with respect to the technology availability in the energy system that is essential to determine how emissions reductions in the energy sector can be fulfilled. The *'NDC FullTech'* scenario includes the full suite of energy technologies represented by GCAM. On the other hand, the *'NDC NOCCS'* scenario is based on the explicit assumption that the expansion of CO_2 capture and geologic storage (CCS) systems is not permitted (all other assumptions are identical to the *NDC FullTech* scenario). New capacities can include nuclear energy in both NDC scenarios. A fundamental motivation for the choice of the technology pathways explored here is that they represent two radically different energy-sector decarbonization routes, each of them with profound consequences for the nexus as a whole. On one side, the *NDC FullTech* scenario allows the opportunity to explore a pathway in which fossil fuel-fired power coupled with CCS, and bioenergy coupled with CCS (BioCCS) become important sources of electricity generation in the long-term. On the other hand, the *NDC NOCCS* scenario is intended to represent a future in which the various limitations surrounding the large-scale deployment of CCS (to be discussed in the following section) could not be overcome and mitigation must rely on other low-carbon sources.

In both policy scenarios, the implementation of the NDCs in GCAM was carried out using economy-wide emissions constraint. This means that the gross GHG emissions (excluding CO_2 land-use and land-cover change − LUC − emissions) were assigned to each GCAM region and the model internally calculated the carbon prices needed to achieve the constraint. The global GHG emission trajectory follows the *'Paris-Increased Ambition'* scenario developed in Fawcett et al. 2015 with updates on the emissions constraints for the seven LAC regions. These updates are based upon the supporting sources listed in the Appendix A. Note that NDCs only cover the period up to 2030. To allow the exploration of nexus transformations in LAC at a level consistent with the 2°C long-term goal set by the Paris Agreement, it is assumed that beyond 2030 the rest of the world puts forward reduction targets with CO_2 emissions intensities decreasing at annual rates implied by the NDCs or 5 percent per year, whichever is higher (Fawcett et al. 2015 provides details on these assumptions and the Appendix A lists the assumptions in LAC).

It is important to acknowledge that actual climate policy approaches do and will significantly differ from the economy-wide carbon prices approach used herein, relying on a range of different sectoral measures from building standards to automobile fuel efficiency to renewable portfolio standards. The implication for the results in this study is that mitigation is focused more heavily on energy supply adjustments than energy demand changes. For this reason, these results are meant to be purely explorative. However, each NDC scenario encompasses relevant multi-sectoral system-wide interactions that provide useful insights to support the points raised in this study.

As previously noted, LAC is characterized by a large share of AFOLU emissions compared to the world average. The four countries analyzed in the present study explicitly included the AFOLU sector in their NDCs, however the potential land-based emissions reductions are incorporated within their total reduction targets. As assessed by previous studies (Damassa et al. 2015; Forsell et al. 2016; Grassi et al. 2017), the NDCs are associated with large uncertainties regarding the actual mitigation role of the land sector. These uncertainties relate to: definition of baselines, historical emissions and removal sources in national inventories; lack of information on accounting methods; absence of quantifiable details of measures or specific targets, among others. Given that the core of the NDC strategies to curb carbon emissions from the land sector in LAC is formed by forest protection efforts, for the NDC scenarios, a land-use policy introduced by a carbon tax on LUC emissions from all land types is imposed. By penalizing terrestrial carbon emissions, land carbon prices affect the economic decisions within the agricultural/land-use model. As a result, this regime restricts forest conversion to agricultural land and incentivizes forest expansion (Calvin et al. 2014; Wise et al. 2009).

The emissions pathways (net emissions including CO_2 LUC emissions) generated by GCAM under all scenarios for the four focus regions are shown in Table 2.1.

Table 2.1 Regional Net GHG emissions ($MtCO_{2e}$) by scenario[a]

GCAM region	Scenario	2010	2020	2030	2040	2050	2030 NDC Target
Argentina	Reference	736	416	493	550	580	483
	NDC_FullTech	736	415	484	488	438	
	NDC_NOCCS	736	415	493	518	460	
Brazil	Reference	2181	1569	1999	2209	2050	1200
	NDC_FullTech	2181	1465	1206	1023	825	
	NDC_NOCCS	2181	1468	1324	1452	1137	
Colombia	Reference	124	236	316	424	444	268
	NDC_FullTech	124	233	266	304	316	
	NDC_NOCCS	124	234	278	392	374	
Mexico	Reference	708	790	943	1051	1153	759
	NDC_FullTech	708	736	759	531	311	
	NDC_NOCCS	708	738	748	543	306	

[a] Global Warming Potentials (GWPs) following official NDC submissions. Brazil and Mexico established GWPs from the IPCC Fifth Assessment Report (AR5). Argentina and Colombia defined GWPs from the Second AR.

2.4 Results and discussion

2.4.1 Energy

Although energy-related emissions have been low in Latin America (about 4% of global energy-related CO_2 emissions in 2015; (IEA 2017)), the region is expected to face increasing energy demand lined up with its economic development and population growth. In the absence of mitigation, the *Reference* scenario projects a 98% increase in primary energy consumption and a threefold increase in electricity generation between 2010 and 2050, with predominance of fossil fuels and a growing role of natural gas (Figures 2.1 and 2.2).

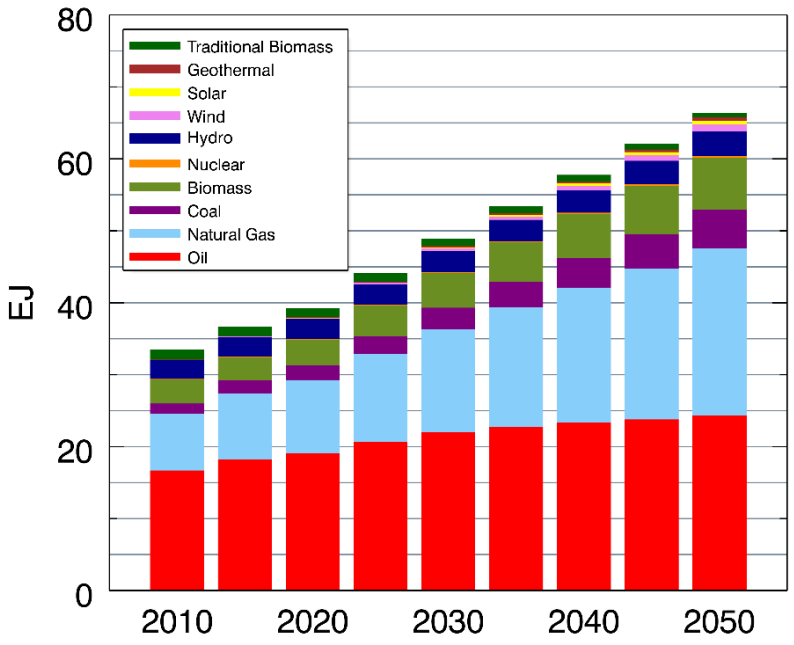

Figure 2.1 GCAM outputs for the *Reference (no policy)* scenario: primary energy consumption by source.

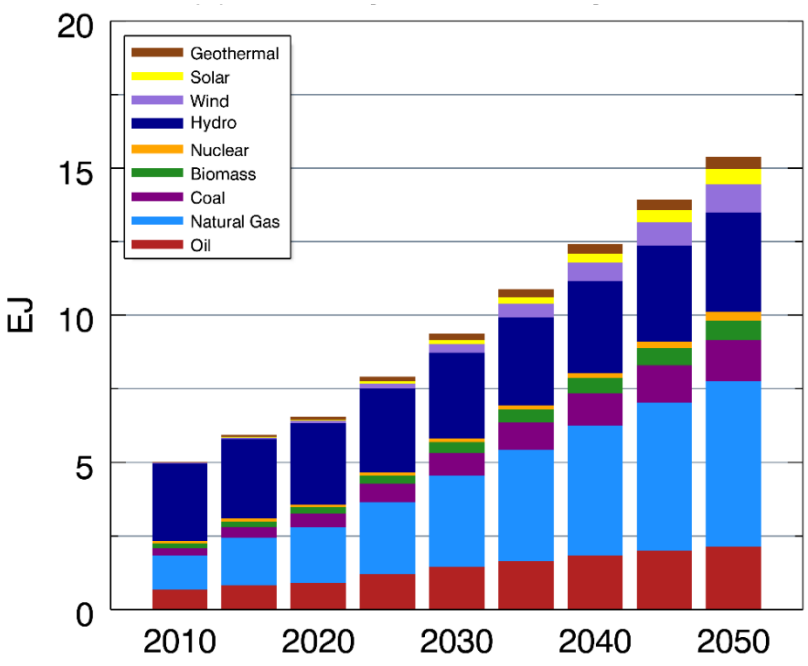

Figure 2.2 GCAM outputs for the *Reference (no policy)* scenario: electricity generation by source.

Thus, gross GHG emissions follow a marked upward trend, in particular, Fossil Fuel and Industrial (FFI) CO_2 emissions, which take larger proportions of the regional emissions up to 2050 (Figure 2.3). The curbing of future energy-related emissions is therefore an important mitigation component in LAC's NDCs. Nevertheless, depending on the available resources and future technology transitions for non-carbon energy sources, substantially different implications on the energy-water-land (EWL) nexus can be expected. Before discussing specific results, it is informative to introduce some of these interplays within a regional perspective.

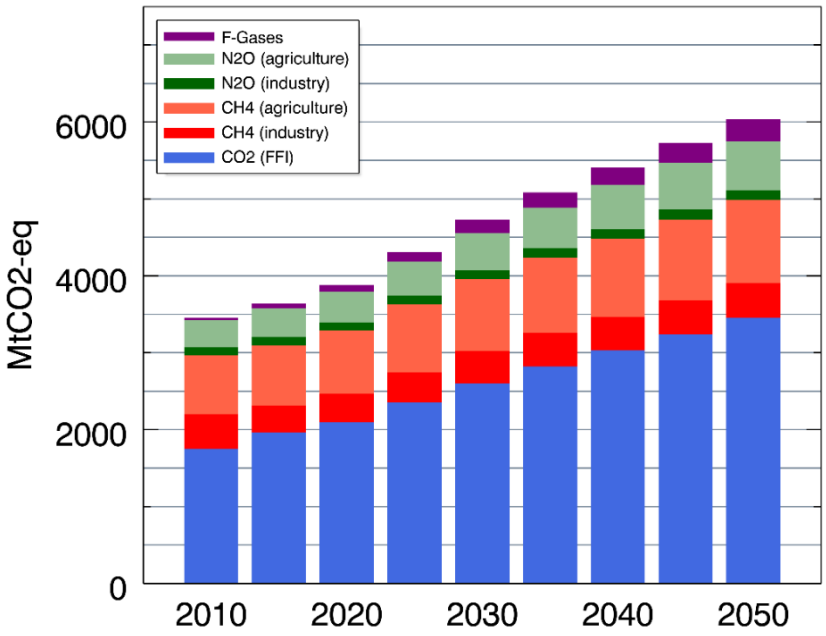

Figure 2.3 GCAM outputs for *the Reference (no policy)* scenario: greenhouse gas emissions (excluding CO_2 LUC emissions) by source.

A first pathway for strong intersections among EWL systems in light of the NDCs is bioenergy. The modern use of bioenergy is recognized as an important strategy to meet part of the future global energy demand while limiting energy-related emissions. The mitigation potential largely increases in the case of BioCCS, which

allows the possibility of deep carbon removals and net negative emissions (van Vuuren et al. 2013). In face of the large-scale bioenergy production necessary for a substantial impact on climate change mitigation (on the order of few hundreds of exajoules (EJ) per year versus present-day levels around 55 EJ; (Calvin et al. 2014)), LAC grows in importance due to its potential for significant increases in production from various feedstock categories (Dallemand et al. 2015). Indeed, LAC is already positioned as a major bioenergy, notably biofuels, producer. Brazil, in particular, has led development for decades focusing on sugarcane products (e.g., bioethanol) that accounted for 17% of domestic energy supply in 2015 (EPE 2016), not to mention the growing utilization of soybeans for biodiesel production. Biofuels markets also exist in Argentina (e.g., biodiesel from soybeans) and Colombia (e.g., sugarcane ethanol, biodiesel from palm oil), whereas Mexico, which set the goal of 35% of the electricity generated from renewable sources plus nuclear energy by 2024, aims to increase feedstock production, mainly from agriculture and forestry (García et al. 2015). Nevertheless, intensively cropping large areas for dedicated bioenergy production inevitably raises serious concerns surrounding land-use impacts and adverse externalities regarding food and water securities.

Other key nexus interactions unleashed by the NDCs, especially relevant for the energy-water subsystem, stem from an increased participation of low-carbon technologies in the energy system. A larger reliance on renewables such as wind and solar or on CCS technologies involve considerable impacts on the water demands for the electricity sector due to the specific water requirements of each technology. The aforementioned nexus implications are further discussed in the upcoming sections.

As illustrated in Figures 2.4 and 2.5, both NDC scenarios entail important transformations of the countries' energy systems relative to the reference case. These include less fossil-fuel based sources resulting from the larger participation of cleaner energy substitutes in the total primary mix. Carbon prices propagating through energy markets along with the expansion of higher-cost lower-carbon technologies stimulate improvements in the efficiency of energy conversion, driving down demand in all countries up to 2050. This effect is more pronounced in the *NDC_NOCCS* scenario given the higher energy costs of non-fossil technologies relative to the CCS-coupled options in the *NDC_FullTech* scenario. In the near-term (2030), changes are relatively small, however, as countries strengthen their mitigation efforts, larger transformations occur over the long-term (2050).

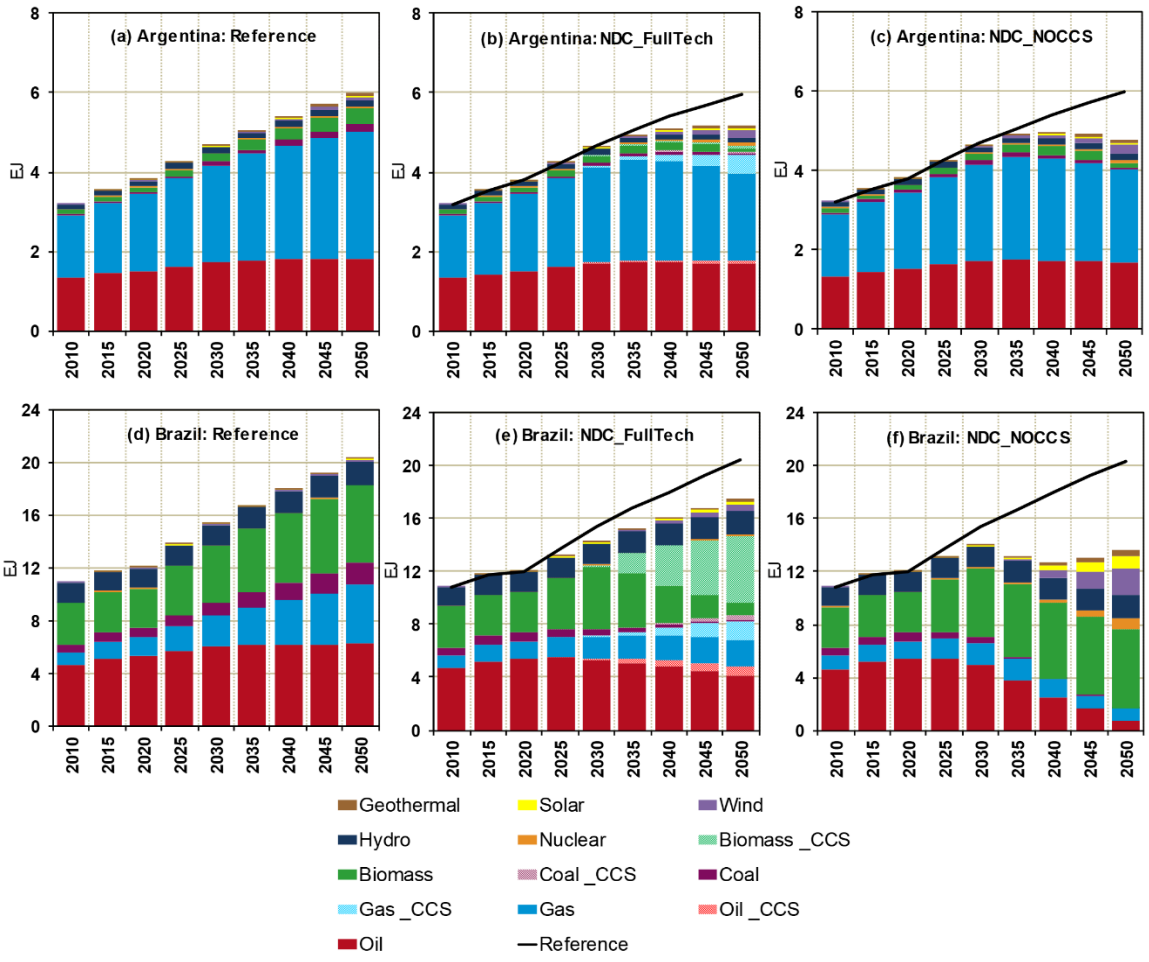

Figure 2.4 Distribution of the primary energy consumption (EJ) for the *Reference* ((A) and (D)), *NDC_FullTech* ((B) and (E)) and *NDC_NOCCS* ((C) and (F)) scenarios in Argentina and Brazil, respectively.

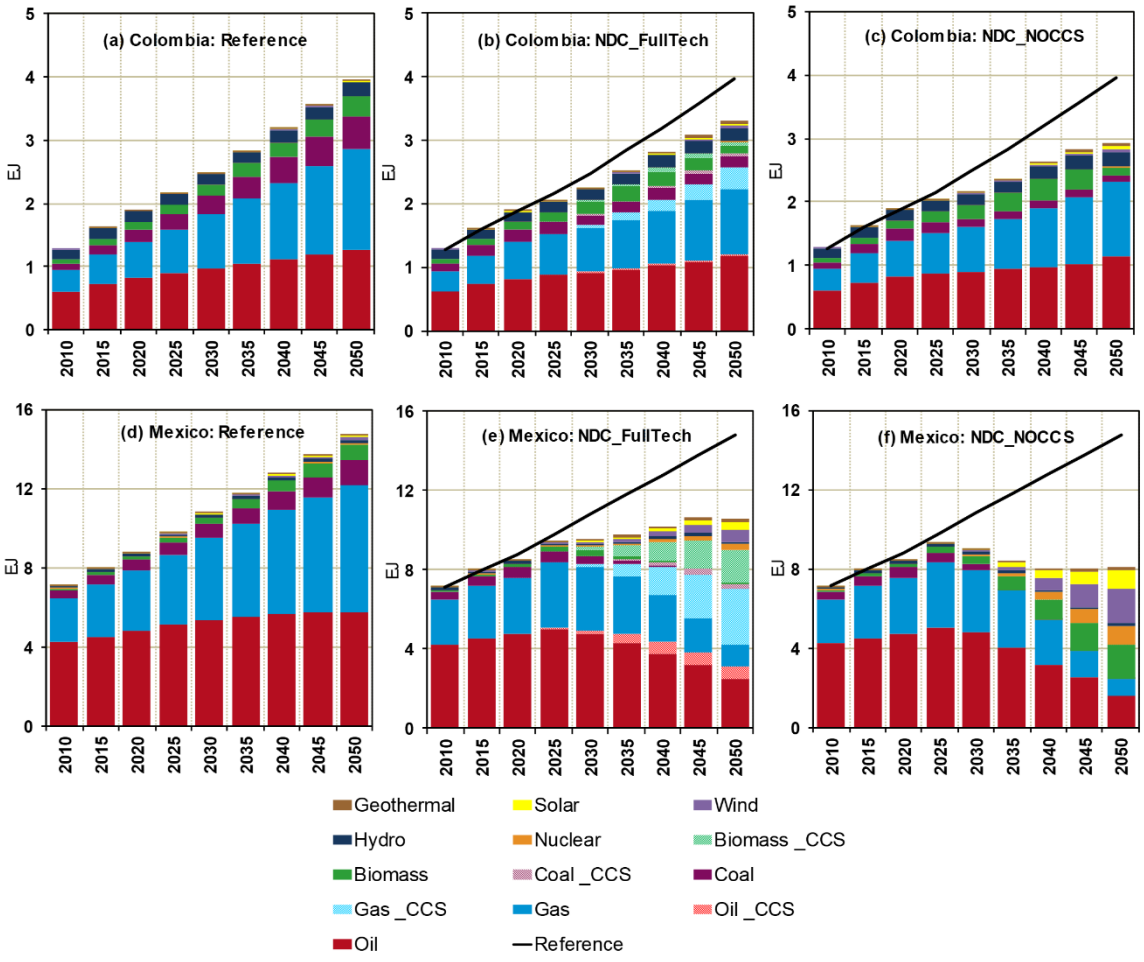

Figure 2.5 Distribution of the primary energy consumption (EJ) for the *Reference* ((A) and (D)), *NDC_FullTech* ((B) and (E)) and *NDC_NOCCS* ((C) and (F)) scenarios in Colombia, and Mexico, respectively.

Except for Argentina, when CCS is unavailable (*NDC_NOCCS* scenario), biomass plays a larger role in the primary mix relative to the *Reference* scenario. In this scenario, although Brazil accounts for the largest participation of biomass in the primary mix (38% and 44% in 2030 and 2050, respectively), Mexico experiences the largest expansion of biomass consumption relative to the reference with percent increases of 34% and 51% (versus 18% and 3% in Brazil) in 2030 and 2050, respectively. Concerning solar, wind and nuclear energy, the differences between both

NDC scenarios are small in the near term, and, overall, these low-carbon sources represent less than 2% of the total primary mix in all countries. Over the long term, the *NDC_NOCCS* scenario induces the expansion of solar, wind and nuclear energy, particularly strong in Mexico where these sources represent about 46% of the primary energy mix (versus 4 to 28% in the other countries). This strong development of renewable and nuclear capacities in Mexico is due to the drastic transformations needed within an energy system heavily based on fossil fuels to achieve an ambitious long-term goal of 50% emissions reduction in 2050 versus 2000 – as stipulated in Mexico's Mid-Century Strategy (SEMARNAT-INECC 2016) – listed in the Appendix A. Without CCS as a viable option, significant mitigation by 2050 involves deep structural changes to develop and expand renewables and nuclear capacities. On the other hand, the contribution of these low-carbon options to the primary mix is much lower in the *NDC_FullTech* scenario (shares of about 12% in Mexico, and 3 to 5% in the remaining countries in 2050) because CCS allows the larger use of fossil fuels.

Under the *NDC_FullTech* scenario, the largest expansion of CCS occurs in Mexico followed by Brazil, reflecting the scale of their energy systems and the amount of mitigation needed in each country. On the other hand, Argentina shows the lowest level of CCS development. BioCCS significantly expands in Brazil whereas the remaining countries develop more natural gas with CCS than BioCCS over the long term. Although the large-scale deployment of CCS is widely accepted as a key strategy to achieve deep CO_2 emissions reductions over the long-term, the viability of such approach is still highly uncertain. Globally, CCS technologies have not yet been broadly deployed commercially. This is due to barriers such as the significant research

& development investments required to overcome the technological challenges involved in their safe and cost-efficient utilization, or even the lack of political and policy support (Haszeldine 2009; Lipponen et al. 2017). In the particular context of LAC, some authors argue that CCS capabilities could be a less viable option compared to other countries for reasons that include lack of major technological and institutional development (Clarke et al. 2016; Lucena et al. 2016). Despite a mature technology, similar arguments hold for nuclear energy when referring to its future viability as an option for mitigation in LAC. Presently, the level of nuclear electricity generation in LAC is low. Nuclear energy in Argentina, Brazil and Mexico accounted for 6.9, 2.9 and 4.8% of their total electricity in 2009 (World Energy Council 2010), respectively (there is currently no nuclear power plant in Colombia). Over the short-term, there is limited growth prospects in nuclear capacity in these countries since only one nuclear plant is under construction in Argentina and Brazil. High operational and investment costs, need of foreign technical expertise and public resistance have slowed down the expansion of nuclear energy in LAC and may prove to be significant obstacles to hamper its future expansion in the region relative to renewables. This study does not take up the question of how likely CCS and nuclear energy are to become viable options for future implementation in LAC, but rather focus on the understanding of their potential nexus implications.

2.4.2 Land

Favored by its vast swathes of productive land, LAC almost tripled its net food production since the early eighties, becoming a major food exporter (ECLAC/FAO/IICA 2012). In the present context of globalized food systems, LAC

accounts for 38% of oil crops, 30% of fruits and 19% of meat global exports (FAO/PAHO 2017). This process, spurred by a monumental global demand growth for agricultural commodities, has induced extensive degradation of native forests, savannas (e.g., the "Cerrado" in Brazil), shrublands and grasslands (e.g., the "Pampas" in Argentina), with South American countries, notably Brazil and Argentina, playing major roles (Aide et al. 2013).

Notwithstanding the fact that most of the projected growth in crop production should derive from higher yields and increased cropping intensity, Latin America in tandem with the sub-Saharan Africa are expected to account for the bulk of future global agricultural land expansion (OECD/FAO 2015). The largest tracts of land with rainfed crop production potential are concentrated in Brazil followed, in LAC, by Argentina, Colombia, Bolivia, Venezuela and Peru (Bruinsma 2009). Nevertheless, such a vast fertile territory is not entirely available for agricultural expansion since it encompasses sensitive ecosystems, protected areas and urban zones. For instance, legally protected reserves and indigenous territories represented 47% of the Brazilian Amazon region in 2012 (Nepstad et al. 2014), with increasing efforts toward forest and land protection regulations in other LAC countries as well (le Polain de Waroux et al. 2019). It is widely agreed that the conversion of such areas into crop or pastoral land implies enormous economic and social costs alongside environmental impacts inconsistent with the land-sector mitigation efforts necessary for climate change stabilization.

In this context, land-energy nexus considerations are central to the bioenergy debate in LAC given the prospects of continued increase in internal and external market

demand for biofuels. Several studies have shown that the large-scale cultivation of bioenergy crops, unless produced from abandoned agricultural or marginal lands, could exacerbate land competition inducing: (1) loss of undisturbed ecosystems (which, in turn, increases LUC emissions that offset the intended mitigation benefits) and biodiversity stocks; and (2) displacement of farmland that contributes to drive up food prices (Calvin et al. 2014; Fargione et al. 2008; Munoz Castillo et al. 2017; Wise et al. 2009). Although the most controversial debate on the impacts to the land sector are around the first-generation bioenergy (food) crops, the second-generation bioenergy can potentially unleash additional impacts if supplied by dedicated plantations (Havlík et al. 2011).

The picture emerging from the above discussion is that, even within a context of relatively land-abundance, future land use and availability in LAC is subjected to various conflicting demands that can be affected by NDCs. In this context, two relevant development NDC modes can be distinguished: (i) increased bioenergy production to accommodate the internal demand for low-carbon sources and exports to regions with limited land and/or feedstock resources, and (ii) stringent actions to conserve and restore natural forests and ecosystems. Figure 2.6 explores these modes by showing the projected distribution of the land use in the four analyzed countries under the two NDC scenarios.

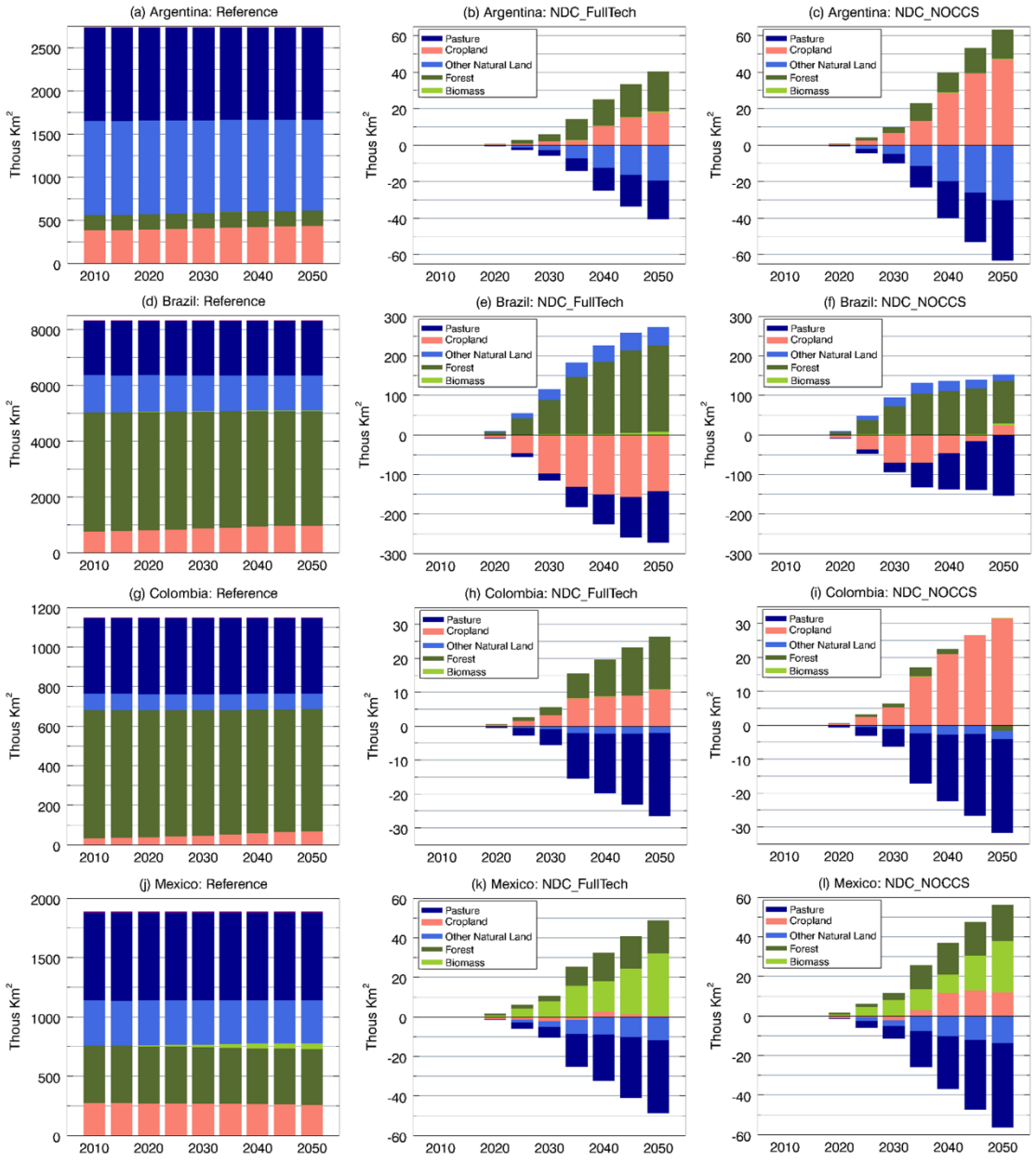

Figure 2.6 Land allocation (thous. Km^2) under the Reference ((A), (D), (G), and (J)). Difference in land allocation between the *NDC_FullTech* and the reference pathways in (B) Argentina, (B) Brazil, (H) Colombia, and (K) Mexico. Difference in land allocation between the *NDC_NOCCS* and the *Reference* pathways in (C) Argentina, (F) Brazil, (I) Colombia, and (L) Mexico.

Focusing on the differences between the *Reference* (left panels of Figure 2.6) and the NDC scenarios, it can be noted that relative changes in land cover associated with dedicated biomass production tend to be pronounced in Mexico. This is due to the cost-efficiency of this option in Mexico given the amount of mitigation required to transform an emissions baseline profile that comprises the largest share of CO_2 FFI emissions among the four focus countries.

In Brazil, the proportional growth in land for bioenergy crop production in both NDC scenarios is far less important than the changes in other land uses (Figures 2.6 D-F). This may seem counter-intuitive considering the current prominent role of Brazil in the bioenergy sector. Referring back to results from the previous section, it can be noted that biomass consumption in the Brazilian primary energy mix under both NDC scenarios is not projected to substantially increase compared with the reference (that already relies on large bioenergy usage). Furthermore, the NDC scenarios include pricing of terrestrial carbon that incurs high economic costs for the large-scale clearing of the carbon-rich forested systems. Since the expansion of land to grow dedicated bioenergy crops is an uneconomic option under the NDC scenarios, the emissions reduction required by the Brazilian NDC needs to be achieved by other low-carbon means. Finally, in Argentina and Colombia, dedicated bioenergy crop production is not projected as a major source of land-use pressure under the NDC scenarios.

Figure 2.6 also reveals that forests expand throughout the 2030-2050 horizon in all countries under both NDC scenarios. The largest increments are projected for Brazil at the expenses of croplands and pasture. As croplands become more profitable, GCAM projects an expansion of croplands into pasturelands and lands dedicated to

other natural systems (e.g., shrublands, savannahs, grasslands, etc.) in both NDC simulations in Argentina and Colombia, particularly in the *NDC_NOCCS* scenario. In Mexico, the long-term expansion of croplands is proportionally less pronounced because of the pressure for land to increase bioenergy production.

2.4.3 Water

LAC is endowed with impressive 32% of the global renewable water resources (FAO 2018b). Despite the overall abundance, water resources are unevenly distributed throughout the region. For instance, Mexico and Argentina experience water deficits, particularly in the northern Mexico and some parts of Argentina where moderate to severe water scarcity conditions last more than six months (Mekonnen; Hoekstra 2016). In fact, the northern and central areas of Mexico, that concentrate 77% of the population and 87% of GDP, constitute prominent examples of low natural availability aggravated by overconsumption of freshwater resources. They also serve to call immediate attention for the fact that water supplies are expected to be placed under increasing stress from socioeconomic trends whose signal can outweigh the effects of climate change in the near future (Vörösmarty et al. 2000).

Under the *Reference* scenario, the water demand for different uses, particularly irrigation, increases at high rates over the coming decades (Figure 2.7). Mexico is the main water user, followed by Brazil (see Figures 2.8(D) and (J)). This is mainly due to the role of irrigated agriculture in Mexico, which currently has the largest area of irrigated land in LAC (about 6.5 million ha) with an infrastructure based predominantly on water-inefficient surface (flood) irrigation techniques. In this regard, Brazil and Argentina also maintain sizable areas of land equipped for irrigation with 2.9 and 2.4

million ha, respectively (FAO 2018b). Also important within this context is the fact that Latin America is characterized by an overall low irrigation efficiency – average of 39% (the highest efficiency is in Brazil with 41%) – contrasting to the global average of 56% (Bellfield 2015).

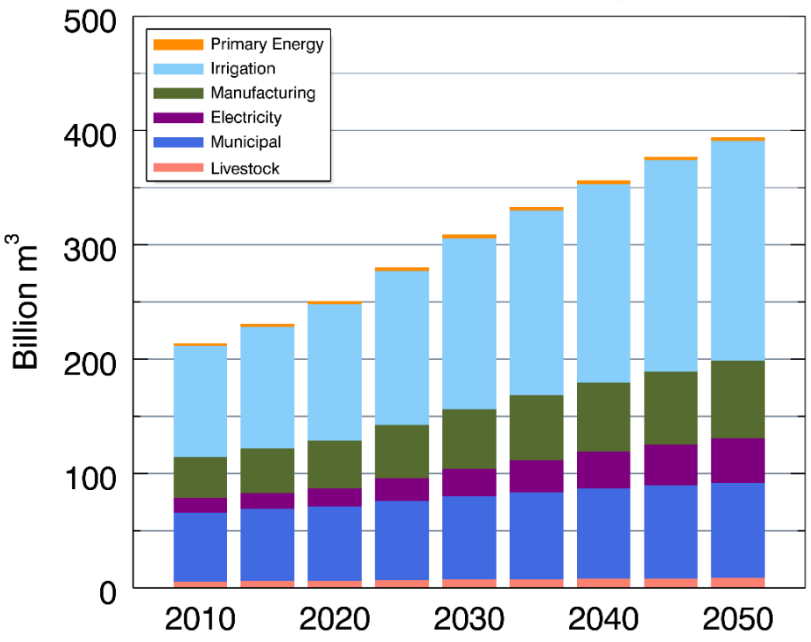

Figure 2.7 GCAM outputs for the *Reference (no policy)* scenario: total water withdrawals by source.

Previous discussion highlights potential implications of NDCs in terms of land-cover change driven by the need to grow dedicated bioenergy crops. Likewise, impacts on water use can be expected. Water requirements for bioenergy crops vary considerably with crop type, climate and soil conditions, but, in general, bioenergy derived from agricultural feedstocks is more water intensive than fossil fuels, particularly in the case of first-generation biofuels (D'Odorico et al. 2018; Hoff 2011). Certain second-generation bioenergy crops have disadvantageous water footprints as well (Gerbens-Leenes et al. 2009; Mathioudakis et al. 2017).

Lastly, NDCs may also imply drawbacks related to water use for power generation. In this sector, LAC is characterized by heavy use of hydropower generation (Figure 2.2), particularly notable in Brazil and Colombia. This option entails significantly lower water consumption (basically due to evaporation losses) than other power generation sources. Although some growth is expected through mid-century, the share of hydropower in the electricity mix should decrease over time. Hence, other generation sources will have to increase participation in the electricity mix to account for the escalating demand in the region. This means that LAC will potentially need to deal with challenges posed by the larger water requirements of conventional thermal power plants. These challenges may be exacerbated under an NDC climate policy if mitigation of energy-related emissions focuses heavily on CCS. Compared with conventional thermal power plants, CCS-based power plants generally have higher water requirements due to additional demands for cooling and other processes that increase water consumption by 37-95% depending on the power plant type (Grubert; Kitasei 2010; Klapperich et al. 2014). On the other hand, climate mitigation through solar photovoltaic (PV) and wind is not water intensive. In operational solar facilities, some water is needed to clean the mirrors/panels. However, concentrating solar power (CSP) systems can be considered as water-intensive as traditional thermoelectric power plants because of the additional water usage for cooling processes that is maximized if wet-cooling methods are employed (Bukhary et al. 2018). The aforementioned differences in water usage between thermal (with or without CCS) and non-thermal renewable types of energy supply are detailed in Table 2.2 (Macknick et al. 2011) . Data are presented in terms of median values of the ranges of water consumption and

withdrawal factors compiled by Macknick et al. 2011. These values are used to specify GCAM water use intensities by electric-sector technologies (Davies et al. 2013). Table 2.2 highlights that a transition toward a less carbon-intensive power sector (through nuclear, CCS or CSP facilities) may result in an increase in total water usage depending on the combination of generating sources and cooling systems employed.

Table 2.2. Water Use Factors for Electricity Generating Technologies (gal/MWh)

Fuel Type	Cooling	Technology	Median Values	
			Consumption	Withdrawal
Nuclear	Tower	Generic	672	1101
	Once-through	Generic	269	44350
	Pond	Generic	610	7050
Natural Gas	Tower	Combined Cycle	198	253
		Steam	826	1203
		Combined Cycle with CCS	378	496
	Once-through	Combined Cycle	100	11380
		Steam	240	35000
	Pond	Combined Cycle	240	5950
	Dry	Combined Cycle	2	2
	Inlet	Steam	340	425
Coal	Tower	Generic	687	1005
		Subcritical	471	531
		Supercritical	493	609
		IGCC	372	390
		Subcritical with CCS	942	1277
		Supercritical with CCS	846	1123
		IGCC with CCS	540	586
	Once-through	Generic	250	36350
		Subcritical	113	27088
		Supercritical	103	22590
	Pond	Generic	545	12225
		Subcritical	779	17914
		Supercritical	42	15046
BioPower	Tower	Steam	235-553	878
	Once-through	Steam	300	35000
	Pond	Steam	390	450
PV	N/A	Utility Scale PV	26	
Wind	N/A	Wind Turbine	0	
CSP	Tower	Trough	865	
		Power Tower	786	
		Fresnel	1000	i
	Dry	Trough	78	
		Power Tower	26	
	Hybrid	Trough	338	
		Power Tower	170	
	N/A	Stirling	5	

i Withdrawal factors assumed to be equivalent to consumption factors.

To provide a perspective on the potential implications of the Paris pledges on national water demands in the focus LAC countries, Figure 2.8 disaggregates differences by sector in water withdrawal estimates between each NDC scenario and the reference. Note that the water demands estimated by GCAM are not constrained in terms of future water supplies, and that climate change impacts are not included. Under both NDC scenarios, the overall picture across the countries, except for Brazil, is one of larger water footprint in a growing pattern until the midcentury. Figure 2.8 also brings out the fact that crop irrigation accounts for great part of the increments in total water withdrawals. Brazil is the only country where the near and long-term total water demands are projected to decline under both NDC scenarios, as well as the specific demand for irrigation (Figures 2.8D-F).

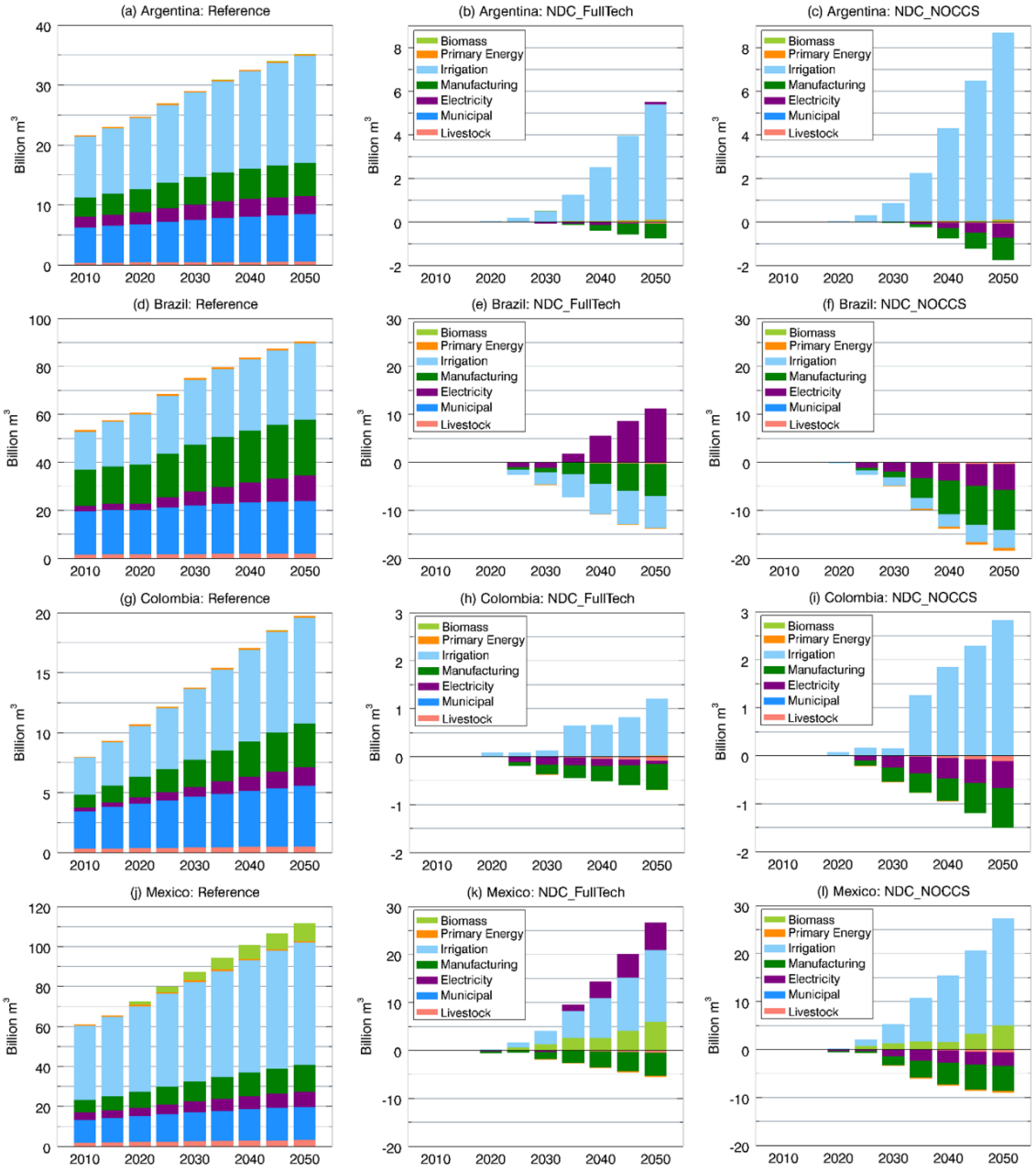

Figure 2.8. Total water withdrawals by sector (billion m^3) under the *Reference* ((A), (D), (G), and (G)). Water withdrawal differences between the *NDC_FullTech* and the reference pathways in (B) Argentina, (E) Brazil, (H) Colombia, and (K) Mexico. Water withdrawal differences between the *NDC_NOCCS* and the reference pathways in (C) Argentina, (F) Brazil, (I) Colombia, and (L) Mexico.

The results from Figures 2.6 and 2.8 point to relevant water-land interactions involving changes in land availability for crop production and changes in agricultural

production that affect the irrigation demands. For example, in Argentina, croplands expansion in both NDC scenarios (recall Figure 2.6) contributes toward increases in crop production (Figure 2.9), putting upward pressure on irrigation demands, whilst, in Brazil where irrigated agricultural production declined, less water is demanded. It is worth noting that, in the context of GCAM, part of the regional changes in irrigation demands can also be associated with changes in crop types since each crop is associated with different irrigation requirements.

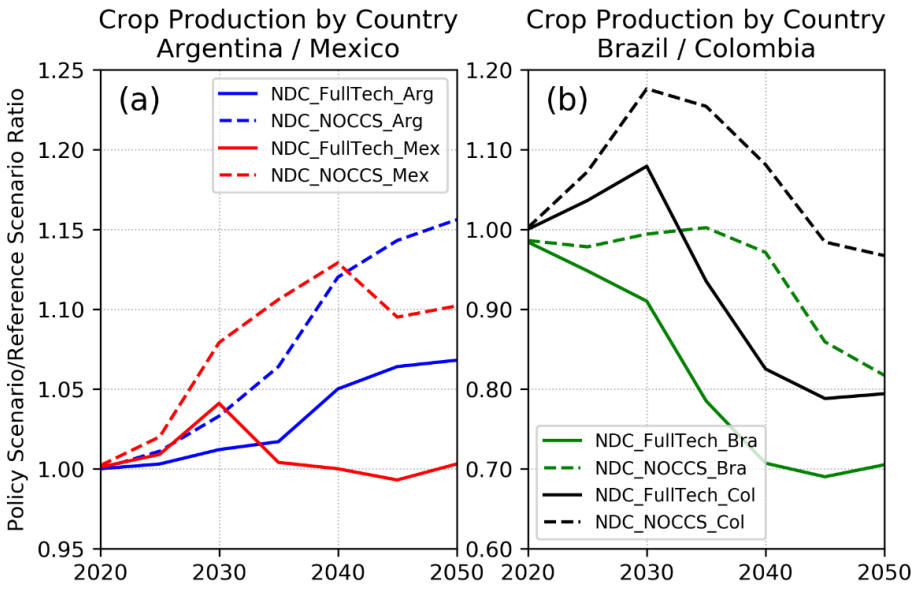

Figure 2.9. Irrigated crop production by country expressed as the ratio between each NDC scenario and the reference scenario.

Regarding irrigation for bioenergy crops, increases in demands relative to the *Reference* scenario are seen in Mexico under both NDC runs in the near and long term (Figures 2.8J-L). This is in line with results from previous sections that point out Mexico as the country with the largest proportional increase in biomass participation in the energy mix and with the most pronounced expansion in land to grow biomass. Both NDC scenarios lead to less water demands in the manufacturing sector over time.

This occurs because of an overall reduction of all goods and services produced in the sector, which is induced by the mitigation policy to reduce the demand for energy.

Across all countries, changes in electricity water withdrawals occur in both NDC scenarios in response to the availability of CCS. In general, both NDC scenarios signal modest water withdrawals reductions relative to the reference in the near term, which are due to small reductions in electricity generation and the consequent lower water usage for power generation. When CCS is available (*NDC_FullTech* scenario), Brazil and Mexico show pronounced increases in water withdrawals over the long term, consistent with the timeframe when CCS is substantially deployed in these countries. On the other hand, lower water demands are noted in Colombia throughout the simulation period. Given the modest level of CCS deployment in the Colombian primary mix (shares of 1% and 14% in 2030 and 2050, respectively), reduced electricity generation, in particular from thermal sources (compared with the reference case) played more relevant roles in reducing water demands. In Argentina, which shows the lowest level of CCS deployment, no significant water demand pressure in the power sector is noted.

In the case of the *NDC_NOCCS* scenario, electricity water demands are consistently lower than the reference in all countries. While in the near-term, this is due to a reduction in power generation, the overall long-term reduction in water withdrawals results from the expansion of wind and solar power (Figure 2.10), despite the increase of the water-intensive nuclear energy in this scenario (recall Figures 2.4 and 2.5). Note that the long-term expansion of solar energy displayed in Figure 2.10 also includes the water-intensive solar CSP technology that responds for most of the

water withdrawal volumes associated with solar energy in 2050. However, the overall net effect of the expansion of renewables in the *NDC_NOCCS* scenario is to reduce power-generation water demands.

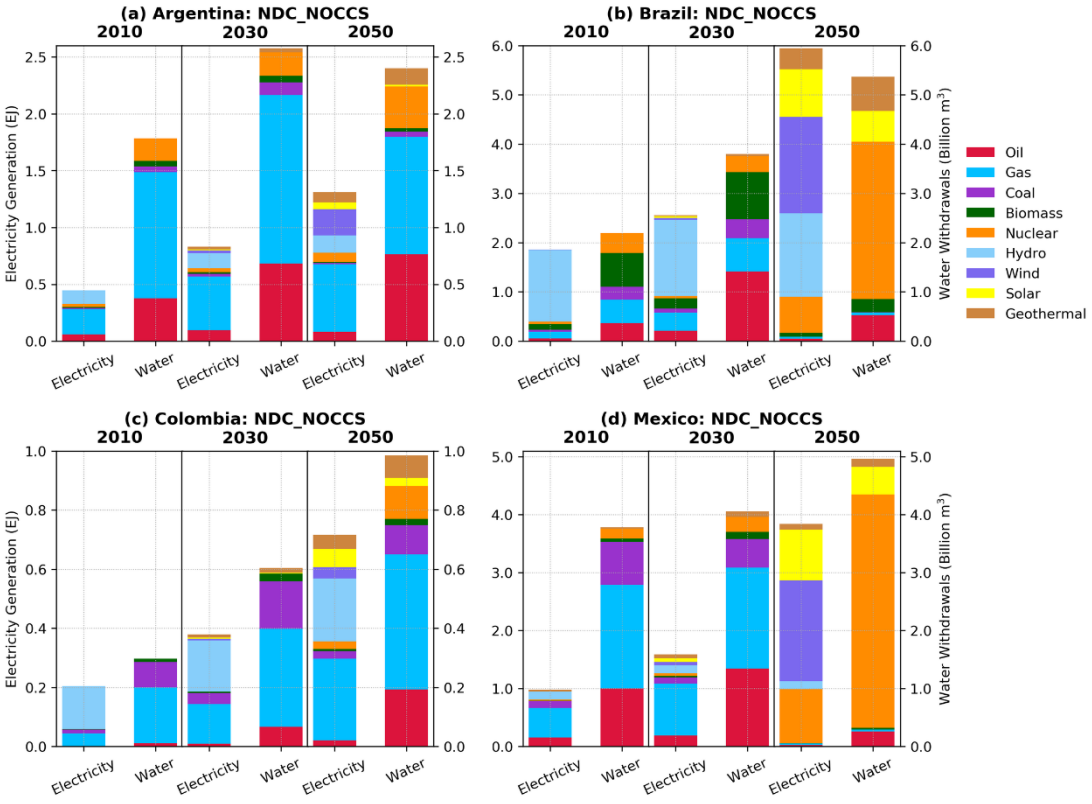

Figure 2.10 Water withdrawals (right bars) by power generation source (left bars) under the *NDC_NOCCS* scenario for (A) Argentina, (B) Brazil, (C) Colombia and (D) Mexico.

2.5 Conclusions

This study presents an integrated assessment of potential implications of mitigation strategies consistent with the Paris Agreement architecture on the EWL nexus resource systems in Latin America. GCAM was used to develop mitigation scenarios in which targets are consistent with the NDCs submitted by Argentina, Brazil, Colombia and Mexico, followed by stringent post-2030 emissions reductions

assumptions. The two policy scenarios explored herein are characterized by differing degrees of low-carbon technology deployments in tandem with a land-sector strategy that prevented forest loss and stimulated afforestation. This approach allowed the opportunity to explore two radically different energy-sector decarbonization routes and their interplays with the land and water sectors in each country. It is found that the policy scenario results entail relevant differences relative to a baseline case: (1) growing irrigation demands up to the midcentury in all countries, except for Brazil; (2) larger irrigation demands to cultivate bioenergy crops in Mexico; and (3) larger electricity water withdrawals in countries that largely deploy CCS over the long-term (Mexico and Brazil) versus reduced demands when CCS is unavailable.

The central insight of this study is that the implementation of NDCs in LAC can result in critical country-level synergies and trade-offs within the nexus domain associated with the portfolio of mitigation strategies. Relevant consequences of mitigation can be unleashed in many ways. One important factor is the range of forest protection measures (a crucial mitigation component in Latin America), which affects the overall cropland availability. This process, in turn, may interfere with food production levels and irrigation demands. For example, in Brazil where the results revealed forested areas growth partially achieved at the expenses of croplands, there were implications in terms of reduced crop production and lower irrigation demands. In addition, the results from Argentina, Colombia and Mexico suggest that non-forested ecosystems, most of them already under serious threats, may be put at additional pressure within a land-sector mitigation framework centered on forest protection. Modeling experiments (Popp et al. 2014) show that, within a forest conservation

scheme, these areas become major options for cropland expansion, thus requiring efficient land management and technological innovations in agriculture for their protection. Within the land and water domains, results from Mexico call for careful consideration on the role of the second-generation bioenergy in future mitigation strategies in face of the land and water requirements to cultivate bioenergy crops. Finally, the role a transition toward less carbon-intensive power sectors may play in increasing electric-sector water usage in LAC was made clear in the results. As previously discussed, low-carbon sources with high water requirements include CCS, which was emphasized in the scenario design of this study, but also solar CSP and nuclear energy.

In face of a potential trade-off between agricultural water demands and climate policy, the results highlight the need of demand-side responses that incorporate improvements in water and land management. Options applicable to the arid and semi-arid regions of Latin America include increased irrigation efficiency and changing cropping patterns toward less water-intensive and drought-resistant crops (Magrin et al. 2014). Given the inefficient irrigation infrastructure in LAC, which is heavily reliant on surface (flood) irrigation – 95.6% of irrigated lands (de Oliveira et al. 2009), important water savings could result from the implementation of modern irrigation methods. Mean differences in field application efficiencies between the least efficient surface systems and the sprinkler and drip systems are about 27 and 40%, respectively, in the South America region (Jägermeyr et al. 2015). These large differences suggest that the additional agricultural water demands found in the results could be reduced by a shift in irrigation technology.

Circumventing climate change through ambitious efforts is the major priority within the Paris Agreement framework. In this context, the full implementation of the current NDCs has been related to important reductions of the post-2020 GHG emissions. Nevertheless, these emission pledges have been considered insufficient to limit global warming to less than 2◦C without a substantial enhancement of global mitigation efforts after 2030 (Fawcett et al. 2015; Rogelj et al. 2016). Ramping-up the stringency of the Paris pledges will be a focus of attention in the coming years as Parties are requested to resubmit their NDCs by 2020, and periodically assess their progress by means of a process known as global stocktake (first global stocktake planned for 2023). To inform the global stocktake process, a number of studies (Iyer et al. 2017; Iyer et al. 2018; Peters et al. 2017) have pointed out the necessity of a systematic and broader process of assessment of the progress of the goals of the Paris Agreement through a multi-objective framework that incorporates, for example, the implications of NDCs on the SDGs.

This study reveals relevant implications for the aforementioned deliberations that will support the updating and enhancing of the NDCs. First, the post-2030 results highlight the potential exacerbation of cross-sectoral implications in the four major LAC economies when mitigation efforts are strengthened. Hence, more ambitious NDCs may imply higher risks of unintended consequences (see further comments on the potential exacerbation of mitigation trade-offs under stringent climate targets below). Second, the clear common objectives within the nexus concept and in the set of goals and targets of the SDGs reinforce the value of an assessment and updating

NDC framework that incorporates considerations on the nexus sectors and their interdependencies as a mean to contribute toward sustainable development.

While this study provides important insights regarding the climate policy (NDCs)-energy-water-land nexus interplays in LAC, any conclusions drawn should be mindful of the assumptions underlying the model and scenarios. A limitation in terms of technology relates to the fact that GCAM currently does not have explicit representations of the various existing irrigation systems, which would be important to guide relevant decision-making in LAC. It is also worth mentioning that GCAM water delivery-efficiency factors, assigned by crop type and region, are held constant over time (Hejazi et al. 2014a). An additional aspect of the modeling approach is that water supply is assumed an unlimited resource. This means that this study does not incorporate feedbacks exerted by physical water constraints from growing regional demands or climate change on energy and agricultural systems. In fact, climate change can result in additional pressure on nexus systems in LAC. This type of concern has been supported by robust differences in regional climate characteristics between present-day and global warming of 1.5°C and between 1.5°C and 2°C warming levels (IPCC 2018). Future research should then be directed at incorporating climate impacts on the water supply as well as on the renewable energy potential to understand how such stressors will propagate across the nexus systems in LAC. Moreover, land policies influence the amount of mitigation effort needed in the energy sector, also interfering with land availability for food production. Hence, these results are sensitive to the land-policy (implemented via terrestrial carbon-prices) applied here. Additional steps toward a better understanding of the implications of climate policies on the EWL nexus

in LAC will require the implementation of comprehensive land-related policies, which will reveal important interplays with the other sectors.

Finally, it is important to note that this analysis focuses on the upper bound of the Paris Agreement long-term climate goals in line with previous literature that has examined 2ºC-compatible scenarios (e.g., Iyer et al. 2015). Nevertheless, the Agreement called for additional efforts to limit end-of-century global warming to 1.5 °C above pre-industrial levels (United Nations 2015a). Previous global-scale studies (Bertram et al. 2018; Rogelj et al. 2015) that have examined differences between 1.5 °C and 2 °C scenarios emphasized that the 1.5 °C target requires faster decarbonization of the energy supply, CO_2 neutrality around the mid-century, net negative emissions in the 2050–2100 period, greater efficiency and demand-side reductions and profound transformations in the land-use. Hence, increasing mitigation ambition from 2.0 ºC to 1.5 ºC may result in greater and no-trivial challenges within the nexus in Latin America. Moreover, the manner in which emission reduction policies are implemented can lead to different pathways in terms of nexus synergies and trade-offs. As shown by Bertram et al. (2018), increasing mitigation ambition from 2ºC to 1.5ºC in scenarios characterized by economy-wide policies implemented via global carbon prices exacerbated trade-offs such as those associated with land requirements for bioenergy, CCS and water extraction. On the other hand, when a range of sustainable policy measures were incorporated into the original scenario design, mitigation risks could be largely alleviated or even compensated. Further research is then needed to examine the implications for the EWL nexus in LAC of the transformations required to meet the 1.5ºC goal to address, for example, the possibility of exacerbation of nexus trade-offs

relative to the 2^{o}C warming level and under which policy mechanisms new stresses or synergies can emerge.

The results and insights outlined above offer an opportunity to discuss a change in the manner current decision-making has been made about NDCs, that is, without sectoral integration and strategic planning to minimize potential nexus trade-offs. Embedding the 'Nexus Approach' in the policy debate regarding NDCs is critical to align a more efficient stewardship of nexus resources with NDCs progressively more stringent with time.

Chapter 3: Power sector investment implications of climate impacts on renewable resources in Latin America and the Caribbean (Santos da Silva et al. 2021)

3.1 Abstract

Climate change mitigation will require substantial investments in renewables. In addition, climate change will affect future renewable supply and hence, power sector investment requirements. This study addresses the implications of climate impacts on renewables for power sector investments under deep decarbonization using a global integrated assessment model. Focus is placed on Latin American and Caribbean, an under-studied region but of great interest due to its strong role in international climate mitigation and vulnerability to climate change. It is found that accounting for climate impacts on renewables results in significant additional investments ($12─114 billion by 2100 across Latin American countries) for a region with weak financial infrastructure. Ii is also demonstrated that accounting for climate impacts only on hydropower – a primary focus of previous studies – significantly underestimates cumulative investments, particularly in scenarios with high intermittent renewable deployment. This study underscores the importance of comprehensive analyses of climate impacts on renewables for improved energy planning.

3.2 Introduction

After the 2015 Paris Agreement, nations worldwide have pursued climate change mitigation strategies in the form of nationally determined contributions (NDCs) and long-term strategies (LTSs). These strategies typically include substantial renewable energy (RE) deployment (Federative Republic of Brazil 2015; India 2015; SEMARNAT-INECC 2016). Nevertheless, climate change might influence RE generation through long-term alterations in various environmental conditions. For example, climate change could affect biomass crop yields and hence biomass potential (IPCC 2012). Likewise, climate change could affect streamflow, with implications for hydroelectricity generation (Schaeffer et al. 2012). Solar power production may be impaired by reduced surface solar radiation (Jerez et al. 2015), or could increase (e.g., concentrating solar power) or decrease (e.g., photovoltaics) with rising air temperatures (Crook et al. 2011; Wild et al. 2017; Wild et al. 2015). Wind power production could be affected by changing wind speed and air density patterns (Eurek et al. 2017; Karnauskas et al. 2018). Hence, planners need to account for climatic impacts on RE during capacity development planning to ensure power system reliability, which is particularly relevant in the context of decarbonization strategies centered on RE expansion.

Most decarbonization scenarios (e.g., those reviewed by the Intergovernmental Panel on Climate Change (IPCC) (IPCC 2014)) suggest that large investments in renewables will be required, particularly under assumptions of limited or no deployment of carbon capture and storage (CCS) and nuclear technologies (Iyer et al. 2017). In this context, there is an open question about how climate impacts on

renewable resources – such as those described above – could alter the understanding of the economic implications and investment needs suggested by alternative decarbonization pathways. Research on this question has been very limited and the majority of mitigation scenarios in the literature do not account for the impacts of climate change. This is the case of the about 900 mitigation scenarios reviewed in the IPCC's Fifth Assessment Report (AR5) (IPCC 2014). Even the few studies exploring climate impacts within the context of decarbonization scenarios have focused only on hydropower without a comprehensive analysis of impacts on all renewable sources.

With growing literature highlighting that the energy sector, including RE production, may face serious impacts due to climate change (Cronin et al. 2018; Solaun; Cerdá 2019; Yalew et al. 2020), there have been efforts to incorporate climate impacts on renewables into energy and integrated assessment models (IAMs) to support decision-making. Methodologically, many of these studies rely on detailed process-based models (for example, hydrologic models, crop models, general circulation models (GCMs)) capable of simulating climate-impacted environmental responses that are used to modify IAM parameters linked to RE production. However, hydropower – the renewable that currently contributes the most to the global electricity supply (IPCC 2012) – has received considerably larger attention from the IAM literature and climate-impact studies in general as pointed out by recent literature reviews (Cronin et al. 2018; Emodi et al. 2019; Solaun and Cerdá 2019; Yalew et al. 2020). IAM-based studies on climate impacts on hydropower (some of them conducted in the context of decarbonization scenarios as mentioned earlier) have been useful in exploring climate change implications for electricity production and capital investments (Arango-

Aramburo et al. 2019; Carvajal et al. 2019; Dowling 2013; Lucena et al. 2018; Savelsberg et al. 2018; Turner et al. 2017; Zhou et al. 2018). Another group of IAM-based studies has addressed impacts on the agriculture sector (which affect biomass potential) by incorporating biophysical crop yield changes (Kyle et al. 2014; Nelson et al. 2014; Ren et al. 2018; Snyder et al. 2019). Regarding the representation of climate impacts on solar and wind resources in IAMs, research efforts are still incipient, and to the best of our knowledge, limited to only two studies (Dowling 2013; Gernaat et al. 2021). Consequently, there is a gap in the literature on a comprehensive analysis of climate impacts on all renewable resources and their implications for electricity sector investments. Studies that focus on climate impacts on individual resources do not account for the compounding effects of climate impacts on multiple renewable sources and may thus under- or over- estimate investment requirements. Another gap in the literature is the lack of regionally-focused studies (Cronin et al. 2018; Solaun and Cerdá 2019). While global studies are useful in characterizing the scale of a problem, policy decisions are made at national to sub-national scales. Hence, regional analyses with focus on national issues and circumstances are important to enhance relevance of the analyses to decision-makers. This study fills both of the above gaps.

In this study, climate impacts on all renewables, namely, hydropower, biomass, solar and wind, are incorporated within the Global Change Analysis Model (GCAM) (Calvin et al. 2019). Using this improved version of the model, changes in electricity generation patterns and future investment needs under decarbonization scenarios are examined. For the purposes of this study, focus is placed on Latin American and the Caribbean (LAC), a greatly under-studied region despite its global relevance. For

instance, in 2017, RE represented about 56% of LAC's electricity generation versus a global average of 26% ((EIA 2019) and Figure 3.1). Hydropower and bioenergy have dominated the regional RE portfolio, however, solar and wind have experienced rapid growth in installed capacity from 0.79 to 27.31 GW between 2008 and 2017 (IRENA 2018). This growth is expected to continue due to strong policies (IRENA 2016), and the strategic role of RE in many LAC countries' climate goals.

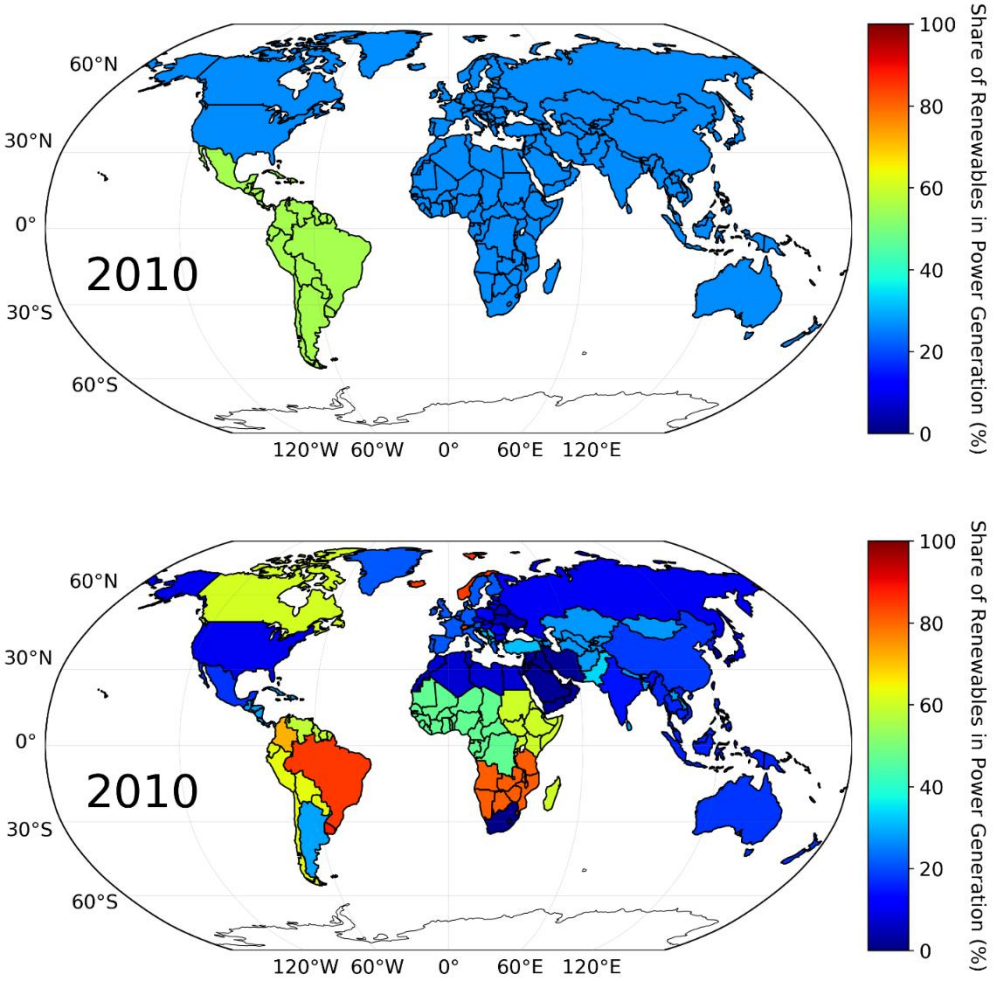

Figure 3.1 Share of renewable energy (bioenergy, geothermal, hydropower, solar and wind) in total electricity generation: in the LAC region compared to the average of the rest of the world (top); and by individual regions (bottom). The share of renewables in power generation was computed as total renewable electricity generation divided by total generation expressed in relative (%) terms. Source: GCAM-LAC total electricity generation by region in 2010 (last calibrated year).

Despite the increasingly important role of RE in LAC, notably in the electricity sector, current regional consumption of fossil fuels remains a challenge for climate mitigation (fossil fuels represented roughly 70% of total primary energy supply (TPES) in 2015 (IEA 2019)). TPES in LAC depends primarily on oil, natural gas, bioenergy, and hydropower (IEA 2019) with large oil and biofuels use in the transportation sector, while hydropower, natural gas and oil comprise most of the electricity supply (as shown earlier in Figures 2.1 and 2.2). However, at sub-regional/country levels, important departures from the overall LAC profile exist. For example, regarding hydropower, which dominates regional electricity mixes (notably in Uruguay, Brazil and Colombia), except for Mexico, Central America and the Caribbean and Argentina where main generating sources are natural gas and oil (Figure 3.2). Absent efforts to constrain emissions, fossil technologies in LAC are projected to expand (van Ruijven et al. 2016) (Figure 3.2 provides projections from the GCAM *Baseline (No Policy)* scenario, which assumes no emissions mitigation actions throughout the 21st century).

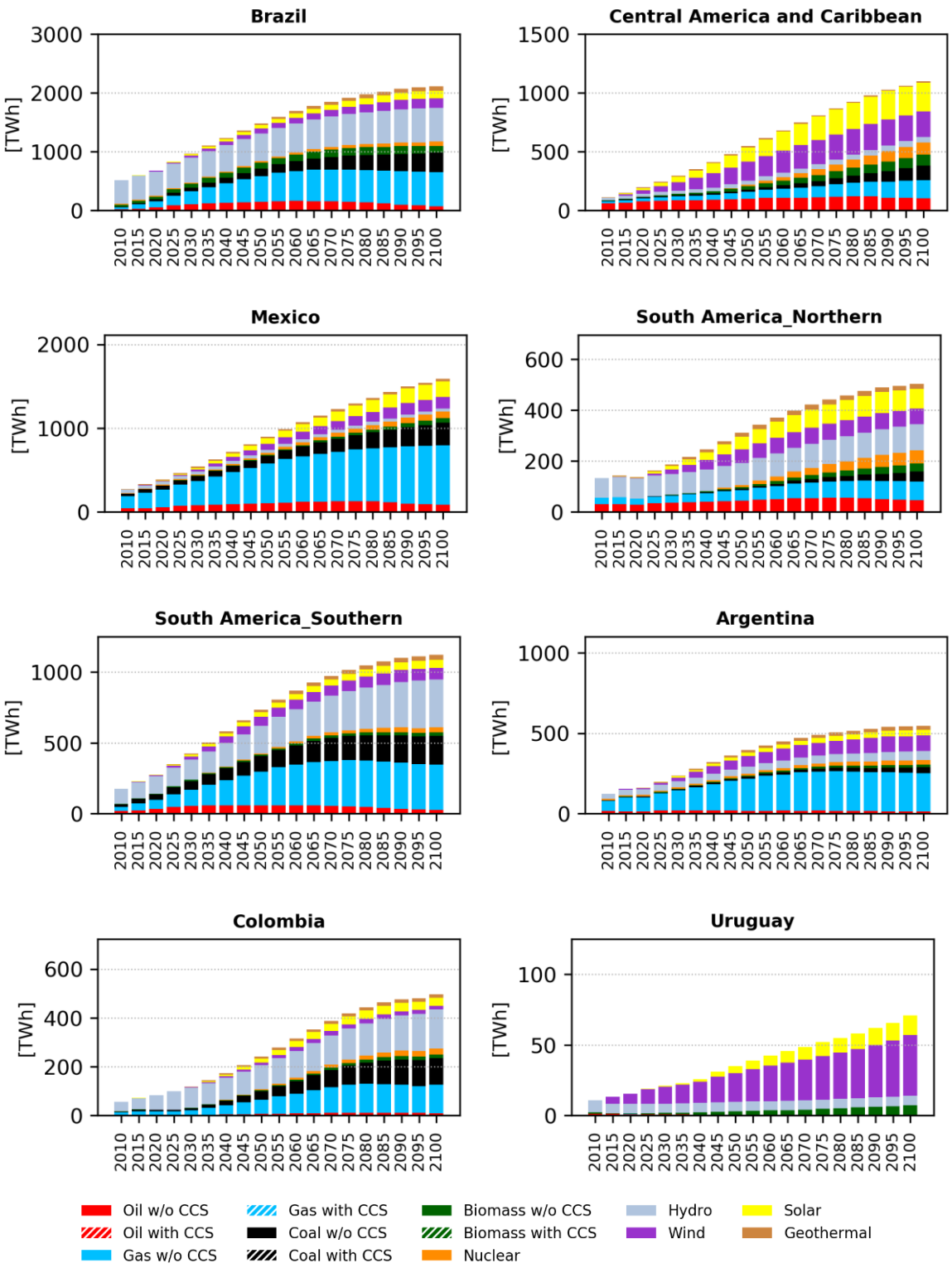

Figure 3.2 Electricity generation by technology in the GCAM *Baseline (No Policy)* scenario for the eight LAC regions represented in GCAM-LAC. (Note that this scenario is identical to the *RCP60_Baseline: No-climate impacts* scenario mentioned below in Table 3.1).

In light of this, previous LAC decarbonization scenarios agree that renewables, mainly biomass, solar and wind as well as CCS technologies applied to fossil fuels and biomass are critical to mitigate energy-sector emissions, with nuclear energy typically playing less relevant roles (Binsted et al. 2020; Calderón et al. 2016; Kober et al. 2016; Lucena et al. 2016; Santos Da Silva et al. 2019; van der Zwaan et al. 2016). In these scenarios, hydropower remains important, but its contribution to regional total generation falls over time, as hydropower capacity expansion is not expected to follow growing demands (Solaun and Cerdá 2019).

Under future climate change conditions, RE production in LAC will potentially face several challenges. By the end of the 21st century, multi-model projections using the representative concentration pathways (RCPs) (IPCC 2014) show mean warming levels reaching 0.6^{o}C to 2.0^{o}C in RCP2.6 and 2.2^{o}C to 7.0^{o}C in RCP8.5, and both positive and negative rainfall anomalies across the region (Magrin et al. 2014). Although there is large uncertainty intrinsic to these climate projections, their effect on future estimates of hydropower potential is manifested in terms of a strong regional variability of impacts from gains in Uruguay and the southernmost basins of Brazil to losses in northern Brazil, Colombia, northern South America, Argentina, and southern South America (Khan et al. 2020; Popescu et al. 2014; Ruffato-Ferreira et al. 2017; Turner et al. 2017). The limited literature focusing on LAC suggests increased wind and solar resource potentials in Brazil (de Jong et al. 2019; Pereira de Lucena et al. 2010; Pereira et al. 2013; Ruffato-Ferreira et al. 2017), and, possibly, a positive general response of the main LAC bioenergy feedstock, sugarcane, to regional climatic changes (Magrin et al. 2014) (more details are provided in the next Section). Despite its large

socioeconomic and physical vulnerability to climate change, LAC has been poorly covered by energy-sector impact studies, which are either global in scope or largely focused on Europe and North America (Cronin et al. 2018; Emodi et al. 2019; Solaun and Cerdá 2019).

3.3 Climate change impacts on the renewable energy supply and potential effects in the Latin America and the Caribbean region

This section briefly reviews major climate change effects on the RE supply. Note that impacts on the whole energy sector, including other relevant aspects such as climate effects on thermoelectric efficiency and transmission systems, extreme events, among others, are not included. These impacts are discussed in Schaeffer et al. 2012, Cronin et al. 2018, and Solaun and Cerdá 2019. This section attempts to emphasize impacts projected for the LAC region published on peer-reviewed articles after 2010, albeit somewhat limited by the weak literature coverage in the region mentioned above.

3.3.1 Bioenergy

Assessing climate impacts on the agricultural system, that can affect biomass production, is complex due to the potential plants exposure to a range of biological and environmental stresses, and to the large uncertainty within the impacts modeling chain that involves general circulation model (GCM) outputs driving responses of crop models spanning different structures, assumptions and approaches. Overall, changes in agricultural yields can be positive or negative depending on the warming levels, rainfall changes and CO_2 fertilization with responses varying widely by crop type and region. CO_2 fertilization is acknowledged as a key modulating mechanism that can partially

offset additional plants transpiration requirements by promoting increased water use efficiency (IPCC 2012). Although there might be some benefits for certain crops at mid- and high-latitude zones at moderate-to-medium levels of local warming (1-3ºC), for a wide range of regions and crops, impacts tend to be predominantly negative, particularly in the tropical regions (IPCC 2014; Rosenzweig et al. 2014). Under higher warming levels, crops can also be more susceptible to deleterious effects associated with plant diseases and pest outbreaks, elevated tropospheric ozone concentration and higher risk of occurrence of extreme events (i.e., heat stress, droughts, floods) (Tubiello et al. 2007).

In LAC, the two most important bioenergy feedstocks are sugarcane and soybeans employed in bioethanol and biodiesel production, respectively. According to the last IPCC report (Magrin et al. 2014), both crops are, in general, likely to respond positively to CO_2 concentration and temperature changes projected for the region, even considering a decrease in water availability. However, a large variability of impacts at smaller sub-regional scales is expected. For example, one study (Marin et al. 2013) used a sugarcane growth model that includes CO_2 fertilization forced by downscaled outputs from two GCMs under high and low emissions scenarios of the IPCC Special Report on Emissions Scenarios (SRES), and found increases in productivity and better water use efficiency for rainfed sugarcane in southern Brazil in all scenarios. Projected yield increases in this region (which is currently the main sugarcane plantation area in the country) ranges between 15 and 59% in 2050 relative to present-day average yield. On the other hand, another modeling study (Carvalho et al. 2015), focusing on a subdomain within the northeastern Brazil (a region considered particularly vulnerable

to climate change where drought events are recurrent), found sugarcane yield reductions by 2040 and 2100 for the moderate A1B SRES emissions scenario. Another study (Rolla et al. 2018) employed the DSSAT cropping system model forced by the CCSM4 climate model, and found significant yield increases of rainfed soybean crops in Central Argentina for the near (2015–2039) and far (2075-2099) horizons relative to present-day conditions under RCPs 4.5 and 8.5. The yield increases were found to be associated with projected increases in summer rainfalls in the region.

3.3.2 Hydropower

Climate change can modify surface runoff owing to shifts in mean annual and seasonal precipitation, in evapotranspiration patterns and in the amount and seasonal cycle of snowmelt (Schaeffer et al. 2012), which would affect the mean river-flow and flow seasonality. In addition, more frequent flooding events may affect the safety of dams' infrastructure. There is also great complexity in assessing climate impacts on hydropower that relate to very region-specific climate responses and local interactions with socioeconomic agents that compete for water resources (Arent et al. 2014). Moreover, the inherent GCMs uncertainty adds up to those arising from distinct global hydrological models (GHMs). The latter can result in a larger spread in simulated streamflow than the spread originating from GCMs (van Vliet et al. 2016b).

Due to the strong non-uniform distribution of projected temperature and precipitation changes around the globe (IPCC 2014), current understanding is that hydropower potentials may increase in certain areas whereas other regions may face a decline. For instance, one study (Hamududu; Killingtveit 2012) projects small global and regional changes in hydropower generation by 2050, with slight increases in some

regions (e.g., Americas by 0.05%), and reductions in other areas (e.g., Europe by –0.16%). Nevertheless, many of the global and regional studies summarized by recent literature reviews (Cronin et al. 2018; Solaun and Cerdá 2019) point out to larger climate-induced changes in runoff, streamflow, hydropower potentials or generation depending on the study scope. According to one recent review (Cronin et al. 2018), positive impacts tend to be located in high latitude areas (e.g., Canada, Russia, northern Europe, northeast China) whereas negative impacts tend to be located in regions such as southern Europe, southern USA, southeast China and southern South America.

Within the LAC domain, potential hydropower generation losses in Brazil, Chile, Colombia and Costa Rica, and substantial uncertainties surrounding Ecuador's hydrological projections have been reported (Solaun and Cerdá 2019). In the particular case of Brazil (one of the largest hydroelectricity producers in the world), a recent study (Ruffato-Ferreira et al. 2017) used the Eta regional model to dynamically downscale projections from the global model HadGEM2-ES under RCPs 4.5 and 8.5. By computing the variation of the water balance index (function of precipitation minus evapotranspiration rates) up to 2100 for the eight main watersheds in the country, the study highlighted a decreasing trend in water availability for watersheds located in the north and center of the country and an increasing trend for southern watersheds in both RCPs. The most pronounced trend of increased water scarcity was found for the northeastern Brazil. In face of a potential marked sub-regional variation of impacts on water availability – as suggested by Ruffato-Ferreira et al. 2017 – it can be expected that the net effect of climate change on the total hydropower potential in Brazil will depend on the location of the installed capacity as well as on the planned capacity

additions. Currently, the majority of hydroelectric power plants are in the Midwest and Southern regions, with the Southwest region accounting for 70% of the hydropower storage capacity (De Souza Dias et al. 2018). However, current government plans of hydropower expansion in Brazil for the next decade focus on the Northwest (i.e., Amazon) region (Almeida Prado et al. 2016).

As noted above, climate impacts on hydropower have been represented in IAMs. For example, one study (Turner et al. 2017) forced a coupled global hydrological and dam model with an ensemble of 16 GCMs (RCPs 4.5 and 8.5), incorporating the projected changes in hydropower potentials in GCAM. The multi-model mean response signaled losses in future hydropower generation in northern South America, Argentina, southern South America, Colombia, and Brazil, albeit with a lack of agreement in the direction of changes for the latter three regions. This same methodology and GCM forcings were employed in regional studies covering Brazil (Lucena et al. 2018) and Colombia (Arango-Aramburo et al. 2019), in which the median changes in hydropower generation up to the mid-century resulted to be negative. However, the spread in simulated 2050 hydropower generation was large, spanning from -13% to +4% in RCP 4.5, and -12% to 2% in RCP 8.5 in Brazil, and from about -20% to 0% for both RCPs in Colombia. In Uruguay, hydrology simulations using the model Xanthos forced by five GCMS and four RCPs provided water supply information that was incorporated in GCAM. This modeling framework projected increases in runoff and hydropower by 2050 across the 20 simulations performed (Khan et al. 2020).

3.3.3 Solar

Solar large-scale electricity generation comprises two main technologies: photovoltaics (PV) and concentrating solar power (CSP). In both cases, the primary climate impact derives from alterations in the spatial and temporal distribution of the incident solar radiation at the surface. Downwelling solar radiation is attenuated through absorption by atmospheric gases (in which water vapor plays an important role) and aerosol particles. Moreover, the incident radiative flux is attenuated through scattering by aerosols, cloud droplets and ice crystals. The aerosol burden of the atmosphere can also influence the amount of incident solar radiation indirectly by affecting cloud properties such as cloud albedo and lifetime. All these atmospheric constituents are subject to changes due to the anthropogenic interference on the climate system. Overall, CSP systems are considered to be more vulnerable than the PV counterparts since the former relies exclusively on the direct component of solar radiation, whereas the latter utilizes both direct and diffuse solar radiation (Arent et al. 2014). Within a global perspective, multi-model end-of-century projections from the Coupled Model Intercomparison Project phase 5 (CMIP5) show consistent reductions in annual mean total cloud cover in low to mid-latitudes under increasing warming levels, notably the RCP8.5 (Collins et al. 2013). However, other effects also play relevant roles with fundamental differences between both technologies.

PV systems rely on panels or modules connecting several PV cells manufactured from a semiconductor material, predominantly silicon. For this technology, increasing mean temperatures negatively affect cell efficiency reducing power output. In general, PV cell efficiency drops approximately 0.5% per 1^{o}C increase

considering PV technologies such as crystalline silicon and thin-film modules (Arent et al. 2014). PV efficiency is also influenced by the wind flow around the module, which produces a cooling effect (Mavromatakis et al. 2010). CSP facilities operate with an array of typically hundreds of high-magnification mirrors or lenses that focus the sun's direct beam radiation on thermally efficient receivers, thereby heating a working fluid that is used to drive steam turbines. CSP outputs increase almost linearly in response to ambient temperature, but the dominant effect lies on the response to solar radiation changes (Crook et al. 2011). Apart from the potential to reduce the amount of incident solar radiation, increased levels of dust and anthropogenic particulate matter being deposited on PV panels and CSP collectors diminish electricity generation (Bergin et al. 2017).

The three following global-scale studies have used large GCM CMIP5 ensembles to investigate climate impacts on PV and CSP outputs, addressing specifically the RCP8.5. The first (Wild et al. 2015), found that the temperature effect is likely to compensate gains from an increase in incoming surface solar radiation, leading to negative trends in PV power output by the midcentury in most parts of the world. Overall, the projected power changes between 2006 and 2049 were about 1%/decade. In contrast, the midcentury CSP output was found to increase over large parts of the globe due to the combined effect of increasing mean temperatures and positive trends in surface solar radiation projected by the CMIP5 models (Wild et al. 2017). In the third study (Zou et al. 2019), increasing trends of PV power (modeled as function of temperature) were found in East Asia, Europe, Central Africa, the northern part of South America, Central America, and central and eastern China in the 2006-

2100 period. Such a trend was attributed to a decreasing trend in the atmospheric aerosols burden. For other regions such as North Africa, Central Asia, Australia, and especially the Tibetan Plateau, decreasing trends of PV power were found, associated with increasing aerosol burdens and cloudiness in the cases of the North Africa and the Tibetan Plateau regions.

The examination of the literature revealed only one study (de Jong et al. 2019) focusing on a LAC domain. This study employed a downscaled regional climate model forced by three CMIP5 GCMs under RCP8.5, and projected a slight increase in average incoming surface solar radiation across most of Brazil. Particularly in the northeastern Brazil (where most of solar and wind power capacities have been concentrated on), the projected increase is of about 3.6% by the 2080s relative to the 1970s.

3.3.4 Wind

The theoretical extractable power of wind is directly proportional to the near-surface wind speed to the third power and air density (Eurek et al. 2017). Hence, the inherent physical relationship involving the general atmospheric circulation, surface pressure and temperature gradients render large to local-scale wind potential sensitive to global warming, resulting in alterations in the mean and extreme wind speeds, direction as well as in the resource variability across different temporal scales (Pryor; Barthelmie 2010, 2013). While changing annual and seasonal mean wind speeds affect power-generation capacity, changes in the magnitude and frequency of extreme wind speeds can affect farms infrastructure through damages to the turbines.

A recent global-scale study (Karnauskas et al. 2018) based on an ensemble of ten GCMs from CMIP5 under RCPs 4.5 and 8.5 portrayed decreases in wind power

across the Northern Hemisphere mid-latitudes and increases across the tropics and Southern Hemisphere (in this case with substantial regional variations and larger sensitivity to the emissions scenario). These responses were attributed to the polar amplification in the northern mid-latitudes, whereas enhanced land–sea thermal gradients governed the tropical and southern subtropical increases. By investigating some focal regional domains in more detail, the study revealed increasing wind power over time for subdomains covering the Mexico-Caribbean and eastern Brazil regions and an opposite pattern in southern South America under the RCP8.5.

Narrowing down to regional impact studies in Latin America, the existing literature has focused in Brazil. Two studies (Pereira de Lucena et al. 2010; Pereira et al. 2013) employed projections from the HadCM3 GCM (dynamically downscaled into regional climate projections) under high and low IPCC SRES emissions scenarios, showing growth in resource availability in most regions over the long term, particularly in the Northeast region of Brazil. From both studies, the most conservative is Pereira et al. (Pereira et al. 2013), in which the average future growth in the wind power density inland for most of Northeast falls within the 15–30% range relative to the 1962-1990 baseline. These earlier findings agree with recent analyses (de Jong et al. 2019; Ruffato-Ferreira et al. 2017), where wind speeds are projected to increase across most of Brazil.

3.4 Methods

3.4.1 GCAM-LAC

This work was carried out in a research version of GCAM v5.1.3 best suited for analyses in LAC (GCAM-LAC) (Khan et al. 2020), in which important model

assumptions have been refined in consultation with local stakeholders. These include socioeconomic drivers, the disaggregation of Uruguay as a distinct geopolitical region and parametric assumptions affecting energy supply, energy demand, and end-use.

3.4.2 Climate impacts on renewables – model representation

GCAM was forced with representations of changing agricultural productivity and hydropower production as well as with climate-impacted solar and wind resource cost-supply curves. These inputs are based on bias-corrected projections from the GFDL-ESM2M, HadGEM2-ES and IPSL-CM5A-LR GCMs obtained from the Inter-Sectoral Impact Model Intercomparison Project (ISIMIP) (Frieler et al. 2017; Warszawski et al. 2014) under RCP2.6 and RCP6.0.

To account for climatic impacts on agricultural productivity that affect the modeled biomass production, crop yields simulated by the parallel Decision Support System for Agrotechnology Transfer (pDSSAT - the parallelized global gridded version of the DSSAT model (Elliott et al. 2014; Jones et al. 2003)) were used to modify GCAM baseline (i.e., no-climate impacts) crop yield change assumptions (based on the Food and Agriculture Organization projections (Kyle et al. 2014)). The pDSSAT dataset comprises gridded annual yield information for both irrigated and rain-fed crops, which allowed climate-induced yield changes to be applied separately into GCAM rain-fed and irrigated crops. Applying yield estimates from pDSSAT into GCAM requires some data processing to accommodate differences in spatial, temporal, and commodity resolutions between pDSSAT and GCAM. One of these key steps is to match crops represented by pDSSAT with the commodities modeled in GCAM. In the specific case of the second-generation bioenergy crops (such as switchgrass,

miscanthus, etc.), which are not represented by pDSSAT, GCAM's biomass crop commodity receives the median of climate impacts to all other commodities. Note that GCAM requires yield change assumptions to calculate the expected land profitability in each model land unit at each time step. Thus, the effect of the climate-impacted yield change assumptions is to modify such profit rates across land units in the model, which are used to determine land allocated to each land type (cropland, biomass, grassland, shrubland, pasture, forest, etc.). The combination of yields and endogenous land allocation determines agricultural production in each land unit at each time step (Kyle et al. 2014). The pDSSAT simulations used in this study are part of the Agricultural Model Inter-comparison Project (AGMIP) (Rosenzweig et al. 2014), and were taken from the experiments that included CO_2 fertilization effects.

Hydrology simulations from the global hydrological model (GHM) Xanthos (Vernon et al. 2019) were used to modify GCAM default hydropower assumptions. Specifically, hydropower default assumptions (derived from the economic and technical potentials estimated by the International Hydropower Association (Calvin et al. 2019)) are exogenous inputs in GCAM containing predetermined quantities of hydroelectricity production (in EJ) for all time steps and regions. These prescribed quantities (read in at the start of a simulation) then determine the temporal evolution of hydropower production by GCAM region. This means that hydropower production does not result from the modeled economic competition like all other power-sector technologies represented in GCAM.

To incorporate gains/losses in hydropower production under evolving climatic conditions, Xanthos is used to provide information regarding renewable water

availability in the 235 large river basins represented in the model, as well as hydropower production. To do so, Xanthos requires gridded monthly precipitation and temperature fields from GCMs to solve for monthly runoff and other variables at grid-cell level globally. Using Xanthos 2.0, future projections of hydropower production were computed through a built-in hydropower module that requires gridded streamflow projections (converted from the simulated runoff) to drive dam simulations. This modeling chain produced modified assumptions of regional hydropower production that incorporate climate change effects. These assumptions were then used to replace default GCAM assumptions as mentioned above.

Climate impacts on solar and wind resource productions are modeled using supply curves. These curves map the availability of energy production as a function of energy price and are important assumptions to the model. The supply curves employed in this study were built upon the global estimates of renewable energy potentials produced as part of the 'ISIpedia-energy protocol' project (Yalew et al. 2020) using climate variables (e.g., solar radiation, temperature, wind speed) from the ISIMIP2b simulations. These data consist of gridded (0.5^{o} spatial resolution) maps of technical and economic potentials for four generating technologies (concentrating solar power, photovoltaics – utility-scale and rooftop – and wind), covering three distinct time-slices (1971–2000: historical conditions; 2031–2070 and 2071–2100: future climate states) produced through methods documented in Gernaat et al. 2021 (Chapter 4 will discuss in details how wind and solar technical potentials are computed in the literature).

ISIpedia information on wind and solar technical potentials (given by the gridded maps of technical potential) and electricity costs (given by the gridded maps of economic potentials), were used to derive three time-varying supply curves per renewable source, GCM and GCAM region (Appendix B; Figures B.1 – B.12), which replaced GCAM default assumptions that do not consider climate change effects on solar and wind sources. In the case of wind, the default supply curves derive from a reanalysis dataset covering the 1980-2009 period (Zhou et al. 2012). Solar energy is modeled as two separate resources: global solar resource and distributed PV (accounting for PV installations on residential and commercial buildings) (JGCRI 2019). While the distributed PV resource is modeled with supply curves derived from an observational solar radiation dataset (Denholm; Margolis 2008), no cost-supply curve is implemented for the global solar primary resource (representing utility-scale solar technologies), which is assumed to be an unlimited resource with very low costs that do not vary with deployment levels (JGCRI 2019).

Replacing GCAM default assumptions by the ISIpedia supply curves has important implications. In GCAM, primary renewable resource production and their resource-related costs serve as inputs to the electricity sector, which contains representations of distinct generating technologies (fossil fuels, geothermal, hydropower, intermittent renewables and nuclear). The cost of generating electricity given by the renewables supply curves represents the fuel costs that GCAM uses to calculate the levelized cost of the technology *T* in time period *t*, $p_{T,t}$, given by:

$$p_{T,t} = \frac{C_{\text{fuel}}}{\eta} + \frac{1000\, C_{\text{capital}}}{8760\ \text{CF}} \times \text{FCR} + \frac{C_{\text{O\&M,fixed}}}{8760\ \text{CF}} + C_{\text{O\&M,variable}} \quad (1)$$

Where C_{fuel} is the fuel cost ($/MWh); η is the power plant efficiency; C_{capital} is the overnight capital cost ($/kW), CF is the capacity factor of the technology, FCR is the fixed charge rate; $C_{\text{O\&M,fixed}}$ is the annual fixed Operation and Maintenance (O&M) cost ($/MW); $C_{\text{O\&M,variable}}$ is the variable O&M cost ($/MWh) and 8760 is the number of hours in a year. The list of electric power generation technologies represented in the model and their input assumptions are available in the literature (Muratori et al. 2017). Thus, higher/lower average availability of a renewable resource due to climate change would translate into shifting supply curves, which would affect C_{fuel} in Eq. 1 above. This would indeed translate into alterations on generating capacity as $p_{T,t}$ is used to compute the share of regional electricity markets each generating technology T captures at time t ($s_{T,t}$). As mentioned earlier, this market competition is modeled by a logit formulation (Calvin et al. 2019) given by (note that hydropower is set aside from economic competition since hydropower production is a fixed input to the model):

$$s_{T,t} = \frac{\alpha_{T,t} p_{T,t}^{\gamma}}{\sum_{T=1}^{N} \alpha_{T,t} p_{T,t}^{\gamma}} \tag{2}$$

Where $p_{T,t}$ is the levelized cost of the technology T in time period t (Eq. 1), γ is an exogenous input shape parameter and $\alpha_{T,t}$ are calibration parameters. This formulation has an important property in that it assigns some market share to expensive technologies, which allows the model to avoid unrealistic "winner take all" responses (Wise et al. 2019). Lastly, it is important to mention that GCAM includes a representation of renewable intermittency. Like most IAMs, this is translated into costs

that vary with the share of renewables in the grid and add to the cost of building new intermittent generation to secure backup capacity.

The impacts on the power system due to climate change on renewables were examined by comparing scenarios with climate impacts on renewables against identical scenarios that neglect these effects (i.e., the No-climate impacts scenarios) according to the scenarios design presented in Table 3.1 below. Note that climate impacts on other relevant aspects of the energy system (e.g., building energy consumption (Clarke et al. 2018), thermal power generation (Bartos; Chester 2015; van Vliet et al. 2016a), transmission infrastructure (Yalew et al. 2020), etc.) were not included in this experimental setup. This means that these results should be interpreted in light of this assumption. Although the modeling framework employed here provides a previously unexplored picture of the effects of climate impacts on all renewables on the power system, future investigation is needed to incorporate impacts on other components of energy system, such as those cited above, which are also acknowledged as key sources of vulnerabilities to the energy system (Yalew et al. 2020).

3.4.3 Calculation of capital investments in the electric power sector

The GCAM representation of capital stock turnover (i.e., the process by which old ‘equipment’ is replaced by new one) in the electric power sector assumes that generating technologies have a prescribed lifetime, and investments in new plants are added by vintage (i.e., period in which the investment is made) in a pace that allows sufficient generating capacity to satisfy demand. Each power plant operates until the end of its lifetime or is retired from production if its operating costs surpass the electricity market price. The new technology investments compete for a share of energy

markets, which is modeled by the logit-choice formulation discussed above. Power-sector capital investments calculation is made as follows (Iyer et al. 2017). Based on GCAM outputs of electricity generation by technology, vintage and period, the first step is to compute new and additional electricity generation for each technology in each period, which is converted to capacity (in GW) via capacity factor assumptions (listed in Appendix B, Tables B.1 and B.2). This can be expressed as:

$$\text{Capacity} = \frac{\text{Generation} \times (2.78 \times 10^5)}{\text{Capacity Factor} \times 8760} \quad (3)$$

Finally, the capacity addition calculated above is multiplied by the overnight capital cost associated with each technology (in $/kilowatt) using assumptions listed in Table B.3 (Appendix B). This yields capital investments (in $ — representative of cumulative investments over a five-year model period) as shown below:

$$\text{Capital investment} = \text{Capacity} \times 10^6 \times \text{Overnight Capital Costs} \quad (4)$$

It is important to mention that capital investments computed by the method outlined here represent the upfront costs that occur at the beginning of the lifetime of a power station. Variable costs (e.g., fuel costs and operation and maintenance costs) and other system costs (e.g., integration) are not included.

3.4.4 Experimental Design

To account for compounding climate impacts on renewables, 9 illustrative scenarios using GCAM are explored (Table 3.1). The scenarios vary across three dimensions, namely, assumptions about the level of climate change mitigation, climate impacts on renewables and technology availability.

Table 3.1 Scenarios explored in this study

		Technology Availability		
		FullTech	NoCCS & NoNewNuc	Baseline
Climate Impacts	None	RCP26_FullTech: No-climate impacts	RCP26_NoCCS & NoNewNuc: No-climate impacts	RCP60_Baseline: No-climate impacts
	Hydropower	RCP26_FullTech: Hydropower	RCP26_NoCCS & NoNewNuc: Hydropower	RCP60_Baseline: Hydropower
	All renewables	RCP26_FullTech: Combined impacts	RCP26_NoCCS & NoNewNuc: Combined impacts	RCP60_Baseline: Combined impacts
Climate Mitigation		RCP2.6		RCP6.0

Along the first dimension, two scenario variants exist. The first refers to scenarios with no explicit climate policy, which lead to a radiative forcing of 6.0 W/m^2 at the end of the century. These scenarios are based on the GCAM Baseline (No Policy) scenario mentioned earlier (note that the RCP60_Baseline: No-climate impacts scenario shown in Table 1 is identical to the GCAM Baseline (No Policy) scenario). Moreover, scenarios with greenhouse gas mitigation policies to reduce radiative forcing are explored. These scenarios assume that countries across the globe (including those in LAC) achieve their NDC commitments through 2030. Beyond 2030, the scenarios assume globally coordinated mitigation efforts compatible with limiting end-of-century temperature rise to 2^{o}C and with the RCP2.6 (Appendix A; Supplementary Note 1).

Along the climate impacts dimension, three variations are explored. The first variation, named No-climate impacts, assumes no climate impacts on renewable resources. The Hydropower scenarios assume climate impacts on hydropower only, allowing a comparison with the approach of prior studies that have investigated electricity-sector implications due to climate impacts on hydropower (Arango-Aramburo et al. 2019; Carvajal et al. 2019; Dowling 2013; Lucena et al. 2018; Savelsberg et al. 2018; Turner et al. 2017; Zhou et al. 2018). The Combined impacts scenarios assume climate impacts on all renewable resources (recall that the representation of climate impacts on renewables in GCAM is discussed in Subsection 3.3.2). The results focus primarily on mean values across all GCMs although the implications for climate model uncertainty are discussed at the end of the Results Section. Note that the RCP2.6 is the lowest projected warming level among the RCPs considered within the IPCC AR5 and ISIMIP, and is consistent with a global warming likely below 2°C above pre-industrial temperatures (IPCC 2014). The RCP2.6 allows climate impacts on renewables being studied in a context of strong climate change mitigation with substantial upscaling of renewable energy. On the other hand, the RCP6.0 represents a high emissions pathway (IPCC 2014).

Along the technology availability dimension, three variations are explored. The Baseline and FullTech scenarios assume that the full suite of power sector technologies represented by GCAM is available globally. However, the FullTech scenario includes CCS technologies that are only deployed in the context of decarbonization. The NoCCS & NoNewNuc scenario assumes no deployment of CCS technologies globally, and no new deployment of nuclear technologies in LAC. The NoCCS & NoNewNuc scenario

represents a high renewable scenario – which is important within the context of LAC where future mitigation strategies are expected to rely heavily on renewables. These scenarios are consistent with many prior mitigation studies (Binsted et al. 2020; Clarke et al. 2014; Santos Da Silva et al. 2019).

3.5 Results

3.5.1 Implications for electricity generation patterns

Consistent with prior literature on LAC decarbonization scenarios (Binsted et al. 2020; Calderón et al. 2016; Kober et al. 2016; Lucena et al. 2016; Santos Da Silva et al. 2019; van der Zwaan et al. 2016), the mitigation RCP26 scenarios entail a significantly larger use of low-carbon energy sources and increased electrification of end-use sectors compared with a Baseline energy technology pathway (Figure 3.3). The RCP26_FullTech family of scenarios represents a diverse array of low-carbon technologies with bioenergy and natural gas plants equipped with CCS playing central roles in mitigation by supplanting the role of fossil-fuel based power generation, particularly, of natural gas, through 2100 (Figures 3.3 and B.13). Under the RCP26_NoCCS & NoNewNuc scenarios, emissions reductions in the power sector are achieved largely through the addition of solar and wind plants (Figures 3.3 and B.14). As noted below, each energy technology pathway offers distinct technological alternatives for adaptation to climate impacts on RE.

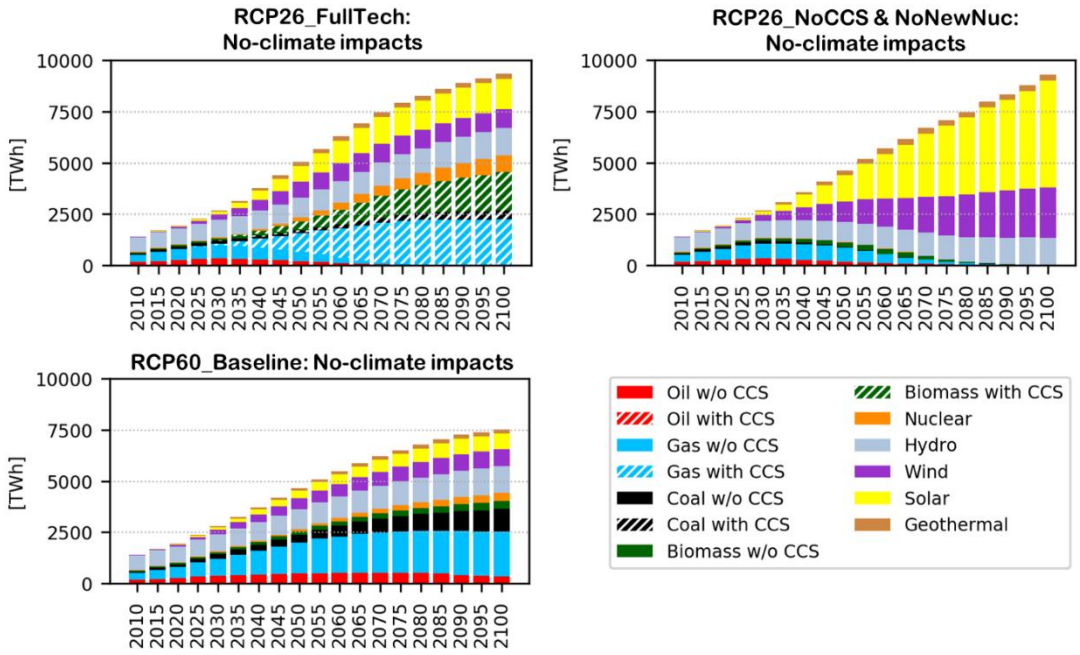

Figure 3.3 Electricity generation by technology in the *RCP26_FullTech: No-climate impacts* scenario (top left), *RCP26_NoCCS & NoNewNuc: No-climate impacts* scenario (top right), and *RCP60_Baseline: No-climate impacts* scenario (bottom left) in LAC.

Figure 3.4 provides an overview of the mean differences in electricity generation for the six climate-impact scenarios relative to the reference *No-Climate impacts* cases. A comparison between the *Combined impacts* and the *Hydropower* scenarios highlights the possibility of an incomplete understanding of the implications of climate change on the power sector without an integrated framework that accounts for impacts on all renewables. Such an issue is apparent in most subregions for two reasons. First, some LAC subregions (particularly Brazil, S. Am. N. and S. Am. S) show nontrivial responses induced by the climate-impacted wind supply-curves (this is better illustrated in Figures 3.5 and 3.6 below). Second, some LAC subregions (Argentina, C. Am/Car. and Mexico) are characterized by lower present-day and projected contributions of hydropower production compared to others (Figure 3.2).

Hence, their national RE portfolios become more sensitive to climate impacts on the non-hydropower renewables. In fact, hydropower is projected to play a less relevant role in total power generation across the entire LAC region (Figures 3.2 and 3.3). Even in Brazil where climate impacts on hydropower largely govern power-sector responses, important differences concerning wind-based generation exist. Conversely, Colombia and Uruguay are noteworthy cases in which climate impacts on hydropower largely dominate the effects on the power system.

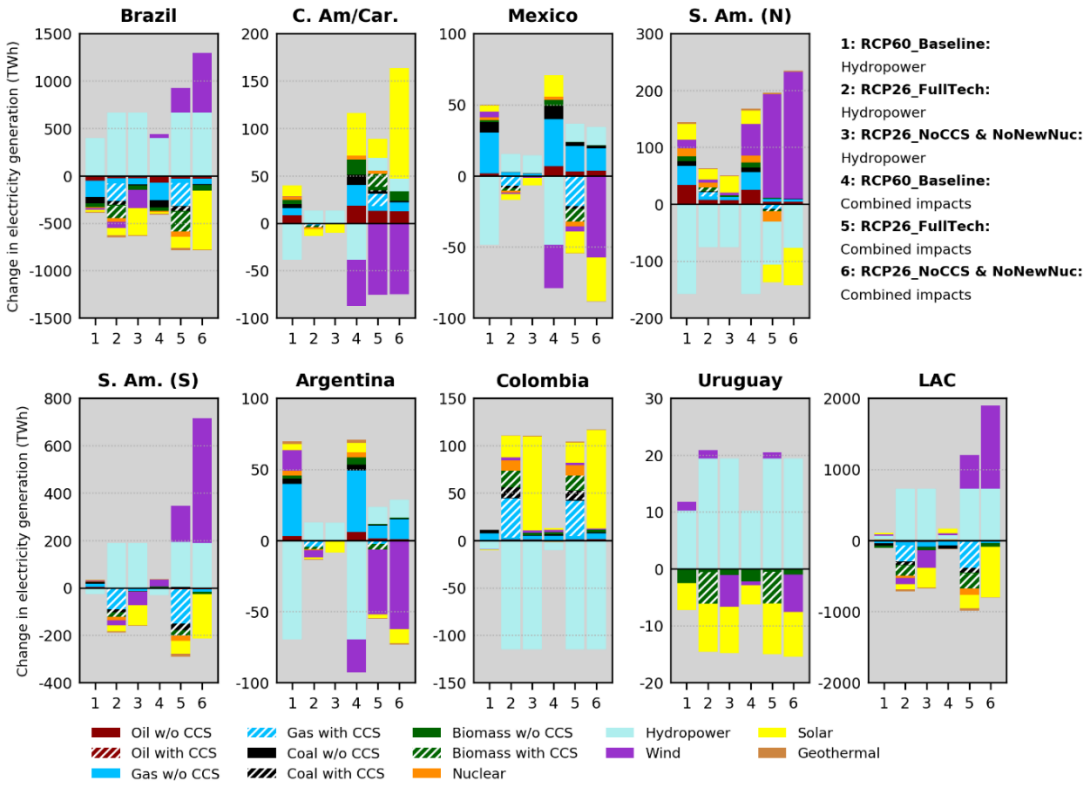

Figure 3.4 Model mean differences in electricity production by technology in LAC assuming climate change impacts on renewables**.** Differences are calculated by technology using cumulative generation (Terawatt-hours – TWh) during the 2020 – 2100 period and are relative to the corresponding No-Climate impacts scenarios. GCAM LAC regions covered: Brazil, Central America and the Caribbean (C. Am/Car.), Mexico, South America_Northern (S. Am. (N)), South America_Southern (S. Am. (S)), Argentina, Colombia and Uruguay. Note the different y axis scales.

Focusing on the RCP26 Combined impacts scenarios (columns 5 and 6 in Figure 3.4), the magnitudes of changes in wind and solar generation tend to be larger in the NoCCS & NoNewNuc relative to the FullTech, since the former is far more reliant on renewables than the latter (Figure 3.3). Nevertheless, the directions of changes in wind generation in the NoCCS & NoNewNuc are largely consistent with the FullTech (except for where this signal is small as noted earlier for Colombia and Uruguay), while differences in other non-hydropower sources are mostly indirect effects (i.e., driven by the changes in hydropower and wind; see Figures 3.5 and 3.6 and discussion below). The results imply that wherever favorable nontrivial signals from the climate-impacted wind resource exist (e.g., Brazil, S. Am. N. and S. Am. S.), wind energy may represent an optimal opportunity to decarbonize the power system, with potential to also serve as a key adaptation strategy to climate-attributable losses in hydropower (e.g., S. Am. N.). Conversely, Argentina and C. Am/Car. may need to increase generation from a mix of alternative sources to compensate for potential reductions in wind power as the projected positive climate effects on hydropower appear insufficient to satisfy demand.

The major driving forces acting on LAC's decarbonizing power sector under multiple simultaneous climate impacts (i.e., under the *Combined impacts* assumption) are better understood by examining results from ancillary experiments which assume climate impacts on each renewable individually (similar to the approach conducted by Turner et al. 2017 for hydropower and by Kyle et al. 2014 for agricultural yields). Specifically, simulations where each climate-impact input is incorporated into GCAM individually were carried out, and the implications for electricity generation per source

considered were assessed (i.e., if climate impacts on wind were incorporated in GCAM, changes in wind power generation were examined and so on). By incorporating the physical impacts of climate change on the RE supply into GCAM, concurrent direct and indirect effects are induced. The former means the direct power-system responses to the climate-impacted RE inputs such as a decline in hydroelectricity production due to reduced streamflow volumes or an increase in bioenergy production due to improved crop yields. The indirect responses derive from feedbacks of the direct effects on the power system. More complex interactions emerge under multiple simultaneous climate impacts. This is illustrated in Figures 3.5 and 3.6. When climate impacts on individual renewables are assumed (a), magnitudes and signs of the resulting direct changes in renewable electricity generation vary considerably across LAC with effects on hydropower- and wind-based generation outweighing those on biomass and solar generation. When all impacts are jointly accounted for in the *Combined impacts* scenarios, bioenergy and solar generation undergo more pronounced variations responding to the compounding indirect effects (price and demand adjusts) driven mostly by hydropower and wind sources (b and c).

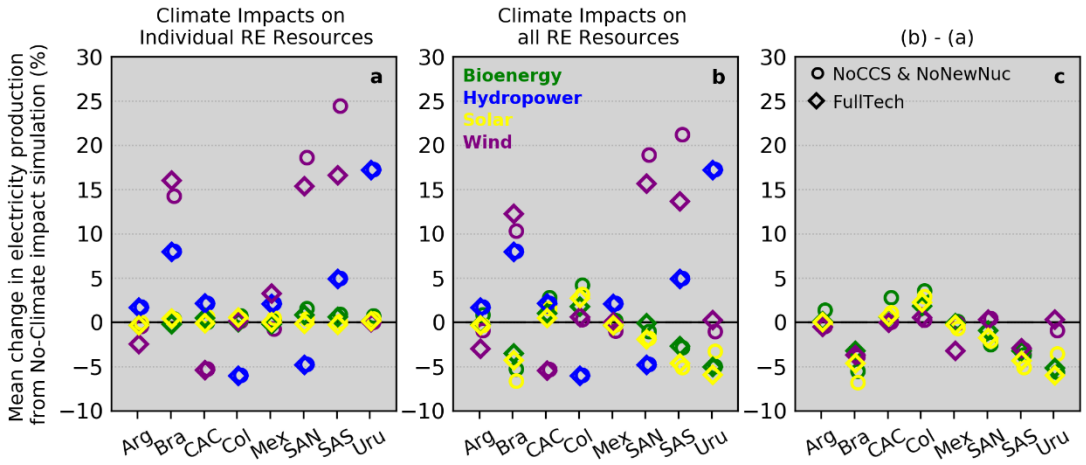

Figure 3.5 Mean changes in electricity generation in LAC assuming climate change impacts on renewables. Changes represent the mean value across GCMs, and are calculated by technology scenario (labelled in **c**) and RE generating source (labelled in **b**) using cumulative generation in the 2020 ─ 2100 period. Percent changes are relative to the corresponding *No-climate impacts* simulations (positive values indicate that scenarios with climate impacts on renewables show higher cumulative generation). **a**. Assumption of climate impacts on each individual renewable source separately. **b**. Assumption of climate impacts on all renewables (*Combined impacts* scenarios in Table 3.1). **c**. Differences between outputs in **b** and **a** (hydropower is not plotted since the temporal evolution of hydroelectricity production per GCAM region is exogenously predetermined, i.e., fixed; thus differences between scenarios **a** and **b** are zero).

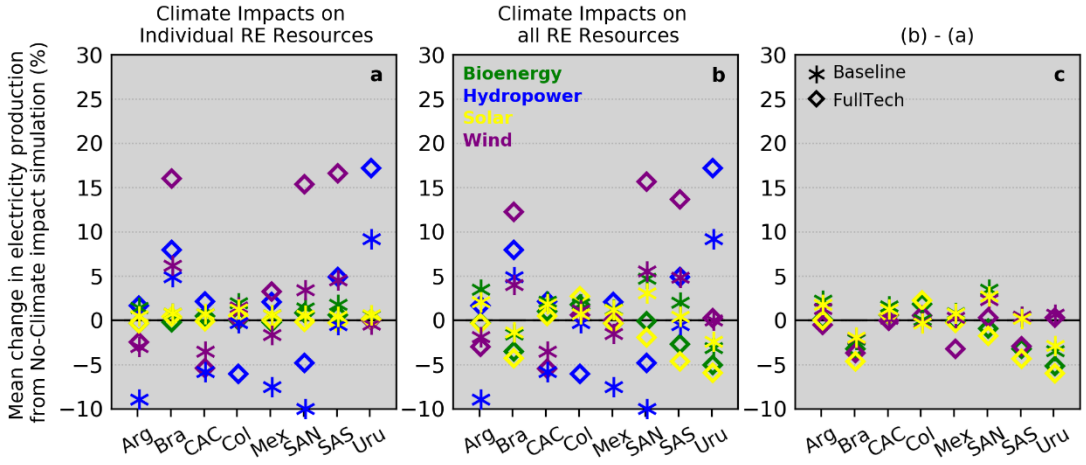

Figure 3.6 As in Figure 3.5 but showing results for the *Baseline* and *FullTech* scenarios.

Figure 3.4 also emphasizes implications from distinct warming levels. A salient response from the Hydropower scenarios (columns 1, 2 and 3 in Figure 3.4) is an

overall deterioration of hydroelectricity production under the RCP6.0. All regions, except for Colombia, experience enhanced reductions in cumulative generation, shifts from generation gains toward losses or less pronounced positive impacts compared to the RCP26 Hydropower scenarios. C. Am/Car., Mexico, S. Am. (N) and Argentina emerge as particularly prone to negative impacts on hydropower as the severity of climate change increases. In these regions, a potential adaptation strategy assessed by GCAM might be to increase fossil fuel based generation (particularly natural gas), which can exacerbate the initial climate change signal via increments in fossil fuel emissions. A comparison between the RCP60_Baseline: Hydropower and RCP60_Baseline: Combined impacts scenarios (columns 1 and 4 in Figure 3.4) reinforces the importance of detailed considerations of multiple impacts, which is particularly prominent in C. Am/Car., Mexico and Argentina. Again, the combination of impacts on hydropower and wind are the leading drivers of the compounding effects on electricity generation, however the direct effects on electricity generation changes induced by the RCP6.0 wind supply curves tend to be less pronounced than those induced by the RCP2.6 curves (Figures 3.5–3.6). This is particularly true for Brazil, S. Am. (N) and S. Am. (S). As a result, these regions experience less pronounced gains in wind-based generation under the RCP60_Baseline: Combined impacts relative to the RCP26_FullTech: Combined impacts case. It is important to note that these distinct outcomes must not be entirely attributed to the climate change signal due to the role of the energy technology pathway by itself. Specifically, under the RCP60_Baseline scenario, the effects produced by the wind supply curves (shown in the Appendix B – Figures B.1–B.12) on wind power generation originate from the lower ends of the

curves as wind power needs are not so prominent in this scenario. Conversely, energy-technology pathways like the FullTech and, in particular, the NoCCS & NoNewNuc rely considerably more on wind power to fulfill climate goals, thus suffering stronger influence from upper portions of the supply curves, in which differences among climate-impacted curves are more pronounced.

In all climate-impact scenarios, much of the differences in electricity generation tend to be more pronounced throughout the 2061-2100 period (Appendix B - Figures B.15─B.22). Given the unique implications each subregion may face due to climate impacts on renewables, these results illustrate how distinct accounting of these impacts in IAMs may affect decision-making. For example, under the RCP60_Baseline scenarios, Argentina is projected to experience a pattern of temporally increasing losses in hydroelectricity production (Appendix B – left panels of Figure B.20), which would require continuously improving adaptation plans. In this regards, modeling impacts only on hydropower implies that increased wind power generation would be among the portfolio of cost-effective adaptation options in Argentina. On the other hand, accounting for impacts in all renewables means that hydropower losses might be progressively exacerbated by losses in wind power generation, requiring a change in the course of power-sector adaptation plans in the country.

3.5.2 Implications for power-sector capital investments

Power-sector capital investments depend on how much generating capacity is installed or retired over time per technology and the marginal costs of building capacity from each technology (Methods - Subsection 3.3.3). Hence, the climate-induced alterations in electricity production patterns discussed so far would have implications

for regional capital investment needs through changes in generating capacity. Under the Combined impacts scenarios, this analysis signals increased needs for capital investments in most LAC subregions until 2100, particularly in the NoCCS & NoNewNuc scenario (Figure 3.7).

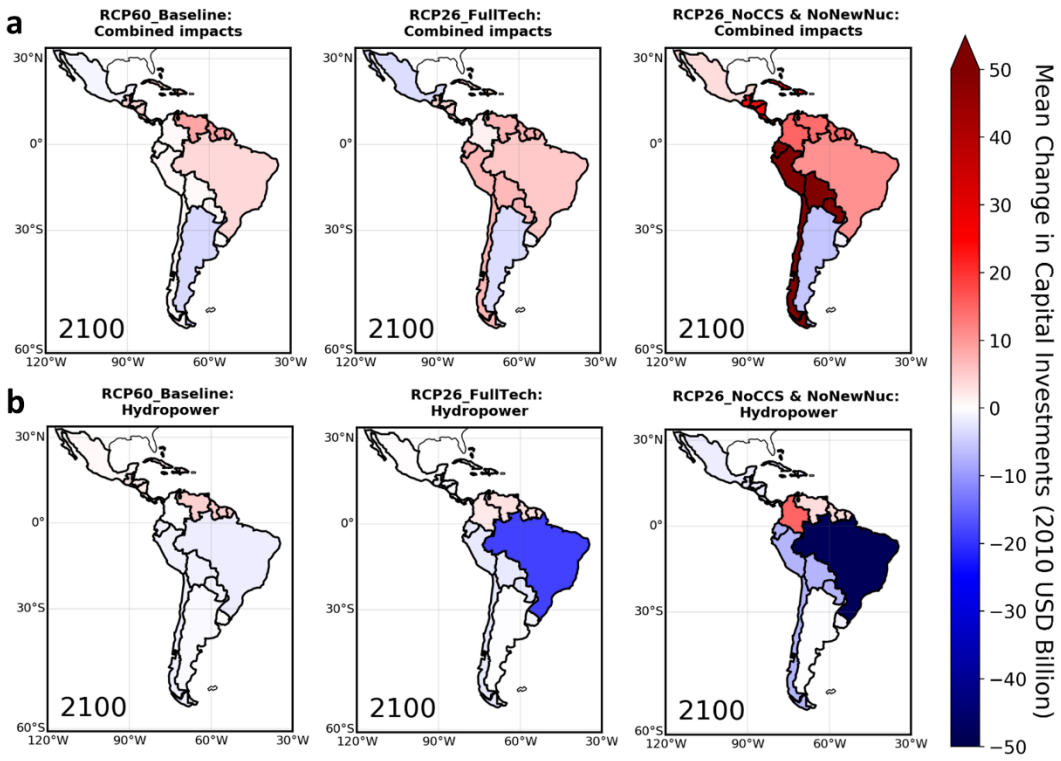

Figure 3.7 Model mean changes in total capital investment requirements in LAC by scenario under distinct assumptions on climate change impacts on renewables. Absolute differences computed under the Combined impacts scenarios (**a**) and Hydropower scenarios (**b**). Changes are calculated using cumulative capital costs (United States dollar – USD) in the 2020 – 2100 period and are relative to the No-Climate impacts scenarios (i.e., positive values mean that scenarios with climate impacts on renewables show increased costs). Full range of estimated costs: USD -48 to +54 billion.

On average, cumulative total capital investment needs in LAC over the 2020–2100 period increase by approximately USD 12–114 billion compared to the No-Climate impacts scenarios (Table 3.2). Putting these results into context, the highest

figure is comparable to LAC's investments in RE accumulated between 2007 and 2015 (of about USD 119 billion), whereas the lowest estimates compare with investments in 2014 or 2015, on the order of USD 15–16 billion (IRENA 2016). Although these additional investments seem small, they could imply significant challenges for the developing economies in LAC, where resources for public investments are scarcer, and private financing costs (closely linked to perceptions of the quality of institutions and associated investment risks (IRENA 2016; Iyer et al. 2015a)) are generally higher compared to the developed world. Among individual subregions, S. Am. (S) stands out with the highest additional investments (of about USD 7–54 billion) in the RCP26 cases. In contrast, investments decrease by USD -0.2 to -5.6 billion in Argentina, Mexico (in the Baseline and FullTech technology cases), and Uruguay.

Table 3.2 Regionally aggregated changes in total capital investments in the LAC electric power sector under the Combined impacts scenarios. Changes represent the mean value (absolute and percentage) across GCMs (the standard deviation of the absolute model mean change is also shown), and calculated using cumulative investments in the 2020 ─ 2100 period. Changes are relative to the No-Climate impacts scenarios (i.e., positive values mean that scenarios with climate impacts on renewables show increased costs).

Region	RCP60_Baseline			RCP26_FullTech			RCP26_NoCCS & NoNewNuc		
	2100			2100			2100		
	Mean ($Bill.)	Mean (%)	Std. ($Bill.)	Mean ($Bill.)	Mean (%)	Std. ($Bill.)	Mean ($Bill.)	Mean (%)	Std. ($Bill.)
Brazil	3.72	0.42	15.54	5.32	0.30	17.84	10.76	0.48	58.74
Central America and Caribbean (C. Am/Car.)	3.75	0.52	2.50	3.93	0.33	11.83	23.65	1.51	45.97
Mexico	-0.81	-0.11	3.71	-3.52	-0.25	16.94	3.28	0.21	17.71
South America_Northern (S. Am. (N))	8.71	2.59	22.98	7.07	1.22	13.54	14.09	1.99	17.55
South America_Southern (S. Am. (S))	0.37	0.07	4.12	6.94	0.88	2.51	54.37	6.11	9.92
Argentina	-3.65	-1.22	1.78	-3.45	-0.53	1.24	-5.55	-0.54	0.66
Colombia	0.48	0.19	1.49	1.28	0.25	1.61	15.13	2.05	5.87
Uruguay	-0.20	-0.34	0.47	-0.75	-0.85	0.71	-1.45	-1.35	0.48
LAC	12.38	0.33	46.91	16.82	0.24	37.49	114.30	1.28	129.76

A breakdown of these total differences by generating source highlights the role of hydropower and wind in altering the net balance of capital investments across LAC (Figure 3.8). The regional differences in investments largely reflect the changes to the electricity technology mix shown in Figure 3.4. Under the RCP26 Combined impacts scenarios, investments in hydropower and wind-based generating capacity increase in LAC until the end-of-century (greatly influenced by the largest magnitudes of changes in Brazil and S. Am. (S)), while solar- and CCS-based generating capacity lose investments. Nevertheless, important regional variations exist as subregions such as C.

Am/Car. and Colombia need to bring solar capacity on line. In the RCP60_Baseline: Combined impacts scenario, the net regional investment in hydropower decreases due to the projected negative climate effects on hydropower in many subregions. In this case, the regional increase in total investments is influenced by a net growth in investments in solar energy.

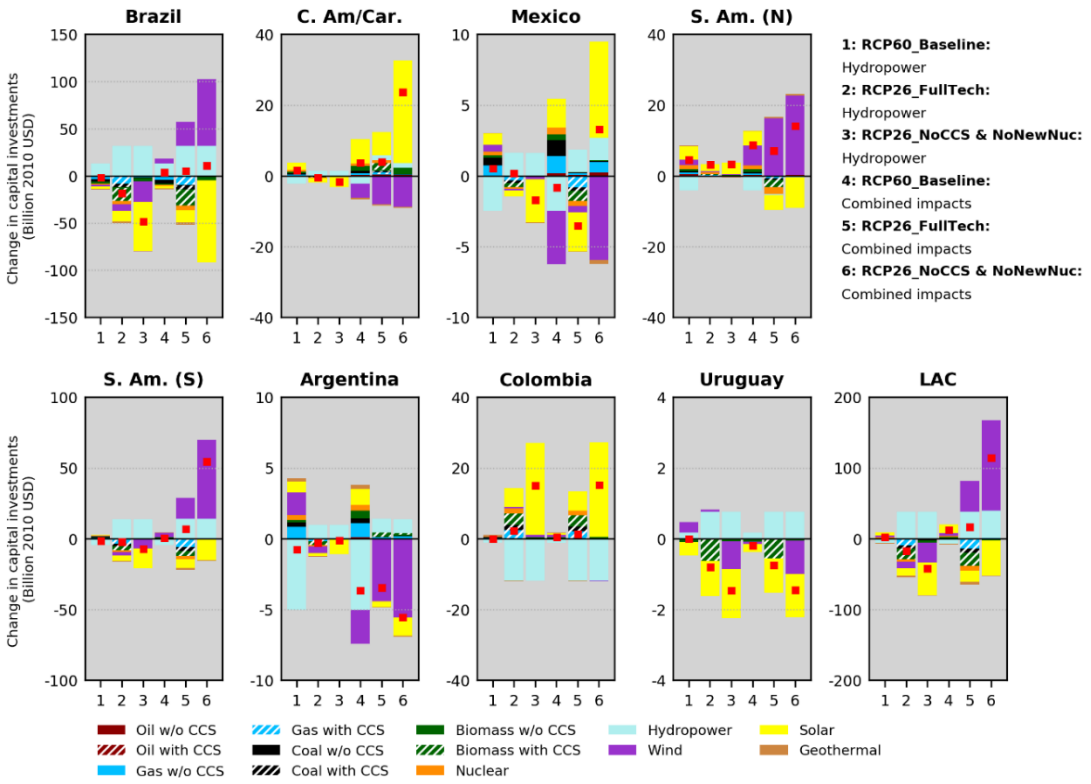

Fig. 3.8 Model mean differences in capital investments by technology in LAC assuming climate change impacts on renewables. Differences are calculated by technology using cumulative investments (USD) in the 2020 – 2100 period. Differences are relative to the No-Climate impacts scenarios (i.e., positive values mean that scenarios with climate impacts show increased costs). The red squares indicate the net of the positive and negative changes for a given scenario (and are equal to the total investment changes plotted in Figure 3.7). Note the different y axis scales.

Figures 3.7 and 3.8 also illustrate marked differences in capital investments when only climate impacts on hydropower are accounted for. In many regions, such differences translate into underestimated investment needs, which are more

pronounced in the RCP26_NoCCS & NoNewNuc case and in Brazil and S. Am. (S.). In these regions, cumulative 2020-2100 capital investment differences in the RCP26_NoCCS & NoNewNuc: Hydropower scenario are approximately USD 60 billion lower than in the RCP26_NoCCS & NoNewNuc: Combined impacts case. Exceptions are Argentina, where reductions in total capital investments in the RCP26 Combined impacts scenarios are considerably larger than in the Hydropower scenarios due to lower wind capacity requirements, and Colombia and Uruguay, where total investment requirements are consistent in both RCP26 climate-impact scenarios because climate impacts on non-hydropower renewables do not play important roles (recall Figure 3.4). Under the RCP60_Baseline scenarios, there are also examples in which the Hydropower case do not show lower investment requirements relative to the Combined impacts case – Mexico and Argentina. However, investment estimates in these subregions under the distinct climate-impact modeling approaches differ markedly.

Although it could be expected that the RCP60_Baseline: Combined impacts scenario would yield considerably larger needs of capital investments in face of more severe climate impacts, it is found that investment changes under the RCP60_Baseline: Combined impacts scenario are predominantly lower than or close to those in the RCP26_FullTech: Combined impacts case (Figure 3.8 and Table 3.2). One key aspect is the overall low reliance of the Baseline pathways on RE as pointed out earlier. Under the RCP60_Baseline scenarios, no cost penalties are imposed for emitting fossil fuels, meaning that it is economically attractive to compensate part of renewable-based generation losses by fossil fuels without CCS, typically less capital-intensive than low-

carbon options. This dynamic is more evident in Argentina and Mexico. These results then emphasize the role of the energy technology strategy in shaping the overall power-sector vulnerability to climate impacts on RE.

It is important to recognize that the investment implications estimated in this analysis are inherently uncertain due to a wide range of outcomes from individual GCM-derived impacts (Figures 3.9–3.10). This wide range relates to the substantial uncertainties in GCM projections of variables such as precipitation, winds and shortwave solar radiation used to force the impact models employed herein. For this reason, uncertainties are high for all technology cases although the NoCCS & NoNewNuc exhibits, for most subregions, the greatest magnitudes of standard deviations associated with the more pronounced mean impacts in this scenario (Table 3.2). Overall, mean impacts estimated for Brazil, C. Am/Car., Mexico and S. Am. (N.) are associated with the largest spread of model outcomes (Figures 3.9–3.10).

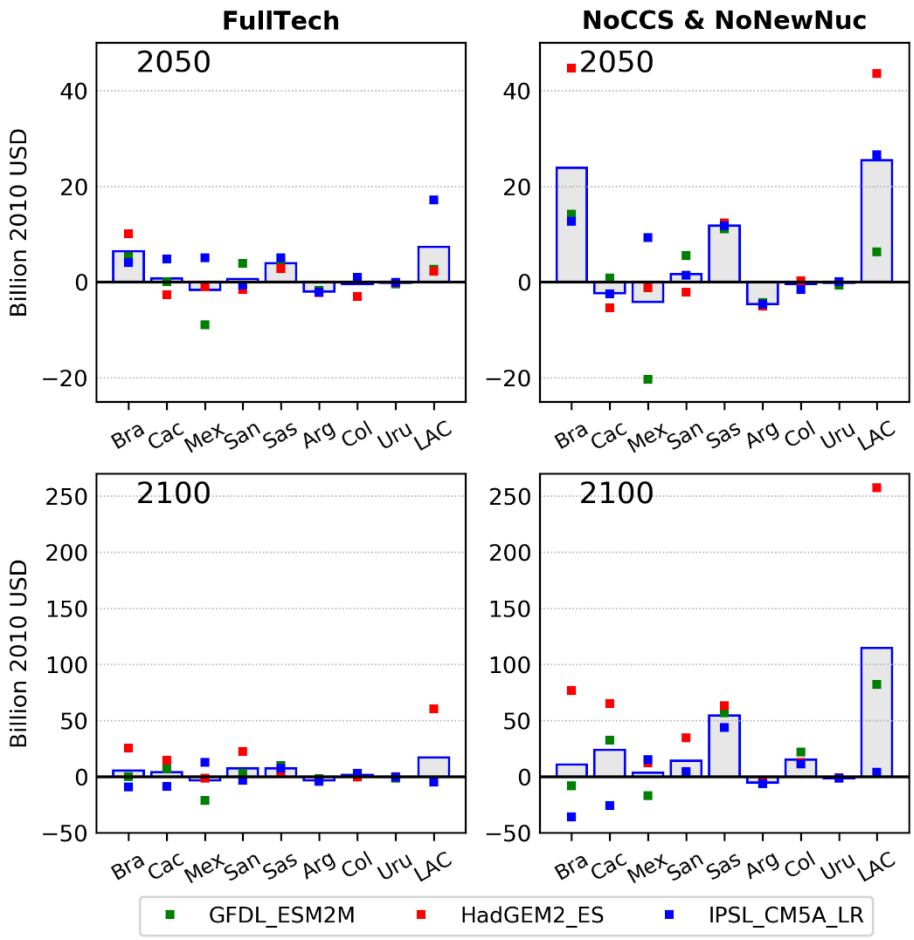

Figure 3.9. Differences in total capital investments in LAC per technology scenario and GCM assuming climate change impacts on all renewables. Changes are calculated using cumulative capital investments in the 2020 ─ 2050 (top) and 2020 ─ 2100 (bottom) periods. Changes are relative to the *No-climate impacts* simulations (i.e., positive values mean that scenarios with climate impacts on renewables show incremental costs). GCAM LAC regions covered: Brazil (Bra), Central America and the Caribbean (Cac), Mexico (Mex), South America_Northern (San), South America_Southern (Sas), Argentina (Arg), Colombia (Col) and Uruguay (Uru).

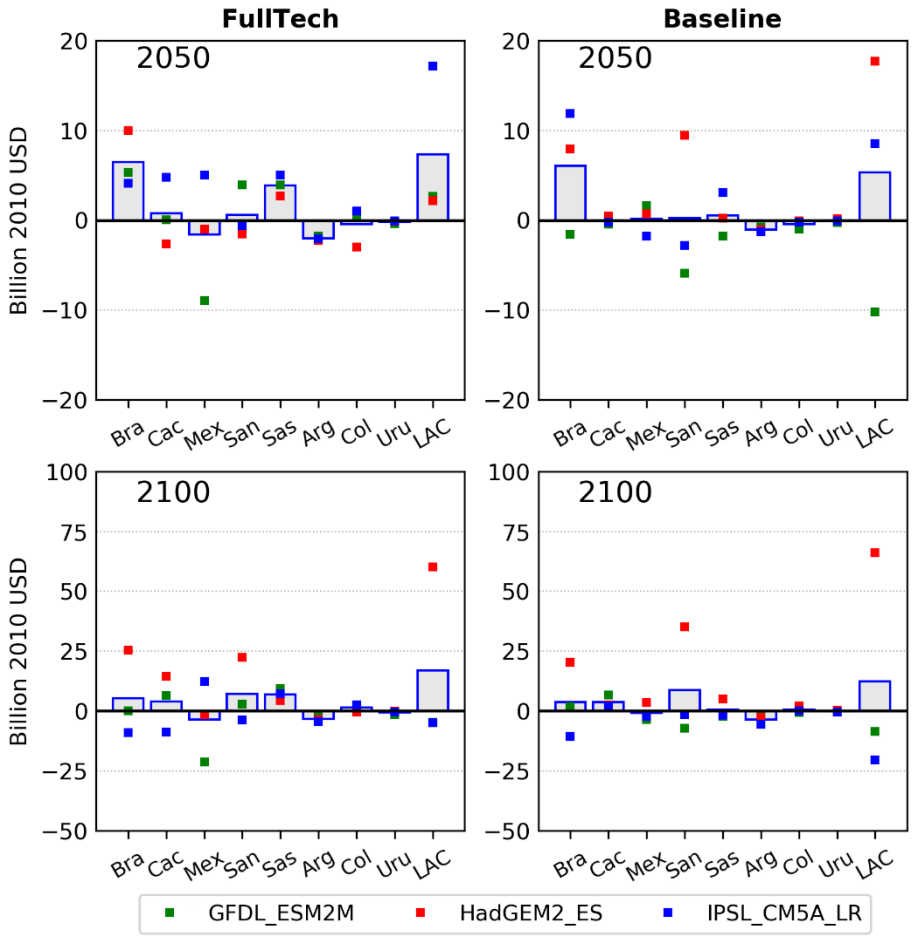

Figure 3.10. As in Figure 3.9 but comparing the *RCP26_FullTech: Combined impacts* and the *RCP60_Baseline: Combined impacts* scenarios. To improve visibility, the y axis scales do not match those presented in Figure 3.9.

Although the ensemble of three climate runs is insufficient to cover the full range of uncertainties across GCMs, it provides initial estimates of overall bounds of economic impacts each region might experience. Importantly, larger confidence is found on investment projections for S. Am. (S), Argentina, Colombia and Uruguay, particularly under the RCP26 cases, reflected in lower standard deviations (relative to their means) than in other subregions (Table 3.2) and agreement on the direction of the investment impact (Figures 3.9–3.10). Future research should employ a larger

ensemble of models to improve overall confidence on the projected changes. Nonetheless, even employing considerably larger ensembles than the one used here, prior studies (Carvajal et al. 2017; Turner et al. 2017) have highlighted the significant decision-making challenge arising from a large spread of individual model outcomes. To improve the resilience of energy systems in light of the large uncertainty in future climate projections, there are arguments supporting "uncertainty-management" methods (Hallegatte 2009) like adaptation strategies that are valid under alternative future outcomes, diversify generation sources and consider a more decentralized small-scale energy structure (Ebinger; Vergara 2011; Hallegatte 2009; Kundzewicz et al. 2018; Miara et al. 2019).

3.6 Discussion and conclusions

The findings of this study underscore the value of a comprehensive analysis of the implications of climate impacts on RE in IAMs so that their aggregate effect on the energy sector can be better understood. This is important because reductions in total power generation due to climate impacts on one RE source may be alleviated or offset by positive impacts on other sources, or simultaneous negative effects in distinct renewables can amplify total generation losses. GCAM results highlight regionally differentiated impacts across LAC power grids due to a combination of vulnerabilities specific to each generation mix and large spatial variability of climate change impacts across LAC. The first component is explored through distinct technology pathways, showing that the generation portfolio plays an important role in alleviating or exacerbating increasing pressure on capital investments due to climate-attributable effects on renewables. Since each energy technology pathway affects the availability

of technology replacement options (each of them characterized by specific costs of installing generating capacity), implications for total capital investments differ markedly.

The key overarching insight from all scenarios explored herein is the risk of misrepresentation of climate change effects on the electric power sector if climate impacts on all renewables are not accounted for. This is particularly evident for the energy pathway with the most pronounced intermittent renewables deployment (i.e., the NoCCS & NoNewNuc), characterized by greatly underestimated capital investment requirements across most of the LAC region when climate impacts only on hydropower are considered. Such an underestimation may result in enhanced power-sector vulnerabilities to climate change.

Given the framework of high deployment of intermittent renewables explored through the mitigation scenarios, accounting for climate impacts on wind in certain LAC subregions was shown to be as relevant as accounting for impacts on hydropower in terms of implications for electricity production. The results also highlighted an overlooked angle related to the fact that climate impacts on wind at the 2^{o}C warming level can positively affect power production in certain LAC subregions (Brazil, S. Am. (N) and S. Am. (S)). This emerges as a strategic opportunity for decarbonization and diversification of regional power mixes. However, the high upfront capital expenditures of wind technologies (and of renewables in general) represent a critical financial barrier to RE deployment, particularly in developing economies, requiring specific policies to create favorable financing conditions (IPCC 2012; IRENA 2016).

The growing trends in LAC's power-sector capital investment requirements reported under multiple RE impacts and technology configurations suggest challenges for the planning of low-carbon capacity additions. On the one hand, a mitigation pathway based on a diversified mix of generating technologies with sizable contributions from fossil-fueled plants with CCS, as illustrated by the RCP26_FullTech scenario, reduces the exposure of the power system to climate impacts on renewables, and may alleviate (or avoid) the necessity of raising investments. However, CCS technologies are not mature, nor have they been widely deployed commercially yet. On the other hand, decarbonizing LAC's power sector largely through climate-sensitive solar and wind technologies may increase risks of higher capital investment requirements, as shown in Table 3.2 for most LAC regions under the RCP26_NoCCS & NoNewNuc: Combined impacts scenario. These larger increases relate to the lower capacity factors of intermittent renewables compared with fossil fuels with CCS technologies deployed in RCP26_FullTech: Combined impacts scenario. This means that intermittent renewables require more generating capacity per unit of electricity produced compared with fossil-fuel technologies with CCS (The Subsection 3.3.3 in Methods shows how capacity factors are used to compute capital investments in this study). Although the value of diversifying the energy portfolio has been recognized as a mean to achieve climate resilient power systems (Ebinger; Vergara 2011), it is crucial that energy planners identify strategies that do not jeopardize climate goals. In this regards, a mixture of renewable and non-renewable energy sources, albeit less vulnerable to climate impacts on renewables, can dampen mitigation efforts unless CCS technologies become technically viable and cost-competitive and/or

comprehensive emissions reductions actions are implemented. Regarding the latter, one alternative might be to focus more heavily on reducing emissions from land and agricultural systems and on enhancing terrestrial sinks for carbon in future decades. This is particularly relevant in LAC where land-related GHG emissions make up a significant share of total emissions (Calvin et al. 2016).

This analysis is the first to assess the potential implications of climate change impacts on the RE supply for power sector investments in LAC, although the methodology can be used to conduct similar analyses for other regions across the globe. Future studies could also benefit from considering the implications of multiple uncertain factors. One critical aspect noted earlier is the uncertainty originating from the GCMs variables. In addition, hydrological and agricultural yields change assumptions are derived from one impact model each (Methods), however, the structure and parameterization of impacts models are known to be a significant source of uncertainty that can rival that of climate models (Rosenzweig et al. 2014; van Vliet et al. 2016b). Another point to note is that the results are focused on aggregated country and regional levels. However, climate change may have distinct and more pronounced effects on smaller sub-national scales. One example is hydropower as climate impacts on runoff patterns are expected to be manifested differently depending on the river basins and sub-basins considered (Ruffato-Ferreira et al. 2017). Hence, further research is needed to develop a finer-resolution multi-impact integrated framework that supports decision-making at sub-national scales. For example, Khan et al. 2020 contribute to fill such a gap by coupling GCAM and a suite of modeling tools to downscale GCAM projections (part of them including climate impacts on hydropower and agricultural

crop yields) onto a grid. This framework was used for a multi-sector assessment of planned policies in Uruguay at a sub-basin scale. Given the possibility of misrepresentation of climate change effects on the power sector highlighted in the results, future high-resolution integrated assessments can benefit from a more comprehensive representation of climate change impacts like the one introduced in this study.

An important caveat of this analysis is that the version of GCAM used in this study represents electricity supply and demand on an annual mean basis assuming, for example, fixed exogenously-defined capacity factors for each power generation technology. Thus, the variability of electricity demand and load at seasonal and daily temporal scales is not considered, which has important implications for decisions on generation infrastructure. The challenge of continuously balancing supply and demand at such finer temporal scales becomes even more complex as the deployment of intermittent solar- and wind-based generation with limited dispatchability increases. Consequently, this analysis likely underestimates rates of capacity additions through 2100 because the annual average supply and demand electricity representation of GCAM smooths out short-term events of peak demand that require the highest electricity outputs. In light of this, the estimates of generation capacity and capital investments should be interpreted as a first-order approximation of the magnitudes of future needs that can be refined by follow-on studies. In this regard, there are ongoing efforts involving GCAM and other IAM groups to improve sub-annual details in power sector representation in IAMs (Pietzcker et al. 2017; Wise et al. 2019). Another consequence of its annual average electricity representation alongside simplifications

of important processes is that GCAM cannot represent climate impacts at short timescales (e.g., seasonal scales). These characteristics also impose challenges for the representation of changes in climate variability and short-term extreme events within IAM frameworks. Hence, this study focuses on implications due to long-term (multi-decadal) mean climatological changes. Future investigation is needed to enhance GCAM modeling capabilities towards finer temporal scales and more detailed representations of power system dynamics. Notwithstanding the limitations above, this study constitutes an additional step toward a more holistic integrated assessment of the potential effects of climate change on the energy sector.

Chapter 4: The role of uncertain renewable resource potentials in solar and wind electricity projections: implications for the GCAM integrated assessment model (Santos da Silva et al., *in prep*)

4.1 Abstract

Integrated Assessment Models (IAMs) are key analytical tools used to project the potential future evolution of the power sector globally, including wind and solar power. To do so, IAMs rely on resource cost-supply curves, which are derived from global assessments of renewable energy potentials. However, estimates of global energy potentials are characterized by large uncertainties stemming from methodological assumptions. Based on a review of parameter values used in prior renewable potentials estimations, this study addresses the implications of these uncertain assumptions for solar and wind electricity projections from a global IAM for the first time. It is found that this parametric uncertainty results in substantial variations in intermittent generation projections, with a prominent role of assumptions related to land-use in both technologies and average turbine installation density for wind onshore. Consequently, the role of these renewables in modeled long-term scenarios can be under- or overestimated relative to other technologies. Some potential implications are highlighted for decision-making on energy planning, climate change mitigation strategies and the adaptation efforts to climate impacts on these renewables. This study underscores the need of further coordination among the integrated assessment modeling community to narrow these uncertainties.

4.2 Introduction

Integrated assessment models (IAMs), such as the Global Change Analysis Model (GCAM) (Calvin et al. 2019), have a long tradition of contributions to the analysis of energy-sector climate change mitigation pathways. These models have contributed, for example, to delineate the important role of renewable energy (RE) in deep decarbonization pathways that can achieve the 2.0^{o}C and 1.5^{o}C climate targets (Clarke et al. 2014; IPCC 2012; Rogelj et al. 2015). However, concerns regarding future vulnerability of RE production to climate change have encouraged more recent IAM development to focus on the modeling of climate impacts on RE to better support energy-sector decision-making.

To represent the physical effects of climate change on RE in IAMs, modelers have employed projections from detailed process-based models (e.g., hydrologic models, crop models, general circulation models (GCMs)) to modify key IAM parameters linked to RE production. Such efforts have focused primarily on impacts on hydropower (Arango-Aramburo et al. 2019; Carvajal et al. 2019; Lucena et al. 2018; Turner et al. 2017) and on the agriculture sector (which affect the biomass potential) (Kyle et al. 2014; Nelson et al. 2014; Ren et al. 2018; Snyder et al. 2019), with virtually no attention to climate impacts on solar and wind, except for one study (Dowling 2013). This panorama is changing. A recent coordinated effort, the 'ISIpedia-energy protocol' (Yalew et al. 2020), proposed an assessment of climate impacts on all renewables at macro-regional to global scales. In the ISIpedia model inter-comparison, participating IAMs implemented a protocol of harmonized scenarios based on climate change input data from the Inter-Sectoral Impact Model Inter-Comparison Project (ISIMIP)

(Warszawski et al. 2014). To allow the representation of climate impacts on solar and wind sources, the ISIpedia project built gridded global estimates of solar and wind energy potentials based on methods recently published (Gernaat et al. 2021). Using this dataset, participating modeling groups were asked to build and implement into models resource supply-cost curves (hereafter referred to as 'supply curves' for simplicity) with the goal of estimating climate change effects on the energy sector. It is worth mentioning that supply curves are essential assumptions within the economic framework of IAMs because they map renewable resource availability at a given energy production cost. As discussed in Chapter 3, these curves affect decision-making on power-sector technologies that are deployed in GCAM.

While the method adopted by the ISIpedia project constitutes a clear advance toward the modeling of climate impacts on solar and wind sources in IAMs, its computation of renewable potentials is based on a fixed pool of assumptions. This means that the uncertainty created by the various assumptions on key parameters used in the computation of renewable potentials remains unaccounted for. Resource potential estimates are hindered by various uncertain assumptions that include, for example, the role of land use, which substantially affects the computed energy potentials. This research calculates global solar and wind technical potentials with the main goal of investigating the impact of their associated parametric uncertainties on solar and wind electricity projections from GCAM, a state-of-the art global IAM linking energy, land, water, climate and economic systems. Although some prior studies (de Vries et al. 2007; Hoogwijk 2004; Rinne et al. 2018; Zhou et al. 2012) have examined the effect of assumptions on specific parameters when computing solar or

wind potentials, no past study has investigated their consequent implications for electricity generation projections from an IAM. Given the role of IAM scenarios in major climate assessments (e.g., the Intergovernmental Panel on Climate Change (IPCC)'s Fifth Assessment Report), it is critically important that the impact of these uncertainties be understood for the construction of credible scenarios.

The analysis is divided into three main sections. First, a literature review is conducted to define a set of 'baseline' or 'central' assumptions and key 'sensitivity' cases (i.e., deviations from the central assumptions) for the computation of onshore wind and solar PV technical potentials. Following the methodology proposed by the ISIpedia intercomparison, these assumptions are then used to calculate historical (defined here as the 1971-2000 period) and future projections of wind and solar technical potentials using input data from the ISIMIP2b GCMs. Finally, supply curves representative of the historical and future periods are built from the central and sensitivity technical potential cases for implementation in GCAM to evaluate implications for wind and solar deployments.

It is important to stress that a formal sensitivity analysis is not conducted here, but rather a first-order assessment that aims at contributing to improvements on the representation of solar and wind power in IAMs, and to the emerging efforts on the modeling of climate impacts on these sources in these models, in which the role of parametric uncertainties in renewable potentials quantification is currently unknown. However, for the sake of simplicity, the term 'sensitivity' is used throughout the text to refer to the various cases in which distinct assumptions on parameter values are tested. These cases are detailed in the Methods section.

As stated above, the novelty of this study is the consideration of the effects of the uncertain estimates of renewable energy potentials embedded in supply curves on wind and solar electricity generation projections from GCAM. In this regard, the specific research questions that motivate this study are: *What are the implication of key parametric uncertainties in the computation of renewable energy potentials for GCAM solar and wind electricity production? Which parameters drive the largest changes? What are the potential implications for decision-making on climate change mitigation and impacts?*

4.3 Background on renewable energy potentials

A number of studies have computed intermittent renewable energy potentials using a common approach that assesses the so-called theoretical, geographical, technical and economic potentials (Bosch et al. 2017; Dupont et al. 2020; Eurek et al. 2017; Gernaat et al. 2021; Hoogwijk 2004; Hoogwijk et al. 2004; Köberle et al. 2015; Rinne et al. 2018; Zhou et al. 2012).

While the theoretical potential is the upper bound of the natural resource availability in any area, the geographical potential explicitly accounts for land use restrictions to identify suitable locations for large-scale renewable electricity generation. Such areas typically include low productivity agricultural and/or pasture land, arid terrain, grasslands and scrublands, while forest and other sensitive ecosystem are deemed unlikely for RE deployment. Other inviable sites include remote high-elevated terrains, urban development, and areas of poor-quality resources. In many studies, the geographical potential at the grid cell level is determined by (1) applying exclusion criteria to remove unsuitable grid cells, and (2) assigning suitability factors

(0 – 1 range; 0 – totally unavailable/unsuitable grid cell; 1 – grid cell area is 100% available) to the non-excluded grid cells based on a land-use and cover map. Next, technical potential is assessed by accounting for factors such as limitations on the conversion from primary to secondary energy and overall losses due to technical and/or operational factors. An example of this constraint is solar energy, in which modern solar photovoltaic (PV) cells can only convert around 20% of the incoming solar radiation into electricity (Gernaat et al. 2021). Finally, the production costs of electricity need to be estimated (based on the total cost for building and operating power plants as well as financing costs), given that renewables must compete for a portion of regional energy markets with other sources. This means that only part of the technical potential can be cost-competitive depending on production costs, which defines the economic potential.

4.4 Methods

4.4.1 Experimental Design

Figure 4.1 summarizes the overall approach and workflow implemented to answer the research questions posed in the Introduction section. Specifically, this work has:

a) built a framework to assess the global wind onshore and solar PV technical potentials based on methods used in prior studies;
b) surveyed the literature to define assumptions for the parameter values (central and sensitivity cases) to be used in the computation of the renewable potentials;

c) used the framework built in (a) to compute renewable potentials for the varying assumptions defined in (b);

d) produced supply curves for all renewable energy potential estimates (wind onshore and solar PV) produced in (c); and

e) implemented the supply curves produced in (d) into GCAM v5.3 to conduct simulations for each supply curve assumption individually.

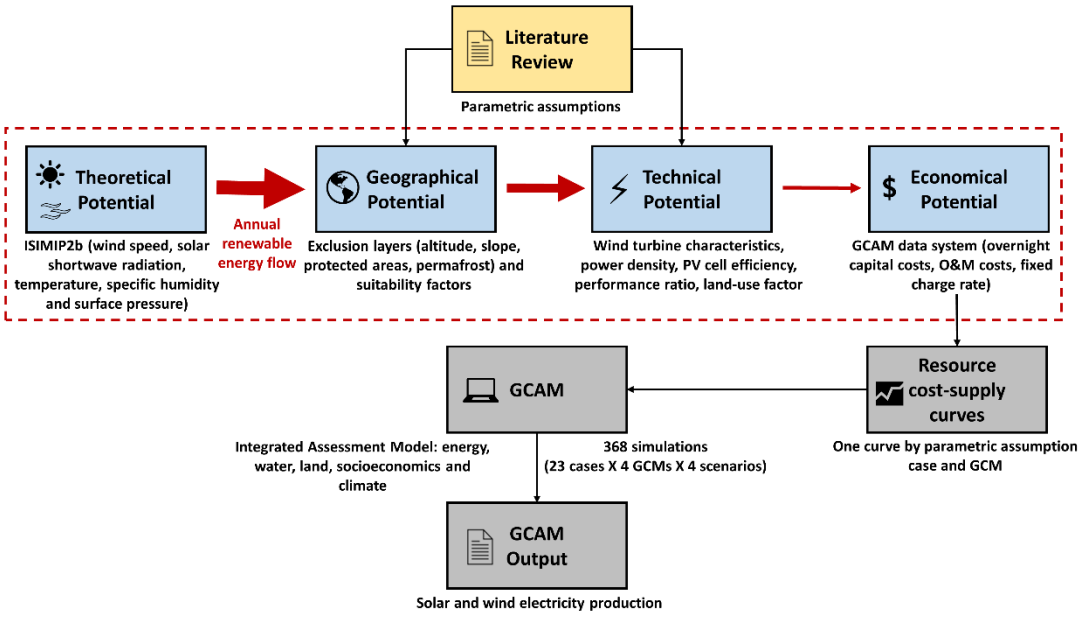

Figure 4.1. Experimental design implemented in this study. Note that the red arrows represent the theoretical upper bound of renewable energy availability (theoretical potential), which is reduced in each step of the calculation of the potentials until the technical potential is estimated.

Details on each step of the method will be provided throughout the following subsections. Note that when describing the equations to compute the technical potentials in subsections 4.4.4 (wind onshore) and 4.4.5 (solar PV), all parameter values provided refer to the central assumptions (labeled *Central* hereafter). The assumptions for all sensitivity cases will be provided later on in subsection 4.4.7, except for the land

suitability factors, which are listed in subsection 4.4.3. The parameter values for the *Central* case are taken exactly as listed in the references that provide the equations to compute the technical potentials. Hence, they are not necessarily the mid-range values across the literature, but rather a benchmark for comparisons with all sensitivity cases analyzed. Tables 4.1-4.2 show that the resource estimates computed under the *Central* case are within the range of results obtained by prior global studies. But above all, these tables highlight the role of methodological aspects in producing uncertainty in resource estimates as shown by the wide range of results. Note that the solar PV technology that this study focuses on refers to utility-scale systems, i.e., large-scale power plants, which are modeled separately from the smaller distributed rooftop PV systems in GCAM. Next, the methodology employed in this study is presented in detail.

Table 4.1 Comparison of results of this study with other analyses (global wind onshore).

Reference	Data Source	Spatial Resolution	Period	Technical Potential (PWh/y)
Bosch et al. 2017	NASA's Modern-Era Retrospective analysis for Research and Applications, version 2 (MERRA-2) and the DTU Global Wind Atlas	1 km	1979-2013	587 (excluding areas with capacity factors < 15%)
Deng et al. 2015	Climate Research Unit (CL2.0) Database	1 km	2010	7-47[a]
Eurek et al. 2017	NCAR's Climate Four Dimensional Data Assimilation	0.4º	1985-2005	557
Hoogwick et al. 2004	Climate Research Unit Database	0.5º	1960-1990	96
Lu et al. 2009	Goddard Earth Observing System Data Assimilation System (GEOS-5 DAS)	2/3° longitude x 1/2° latitude (~66.7 x 50km at midlatitudes)	2006	(a) 1100; (b) 690 (excluding areas with capacity factors < 20%)
Zhou et al. 2012	Climate Forecast System Reanalysis/NCEP	0.3125°	1980-2009	(a) 120 (at costs below 9 cents/kWh); (b) ~330[b] (no cost cutoff)
This study	ISIMIP2b GCMs	0.5º	1971-2000	447-455

Notes:

[a] Depends on the land availability scenario (low, medium, and high cases). This study also makes estimates for 2030 and 2070 (based on the assumption of improvement in technological parameters) not reported here.

[b] Inferred from Fig. 2 from Zhou et al. 2012.

Table 4.2 Comparison of results of this study with other analyses (global solar PV).

Category	Data Source	Spatial Resolution	Period	Technical Potential (PWh/y)
Deng et al. 2015	NASA Langley Research Center Surface Meteorological and Solar Energy dataset (SSE)	1 km	2010	25-223[a]
Dupont et al. 2020	World Bank Group ESMAP. Global Solar Atlas	0.1°	Not explicitly stated	1194
Hoogwick 2004	Climate Research Unit Database	0.5°	1960-1990	366
Koberle et al. 2015	NASA Langley Research Center Surface Meteorological and Solar Energy dataset (SSE – Release 6.0)	0.5°	1983-2005	101
Korfiati et al. 2016	NASA Langley Research Center Surface Meteorological and Solar Energy dataset (SSE – Release 6.0)	1 km	Not explicitly stated	613
This study	ISIMIP2b GCMs	0.5°	1971-2000	205-208

Notes:

[a] Depends on the land availability scenario (low, medium, and high cases). This study also makes estimates for 2030 and 2070 (based on the assumption of improvement in technological parameters) not reported here.

4.4.2 Datasets

Tables 4.3-4.4 describe the climate input data (which provides the spatiotemporal distribution of the theoretical potential) and datasets utilized for the assessment of the geographical potential, respectively.

Table 4.3 Overview of the climate model data used in the analysis.

Climate model data	Bias-corrected projections from ISIMIP 2b (Frieler et al. 2017)
GCMs	GFDL-ESM2M, HadGEM2-ES, IPSL-CM5A-LR, and MIROC5
Climate scenarios	RCP2.6 and RCP8.5
Climate data spatial resolution	0.5° × 0.5°
Climate variables utilized (short name | units)	Near-surface specific humidity (HUSS | $kgkg^{-1}$) Surface pressure (PS | Pa) Surface-downwelling shortwave radiation (RSDS | Wm^{-2}) Near-surface wind speed (SFCWIND | ms^{-1}) Near-surface air temperature (TAS | K)
Data availability	Publicly available at: https://esg-pik-postdam.de/search/isimip

Table 4.4 Datasets used for the assessment of the geographical potential[a]

Category	**Dataset and reference**	**Dataset resolution**
Elevation	EarthEnv (Amatulli et al. 2018)	25 arc-minute (~50 km)
Land use/land cover	GlobCover 2009 (Bontemps et al. 2011)	30 arc-seconds (~1km)
Permafrost	Global Permafrost Zonation Index Map (Gruber 2012)	30 arc-seconds (~1km)
Protected areas	World Database on Protected Areas (WDPA) (UNEP-WCMC 2019)	Variable[b]: geodatabase comprising two classes of spatial data: polygons (distinct sizes) delineating boundaries and data points (point location and an area)
Slope	EarthEnv (Amatulli et al. 2018)	25 arc-minute (~50 km)

Notes:
[a] All geospatial fields were regridded onto a common 0.5° by 0.5° grid in order to match the grid spatial resolution of the input climate data.
[b] Dataset was converted to a raster (rows and columns of cells) with 0.5° × 0.5° spatial resolution.

4.4.3 Geographical Potential

Using the datasets listed in Table 4.4 and the exclusion criteria summarized in Table 4.5, terrain deemed unsuitable for a given technology is excluded. Next, the remaining grid cells receive suitability factors (Tables 4.6-4.7) based on their land cover types. This approach is formalized in Eq. (1), in which the geographical potential represents the suitable area available for RE production (A) within any grid cell i

(Hoogwijk 2004). Figures 4.2-4.3 show the suitability maps by technology resulting from the geographical constraints applied.

$$A_i = f_i \cdot a_i \quad (1)$$

where a_i is the grid cell area (Km^2) and f_i is the suitability factor in cell i.

Table 4.5 Summary of geographic exclusion criteria (based on the references listed).

Category	**Criteria: onshore wind (Eurek et al. 2017)**	**Criteria: solar PV (Deng et al. 2015; Gernaat et al. 2021)**	**Criteria: solar CSP[a] (Deng et al. 2015; Gernaat et al. 2021)**
Elevation	100% exclusion for areas with elevation greater than 2500 m.	No constraint applied.	No constraint applied.
Land use/land cover	100% and partial exclusions based on suitability factors (Table 4.6).	100% and partial exclusions based on suitability factors (Table 4.7).	100% and partial exclusions based on suitability factors (Table 4.7).
Permafrost	100% exclusion for areas classified as permafrost.	No constraint applied.	No constraint applied.
Protected areas[b]	100% exclusion for protected areas with International Union for the Conservation of Nature (IUCN) rankings codes of: I (Strict Nature Reserve and Wilderness area); II (National Park), and III (Natural Monument or feature).	100% exclusion for protected areas with International Union for the Conservation of Nature (IUCN) rankings codes of: I (Strict Nature Reserve and Wilderness area); II (National Park), and III (Natural Monument or feature).	100% exclusion for protected areas with International Union for the Conservation of Nature (IUCN) rankings codes of: I (Strict Nature Reserve and Wilderness area); II (National Park), and III (Natural Monument or feature).
Slope	100% exclusion for areas with average slope greater than 20%.	100% exclusion for areas with average slope greater than 27%.	100% exclusion for areas with average slope greater than 4%.

Notes:

[a] Assumptions for the solar CSP technology will be discussed in subsection 4.4.9.

[b] All technologies are assumed to follow the same exclusion criteria as in Eurek et al 2017.

Table 4.6 Suitability factors by sensitivity case (wind onshore) applied to the land cover map categories.

Land cover category (GlobCover dataset)	Suitability factors by sensitivity case[a]			
	Central[b]	S_low[c]	S_low_II[d]	S_high[e]
Post-flooding or irrigated croplands (or aquatic)	0	0	0	0
Rainfed croplands	70%	60%	3%	100%
Mosaic cropland (50-70%) / vegetation (grassland/shrubland/forest) (20-50%)	70%	60%	3%	100%
Mosaic vegetation (grassland/shrubland/forest) (50-70%) / cropland (20-50%)	70%	60%	3%	100%
Closed to open (>15%) broadleaved evergreen or semi-deciduous forest (>5m)	10%	0	0.5%	0
Closed (>40%) broadleaved deciduous forest (>5m)	10%	0	0.5%	0
Open (15-40%) broadleaved deciduous forest/woodland (>5m)	10%	0	0.5%	0
Closed (>40%) needleleaved evergreen forest (>5m)	10%	0	0.5%	0
Open (15-40%) needleleaved deciduous or evergreen forest (>5m)	10%	0	0.5%	0
Closed to open (>15%) mixed broadleaved and needleleaved forest (>5m)	10%	0	0.5%	0
Mosaic forest or shrubland (50-70%) / grassland (20-50%)	50%	10%	3%	100%
Mosaic grassland (50-70%) / forest or shrubland (20-50%)	65%	10%	3%	100%
Closed to open (>15%) (broadleaved or needleleaved, evergreen or deciduous) shrubland (<5m)	50%	20%	3%	100%
Closed to open (>15%) herbaceous vegetation (grassland, savannas or lichens/mosses)	80%	20%	3%	100%
Sparse (<15%) vegetation (woody vegetation, shrubs, grassland)	90%	20%	3%	100%
Bare areas	90%	10%	3%	100%
Urban areas, water bodies, permanent snow and ice	0	0	0	0

[a] The complete list of sensitivity cases analyzed in this study is provided in subsection 4.4.7. This table provides the specific values for the *Central* and sensitivity cases concerning only suitability factors.

Suitability factors based on: [b] Eurek et al. 2017, [c] Zhou et al. 2012 (low case), [d] Deng et al. 2015 (low case) and [e] Lu et al. 2009.

Table 4.7 Suitability factors by sensitivity case (solar PV) applied to the land cover map categories.

Land cover category (GlobCover dataset)	Suitability factors by sensitivity case[a]			
	Central[b]	S_low[c]	S_low_II[d]	S_high[e]
Post-flooding or irrigated croplands (or aquatic)	0	0	0	0
Rainfed croplands	1%	0.1%	0.5%	10%
Mosaic cropland (50-70%) / vegetation (grassland/shrubland/forest) (20-50%)	1%	0.1%	0.5%	5%
Mosaic vegetation (grassland/shrubland/forest) (50-70%) / cropland (20-50%)	1%	0.1%	0.5%	5%
Closed to open (>15%) broadleaved evergreen or semi-deciduous forest (>5m)	0	0	0	0
Closed (>40%) broadleaved deciduous forest (>5m)	0	0	0	0
Open (15-40%) broadleaved deciduous forest/woodland (>5m)	0	0	0	0
Closed (>40%) needleleaved evergreen forest (>5m)	0	0	0	0
Open (15-40%) needleleaved deciduous or evergreen forest (>5m)	0	0	0	0
Closed to open (>15%) mixed broadleaved and needleleaved forest (>5m)	0	0	0	0
Mosaic forest or shrubland (50-70%) / grassland (20-50%)	1%	0.5%	1%	5%
Mosaic grassland (50-70%) / forest or shrubland (20-50%)	1%	0.5%	1%	5%
Closed to open (>15%) (broadleaved or needleleaved, evergreen or deciduous) shrubland (<5m)	1%	0.5%	1%	10%
Closed to open (>15%) herbaceous vegetation (grassland, savannas or lichens/mosses)	1%	0.5%	1%	10%
Sparse (<15%) vegetation (woody vegetation, shrubs, grassland)	1%	0.5%	1%	10%
Bare areas	5%	0.5%	1%	10%
Urban areas, water bodies, permanent snow and ice	0	0	0	0

[a] The complete list of sensitivity cases analyzed in this study is provided in subsection 4.4.7. This table provides the specific values for the *Central* and sensitivity cases concerning only suitability factors.

Suitability factors based on: [b] Gernaat et al. 2021, Hoogwick 2004 and Korfiati et al. 2016, [c] Deng et al. 2015 (low case), [d] Deng et al 2015 (medium case) and [e] Dupont et al. 2020.

Note that this study follows the approach by Gernaat et al. 2021, Hoogwick 2004 and Deng et al. 2015 in the case of solar PV, and by Eurek et al. 2017 and Zhou et al. 2012 in the case of wind onshore and do not exclude any area based on a minimum threshold for resource intensity. However, there are variations in the literature as resource quality cutoffs have been assumed in prior assessments of solar PV potential (Korfiati et al. 2016) and wind potential (Hoogwick et al. 2004).

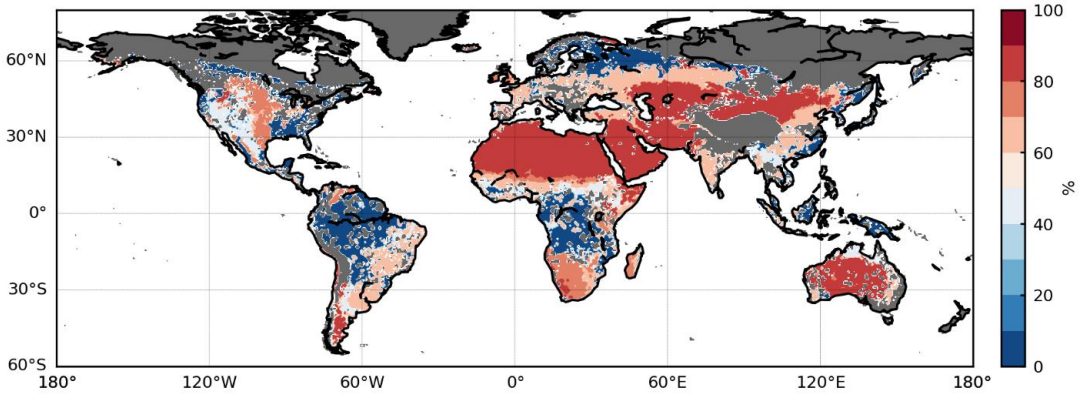

Figure 4.2. Land suitability map (%) for wind turbine deployment using the exclusion criteria in Table 4.5 and suitability factors in Table 4.7 at grid cell level under central assumptions. Gray areas correspond to grid cells that are entirely excluded.

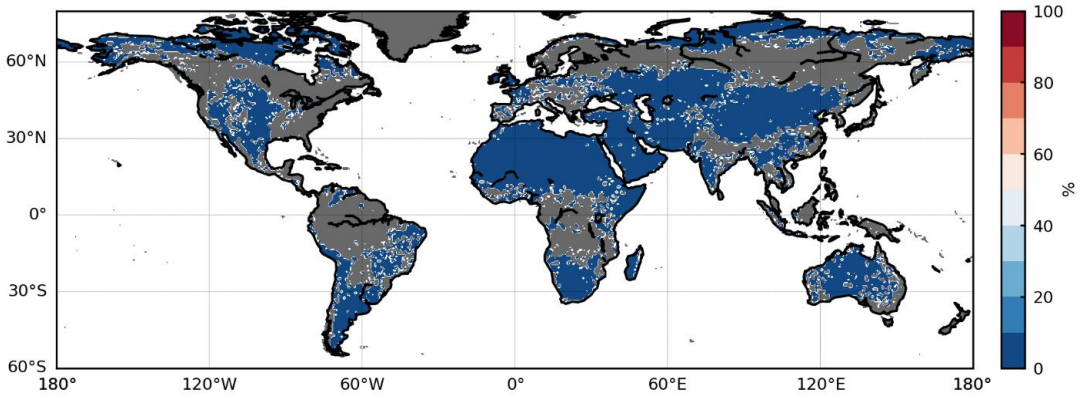

Figure 4.3. Land suitability map (%) for solar PV deployment using the exclusion criteria in Table 4.5 and suitability factors in Table 4.6 at grid cell level under central assumptions. Gray areas correspond to grid cells that are entirely excluded.

4.4.4 Technical Potential – Wind Onshore

The geographical potential computed in the previous subsection (Eq. 1) expresses the suitable area for renewable energy production in grid cell i (A_i). Using this information, the wind onshore technical potential, E_i, in grid cell i (kWh/year) is computed as (Eurek et al. 2017):

$$E_i = A_i \cdot D \cdot h \cdot \left(\frac{\overline{P_i} \cdot \eta_{avail} \cdot \eta_{array}}{P_{rated}} \right), \quad (2)$$

where D is the average wind turbine installation density, namely power density (assumed 5.3 MW Km^{-2}), which depends on the spacing between turbines; $\overline{P_i}$ is the yearly-averaged wind power (MW) in grid cell i (see details below); η_{avail} is the average availability of the wind turbine (assumed 0.95) to account for the fraction of the year in which a turbine is not operating due to maintenance and/or breakdowns; η_{array} is the wind farm array efficiency (assumed 0.90) to account for losses in farm arrays due to the air flow interference on downward turbines known as wake losses; P_{rated} is the turbine rated power (MW), i.e., the maximum power output generated by a turbine model under the optimum range of wind speed values for the model (see Figure 4.4); and h is the number of hours in a year.

The kinetic energy of the wind when intercepted by the blades of a turbine is a well-established function of the wind speed at the rotor height, air density and the area swept by the rotor blades (Eurek et al. 2017; Lu et al. 2009). This relationship is embedded in the power curve of each wind turbine model. In wind potential assessments, wind power is typically computed using the power curve of a representative wind turbine. This same approach is followed here. Table 4.8 summarizes the main steps of the wind power computation method employed, which is followed by the specific equations utilized in such a computation.

Table 4.8 Steps for the computation of wind power.

Step	Justification	Method	Reference
Selection of representative turbine model | Construction of power curve function.	Power curves provide wind power as function of wind speed at the rotor height taking into consideration the specific design and characteristics of each turbine model. Based on the wind power-wind speed data pairs provided by the power curve, a function that returns wind power for any input wind speed can be derived.	Selection of a turbine model and use of its power curve points to build an algorithm that computes wind power as a function of wind speed. For the *Central* case, the selected model is the Vestas V136-3.45 MW with a 125-m hub height (power curve provided in Figure 4.4). These choices represent both a modern technology and the current trend of installations at growing hub heights.	The representative wind turbine model and choice of hub height[a] are based on Rinne et al. 2018. The wind power method is widely used in the literature.
Extrapolation of 10-m wind speed to the rotor height.	Wind speed outputs from GCMs are provided at the 10-m level, however wind power must be computed at the rotor height.	Power law equation.	Karnauskas et al. 2018
Correction of wind speed for air density.	Power curves provided by manufacturers assume standard atmospheric conditions (air density of 1.225 kg/m^3, air temperature of 15 °C and pressure of 1 atmosphere).	Wind speed is scaled for air density based on the ideal gas law, which requires GCM outputs of atmospheric pressure at the station level, surface temperature and specific humidity.	Karnauskas et al. 2018

[a] The hub height refers to the height of the rotor above the ground. This term is also referred to as rotor height.

a) Wind power computation: extrapolation of 10-m wind speed to the rotor height

Following prior studies (Karnauskas et al. 2018; Tobin et al. 2015), the power law is used to extrapolate 10-m wind speeds to the turbine hub height H with W_H as the wind speed (m/s) at the hub height, W_{10} as the wind speed (m/s) at 10 m and α as the power exponent assumed 1/7 (Eq. 3).

$$W_H = W_{10} \cdot \left(\frac{H}{10m}\right)^{\alpha} \quad (3)$$

The empirical power law equation is widely used by the wind industry to extrapolate wind speeds to higher levels. Regarding this method, Tobin et al. 2015 note that the typical power exponent value of 1/7 corresponds to neutral stability conditions and smooth open terrain, and tested an alternative formulation that accounts for spatio-temporal variations of the wind speed. The study concluded that the dynamic coefficients tested have only slightly affected wind power computation.

b) Wind power computation: correction of wind speed for air density

While computing wind power, procedures described by Karnauskas et al. 2018 are followed to adjust wind power for air density. This is necessary given the direct dependence of wind power on air density (which varies largely with the altitude of the site) and the fact that power curves are provided by manufacturers under the assumption of standard atmospheric conditions (air density of 1.225 kg/m^3, air temperature of 15 °C and pressure of 1 atmosphere).

First, dry air density ρ_d (kg/m^3) is calculated using the ideal gas law:

$$\rho_d = \frac{P}{R \cdot T} \quad (4)$$

where P is the surface pressure (Pa), T is the surface air temperature (K) and R = 287.058 J kg^{-1} K^{-1}. Dry air density is used to compute the moist air density ρ_m, which corrects air density for humidity.

$$\rho_m = \rho_d \cdot \frac{1+q}{1+0.609 \cdot q} \tag{5}$$

where q is the specific humidity (kg/kg). Next, the hub height wind speed W_H is corrected for air density using

$$W_{H\_cor} = W_H \cdot \left(\frac{\rho_m}{1.225}\right)^{1/3} \tag{6}$$

Lastly, the turbine power curve is used to derive a function that relates wind power and the corrected hub height wind speed, i.e.,

$$P = f(W_{H\_cor}). \tag{7}$$

Details on how function f was modeled are provided in the Figure 4.4 below. For each grid cell, wind power is computed at the native daily temporal resolution of ISIMIP2b climate data. Daily wind power series are averaged within each year of interest to derive annual means, which are used to estimate the wind technical potential via Eq. 2. This is done because the use of GCM outputs averaged across low temporal frequencies prior to computing wind power have been shown to underestimate wind power values (Karnauskas et al. 2018).

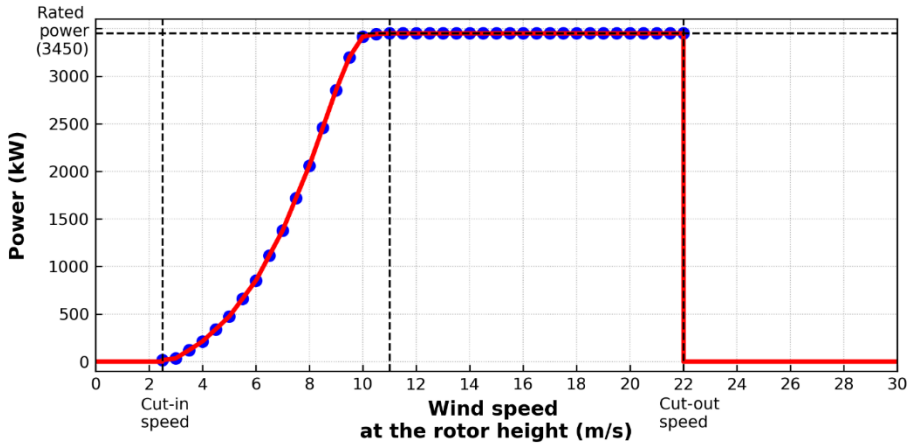

Figure 4.4. Power curve for the wind turbine Vestas V136-3.45 selected as the representative model under *Central* assumptions. Blue dots represent the paired wind speed–power data taken from the power curve. The dashed lines mark specific wind speeds that characterize wind turbine models: the cut-in wind speed (2.5 m s^{-1}), cut-out wind speed (22 m s^{-1}) and rated wind speed (11 m s^{-1}). There is no energy output below the cut-in and above the cut-out wind speed, while the output is maximum (3450 kW – rated power) between the rated wind speed (11 m s^{-1}) and the cut-out wind speed. The red line represents the power curve function used in this study to compute wind power obtained by (1) performing a linear interpolation between the power curve (blue) points, and (2) assigning 0 kW for wind speeds below the cut-in and above the cut-out wind speeds.

4.4.5 Technical Potential – Solar PV

The solar PV technical potential ($E_{PV,i}$) in grid cell *i* (kWh y^{-1}) is computed as (Gernaat et al. 2021; Hoogwijk 2004):

$$E_{PV,i} = 10^3 \cdot \overline{I_i} \cdot A_i \cdot h \cdot \eta_{LPV} \cdot \eta_{PV} \cdot PR \quad (8)$$

where $\overline{I_i}$ is the yearly-averaged solar radiation (W m^{-2}) in grid cell *i*; A_i is the suitable area in cell *i* (Km^2; Eq. 1); h is the number of hours in a year; η_{LPV} is the land use factor (assumed 0.47), which accounts for the fraction of the suitable area actually covered by PV panels since there is spacing between the panels; and PR is the performance ratio of the PV system (assumed 0.85), which expresses the ratio between the actual

output of the system and the performance under standard test conditions (STC) (standardized set of conditions under which solar panels are tested) to account for the overall efficiency losses within any PV system.

The term η_{PV} is the PV panel efficiency, which is affected by atmospheric conditions according to Eq. 9.

$$\eta_{PV} = \eta_{Panel} \cdot (1 + \gamma(T_{cell,i} - T_{STC})) \quad (9)$$

where η_{Panel} is the standard efficiency of a PV panel (assumed 17% – an average value in the market); T_{STC} is the temperature under STC (25°C); and the thermal coefficient γ is taken as −0.005 °C^{-1}, denoting the typical response of the monocrystalline silicon solar panels widely used in the world market today.

The dependence of T_{cell}, the PV cell temperature, on the ambient temperature (TAS in °C), solar radiation (I in W m^{-2}) and surface wind speed ($sfcWind$ in m s^{-1}) is given by

$$T_{cell,i} = c_1 + c_2 TAS_i + c_3 I_i + c_4 sfcWind_i \quad (10)$$

where c_1 = 4.3 °C, c_2 = 0.943, c_3 = 0.028 °C m^2 W^{-1} and c_4= − 1.528 °C s m^{-1}.

4.4.6 Technical Potential Maps

Following prior studies (Gernaat et al. 2021; Hoogwijk et al. 2004; Zhou et al. 2012), each technology technical potential case is calculated on a yearly basis and the resulting energy outputs are averaged over 30-yr periods (1971–2000, 2011–2040, 2041–2070 and 2071–2099) for each GCM. Figures 4.5–4.6 show the technical

potential maps by technology for the 1971-2000 period resulting from the methodology described above using input data from the IPSL-CM5A-LR model as example. Note that the parameter values listed in the equations above constitute the central assumptions for this study.

Overall, the technical potential maps shown in Figures 4.5–4.6 are in qualitative agreement with similar results found in the literature with respect to areas with high and low resource quality (although there are some differences with respect to excluded areas given the different assumptions). For example, Figure 4.5 shows high-quality wind resource areas in Northern Africa, Eastern Africa, Australia, Southern South America, Central USA zones, and some portion of Central and Eastern Asia, which is in line with results by Lu et al. 2009 and Karnauskas et al. 2018. In the case of solar PV (Figure 4.6), the largest potential areas are found in Northern Africa and Middle East, which agrees with similar results by Korfiati et al. 2016.

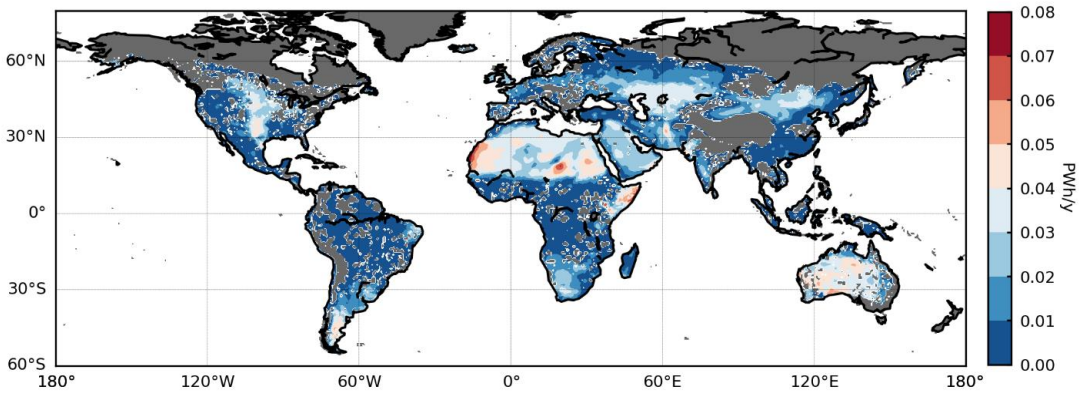

Figure 4.5. Global wind onshore technical potential computed using the suitability map displayed in Figure 4.2 and Equations 2–7 (*Central* case). Input climate data: IPSL-CM5A-LR (1971–2000). Gray areas correspond to grid cells that are entirely excluded.

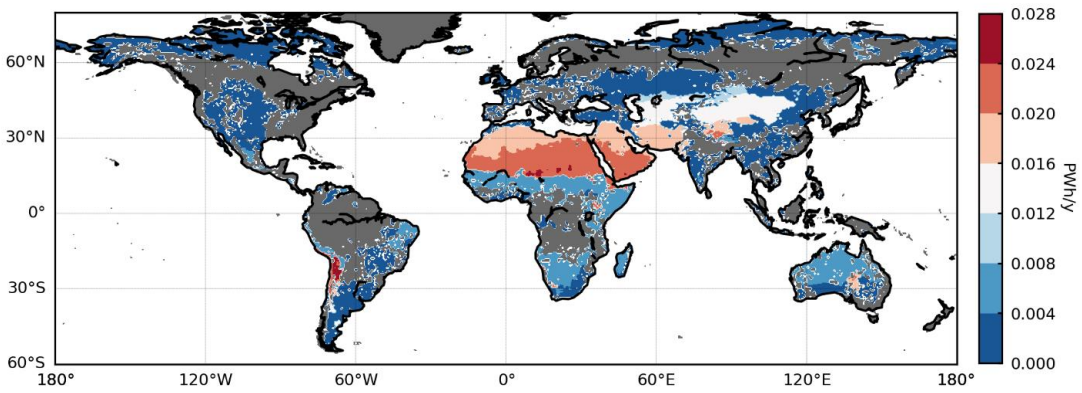

Figure 4.6 Global solar PV technical potential computed using the suitability map displayed in Figure 4.3 and Equations 8–10 (*Central* case). Input climate data: IPSL-CM5A-LR (1971–2000). Gray areas correspond to grid cells that are entirely excluded.

4.4.7 Sensitivity Cases

Tables 4.9–4.10 summarize which parametric assumptions are analyzed in this study and the references from which they are taken from. These assumptions then reflect a range of values used by prior studies.

Table 4.9 Parametric assumptions for all cases analyzed for the onshore wind technology.

Parameter	Case label	Reference	Value
Power output estimate[a]	Central	Rinne et al. 2018	Turbine technology Vestas V136-3.45; hub height = 125m
Power output estimate	E101_3.05	Höltinger et al. 2016	Turbine technology Enercon E101-3.05; hub height = 135m
Power output estimate	GE_2.5-100	Lu et al. 2009	Turbine technology General Electric GE 2.5-100; hub height = 100m
Power output estimate	V90_2.0	Bosch et al. 2017	Turbine technology Vestas V90-2.0; hub height = 100m
Suitability factors	Central	Eurek et al. 2017	See Table 4.6
Suitability factors	S_low	Zhou et al. 2012	See Table 4.6
Suitability factors	S_low_II	Deng et al. 2015	See Table 4.6
Suitability factors	S_high	Lu et al. 2009	See Table 4.6
Power density	Central[b]	Rinne et al. 2018; Eurek et al. 2017	5.3 MW Km^{-2}
Power density	Pdens_1	Adams and Keith 2013	1.0 MW Km^{-2}
Power density	Pdens_9	Lu et al. 2009	9.0 MW Km^{-2}
Power density	Pdens_13	Rinne et al. 2018[b]	13.0 MW Km^{-2}
Hub height[c]	Central	Rinne et al. 2018	125
Hub height	Hub_75	Rinne et al. 2018	75
Hub height	Hub_100	Rinne et al. 2018	100
Hub height	Hub_150	Rinne et al. 2018	150

Notes:
[a] Figure 4.7 shows the power curves of all turbine models analyzed in this study.
[b] The high power density case is set to 13.0 MW Km^{-2} given that the upper bound limit for this parameter in the literature has been shown by Rinne et al. 2018 to be in the 12-15 MW Km^{-2} range.
[c] As shown by Rinne et al. 2018, many previous assessments have assumed hub heights within the 70-100 m range.

Table 4.10 Parametric assumptions for all cases analyzed for the solar PV technology.

Parameter	Case label	Reference	Value
Performance ratio (PR)	Central	Gernaat et al. 2021	0.85
Performance ratio (PR)	PR_75	Deng et al. 2015	0.75
Performance ratio (PR)	PR_90	Used to understand implications from higher assumptions[a]	0.90
Land use factor (η_{LPV})	Central	Gernaat et al. 2021; Koberle et al. 2015;	0.47
Land use factor (η_{LPV})	Nlpv_20	Deng et al. 2015;	0.20
Land use factor (η_{LPV})	Nlpv_30	Deng et al. 2015	0.30
Land use factor (η_{LPV})	Nlpv_100	Hoogwick 2004	1.0
Suitability factors	Central	Gernaat et al. 2021	See Table 4.7
Suitability factors	S_low	Deng et al. 2015 (low case)	See Table 4.7
Suitability factors	S_low_II	Deng et al. 2015 (medium case)	See Table 4.7
Suitability factors	S_high	Dupont et al. 2020	See Table 4.7
Notes: [a] No reference found for a *PR* value higher than the *Central* case.			

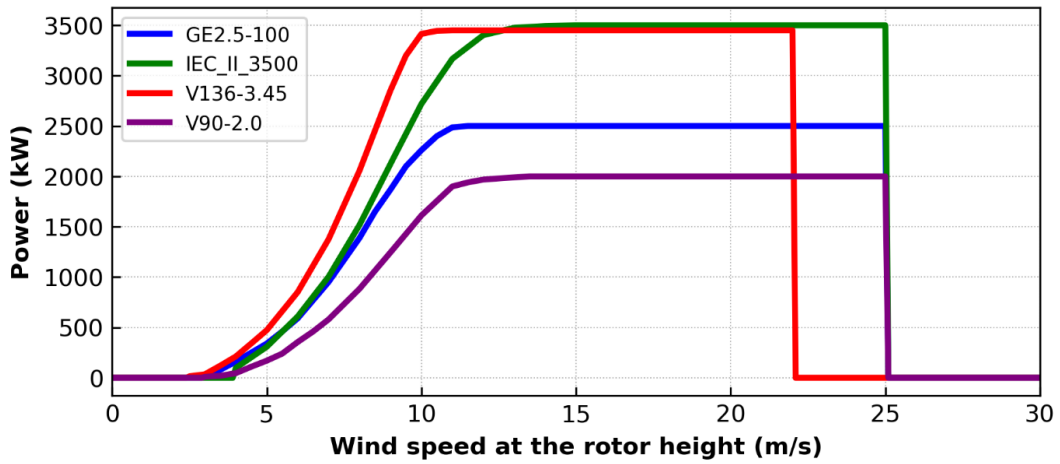

Figure 4.7. Power curves for all wind turbine models analyzed in this study (recall that the turbine model for the *Central* case is the Vestas V136-3.45).

4.4.8 Implementation of supply curves in GCAM

As noted earlier, supply curves (a representation of economic potential) are key assumptions in GCAM as well as in other IAMs. They represent costs of generating power from renewable resources that increase with additional development as the least-cost sites (those with higher quality resources) are used first. To produce the supply curves used in this study, each global 30-yr average potential map is used to obtain the total technical potential in all GCAM regions. The total regional potential is then divided into classes spanning low- to high-quality resource categories so that each class corresponds to a point in the supply curve. The computation of the costs of electricity is carried out using the GCAM data system (Calvin et al. 2019) framework (the open-source R package that processes and produces all GCAM input files). This package computes the cost of energy for each point in the curve based on GCAM economic information of capital costs, operation and maintenance costs and fixed charge rate (listed in Iyer et al. 2017). This is the same process used to build the default wind onshore supply curves that are part of the GCAM core version. Note that the wind onshore supply curves produced here replaced the default GCAM supply curves produced from the wind onshore potentials computed by Eurek et al. 2017. As mentioned in Chapter 3, the utility-scale solar technologies in the GCAM core version do not rely on supply curves. Hence, the solar supply curves produced in this study replaced the default assumption of unlimited solar resources. To produce the solar supply curves, the original GCAM data system R code for wind onshore was modified to account for the costs of solar energy.

Supply curves for all cases were implemented in GCAM for the long-term assessment of implications for the power sector. As mentioned in Chapter 3, these curves affect GCAM technology competition. Figure 4.8 shows examples of supply curves for the USA for some selected cases.

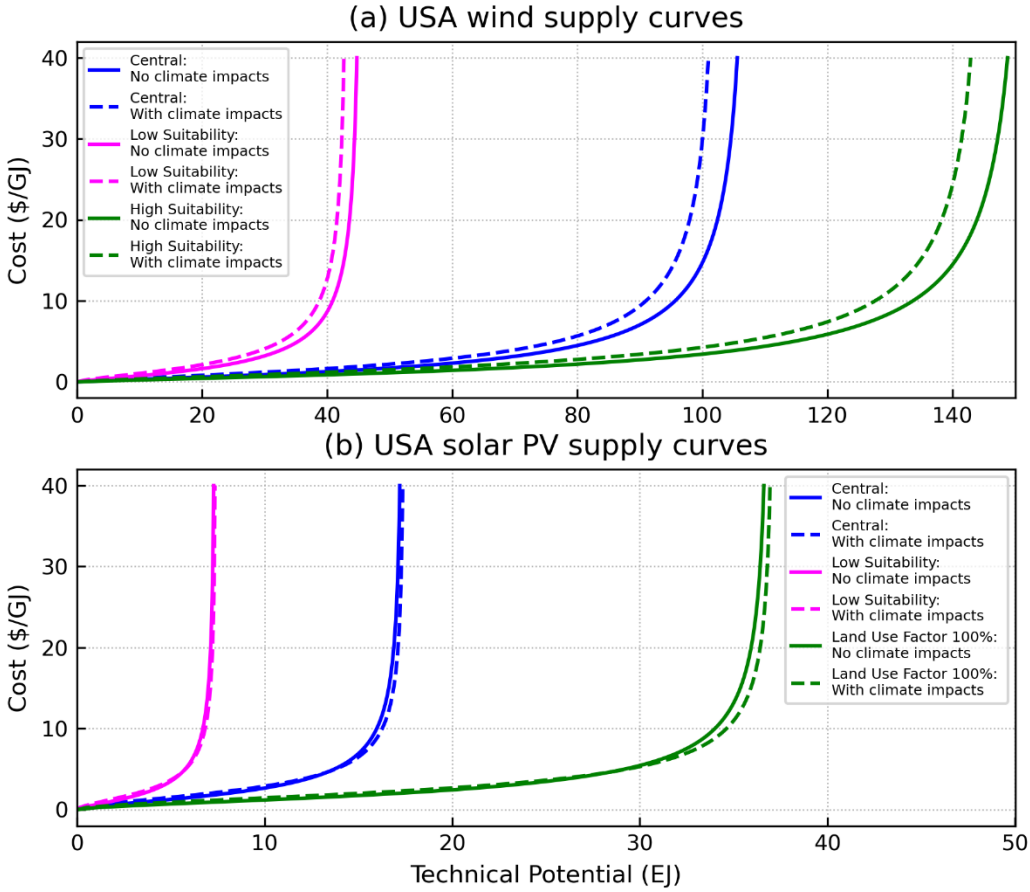

Figure 4.8. Examples of (a) wind onshore supply curves and (b) solar PV supply curves for the USA. Curves represent sensitivity cases (solid lines, period: 1971-2000) and climate change impacts on the technical potential (dashed lines, period: 2071-2099). In this example, input data derive from the IPSL-CM5A-LR model under RCP2.6.

4.4.9 Additional assumptions: solar CSP

An important note about the implementation of the solar PV supply curves in GCAM is that it can only be made in conjunction with the implementation of supply curves for the concentrated solar power (CSP) technology. Although this study has not examined the implications of the parametric assumptions for the solar CSP technical potential, a calculation of the global solar CSP technical potential was made to produce regional supply curves for the GCAM solar CSP technology. To do so, the methodology from the ISIpedia project (Gernaat et al. 2021) was followed. The main reason for this choice is that it accounts for climate change effects on the solar CSP technical potential, allowing a consistent assumption of climate effects on both the solar CSP and solar PV technical potentials and on the derived supply curves. Next, the approach to compute the global CSP technical potential is detailed.

- Geographical potential (A_i): computed using Eq. 1, exclusion criteria in Table 4.5 and suitability factors listed in Table 4.7 (same suitability factors used for solar PV). Figure 4.9 shows the land suitability map (%) for solar CSP.

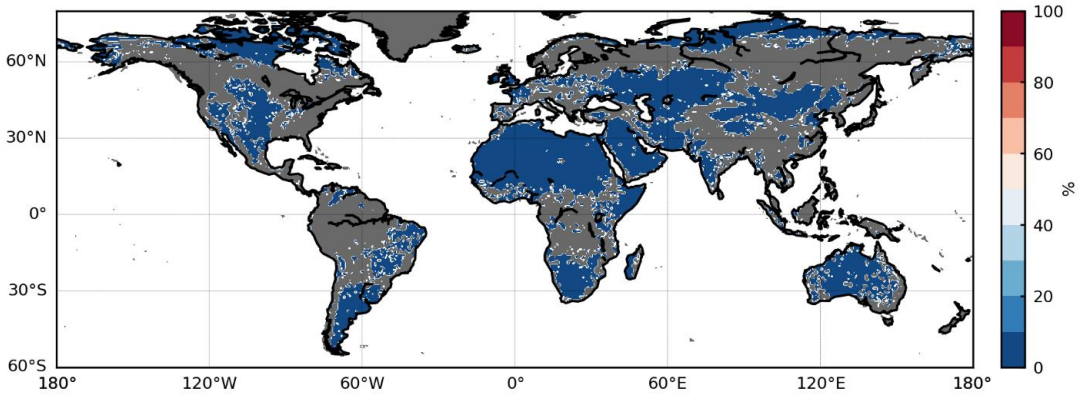

Figure 4.9. Land suitability map (%) for solar CSP deployment using the exclusion criteria in Table 4.5 and suitability factors in Table 4.7 at grid cell level. Gray areas correspond to grid cells that are entirely excluded.

- Technical potential: Likewise the wind and solar PV technical potentials, it is necessary to define the representative technology. The method employed by Gernaat et al. 2021 assumes that the parabolic trough technology is the reference technology given it is the most mature CSP technology in the market (Köberle et al. 2015). Using this assumption, the CSP technical potential ($E_{CSP,i}$) in kWh/year is calculated using Eq. 11,

$$E_{CSP,i} = \overline{I_i} \cdot h \cdot A_i \cdot \eta_{LCSP} \cdot \left(\frac{\eta_{CSP}}{FLH_i}\right) \quad (11)$$

where $\overline{I_i}$ is the yearly-averaged solar radiation (kWh m^{-2} y^{-1}) in grid cell *i* assuming a minimum resource intensity of 1095 kWh m^{-2} y^{-1} (grid cells are excluded if not satisfying this operational threshold); η_{LCSP} is the CSP land use factor (assumed 0.37) that accounts for the fraction of the suitable land actually covered by collectors given the spacing between them; h is the number of hours in a year; and FLH_i is the number of full load hours (h) of the reference CSP power plant, i.e., the number of hours a year that the CSP plant operates at the maximum rating. FLH_i is computed using the linear regression equation derived by Köberle et al. 2015 (in which FLH_i is a function of $\overline{I_i}$). The term η_{CSP} is the CSP efficiency formulated to account for changes in CSP potential as a function of atmospheric parameters, given by:

$$\eta_{CSP} = \eta_r \cdot \left(k_0 - \frac{k_1(T_f - T_i)}{I_i}\right). \quad (12)$$

As noted by Gernaat et al. 2021, in a CSP plant, heat is captured by the solar collectors and transported to a Rankine cycle turbine to produce electricity. This generation process is characterized by an efficiency η_r, which is the efficiency of the

Rankine cycle (assumed to remain static as 40%). In Eq. 12, T_f is the temperature of the fluid in the absorber (115 ^{o}C), T_i is the air temperature, I_i is the solar radiation (in W m^{-2}), k_0 = 0.762, and k_1 = 0.2125 W m^{-2} ^{o}C^{-1}. Note there is a caveat in the ISIMIP2b dataset which does not provide direct normal radiation. The latter is used in CSP technical potential assessments because CSP systems only utilize direct solar radiation. The ISIMIP2b RSDS variable (i.e., the total global solar radiation) is used in the study by Gernaat et al. 2021 as an estimate for the I_i term, which is followed here. Table 4.11 shows a comparison with CSP technical potential estimates from other global studies and Figure 4.10 shows the CSP technical potential map derived from the implementation of all steps listed above.

Table 4.11 Comparison of results of this study with other analyses (global solar CSP).

Reference	Data Source	Spatial Resolution	Period	Technical Potential (PWh/y)
Deng et al. 2016	NASA Langley Research Center Surface Meteorological and Solar Energy dataset (SSE)	1 km	2010	98-808[a]
Dupont et al. 2020	World Bank Group ESMAP. Global Solar Atlas	0.1^{o}	Not explicitly stated	294
Koberle et al. 2015	NASA Langley Research Center Surface Meteorological and Solar Energy dataset (SSE – Release 6.0)	0.5^{o}	1983-2005	173
Trieb et al. 2009	NASA Langley Research Center Surface Meteorological and Solar Energy dataset (SSE – Release 6.0)	1 km	1983-2005	2946
This study	ISIMIP2b GCMs	0.5^{o}	1971-2000	577-579

Notes:

[a] Depends on the land availability scenario (low, medium, and high cases). This study also makes estimates for 2030 and 2070 (based on the assumption of improvement in technological parameters) not reported here.

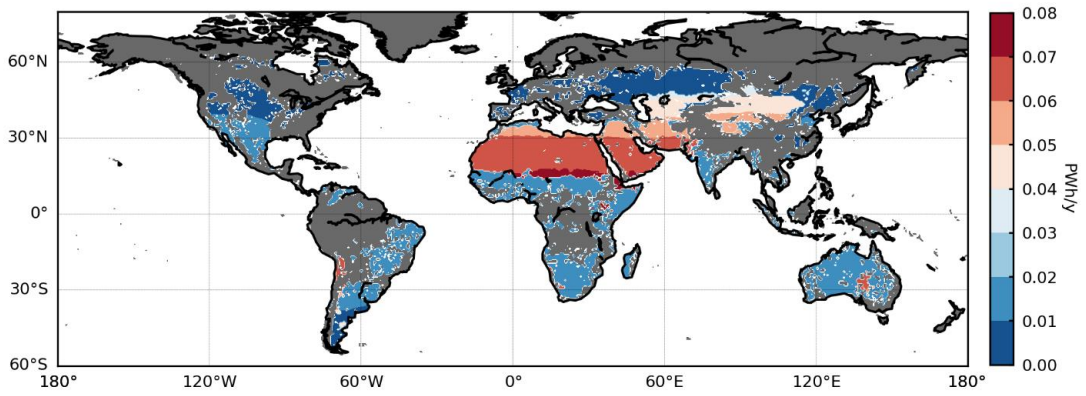

Figure 4.10 Global solar CSP technical potential computed using the suitability map displayed in Figure 4.9 and Equations 11–12. Input climate data: IPSL-CM5A-LR (1971–2000). Gray areas correspond to grid cells that are entirely excluded.

Having computed the global CSP technical potential using the assumptions listed above, solar CSP supply curves were derived (as in subsection 4.4.8) and implemented in GCAM in tandem with the solar PV supply curves. It is important to mention that the same solar CSP supply curves were used in all GCAM simulations for the solar PV sensitivity cases.

4.4.10 Scenarios

The effects of the implementation of supply curves based on distinct resource estimates are analyzed in the context of scenarios that vary according to the climate mitigation and climate impacts dimensions (Table 4.12).

Table 4.12 Scenarios explored in this study.

Scenario	Description[a,b,c]
Baseline_NoCI	Baseline scenario with no price or constraints on greenhouse gas emissions. This scenario assumes no climate impacts on solar and wind, utilizing supply curves from the historical 1971–2000 period throughout the entire simulation.
RCP2.6_NoCI	Climate policy scenario in which the end-of-century radiative forcing target is specified to reach 2.6 W m^{-2} (consistent with a 2°C scenario)[d]. This scenario assumes no climate impacts on solar and wind, utilizing supply curves from the historical 1971–2000 period throughout the entire simulation.
Baseline_CI	Baseline scenario with no price or constraints on greenhouse gas emissions. This scenario assumes climate impacts on solar and wind, utilizing supply curves produced from climate input data from the RCP8.5.
RCP2.6_CI	Climate policy scenario in which the end-of-century radiative forcing target is specified to reach 2.6 W m^{-2} (consistent with a 2°C scenario). This scenario assumes climate impacts on solar and wind, utilizing supply curves produced from climate input data[e] from the RCP2.6.

Notes:

[a] Socioeconomic assumptions in all scenarios are consistent with the Shared Socioeconomic Pathway (SSP) 2, which reflects a world in which social, economic and technological future trends do not differ markedly from historical patterns (Riahi et al. 2017).

[b] The supply curves (varying by climate impact assumptions) are implemented individually by renewable technology. This means that when a supply curve is implemented for the wind technology, the solar technology keeps the GCAM default assumptions and vice-versa.

[c] The scenarios do not account for climate impacts in other renewables such as biomass and hydropower or in water availability since this scenario framework aims to help understanding the interplays between climate impacts on solar and wind and the uncertain supply curve inputs.

[d] To achieve the target, the model iteratively solves for the global carbon price pathway needed.

[e] For the climate impacts (CI) scenarios, supply curve assumptions change over time and are implemented for the periods 2011-2040, 2041-2070 and 2071-2099 based on the 30-yr average potentials of each period. This is in line with the methodology of the ISIpedia project (Gernaat et al. 2021).

4.5 Results and Discussion

4.5.1 Implications for the global technical potentials and electricity production

Figure 4.11 ((a) and (c)) summarizes the strong effect of the distinct parameter assumptions on the quantification of wind and solar PV technical potentials, respectively, by comparing the changes associated with each sensitivity case with the technical potentials produced under the *Central* case. Land use parameters (i.e., suitability and land-use factors) play critical roles for both technologies. The wind potential is also strongly influenced by the choice of the average turbine installation density with the high power density case (*Pdens_13*) showing the largest deviation from the central assumption. Another important assumption is how wind power is computed. In this regard, these results contrast the effect of the combination of a modern turbine technology (Vestas V136-3.45 – a technology from 2015 according to the https://www.thewindpower.net) and a taller hub height (125 m), as assumed in the *Central* case, against a past turbine model (V90-2.0 MW – a technology from 2004) placed at a lower hub height (75 m). The latter leads to ~30% reduction relative to the *Central* case. The other assumptions (hub height in the case of wind, performance ratio in the case of solar PV) show considerably lower relative changes than land-related parameters. However, the low hub height assumption (75 m) leads to non-trivial reductions in wind potential of ~17%.

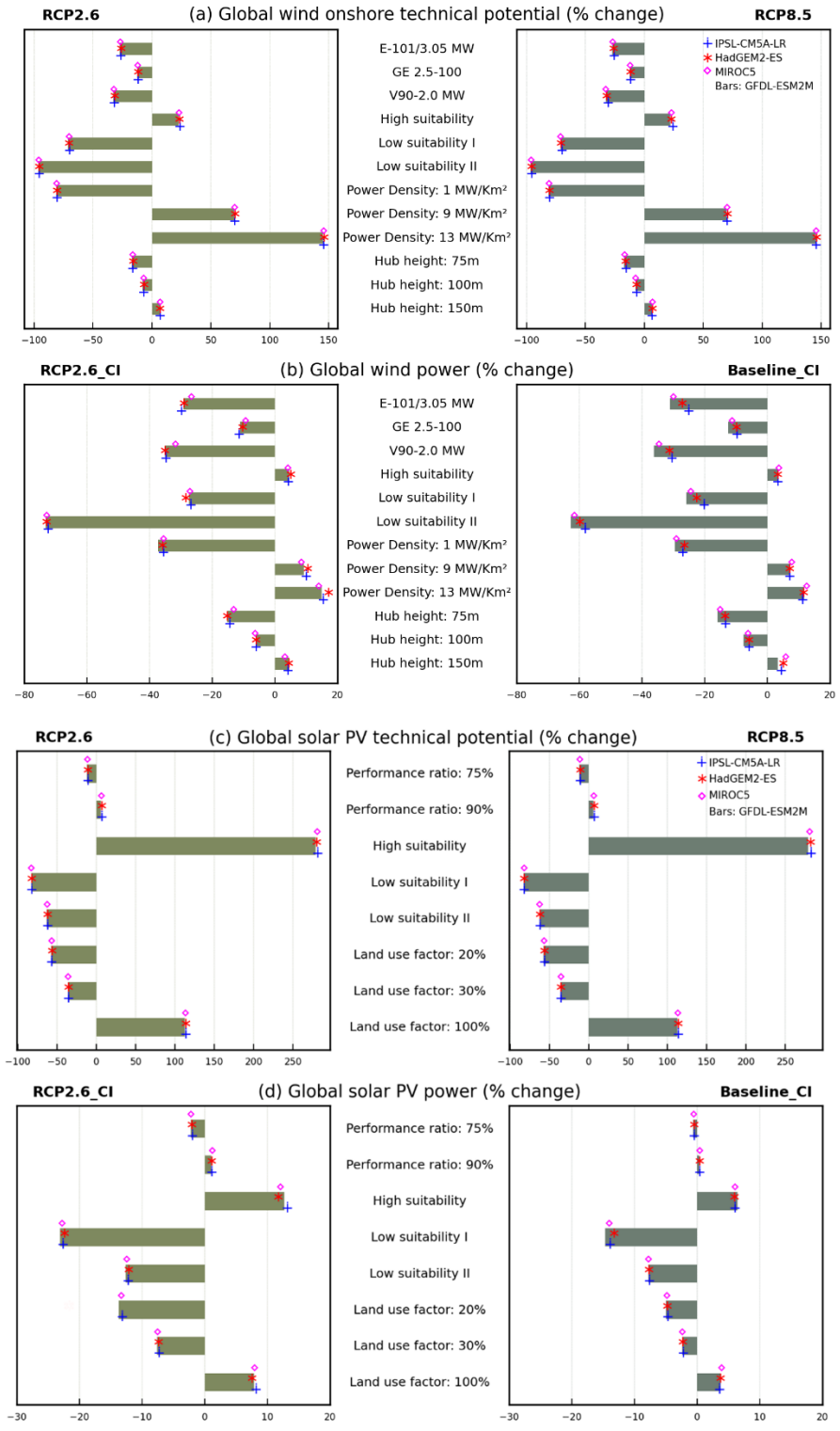

Figure 4.11. (a) Changes in the global wind onshore technical potential relative to the *Central* case by sensitivity case and RCP. Technical potentials are computed for the 2071-2099 period. (b) Changes in the global wind power generation by sensitivity case and scenario in 2100 (climate impact *"CI"* assumptions). Changes are relative to a GCAM simulation using supply

curves produced from the *Central* technical potential case. (c) As in (a) but for the global solar PV technical potential. (d) As in (b) but for the global solar PV power. (Note: the solar PV case assuming land use factor of 20% has not solved for the RCP2.6_CI scenario using the HadGEM2-ES input data).

When supply curves produced from all technical potential cases are implemented in GCAM, the corresponding changes in the 2100 global wind and solar PV electricity generation reproduce the patterns of change in the input potentials (Figure 4.11(b) and (d)). That is, positive changes in generation compared with the *Central* case are in line with increased technical potentials, and vice-versa. Importantly, technical potential cases with the largest deviations from central assumptions result in the largest changes in generation, which can be very pronounced depending on the case. For example, the low suitability (*S_low_II*) case for wind results in very large reductions in generation ranging between 58% and 73% depending on the GCM input and scenario. It can be noted that negative changes in electricity generation are more prominent than the positive ones even for a very large increase in potential like in the high suitability case of solar PV. This is because GCAM, like most IAMs, imposes limitations to substantial deployment of solar and wind capacities to account for the added cost of managing the inherent intermittency of these resources. As mentioned earlier in Chapter 3, this is done through costs that vary with the fraction of renewables in the grid and add to the cost of building new intermittent generation to secure backup capacity.

Interestingly, the above general sensitivity patterns are largely consistent across warming scenarios, GCM input assumptions, GCAM scenarios and periods. Concerning the latter, it is worth noting that the global technical potentials computed using data from the historical (1971-2000) period, and the 2100 intermittent electricity

production simulated using supply curves from the historical period (i.e., the no climate impacts "*NoCI*" assumption in Table 4.12) unveil similar patterns of changes as those shown in Figure 4.11 (Appendix C; Figure C.1). All the above results then highlight the role of the parametric assumptions in resource estimates as a significant source of uncertainty in the modeling of intermittent electricity generation in GCAM.

4.5.2 Implications for the analyses of climate impacts on global technical potentials

As mentioned earlier, the implications of uncertainties in resource estimates for climate-impact analyses on the energy sector, such as the recent ISIpedia intercomparison, are currently unknown. To start investigating this matter, Tables 4.13-4.14 present the relative (%) changes in the mean end-of-century (2071-2099) technical potentials from the historical period. The multi-model impact assessments presented in Tables 4.13-4.14 indicate modest climate change impacts on solar and wind technical potentials at the global scale, which is in line with prior literature (Gernaat et al. 2021; IPCC 2012). These results also show that within this relative context, changes by GCM are not markedly affected by the parametric choice and that the small variations are further smoothed out by the multi-model means. However, the relative context masks the large absolute differences across the sensitivity cases that are reflected in the derived supply curves. These absolute differences and their effects on the supply curves (i.e., changes in the cost of energy and resource availability) are the key pieces to the understanding of the potential implications of the parametric uncertainties for the analysis of regional impacts, which will be discussed later in this dissertation.

Table 4.13 Relative changes in the global wind technical potential by case, GCM and RCP (mean 2071-2099 potentials relative to the historical 1971-2000 potentials).

% Differences relative to historical: Global Wind Technical Potential										
Case	HadGEM2-ES		GFDL-ESM2M		IPSL-CM5A-LR		MIROC5		Multi-model Mean	
	RCP2.6	RCP8.5	RCP2.6	RCP8.5	RCP2.6	RCP8.5	RCP2.6	RCP8.5	RCP2.6	RCP8.5
Central	-1.0	-1.8	-0.7	-1.3	0.9	7.6	-0.9	-4.9	-0.4	-0.1
E101_3.05	-1.0	-1.8	-0.8	-1.4	0.7	8.8	-1.1	-5.4	-0.5	0.1
GE_2.5-100	-1.0	-1.9	-0.7	-1.3	0.8	7.9	-1.0	-5.1	-0.5	-0.1
V90_2.0	-1.1	-2.0	-0.8	-1.5	0.7	9.5	-1.3	-5.8	-0.6	0.0
S_high	-1.0	-2.0	-0.8	-1.8	1.3	8.6	-0.7	-5.0	-0.3	0.0
S_low	-0.8	-3.9	-0.6	-1.6	2.5	10.1	0.0	-5.8	0.3	-0.3
S_low_II	-0.9	-2.0	-0.7	-1.5	1.3	8.5	-0.4	-4.9	-0.2	0.0
Pdens_1	-1.0	-1.8	-0.7	-1.3	0.9	7.6	-0.9	-4.9	-0.4	-0.1
Pdens_9	-1.0	-1.8	-0.7	-1.3	0.9	7.6	-0.9	-4.9	-0.4	-0.1
Pdens_13	-1.0	-1.8	-0.7	-1.3	0.9	7.6	-0.9	-4.9	-0.4	-0.1
Hub_75	-1.0	-1.9	-0.7	-1.4	0.8	8.4	-1.1	-5.3	-0.5	0.0
Hub_100	-1.0	-1.9	-0.7	-1.3	0.8	7.9	-1.0	-5.1	-0.5	-0.1
Hub_150	-1.0	-1.8	-0.6	-1.3	0.9	7.3	-0.8	-4.8	-0.4	-0.1

Table 4.14 Relative changes in the global solar PV technical potential by case, GCM and RCP (mean 2071-2099 potentials relative the historical 1971-2000 period).

% Differences relative to historical: Global Solar PV Technical Potential										
Case	HadGEM2-ES		GFDL-ESM2M		IPSL-CM5A-LR		MIROC5		Multi-model Mean	
	RCP2.6	RCP8.5	RCP2.6	RCP8.5	RCP2.6	RCP8.5	RCP2.6	RCP8.5	RCP2.6	RCP8.5
Central	-0.4	-3.8	0.3	-2.0	-0.3	-2.4	-0.1	-3.2	-0.1	-2.9
PR_75	-0.4	-3.8	0.3	-2.0	-0.3	-2.4	-0.1	-3.2	-0.1	-2.9
PR_90	-0.4	-3.8	0.3	-2.0	-0.3	-2.4	-0.1	-3.2	-0.1	-2.9
V90_2.0	-0.4	-3.8	0.3	-2.0	-0.3	-2.4	-0.1	-3.2	-0.1	-2.9
S_high	-0.3	-3.2	0.3	-2.0	0.3	-1.5	0.3	-2.8	0.2	-2.4
S_low	-0.6	-3.7	0.1	-2.3	0.1	-1.9	-0.1	-3.3	-0.1	-2.8
S_low_II	-0.5	-3.5	0.2	-2.2	0.2	-1.7	0.1	-3.0	0.0	-2.6
Nlpv_20	-0.4	-3.8	0.3	-2.0	-0.3	-2.4	-0.1	-3.2	-0.1	-2.9
Nlpv_30	-0.4	-3.8	0.3	-2.0	-0.3	-2.4	-0.1	-3.2	-0.1	-2.9
Nlpv_100	-0.4	-3.8	0.3	-2.0	-0.3	-2.4	-0.1	-3.2	-0.1	-2.9

4.5.3 Implications for the regional technical potentials and electricity production

In this subsection, the results from the GFDL-ESM2M model for the historical period are used as example since the qualitative insights of this discussion are not affected by the choice of GCM or period of the resource estimate. (Appendix C; Figures C.2-C.9 provide the technical potential sensitivity case results for the four ISIMIP2b GCMs, two emissions scenarios and two periods (1971-2000 and 2071-2099), which highlights no major effects on the patterns of sensitivity presented).

Not surprisingly, the regional patterns of changes in technical potentials are consistent with the global results (Figures 4.12(a) and 4.13(a)). While changes in certain parameters affect the computation of technical potentials equally in all regions (e.g., power density, performance ratio and solar PV land use factor), effects from other sensitivity cases vary regionally with some of them displaying strong variation (notably the suitability cases). For example, reductions in solar PV technical potential range between -1 and -79% in the *S_low_2* case (compared with the *Central* case) depending on the land cover distribution in each region. On the positive side, the *S_high* case of solar PV is an example of very strong relative changes and marked regional variability (between 111% and 900%).

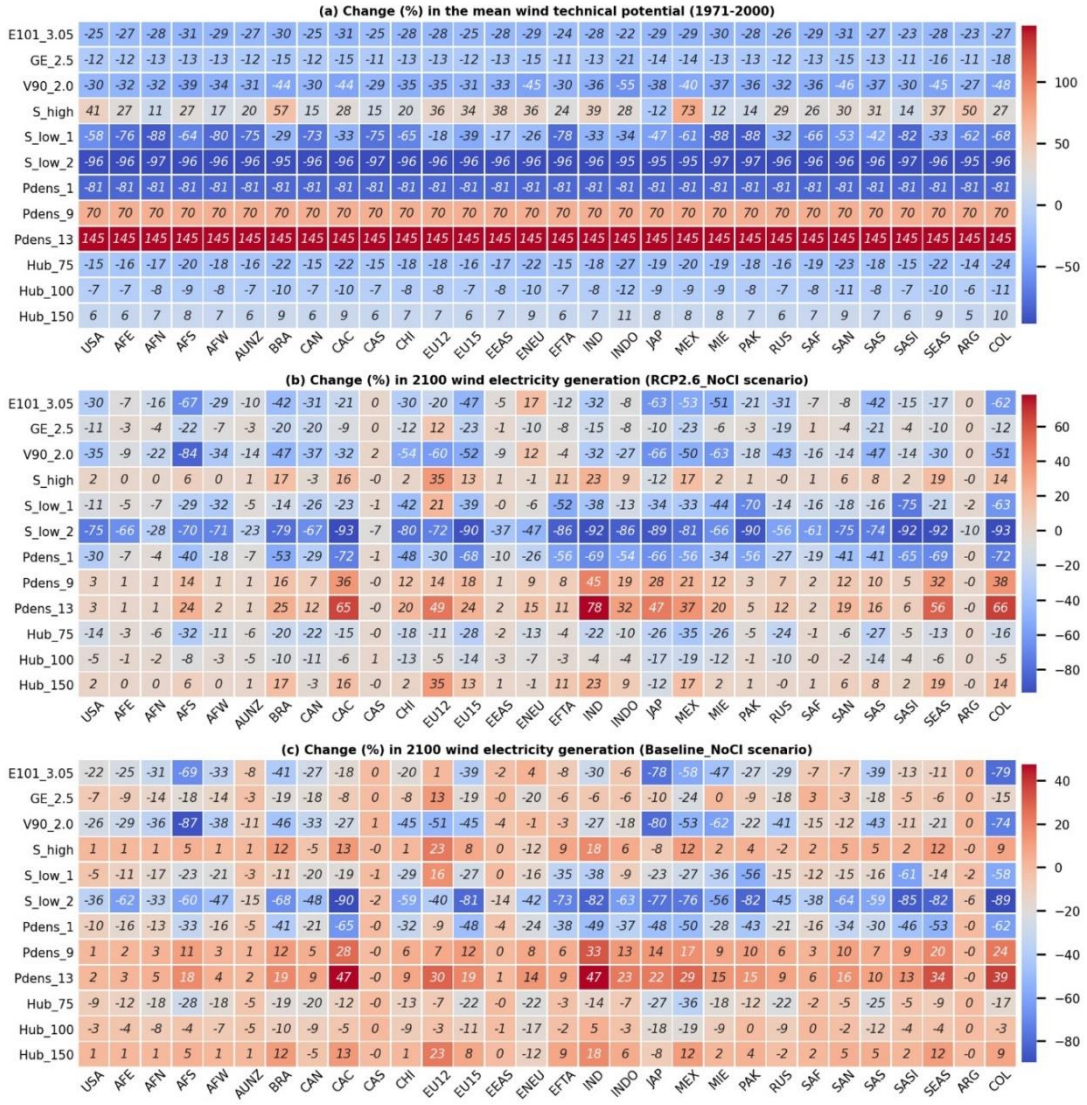

Figure 4.12. (a) Relative changes in wind onshore technical potential from central assumption by sensitivity case and GCAM region (input data: GFDL-ESM2M model – 1971-2000). (b) Relative changes from the *Central* case in wind onshore electricity production in 2100 (*RCP2.6_NoCI* scenario) (all cases used supply curves from the historical period throughout the entire simulation). (c) As in (b) but for the *Baseline_NoCI* scenario. Note that this study excludes two GCAM regions: Taiwan and South Korea. In these regions, the spatial resolution of this analysis (0.5 degree) does not allow sufficient number of points to produce a supply curve in all sensitivity cases.

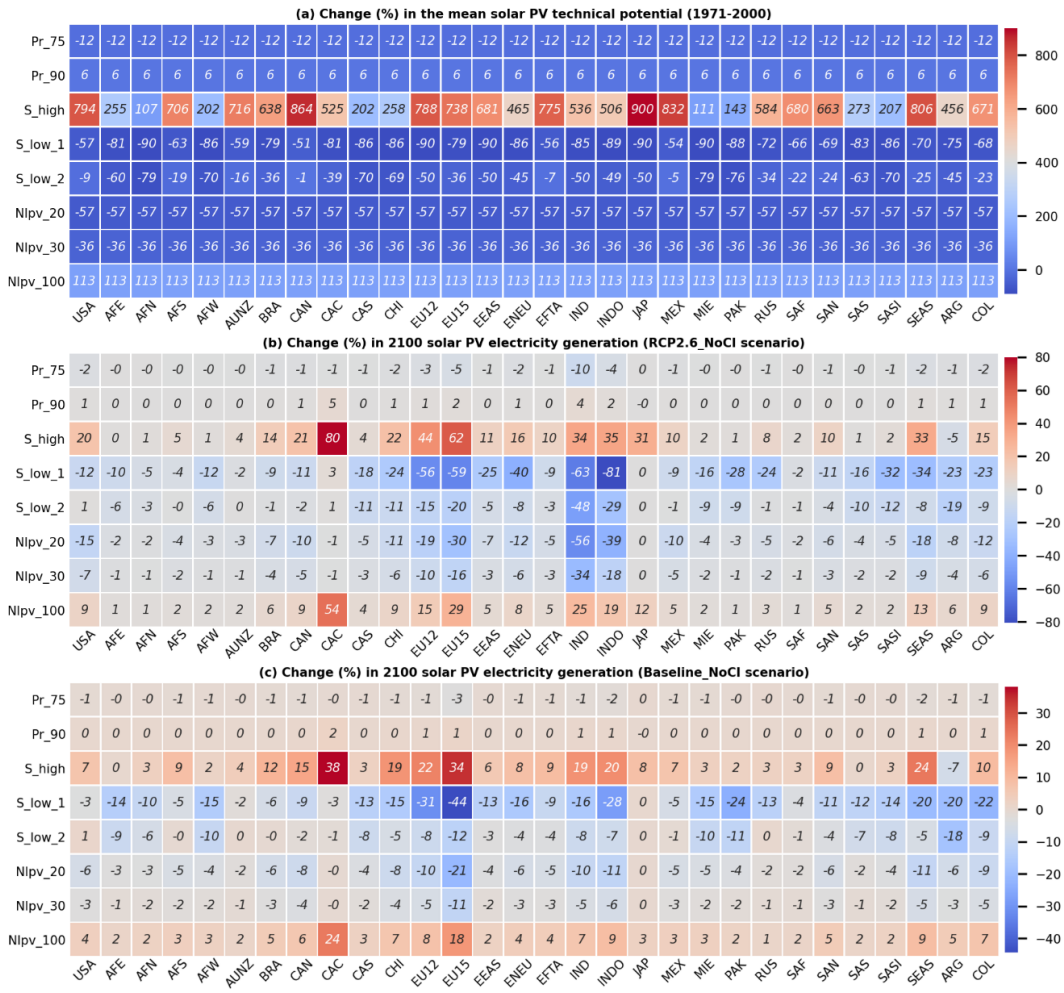

Figure 4.13. As in Figure 4.12 but for the solar PV technology.

With respect to the regional solar and wind electricity generation responses, their sensitivity to the distinct parametric assumptions is large like in the global situation, with the resulting changes from the *Central* case varying substantially by region (Figures 4.12-4.13 (b) and (c)). For example, wind power reductions under the *Pdens_1* case can be lower than -1% in Argentina (ARG) up to -72% in Colombia (COL) (*RCP2.6_NoCI* scenario). This marked regional variation is determined by two main factors: the ratio between electricity demands and technical potentials embedded in the supply curves and the effect of the shifting supply curves on GCAM regional

power-sector market competition. The first factor means that in regions where the demand for electricity is high compared with the available resource (i.e., the technical potential), differences among the distinct supply curves are more pronounced, which contributes toward larger differences in electricity generation. Conversely, with low ratios between electricity demands and technical potentials, the effects from the shifting supply curves originate from the lower ends of the curves in which differences among the supply curves are lower. The second and most important factor relates to how the modeled electricity market shares are distributed among the various technologies in GCAM. As detailed in prior literature (Calvin et al. 2019; Wise et al. 2019) and explained in Chapter 3, the decision to invest in additional capacity is based on the costs of energy production per technology (least-cost technology options capture the largest shares of markets although the other options also gain some market share). As shown in Chapter 3, the cost of individual power-sector technologies in GCAM depends on amortized capital costs, operations and maintenance (O&M) costs, fuel costs, efficiency of the power plant and capacity factor of the technology (other factors like the intermittency costs mentioned above and the price of carbon also affect the cost of individual technologies). While most of these parameters are fixed assumptions within the model (assumptions listed in Iyer et al. 2017), fuel costs are computed internally based on the supply curves. Thus, higher/lower availability of the intermittent renewable resource represented in the supply curves alter fuel costs, which in turn affect the cost of the renewable technology. This has direct implications on the economic competitiveness of solar and wind relative to other technologies. In other

words, solar and wind technologies can gain or lose importance within regional electricity markets depending on the sensitivity case.

A major insight from Figures 4.12-4.13 is that the role of intermittent renewable generation could be considerably under or overestimated relative to other technologies in some regions depending on the sensitivity case. This interferes with model's ability to provide decision support. As the model needs to balance electricity supplies and demands in all regions and all periods, reduced projections force the model to replace generation lost by enhancing the deployment of other technologies, while increased solar or wind generation diminishes the importance of other technologies in the power system. The first is illustrated in Figures 4.14-4.15 for the six cases with the overall largest reductions in wind onshore technical potential. Under the mitigation *RCP2.6_NoCI* scenario, reductions in wind onshore power are split among various low-carbon technologies in proportions that vary depending on the region (Figure 4.14). For example, nuclear energy is the most important replacement technology in China (CHI) followed by carbon capture and storage (CCS) technologies whereas the opposite is seen in the USA. Along similar lines, nuclear generation largely grows in importance in the modeled European (EU-15) power system, but the increase in wind offshore predominates in all sensitivity cases. For the *Baseline_NoCI* scenario, in which greenhouse gas (GHG) emissions are unconstrained, the GCAM assessment for the loss of wind generation is an overall higher value of carbon-intensive technologies in many regions, which include major economies such as USA, China, EU-15 and India (IND) (Figure 4.15). The overall implication for decision-making is that each replacement technology that grows in importance in GCAM scenarios due to an undermined role of

the wind technology would be associated with challenges, such as larger land and/or water requirements, public opposition issues, higher investment requirements or increased GHG emissions. An overestimated role of wind power in future scenarios also has significance because it can lead, for example, to similarly overestimated assessments of investments in generating facilities as well as in transmission infrastructure.

The above-mentioned substitution effect is also seen for solar albeit with lower generation figures as regional solar production in GCAM is typically lower than wind onshore power (except for few regions with very high solar resources) (Figures 4.16-4.17). Unlike the wind onshore sensitivity cases, wind offshore, in general, does not represent a major replacement technology for losses in solar power under the *S_low_1*, *S_low_2, Nlpv_20* and *Nlpv_30* sensitivity cases. In fact, changes in wind offshore are negative in many regions. Note that the sensitivity cases for solar PV shown in Figure 4.16 also include the *S_high* and the *Nlpv_100* cases associated with increases in solar PV generation. China is used again as an illustrative example. In this region, nuclear energy followed by CCS are the most important replacement technologies under the *RCP2.6_NoCI* scenario for those sensitivity cases that reduced solar PV generation. Conversely, these sources become less relevant in the *S_high* and *Nlpv_100* cases. For the *Baseline_NoCI* scenario (Figure 4.17), India shows notable changes in fossil fuels generation. In India, cumulative changes in electricity from fossil fuels vary largely from -525 to 340 TWh throughout all sensitivities. The above examples highlight the ambiguity created by the parametric uncertainties concerning the role of each technology in the power system. This suggests challenges, for example, for the

delineation of decarbonization strategies as the level of mitigation effort needed varies as shown by the example of India under the *Baseline_NoCI* scenario.

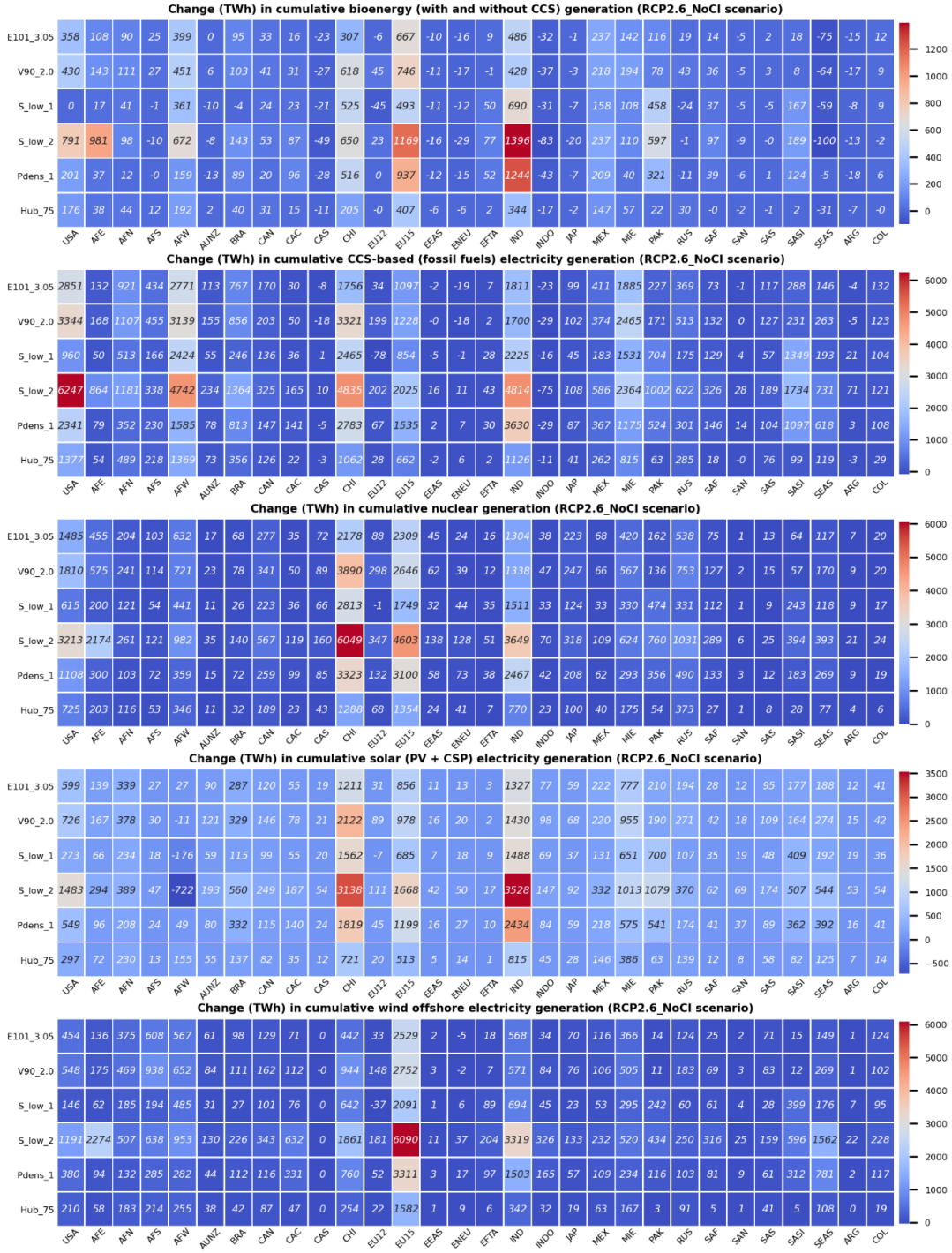

Figure 4.14. Changes in cumulative (2020-2100) electricity production by generating technologies relative to the wind onshore *Central* case (*RCP2.6_NoCI* scenario).

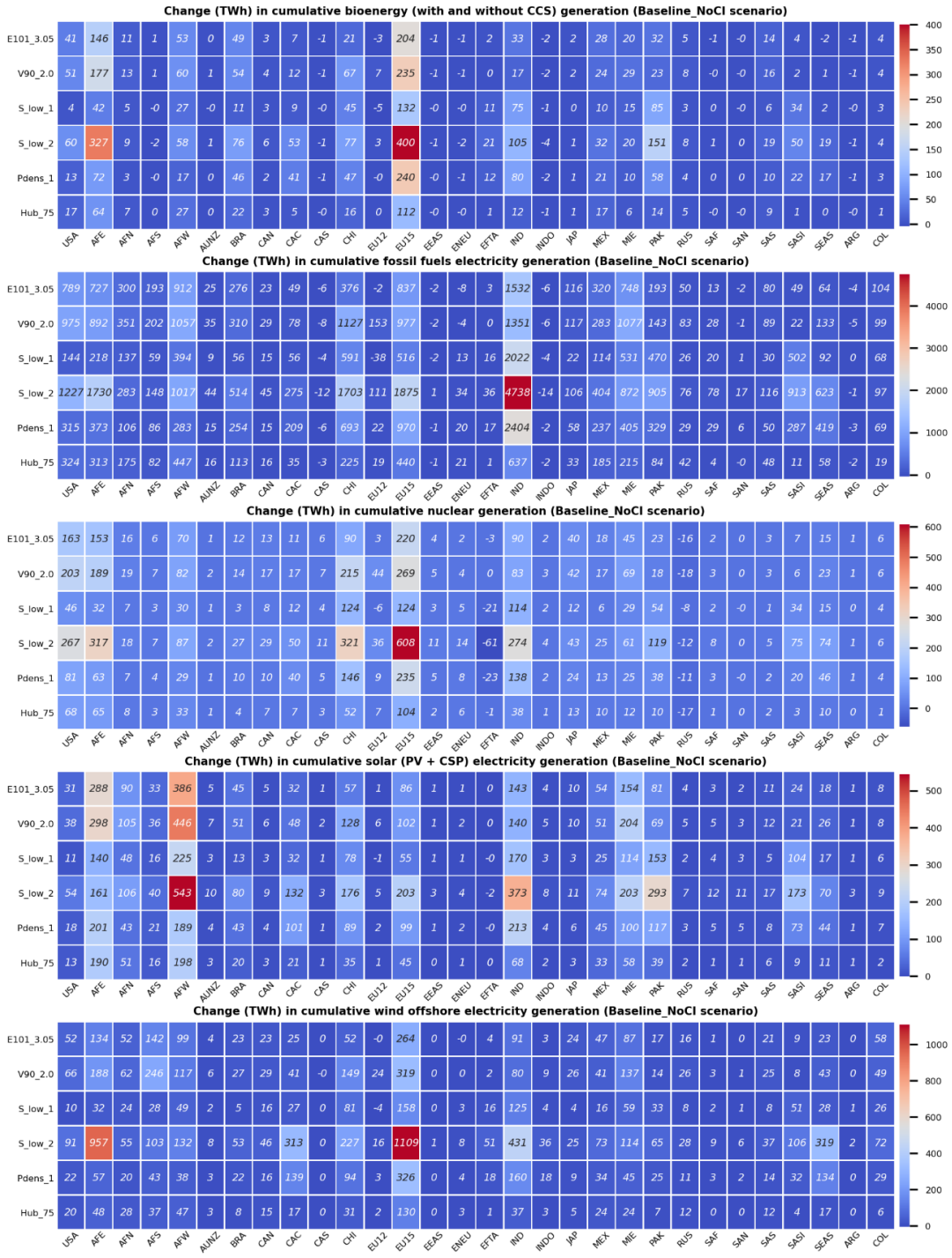

Figure 4.15. As in Figure 4.14 but for the *Baseline_NoCI* scenario.

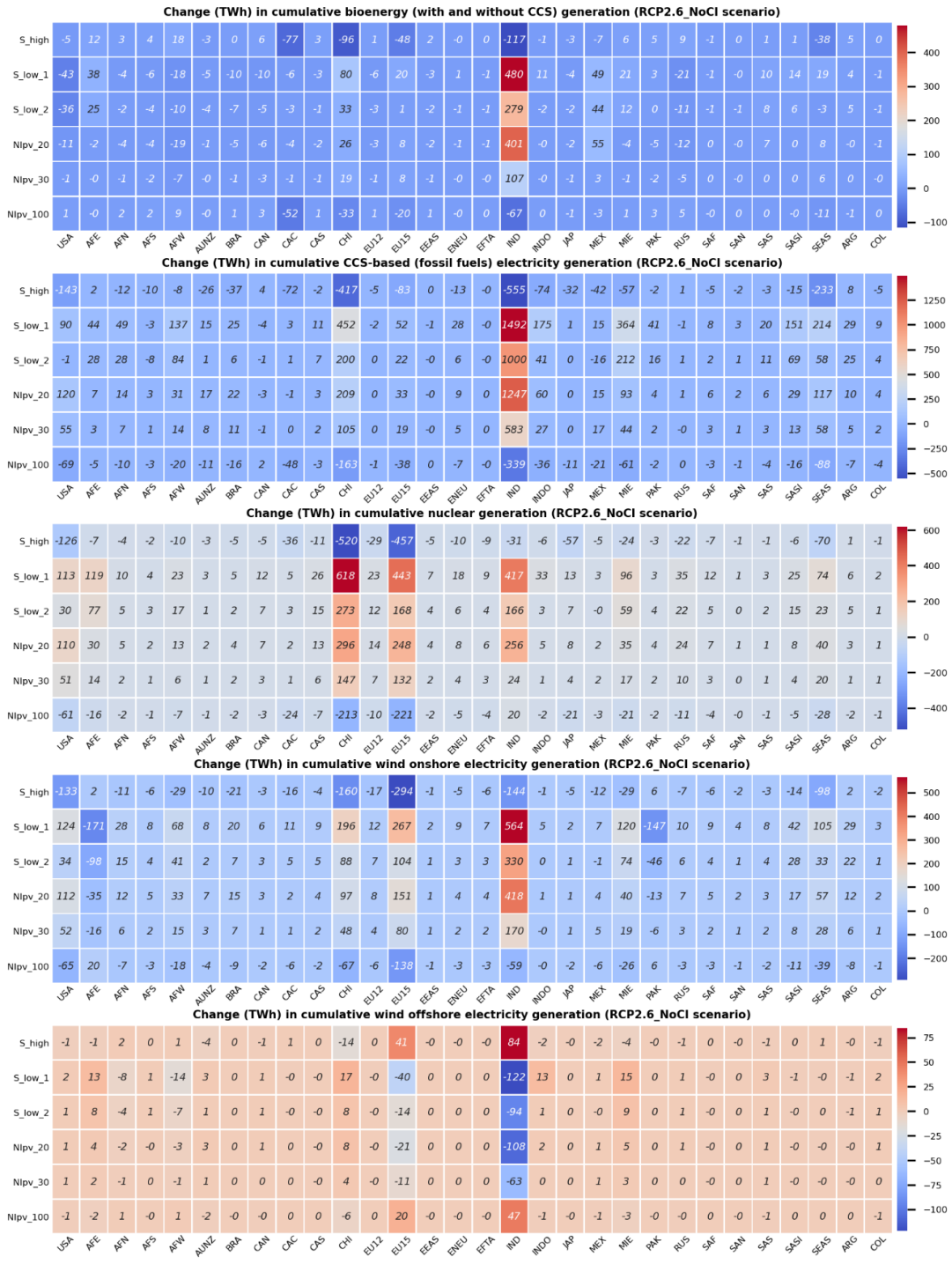

Figure 4.16. Changes in cumulative (2020-2100) electricity production by generating technologies relative to the solar PV *Central* case (*RCP2.6_NoCI* scenario).

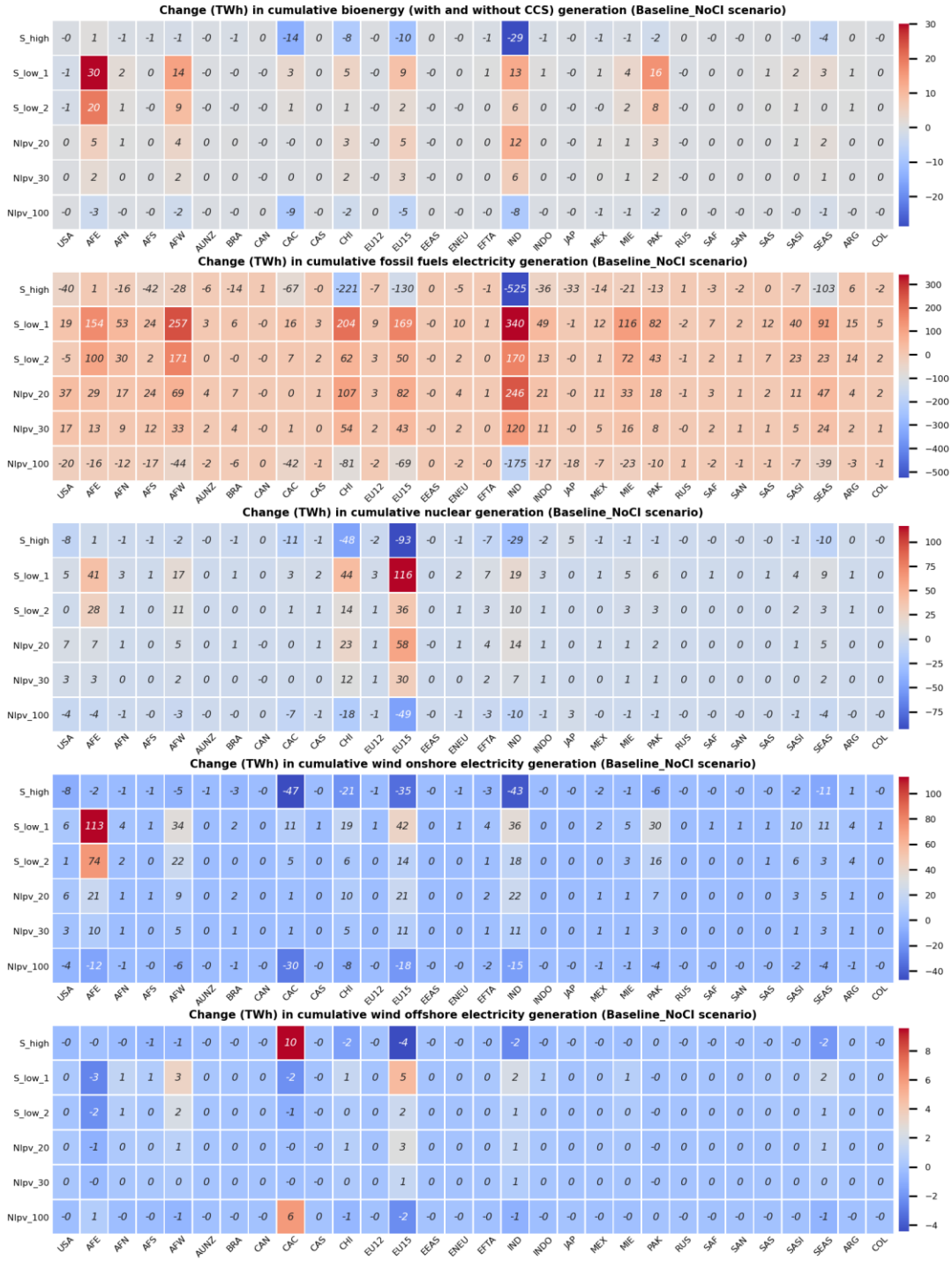

Figure 4.17. As in Figure 4.16 but for the *Baseline_NoCI* scenario.

4.5.4 Implications for the regional analyses of climate change impacts on the energy sector

GCM projections are largely uncertain for reasons that include our incomplete understanding of certain physical processes or inability to represent them accurately in the model as well as uncertainty in model parameters (Knutti et al. 2010). Due to these deficiencies, long-term projections made using different GCMs lie within an 'uncertainty envelope' in which the spread of outcomes challenges the planning of adaptation measures. This is illustrated in Figures 4.18-4.19 for changes in solar and wind resources using the ISIMIP2b GCMs. These changes strongly vary by region and, in general, the magnitudes and uncertainties of regional impacts under RCP8.5 tend to be larger than for the RCP2.6 scenario. In agreement with a recent global analysis also based on ISIMIP2b climate models (Gernaat et al. 2021), mean changes in the wind resource are considerably more pronounced than changes in solar PV energy. In this regard, another recent study (Karnauskas et al. 2018) using 10 CMIP5 GCMs has reported pronounced changes in the projected wind power under RCP8.5 for distinct regional domains around the world (for example, 42% in eastern Brazil and 41% in northeastern Australia by 2100).

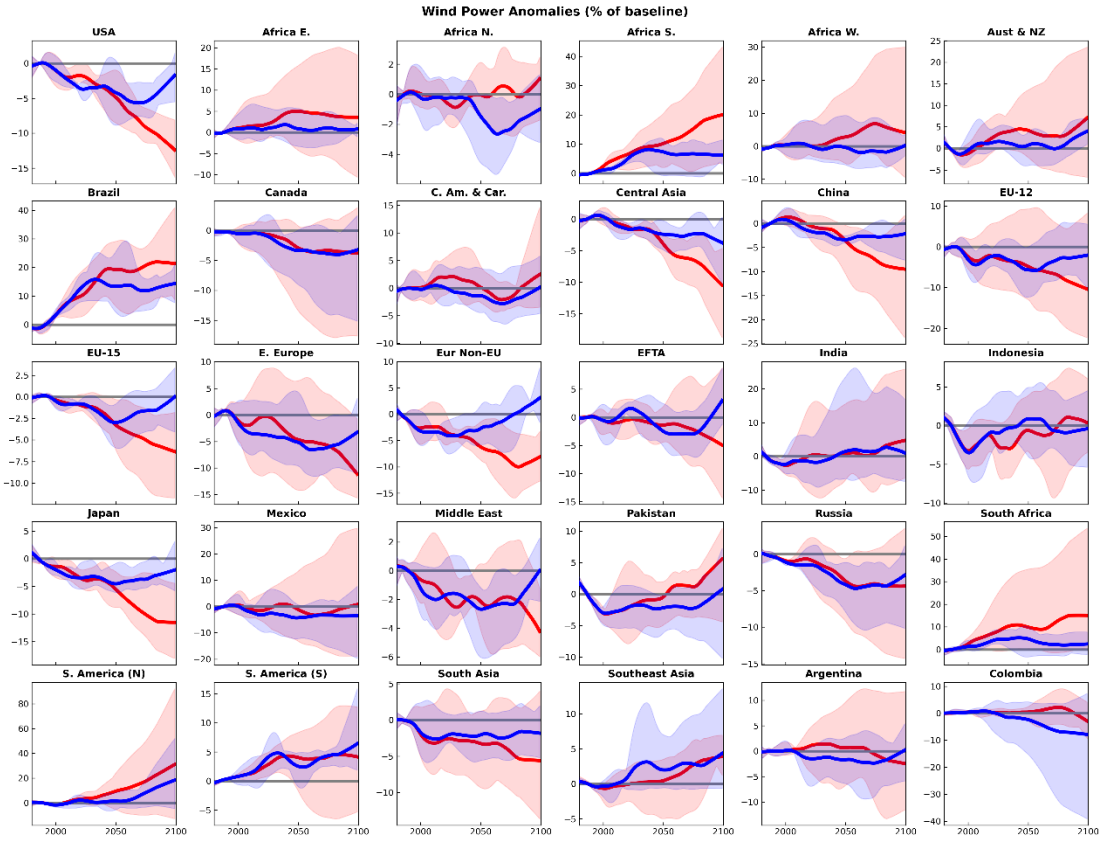

Figure 4.18. Evolution of wind power anomalies for the 30 GCAM regions analyzed in this study over the twenty-first century. Time series of changes in wind power (% of the baseline period 1971-2000) averaged across each region based on data from the four ISIMIP2b GCMs under RCP2.6 (blue) and RCP8.5 (red). Shadows show the ensemble spread and solid lines depict the ensemble mean values. Regional raw series are smoothed using the LOWESS filter with a window span of 25% of the 1971-2099 period (~30 years), which suppresses interannual variability. Note the different y axis scales.

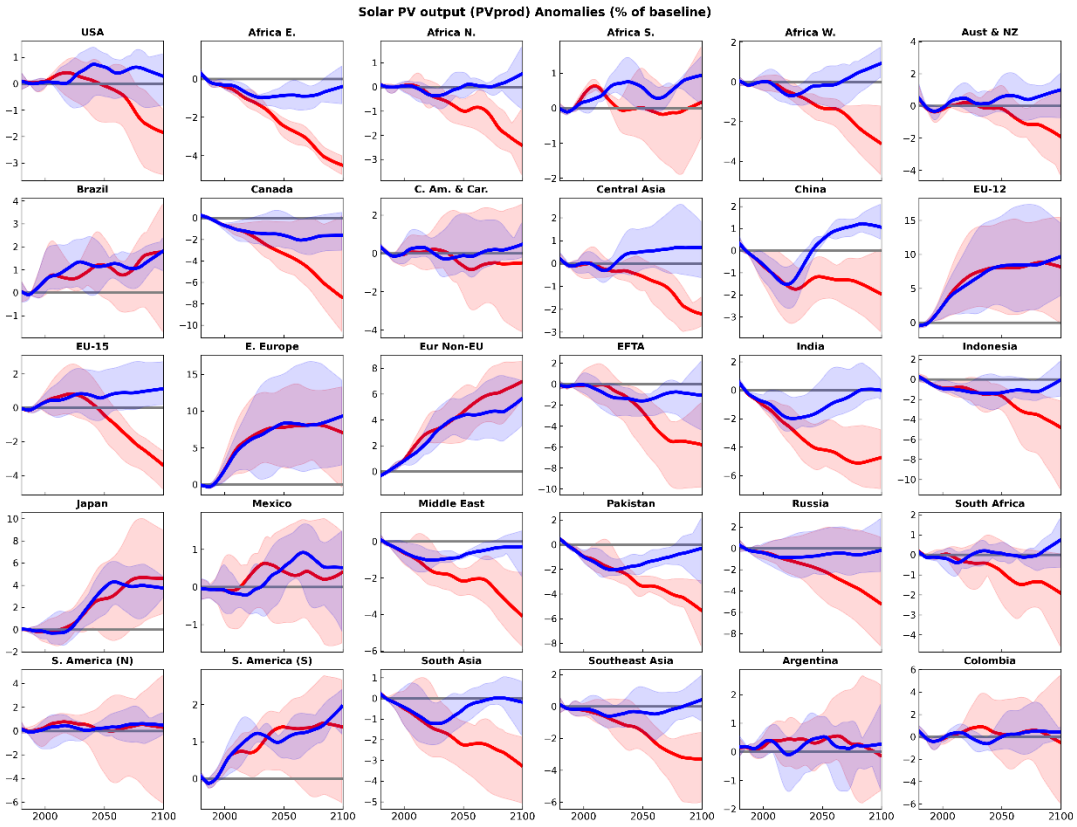

Figure 4.19. Evolution of PV power production anomalies for the 30 GCAM regions analyzed in this study over the twenty-first century. Time series of the estimated PV power production anomalies computed similarly as in Figure 4.18. PV power production (PV_{prod}) computed as $PV_{prod} = \eta_{PV} \cdot \overline{I_t}$ (Crook et al. 2011), with η_{PV} , PV panel efficiency, defined as in Eq. 9 and $\overline{I_t}$, the yearly-averaged solar radiation as in Eq. 8.

The uncertainty in future GCM projections is a known challenge within the climate change science. Given the repercussions in GCAM's projections of solar and wind electricity generation stemming from the uncertainties in renewables resource estimates discussed earlier, it is also important to understand how the assessment of climate impacts on regional intermittent renewable generation made using GCAM might be influenced by this type of uncertainty. Using again the GFDL-ESM2M model for illustration (because these insights are independent of the choice of GCM), Figures

4.20-4.21 show that the aforementioned parametric uncertainty translates into a considerable spread of differences in regional technical potentials (Appendix C; Figures C.10-C.11 provide the multi-model means). For example, in the USA, where the GFDL-ESM2M model projects reductions in both the solar PV and wind technical potentials, such a pattern means a range of differences between -159 (-139) and -8462 (-7666) TWh for the wind potential and between -63 (-21) and -1251 (-428) TWh for the solar potential under RCP8.5 (RCP2.6).

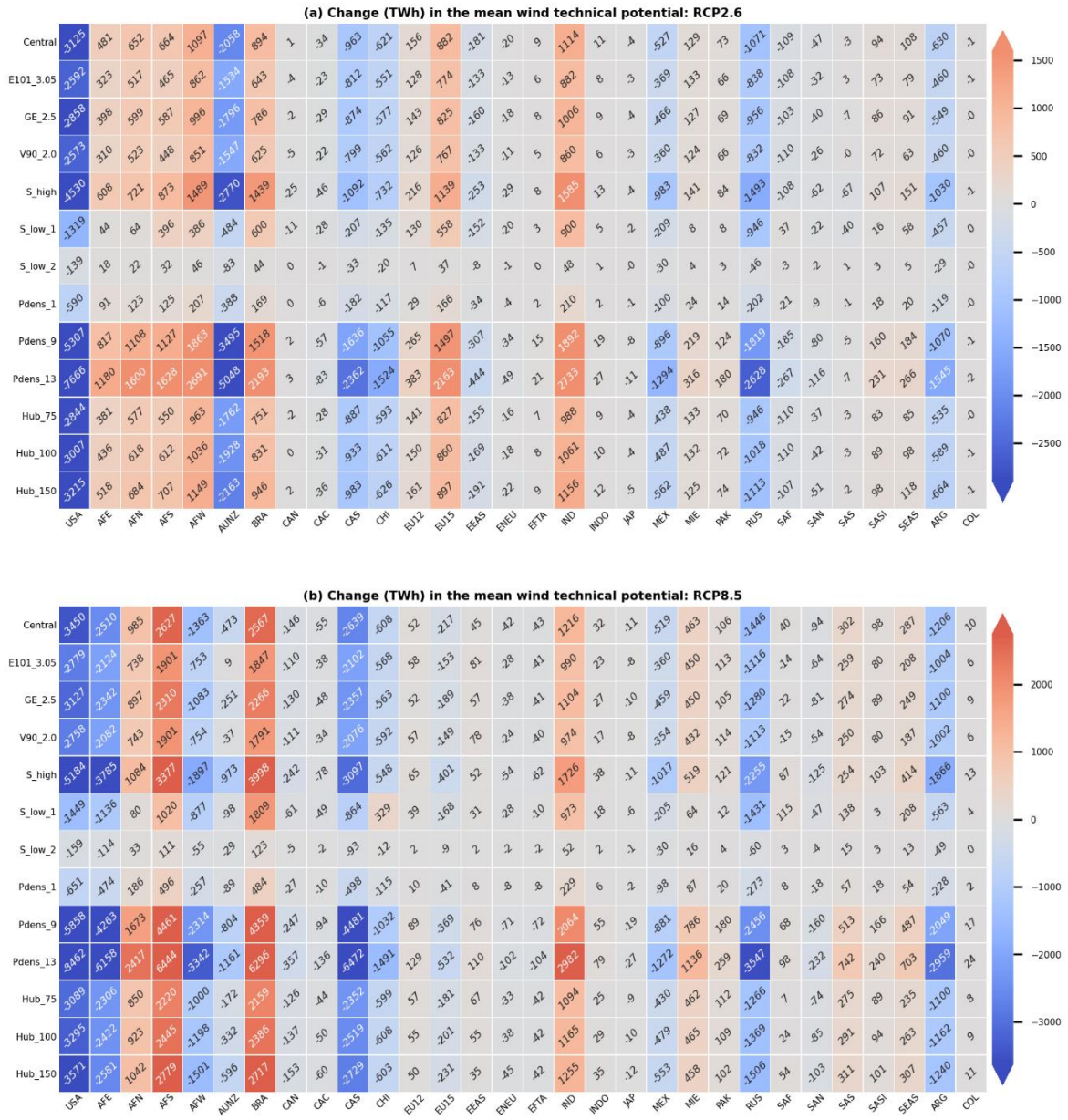

Figure 4.20. Change in annual mean wind technical potential (TWh) in 2071-2099 relative to the historical period (1971-2000) by forcing scenario (Input climate data: GFDL-ESM2M).

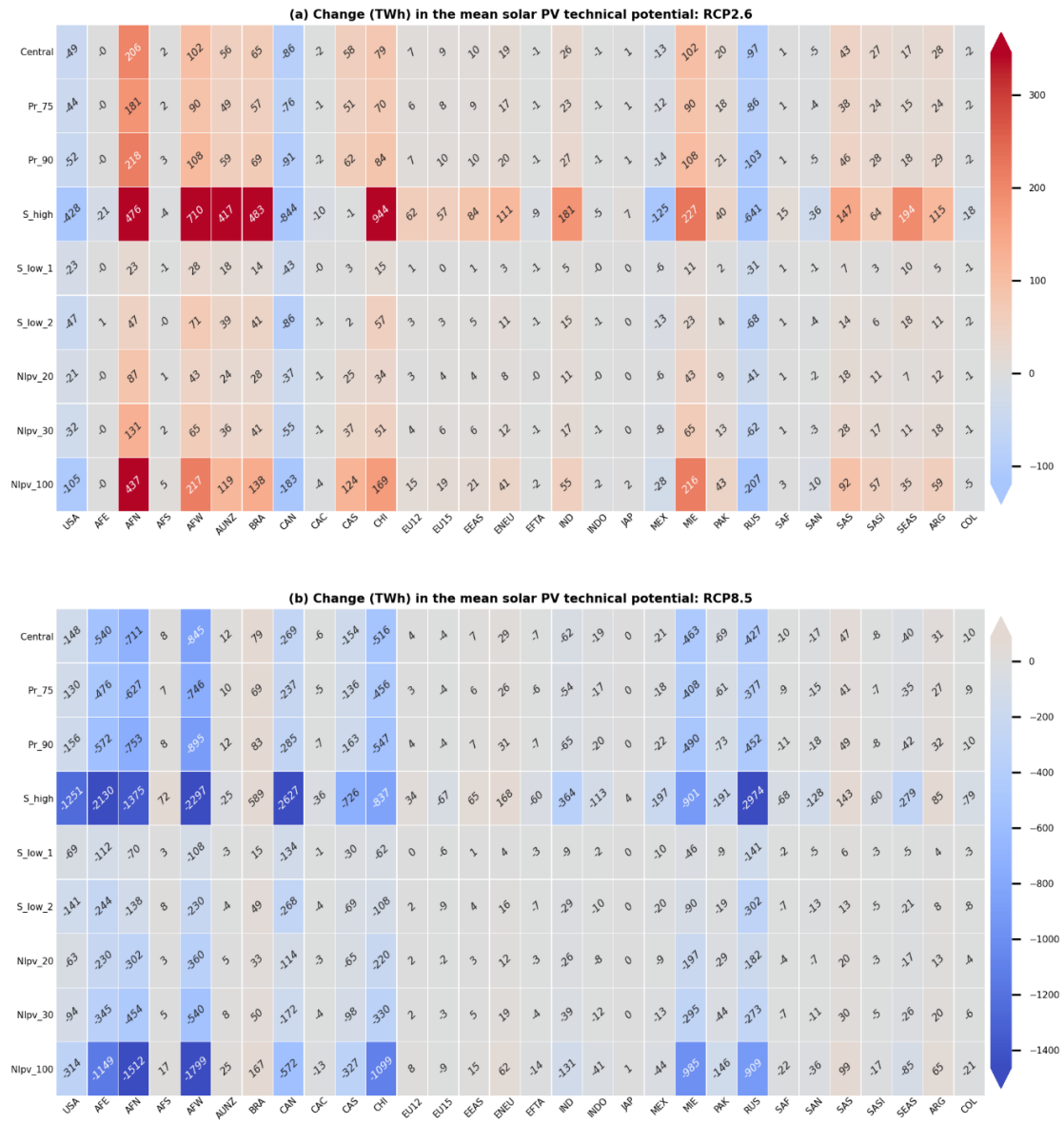

Figure 4.21. Change in annual mean solar PV technical potential (TWh) in 2071-2099 relative to the historical period (1971-2000) by forcing scenario (Input climate data: GFDL-ESM2M)

For the supply curves derived from the sensitivity cases under climate change assumptions these large variations with respect to the estimates of absolute differences in technical potentials translate into differentiated inputs into GCAM (in terms of cost and resource availability changes) that affect the economic decisions in the power sector differently. Figures 4.22–4.25 show that there are differing responses in

cumulative electricity generation changes to similar climate forcings due to the different supply curve assumptions. However, these effects vary substantially from region to region. For wind power in the *RCP2.6* scenarios, relevant effects are found in certain regions such as the USA, in which changes range between ~-3.5% and -15% considering the GFDL-ESM2M model, or the South America Southern and Middle East regions with changes ranging between 5% and 40% and -5% and -25%, respectively, for the MIROC5 model. Considering the *Baseline* scenarios, there are examples of more pronounced effects like in Brazil with relative changes in generation varying between ~18% and 60% for the GFDL-ESM2M forcing or in Southern Africa with changes between 20% and 65% for the IPSL-CM5A-LR model. On the other hand, these differences are generally unimportant in regions where the climate change forcing is weak like in Indonesia in both set of scenarios. The latter helps to explain the situation of solar power. Changes in solar electricity production are predominantly lower than those in wind power because of the less pronounced climate impacts in solar mentioned above. Hence, the effects from the varying supply curves, although evident in Figures 4.24-4.25, tend to be less impactful than in wind. This implies that within a context of weaker impacts, the effects from the parametric uncertainty play a less relevant role in affecting the overall assessment of climate impacts on renewable generation using GCAM. For example, in the USA, the change in solar generation considering the GFDL-ESM2M model in the *RCP2.6_CI* scenario for the *Central* case is of ~-2.5% relative to the *RCP2.6_NoCI* scenario whereas the range of variation across all cases lies between -0.5% and -3.5%. These changes are even less pronounced under the *Baseline* scenarios. There are also few examples in which the overall

generation changes are more pronounced, but the parametric uncertainty effect is not relevant. These regions include Canada, Europe Eastern and Russia under both set of scenarios. On the other hand, important changes due to the parametric effect are found in few regions like European Free Trade Association under both the *RCP2.6* and *Baseline* scenarios for the MIROC5 model (changes varying between ~-3 and -20%).

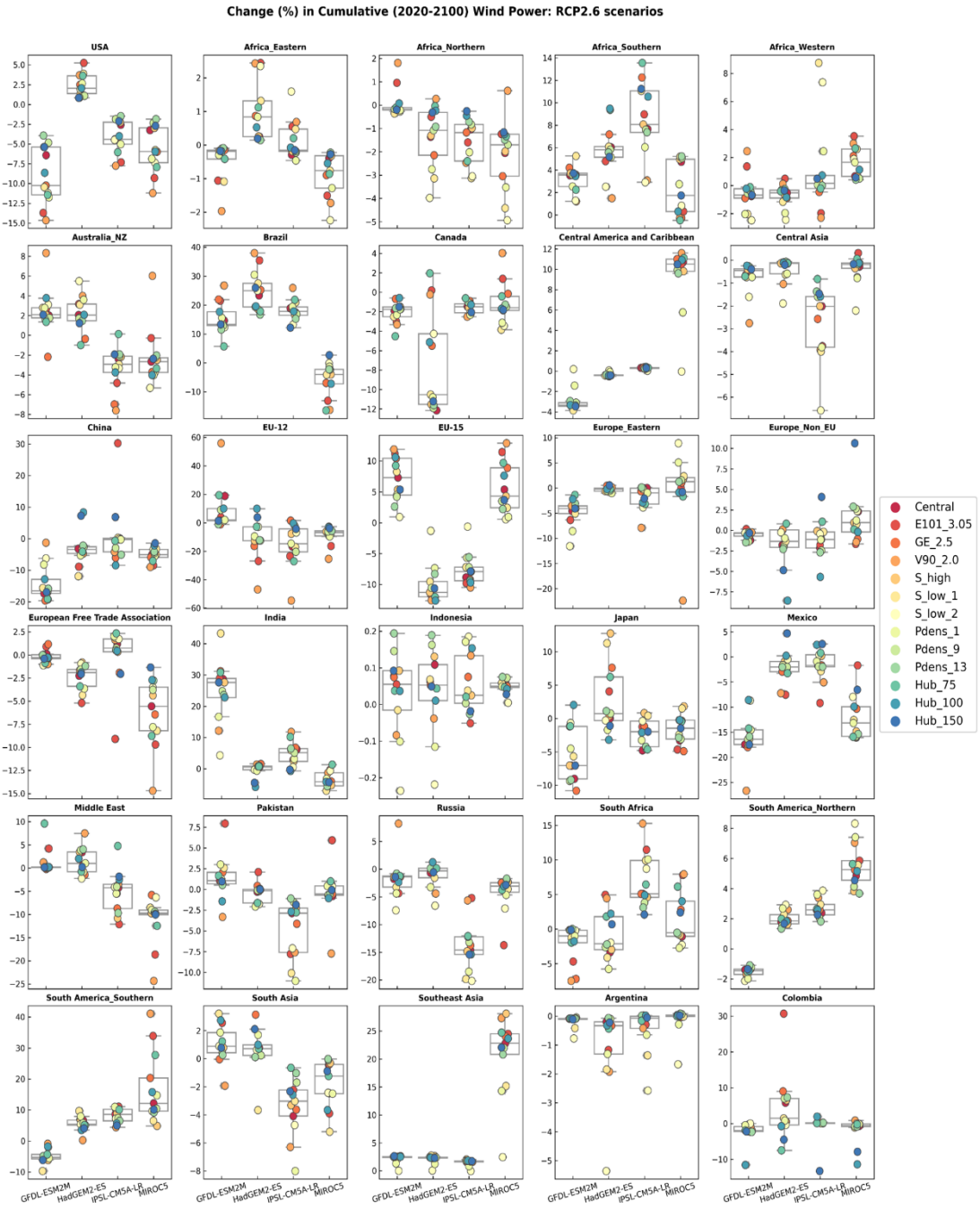

Figure 4.22. Regional changes (%) in cumulative (2020-2100) wind power generation: *RCP2.6_CI* scenario relative to the *RCP2.6_NoCI* scenarios.

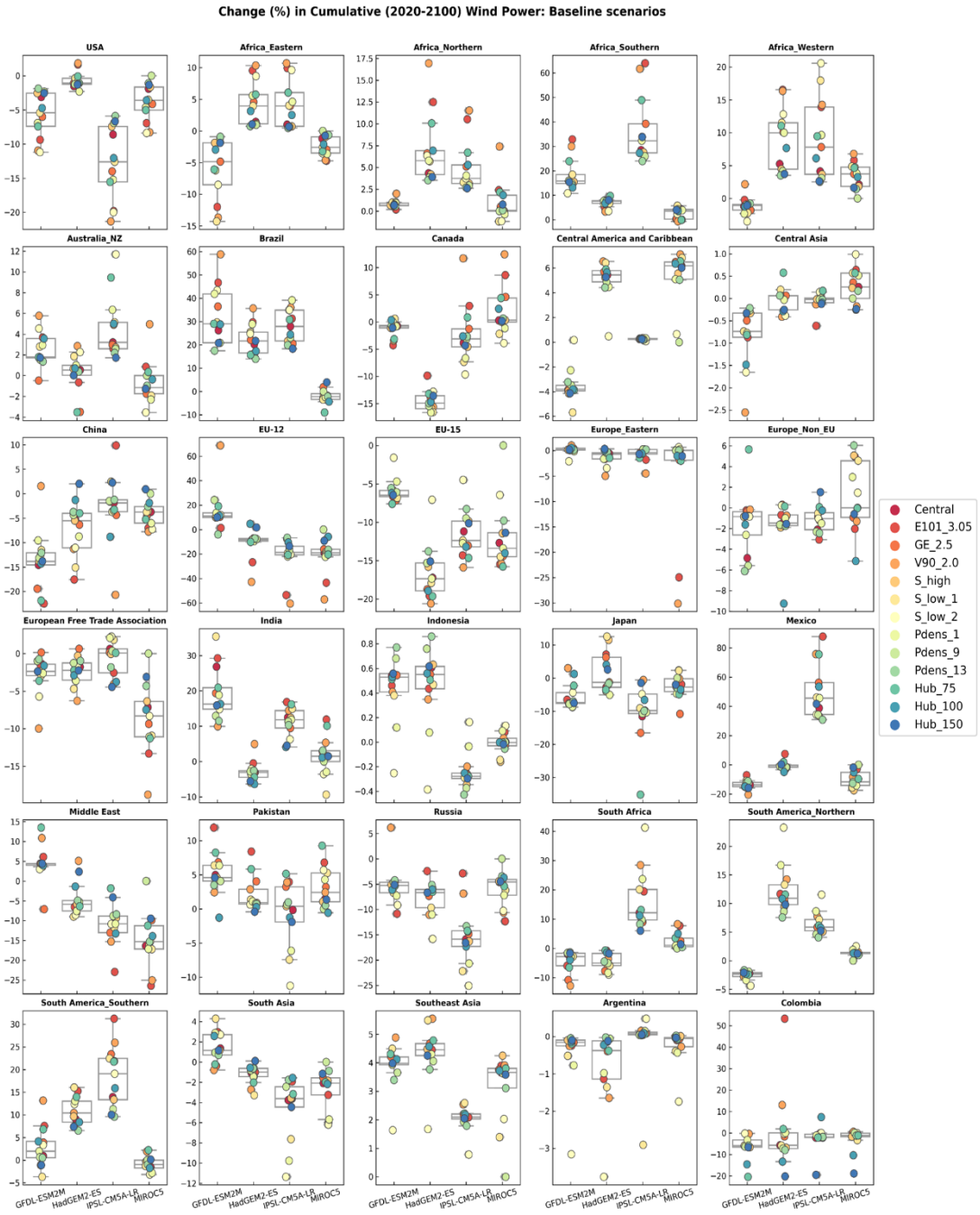

Figure 4.23. Regional changes (%) in cumulative (2020-2100) wind power generation: *Baseline_CI* scenario relative to the *Baseline_NoCI* scenarios.

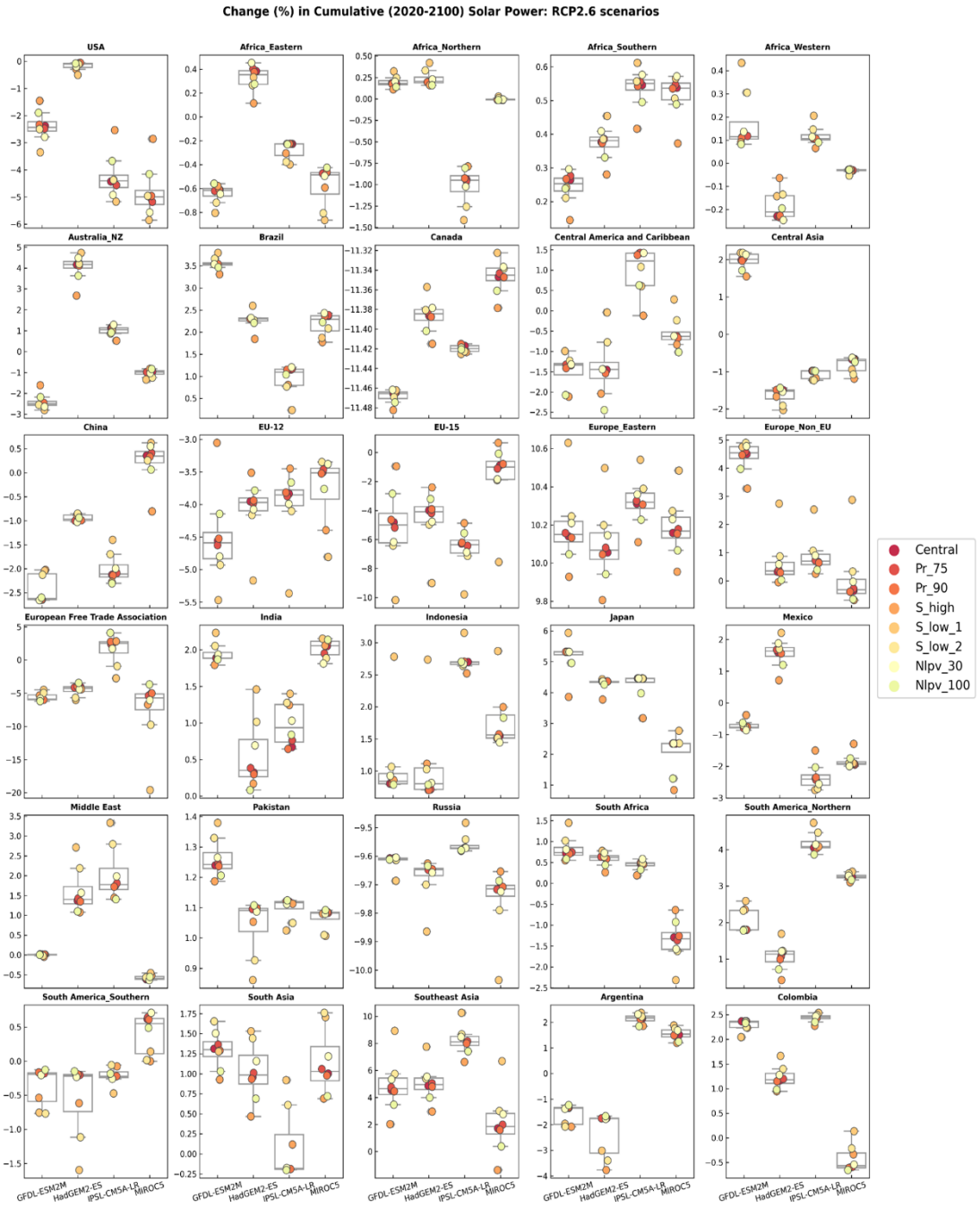

Figure 4.24. Regional changes (%) in cumulative (2020-2100) solar power generation: *RCP2.6_CI* scenario relative to the *RCP2.6_NoCI* scenarios.

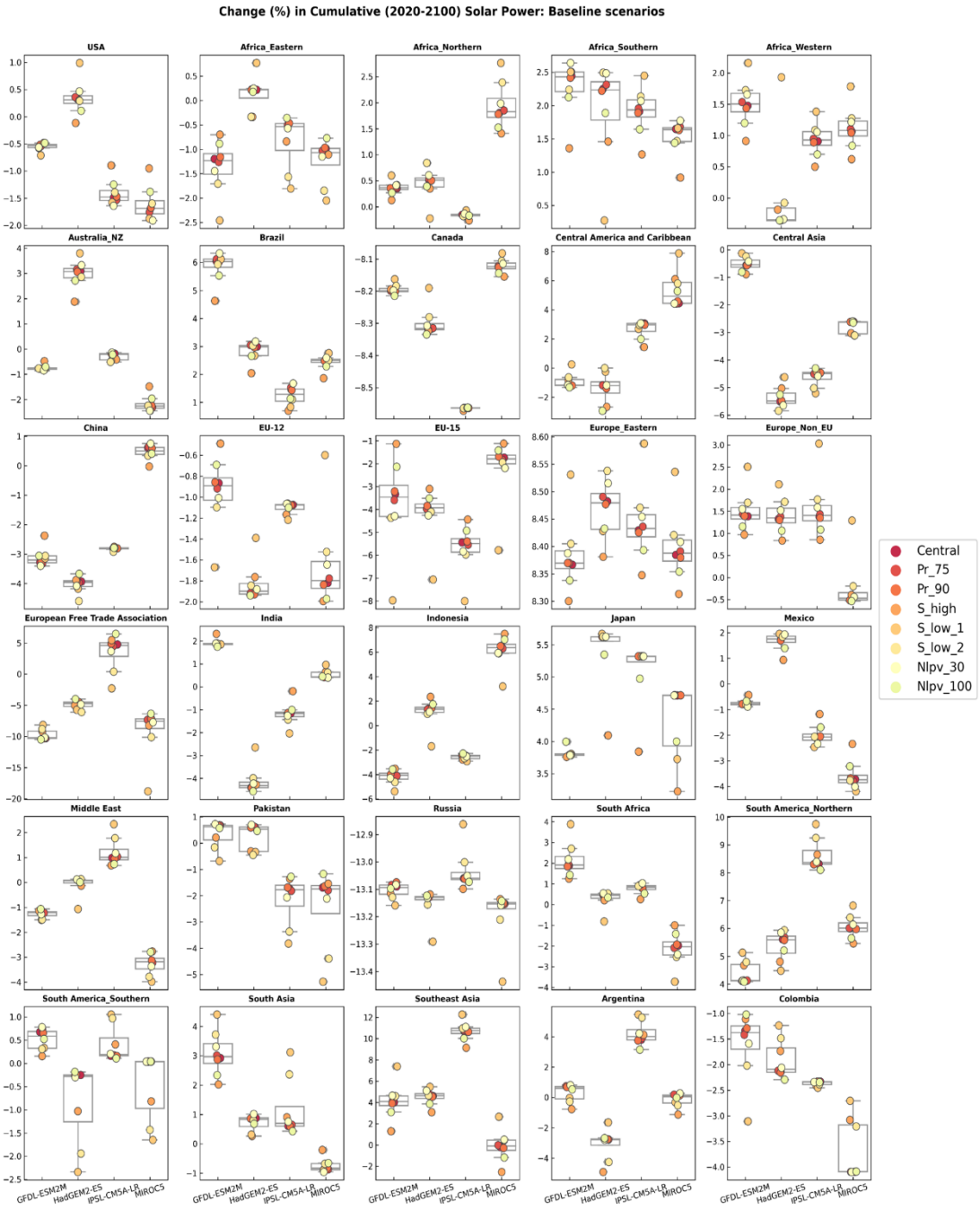

Figure 4.25. Regional changes (%) in cumulative (2020-2100) solar power generation: *Baseline_CI* scenario relative to the *Baseline_NoCI* scenarios.

Figures 4.22-4.25 also contrast the effects from uncertainties due to GCM projections against those from the supply curve assumptions. There are large disparities on the projections of changes in generation due to the choice of GCM. This can be illustrated with the case of the EU-15 region under the *RCP2.6* scenarios for wind. It can be noticed that the choice of GCM markedly shifts the distributions with two GCMs pointing out positive effects whereas the other two indicate negative impacts. This lack of agreement creates ambiguity with respect to the direction of the climate change impact. Likewise effects associated with GCM uncertainty, effects from the parametric uncertainty create decision-making challenges. As noted above these effects are large for some regions, particularly for wind power. This is the case of India in the *RCP2.6* scenarios. In this region, the wind power change projections from the GFDL-ESM2M model reveals a wide range of outcomes associated with the sensitivity cases (~5% to 45%). This is larger than the differences across all GCMs (using the median of the distributions as the reference for comparison). Moreover, effects concerning the direction of changes can be noticed in few regions like the Europe_Non_EU region in the *Baseline* scenarios of wind power for the MIROC5 model (changes within -5% to +6%).

For a better understanding of the implications for GCAM electricity projection changes due to the adoption of different supply curve assumptions, it is instructive to focus on a smaller set of regions and sensitivity cases. For wind power, the distinct input assumptions result in notable differences in gains or losses in power production in each region (Figure 4.26). In Central Asia, for example, the total loss of wind power under the Low Suitability_II (*S_low_II* in prior figures) case is more than double the

losses found in all other cases. Conversely, in Brazil, the lowest wind power gains are found in the *Low Suitability II* and *Hub Height 75 m* cases, which are about one third of the increases found in the *Central*. Each sensitivity case can impact wind power changes very differently. This is seen for the *Low Suitability II*, which is associated with the largest generation losses in Central Asia and Russia, as well as with the smallest negative differences in China and Mexico. As mentioned earlier, the final effect on generation changes depends on how the power-sector market competition is affected by each supply curve. Generally, the *Low Suitability_II* and the lowest power density case (*Pdens_1* in prior figures*)* cases are associated with the most marked differences relative to the *Central* case.

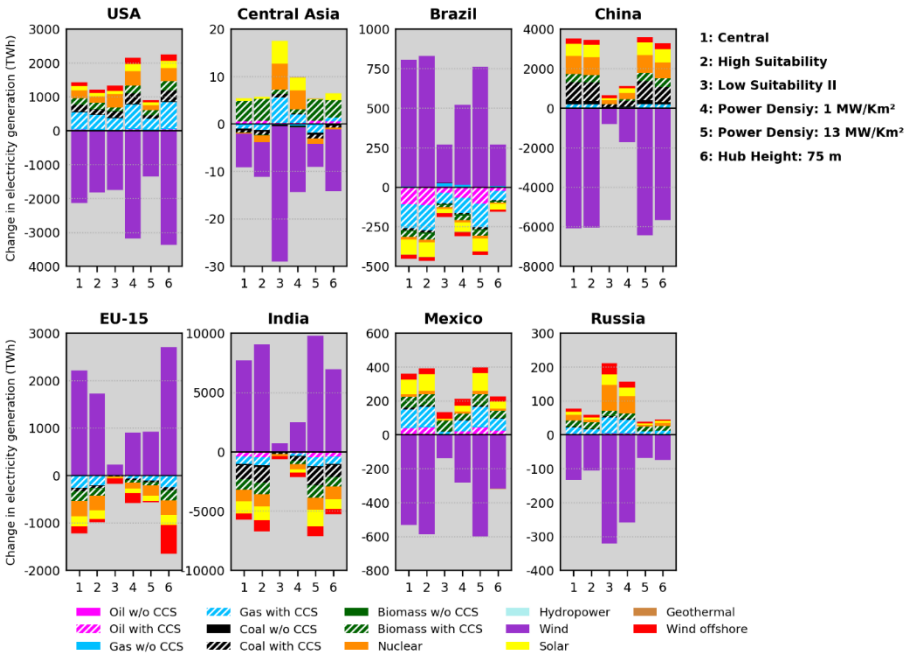

Figure 4.26. Regional differences in electricity production by technology assuming climate change impacts on wind only. Differences (*RCP2.6_CI - RCP2.6_NoCI* scenarios) are calculated by technology using cumulative generation during the 2020─2100 period. Note the different y axis scales.

Results for the *Baseline* scenarios (forced with input climate data from RCP8.5) show similar patterns but considerably lower absolute differences compared with the *RCP2.6* scenarios (except for Brazil) (Figure 4.27). Although counterintuitive given

the overall more pronounced climate impacts on technical potentials under the RCP8.5, having significantly more renewables in the power mix, as seen in the *RCP2.6* scenarios with about ~three times more renewables in 2100, contributes considerably more to accentuate the magnitudes of impacts in generation. It can be noted that the relative differences among sensitivity cases are less pronounced compared with the *RCP2.6* scenarios in regions like Brazil, China, Mexico and Russia.

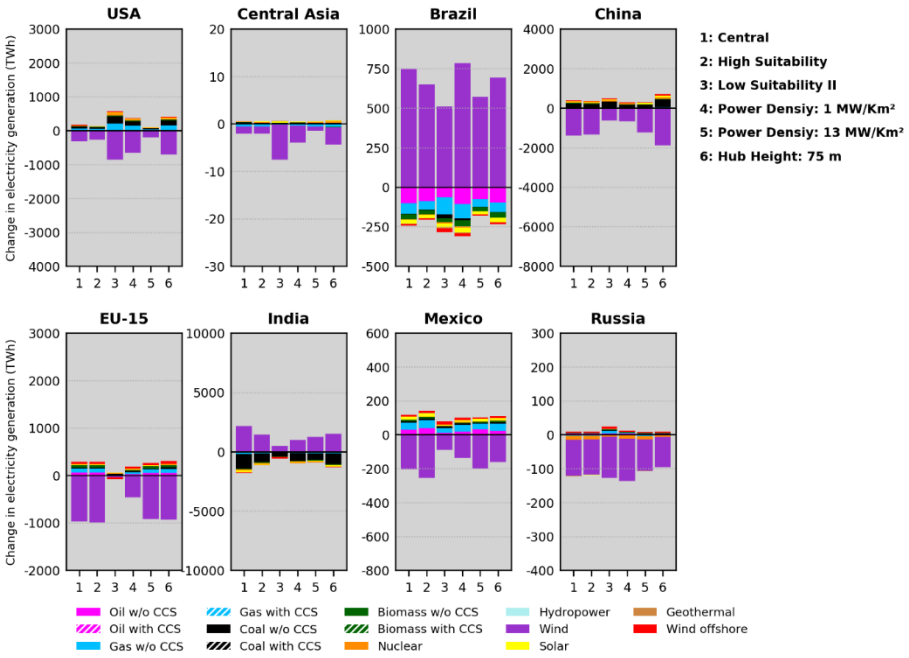

Figure 4.27. Regional differences in electricity production by technology assuming climate change impacts on wind only. Differences (*Baseline_CI - Baseline_NoCI* scenarios) are calculated by technology using cumulative generation during the 2020─2100 period. Note the different y axis scales.

In the case of solar power, the variation of differences across sensitivity cases is, in general, less marked than in wind power (Figures 4.28-4.29). In certain regions there is no major effect from the different supply curve assumptions, particularly under the *Baseline* scenario. The most notable exception is the EU-15 region (USA and Mexico also show some considerable differences relative to the *Central* case under the *RCP2.6* scenarios).

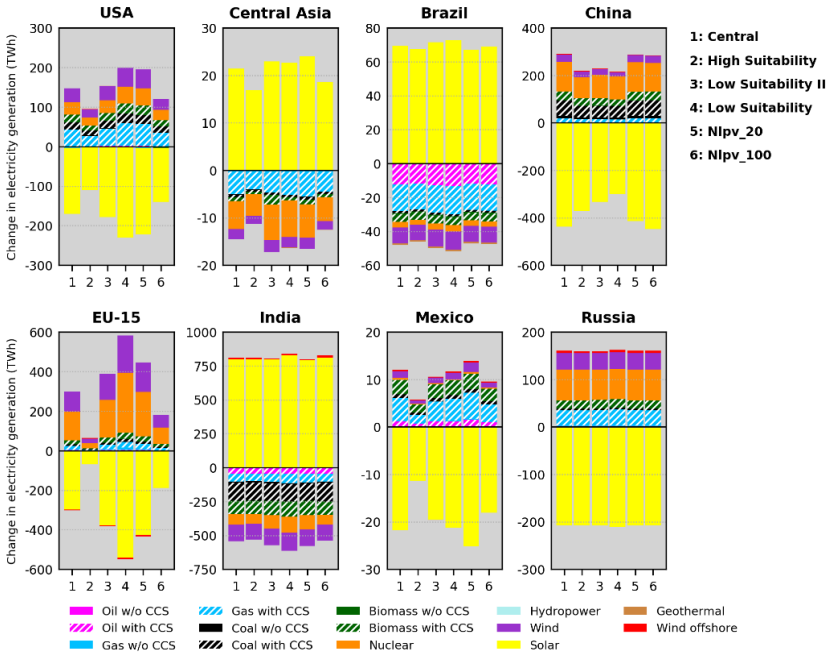

Figure 4.28. Regional differences in electricity production by technology assuming climate change impacts on solar only. Differences (*RCP2.6_CI – RCP2.6_NoCI* scenarios) are calculated by technology using cumulative generation during the 2020─2100 period. Note the different y axis scales.

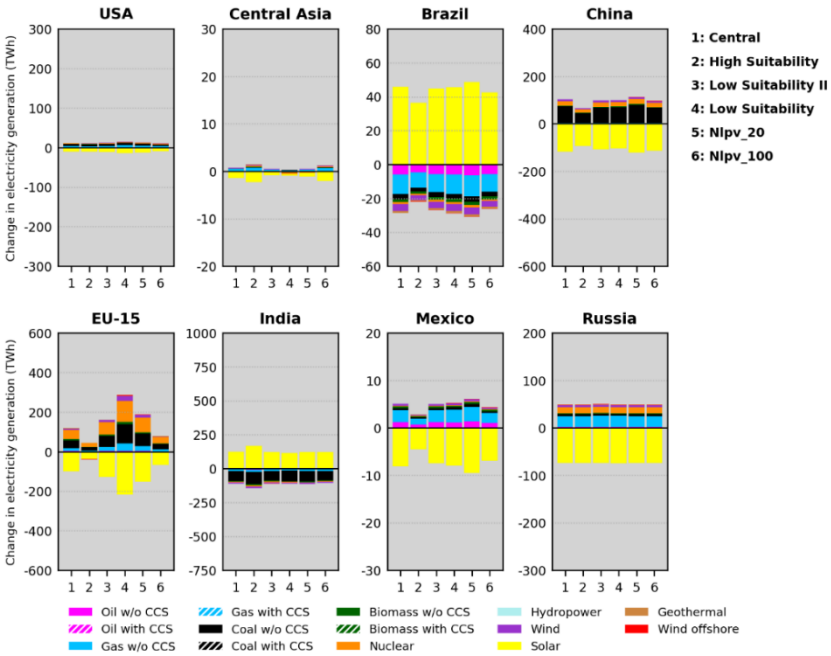

Figure 4.29. Regional differences in electricity production by technology assuming climate change impacts on solar only. Differences (*Baseline_CI - Baseline_NoCI* scenarios) are calculated by technology using cumulative generation during the 2020─2100 period. Note the different y axis scales.

From the above discussion, the most relevant insights are that the uncertainties embedded in the resource estimates can affect the level of adaptation effort the model uses to compensate for deteriorated generation or modify the model assessment of positive effects on generation. As shown in Figure 4.26, the effort and technology options to compensate for wind power losses in Central Asia in the *Low Suitability II* case markedly differs from those in the *Central* case. The first case uses as adaptation options generation from natural gas with CCS and nuclear sources that are not contemplated by the *Central* case as well as significantly more solar power. Conversely, the uncertainty surrounding possible gains in wind-based generation in Brazil or in India in the *RCP2.6_CI* scenario can have repercussions on derived analyses, such as the assessment of capital investment requirements, which may be overestimated. This is more likely to happen in scenarios with pronounced deployment of intermittent renewables since prior analyses have shown they are associated with larger needs of capital investments (Iyer et al. 2017; Santos da Silva et al. 2021)

Conclusions

Renewable energy is expected to play an increasingly important role in meeting ambitious global objectives, such as the sustainable development goals and climate change mitigation. To understand the future contribution of intermittent renewables into these objectives, policy-makers have relied heavily on scenarios from IAMs such as GCAM. As one of the main goals of IAM scenarios is to explore distinct energy technology pathways, it is essential to understand how sources of structural uncertainties in IAMs can affect electricity projections from these models.

This study is the first to investigate the implications for an IAM of the uncertain assumptions on parameter values used to quantify the solar and wind technical potentials. Specifically, a framework has been developed to compute the solar PV and wind global technical potentials to produce distinct estimates using varying assumptions of key parameters used in the computation of these potentials. The various technical potentials estimates were used to produce supply curves that were implemented in GCAM for the assessment of the consequences for the intermittent renewable electricity generation. The results demonstrate that the GCAM solar PV and wind power projections are markedly affected by the parametric uncertainties embedded in the supply curves. Although GCAM has been used in this analysis, this result is relevant to the broad IAM community since many IAMs rely on supply curves to model solar and wind resource availability and costs of production.

The ensemble of technical potential cases investigated in this analysis were produced based on a literature review, which identified a list of parametric assumptions used to compute solar PV and wind technical potentials in prior studies. This survey by

itself constitutes an important contribution to the scientific community since it can help to guide future RE potential assessments and sensitivity studies. It is shown that the choice of parameters related to land-use together with power density (i.e., the average turbine installation density) in the case of wind onshore have a significant impact on the technical potential estimate. In the case of the wind technical potential, the choice of the turbine technology is also important. These cases of larger impact on the technical potential are the most influential in GCAM electricity projections, although assumptions that reduce the technical potential are more impactful than the ones that increase the potential due to the model's limitation on substantial RE deployment. Depending on the input supply curve assumption, intermittent RE generation can be greatly increased or reduced, which affects the role of the renewable relative to other technologies in quantitative IAM scenarios. This has repercussions for the overall energy system planning and for the assessment of climate change mitigation strategies.

The results also highlight potential implications for the analyses of climate change impacts on solar and wind sources that rely on the implementation of climate-impacted supply curves as proposed by recent studies (Gernaat et al. 2021; Yalew et al. 2020). It is found that GCAM can translate the uncertainty in the input assumptions into a range of projected outcomes expressing gains in RE generation or varying degrees of adaptation effort (as well as adaptation options). However, the extent to which uncertainties in resource estimates affect the analysis of climate impacts on the energy sector using GCAM scenarios depends on the modeled mitigation effort and on the severity of the climate impact signal. Hence, mitigation scenarios with large deployment of intermittent RE and that account for climate impacts on wind are the

most affected. Although not verified in this study, the results suggest that the implications for climate change analyses could be even more pronounced in mitigation scenarios with limited or no deployment of CCS and nuclear technologies, in which emissions reductions from the power sector are largely achieved with the addition of intermittent renewables. It is also concluded that the parametric uncertainty explored in this study can be as challenging for decision-making as the uncertainty associated with GCMs projections.

Depending on the spread of projected outcomes, there may be important cascading effects on other derived quantitative estimates, such as capital investment requirements, as noted earlier. An exploration of this potential effect merits future work. This work stresses that the parametric assumptions tested here were chosen for their potential effect on the resource estimates. However, this list is by no means exhaustive and could be expanded in future studies. Examples of parameters not tested are array availability and array efficiency in the case of wind and panel efficiency in the case of solar PV. Future studies should also expand this analysis to other GCAM technologies not covered in this study: solar CSP, solar rooftop PV and wind offshore. The climate impacts dimension of the scenarios analyzed in this study focuses on wind and solar for a specific analysis of the interplays between climate impact assumptions on these sources and the uncertainty stemming from the supply curves. Future work could expand this framework by including climate impacts on the other renewables, i.e., agricultural crop yields that affect biomass and hydropower, and on the water supply. This will help to understand if within a context of multiple and simultaneous

impacts, the effects from the parametric uncertainty on solar and wind projections might be dampened or exacerbated.

The results underscore the need of careful consideration of the parametric choice in RE technical potential estimates. However, narrowing this type of uncertainty is a difficult undertaking. Prior studies (Bosch et al. 2017; Deng et al. 2015; Rinne et al. 2018) have emphasized the quality of the datasets used pointing out for the need of high-resolution datasets and analyses. In this regard, it is acknowledged that this study is conducted within a relatively low resolution (0.5^{o} spatial resolution), which is sufficient to support the points raised in this research although it misses details at finer local scales. However, even with the use of high-resolution/high-quality datasets, certain assumptions will continue to be highly uncertain, such as the land suitability factors. As seen in the results, the assumptions concerning suitability factors are highly influential, but there is no methodology to derive them. These factors have been derived based on authors' judgement. Indeed, even recent analyses (Bosch et al. 2017; Eurek et al. 2017; Gernaat et al. 2021) use suitability factor assumptions from studies published in the 2000's highlighting the difficulty to develop more precise approaches. For this reason, recent RE technical potential estimates (Deng et al. 2015; Rinne et al. 2018) have defined distinct land-use scenarios to try to improve upon this uncertainty issue. This could be considered the path forward for the other influential parameters. In this regard, De Vries et al. 2007 have suggested that 'scenario-based' assessments could be useful in communicating the wide range of outcomes resulting from the uncertain factors such as land use and technology. However, a deeper understanding of the implications of this uncertainty issue for IAM projections will require sampling of

a broader range of technical potential cases than the ones explored in this study within a formal sensitivity analysis. In this context, a more robust analytical framework appears particularly relevant for climate change analyses incorporating impacts on solar and wind supply curves because of the complexity added by the uncertainties from the GCM projections. The results then suggest the need of an ample debate within the IAM community that might result, for example, in a subsequent model intercomparison exercise using models with varied representations of energy systems. This would allow an understanding of the effects of the uncertain supply curves on the long-term energy scenarios from these models. As acknowledged in the literature, such diagnostic experiments are needed for a more explicit and transparent treatment of the deep uncertainties and structural dynamics in IAMs (van Vuuren et al. 2010).

Chapter 5: Concluding Remarks and Future Work

5.1 Concluding Remarks

Integrated assessment modeling is a vital piece of climate change science, particularly as it relates to important societal sectors such as energy, water and land. There is a wide recognition of the need of meaningful and credible IAM scenarios to support decision-making and the climate change science in general. To maximize the usefulness of IAM scenarios, the IAM community has recently prioritized assessments of country-specific mitigation policies over analyses at highly aggregated spatial-scales as well as research on the interactions across climate impacts, sectors, and sustainable development objectives (Fisher-Vanden; Weyant 2020). This dissertation aims to contribute to these recent research efforts, exploring specific research gaps within the contemporary IAM research that represent clear opportunities to enhance the value of GCAM scenarios to decision makers and contribute toward future model developments.

Chapters 2-4 together contribute in three important ways to the overarching goal of the study. First, the research presented in all chapters are novel in scope, encompassing questions that have received little or no attention by the IAM community. The second contribution lies on their relevant specific approaches and insights that offer improvements relative to prior analyses. Lastly, the code used to produce the solar and wind technical potentials in Chapter 4 will be made available to the scientific community. This code (written in Python) will become part of the suite

of open-source packages of the Joint Global Change Research Institute (which are hosted at https://github.com/JGCRI). This package is expected to help researchers build renewable technical potential assessments based on the assumptions described in Chapter 4. The IAM community can, for example, produce resource estimates based on different parametric assumptions and examine the effect of supply curves produced from these estimates in IAMs. Besides the open-source approach, the code has the advantage of being modular so that users can customize or replace individual components.

The following findings are provided by the completion of this Ph.D. dissertation:

Chapter 2

Research question: *What type of implications might be triggered by NDC mitigation strategies in line with the climate goals of the Paris Agreement on the EWL nexus resource systems in Latin America*?

By developing mitigation scenarios in which targets are consistent with the NDCs submitted by Argentina, Brazil, Colombia and Mexico, followed by stringent post-2030 emissions reductions assumptions, implications have been found associated with the portfolio of mitigation strategies in place. Those can be summarized as follows: (1) growing irrigation demands up to the midcentury in all countries, except for Brazil (associated with the land- and water-use impacts of forest protection measures); (2) larger irrigation demands to cultivate bioenergy crops in Mexico (land- and water-use impacts of energy decisions); and (3) larger electric-sector water withdrawals in

countries that largely deploy CCS over the long-term (Mexico and Brazil) versus reduced demands when CCS is unavailable (water-use impacts of energy decisions).

Key Insights:

(1) The analysis of mitigation scenarios using Latin American countries as case studies demonstrates that multi-sector modeling is critical for assessing the EWL nexus because of the diverse constraints on EWL resources and the interactions with policies affecting different sectors.

(2) Mitigation pathways need to be assessed within an EWL nexus perspective that balances interactions across multiple sectors to better understand the trade-offs and synergies associated with meeting future climate goals.

Implications for policy-/decision-making:

The Paris Agreement includes a framework in which countries report their emissions periodically and monitor the progress of their pledges ('global stocktake'). This process intends that countries can enhance their commitments to make sure that the long-term goals of the Paris Agreement can be achieved. Given the possibility of negative repercussions of mitigation policies on the EWL nexus resources as highlighted in this analysis, the results suggest that considerations concerning EWL nexus issues should be accounted for during the review process of NDCs. In other words, the results suggest revising the NDCs within an integrated multi-sector analysis that can identify key areas of conflicts across EWL nexus sectors. This is in line with arguments in the literature (Iyer et al. 2017, Iyer et al. 2018, Peters et al. 2017) that highlight the value of a broader process of assessment of the progress of the NDCs through a multi-objective

framework that incorporates, for example, the implications of NDCs on sustainable development objectives.

Chapter 3

Research question: *What are the implication of climate impacts on renewables on the electricity sector in Latin America in terms of electricity generation and capital investment requirements? How do these implications change under alternative energy technology pathways and modeling approaches?*

By developing scenarios that vary across the level of climate change mitigation, climate impacts on renewables and technology availability, likely implications have been found on electricity generation due to climate impacts that vary strongly by region. It is found that accounting for climate impacts on renewables can result in additional investments ($12─114 billion by 2100 across Latin American countries) for a region with weak financial infrastructure. It is also demonstrated that accounting for climate impacts only on hydropower – a primary focus of previous studies – can significantly underestimate cumulative investments, particularly in scenarios with high intermittent renewable deployment.

Key Insights:

(1) IAM scenarios that explore the consequences of climate change impacts on renewable energy for the electric power sector need to adopt a comprehensive modeling approach that accounts for climate change impacts in all renewables.

(2) There are risks of misrepresentation of climate change effects on the electric power sector if climate impacts on all renewables are not accounted for in the

modeled scenarios, particularly for energy pathways with pronounced intermittent renewables deployment.

Implications for policy-/decision-making:

The multi-impact modeling framework presented in this study can be used by energy planners to understand the overall vulnerability of regional power systems to climate impacts on renewables under alternative mitigation and no-policy scenarios and to assess the potential monetary consequences for the planning of generation capacity.

Chapter 4

Research question: *What are the implication of key parametric uncertainties in the computation of renewable energy potentials for GCAM solar and wind electricity production? Which parameters drive the largest changes? What are the potential implications for decision-making on climate change mitigation and impacts?*

Based on a review of parameter values used in prior renewable potentials estimations, it is found that this parametric uncertainty results in substantial variations in intermittent generation projections with a prominent role of assumptions related to land-use in both solar PV and wind onshore technologies and average turbine installation density for wind onshore. Consequently, the role of these renewables in modeled long-term scenarios can be under- or overestimated relative to other technologies.

Key Insights:

(1) GCAM projections of solar PV and wind onshore electricity generation can be largely affected by methodological uncertainties in the computation of

renewable energy potentials that are used to produce the resource cost-supply curves needed as input assumptions to IAMs.

(2) There may be potential implications for decision-making on energy planning, climate change mitigation strategies and the adaptation efforts to climate impacts on these renewables. However, these implications are highly dependent on the mitigation effort and on the severity of the climate change signal. Hence, they are expected to be more prominent in mitigation scenarios with high intermittent renewable deployment and that account for climate impacts on wind.

Implications for policy-/decision-making:

The results of Chapter 4 aim to support an ample discussion within the IAM community toward a better understanding of the effects of the uncertain renewable potentials on IAM's projections of solar and wind power. This process is expected to guide follow-on research intended to better inform the construction of renewable supply curves for implementation in IAMs.

The overarching message from this dissertation is that the usefulness of the GCAM mitigation and impact scenarios to decision-making is enhanced within a more holistic view in which key interactions (cross-sectoral, multiple impacts) are accounted for by the modeling framework, and modeling structural uncertainties are diagnosed.

Despite the contributions highlighted above, it is important to acknowledge the limitations of this dissertation. The three analyses presented here are built upon modeling experiments, and hence, are subject to the limitations inherent of the

modeling framework. As mentioned in the introductory Chapter 1, GCAM represents five systems (energy, water, land, socioeconomics, and climate) and their key interactions. However, important feedbacks are missing in GCAM. For example, GCAM is coupled with the SCM Hector, which tracks emissions from all sectors and derives the global mean radiative forcing and the global mean temperature change. Such a coupling is one way as there is no dynamic feedback between Hector and GCAM systems based on the radiative forcing achieved. This has implications for the modeled systems. One key example is the land sector. For example, the resulting changes in temperature computed by Hector do not feedback into GCAM crop yields. Consequently, there is no repercussion from these changes on land allocation and on the modeled agricultural supply. This includes any potential effect on biomass crop yields and on the resulting biomass production, which is not exchanged with the energy system. Indeed, the energy system is another important pathway through which human and climate systems directly interact. In this regard, changes in the mean global temperature computed by Hector do not feedback into the energy system through effects on demand (e.g., heating and cooling) or on the supply (e.g., temperature-related effects on thermal power generation). Within this context, it is also important to stress that the climate information from the GCMs and physical impact models (employed in Chapters 3 and 4) are passed into GCAM in a one-way fashion (with data passed through input files to GCAM). This approach has the advantage of transparent information exchange and flexibility (van Vuuren et al. 2012), but it has implications for the results of this study since GCAM captures the effect of the climate on the renewable supply and the resulting effects on GHG emissions but not the influence of

these changes in emissions back on the system. The ability to model bidirectional climate feedbacks in IAMs is acknowledged as a key research need in integrated assessment modeling, and only a limited number of IAM studies has employed a two-way coupling approach (Calvin and Bond-Lamberty 2018). Despite the growing awareness of the need of assessing the sign and magnitude of human-Earth system feedbacks, scholars have pointed out the enormous challenges resulting from the complexity of the full coupling of human and climate/impact models and the associated computational costs, arguing for a balance between these additional costs and the analytical gains (Calvin and Bond-Lamberty 2018; van Vuuren et al. 2012).

It is also important to consider the sources of uncertainties in the results of this dissertation. In Chapter 2, socioeconomic assumptions follow the "Middle of the Road" SSP 2. Using the other four SSPs, which span a wide uncertainty range in terms of long-term demographic and economic projections, would have produced distinct effects on the demand for EWL nexus resources, which may have exacerbated or dampened the nexus trade-offs found. Chapter 3 utilized climate impacts produced by an ensemble of three GCMs. Expanding the number of GCMs will help to improve the robustness of the results. Moreover, only one hydrological and one crop model were used to derive the climate impacts inputs of hydropower and crop yield changes, respectively. Previous studies have highlighted the large uncertainty resulting from these impact models, which is comparable to that of climate models (Rosenzweig et al. 2014; van Vliet et al. 2016b). Hence, expanding the number of impact models will help to better characterize this relevant source of uncertainty. Results from Chapter 3 were also produced under socioeconomic assumptions consistent with the SSP 2 (except for

Argentina, Colombia, and Uruguay). Changing the socioeconomic assumptions is unlikely to alter the main qualitative insight of the study, i.e., the value of a multi-impact modeling approach. However, it would have resulted in a distinct estimate of capital investment requirements in Latin America. Hence, future work could explore the uncertainty space concerning socioeconomic assumptions in that study. In this regard, the exploration of alternative socioeconomic assumptions in Chapters 2 and 3 could benefit from a more robust process of scenarios generation such as that from a recent work (Lamontagne et al. 2018). This study proposed a scenario matrix framework to generate a large ensemble of scenarios that systematically sample the SSP set of assumptions. Future research could include experimenting with different climate change mitigation scenarios since the illustrative scenarios developed for Chapters 2 and 3 lie among the various pathways that can achieve the same climate goals outlined in those studies. In Chapter 4, additional experimentation with different GCMs, socioeconomic assumptions and climate mitigation scenarios could be made and would change the quantitative outputs obtained. However, they would not alter the main qualitative insights concerning the uncertainty on the computation of the renewable potentials and their large effects on the GCAM's projected solar and wind power. For the purposes of the third study, the main uncertainty is the IAM selection. As mentioned in Chapter 4, repeating the same modeling experiments conducted with GCAM using other IAMs has the potential to lead to valuable insights for the IAM community in general.

5.2 Future Work

In addition to the more comprehensive coverage of the underlying uncertainties mentioned above, further opportunities to refine this research exist. An analysis of the relationship between climate change mitigation and EWL resource constraints at finer-resolutions than the national-level scale of Chapter 2 would be valuable for the countries examined. Equally relevant is to examine the interplays with climate change impacts on EWL systems at subnational levels to help guide local decisions. These efforts could benefit from recent modeling tools developed to downscale GCAM land and water sector projections to higher spatial resolutions as done for the EWL nexus case study in Uruguay (Khan et al. 2020). However, there is need of analytical approaches to downscale GCAM energy-sector projections to finer resolutions, which is a current focus of research interest. Future work could also examine the interplays between climate change mitigation and EWL resources under more stringent mitigation targets, such as the 1.5°C warming level since the mitigation scenarios in Chapter 2 are in line with the 2.0°C climate goal. As discussed in the literature (e.g., Rogelj et al. 2015), 1.5°C scenarios are characterized by a faster shift away from traditional fossil-fuel use towards large-scale low-carbon energy supplies and carbon-dioxide removal, which may have more pronounced consequences on EWL sectors.

Additional future work could expand on the assessment of methodological uncertainties conducted in Chapter 4. This could be done by examining parameter values or changes in the formulation to compute the potentials that are not evaluated in the study. Future studies could also expand this analysis to other GCAM power-sector technologies not covered in this study: solar CSP, solar rooftop PV and wind offshore.

Lastly, a formal sensitivity analyses, systematically decomposing the individual and combined influence of each parameter could provide important additional insights. For example, Chapter 4 focuses on individual sensitivities that are computed by varying just one factor at a time. However, this could be refined in future studies to investigate whether interactions across factors can amplify or smoothen individual effects.

Appendices

Appendix A: Supplementary Material - Chapter 2

Supplementary Notes

Supplementary Note 1

As noted in Chapter 2, this study explores two climate change mitigation scenarios: *NDC_FullTech* and *NDC_NOCCS*. Both scenarios are based on the *'Paris-Increased Ambition'* scenario developed in Fawcett et al. 2015, in which the main assumptions are: (1) countries achieve their NDCs through 2030; and (2) beyond 2030 CO_2 emissions intensities decrease at annual rates implied by the NDCs or 5% per year, whichever is higher. However, for the Latin America and the Caribbean (LAC) region, the emissions constraints were revised based upon the supporting sources and assumptions listed below.

Table A.1 Supporting sources and assumptions by GCAM region in LAC.

GCAM Region	Long-term (post-2030) Goal	Notes
Argentina	The conditional NDC target is assumed to be achieved by 2050	Emissions constraints revised according to the First Revision of Argentina's NDC [1]
Brazil	Emissions constraints extrapolated from 2025-2030 rate of emissions reduction until 2050	Revised emissions constraints based on [2] and Forsell et al. 2016
Central America and Caribbean	5% annual rate of improvement in GHG emissions per unit of Gross Domestic Product (GDP) beyond 2030	
Colombia	2050 long-term target (30% reduction in all GHG below BAU) based on [3]	Revised emissions constraints based on [3]
Mexico	Emissions extrapolated from 2030 NDC emissions level towards the 2050 target stipulated in [4] (50% reduction of GHGs in 2050 compared to Mexico's 2000 emissions: about 311 $MtCO2_e$ in 2050)	Revised emissions constraints based on Forsell et al. 2016 and [4]
South America_Southern	5% annual rate of improvement in GHG emissions per unit of Gross Domestic Product (GDP) beyond 2030	
South America_Northern	5% annual rate of improvement in GHG emissions per unit of Gross Domestic Product (GDP) beyond 2030	

Sources:

[1] https://www4.unfccc.int/sites/NDCStaging/Pages/All.aspx

[2] MMA. Fundamentos para a elaboração da Pretendida Contribuição Nacionalmente Determinada (NDC) do Brasil no contexto do Acordo de Paris sob a UNFCCC [Internet]. Brasilia; 2016. Available from: http://www.mma.gov.br/images/arquivos/clima/convencao/indc/Bases_elaboracao_iNDC.pdf

[3] Cadena A, Bocarejo JP, Rosales R, Arguello R, Delgado R, Flórez E, et al. Upstream analytical work to support development of policy options for mid- and long-term mitigation objectives in Colombia (Anexo A – Documento Técnico de soporte para la iNDC colombiana, pp. 27). [Internet]. Bogotá; 2015. Available from: http://www.minambiente.gov.co/images/cambioclimatico/pdf/documentos_tecnicos_soporte/Contribución_Nacionalmente_Determinada_de_Colombia.pdf

[4] INECC-SEMARNAT. First Biennial Update Report to the United Nations Framework Convention on Climate Change. [Internet]. Mexico City; 2015. Available from: http://unfccc.int/files/national_reports/non-annex_i_parties/ica/technical_support_for_the_ica_process/application/pdf/executive_summary.pdf

Supplementary Figures

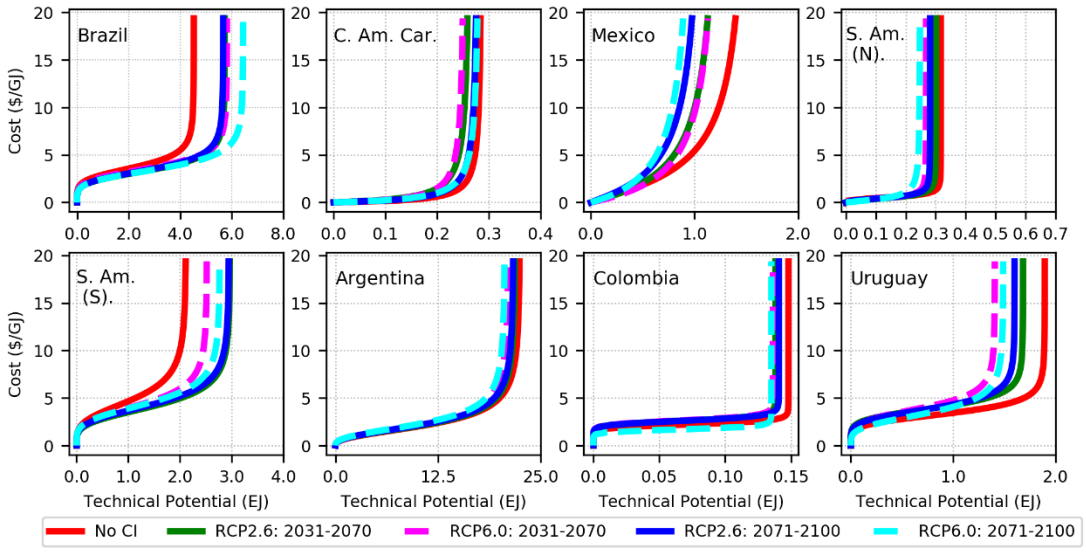

Figure B.1 Latin America and Caribbean cost-supply curves for wind energy using climate inputs from the GFDL-ESM2M model under RCPs 2.6 and 6.0. Cost-supply curves for three different periods were implemented in GCAM: two curves representing future climate states and one curve produced from data corresponding to the model historical period (labeled "No CI").

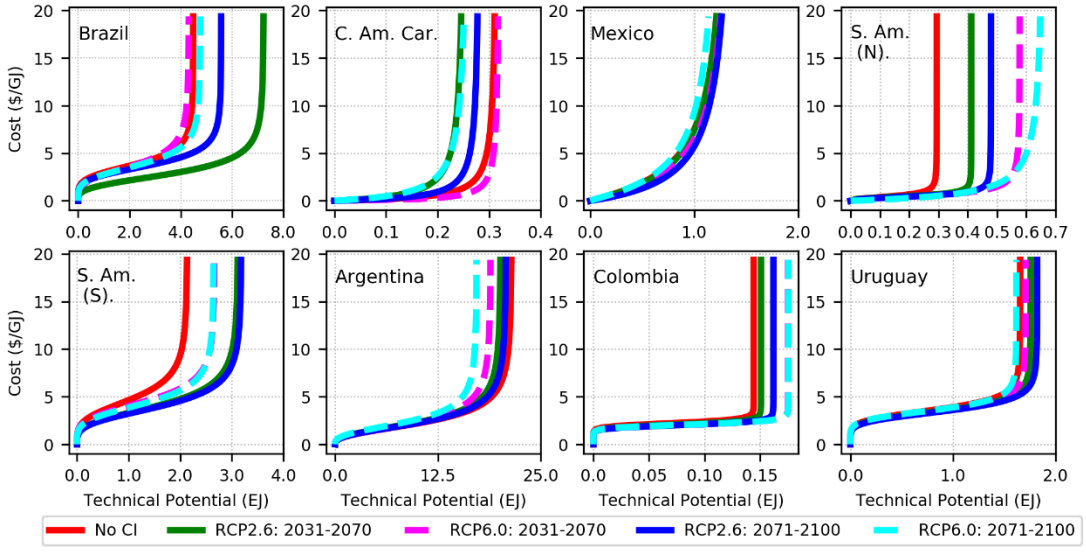

Figure B.2 As in Figure B.1 but using climate inputs from the HadGEM2-ES model.

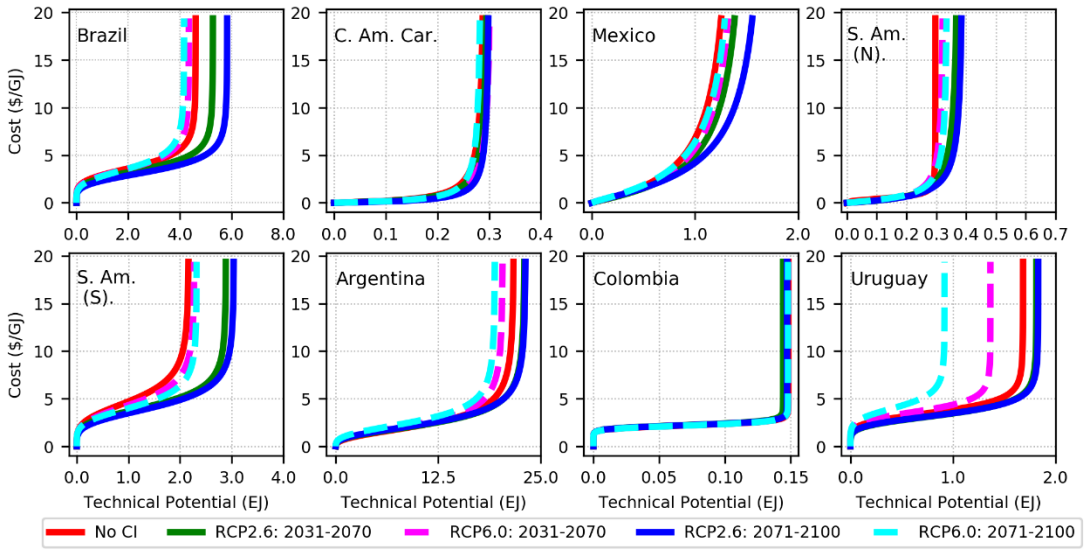

Figure B.3 As in Figure B.1 but using climate inputs from the IPSL-CM5A-LR model.

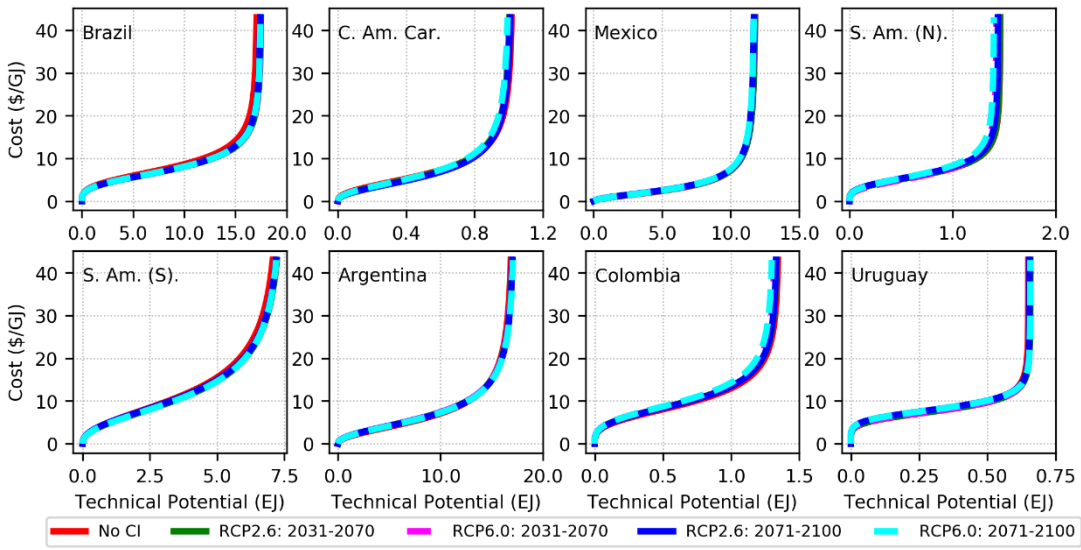

Figure B.4 Latin America and Caribbean cost-supply curves for solar (PV) energy using climate inputs from the GFDL-ESM2M model under RCPs 2.6 and 6.0. Cost-supply curves for three different periods were implemented in GCAM: two curves representing future climate states and one curve produced from data corresponding to the model historical period (labeled "No CI").

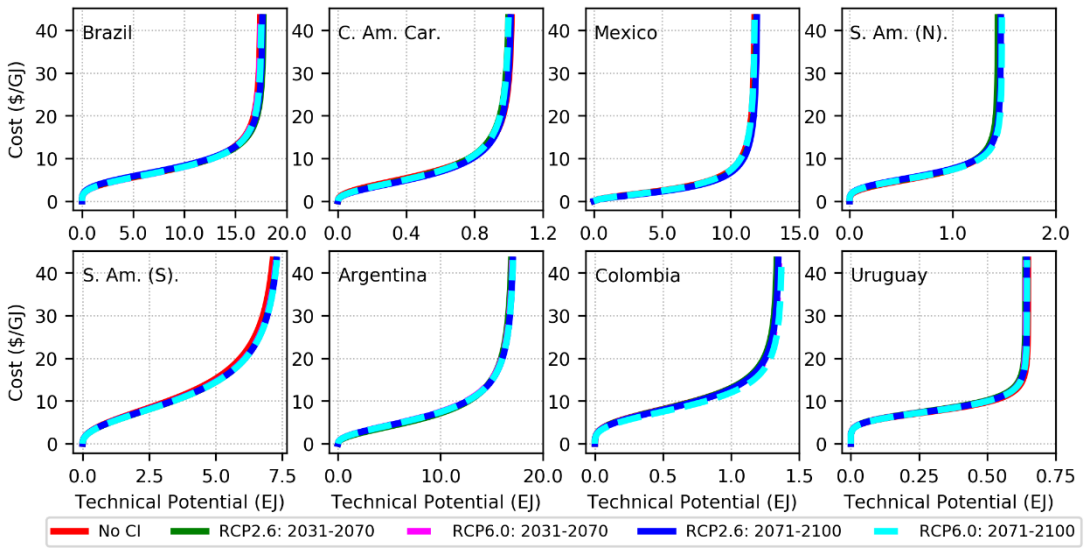

Figure B.5 As in Figure B.4 but using climate inputs from the HadGEM2-ES model.

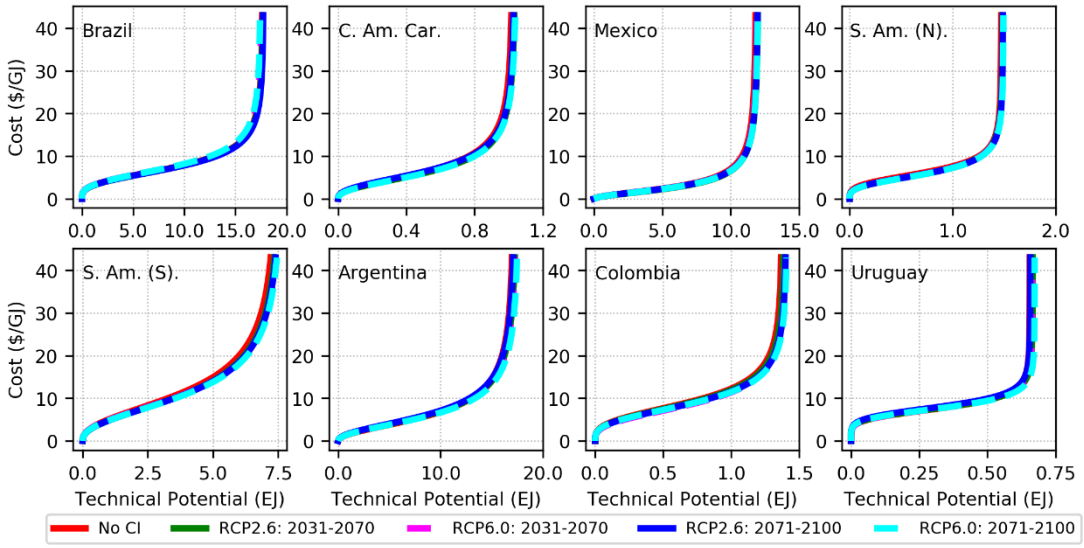

Figure B.6 As in Figure B.4 but using climate inputs from the IPSL-CM5A-LR model.

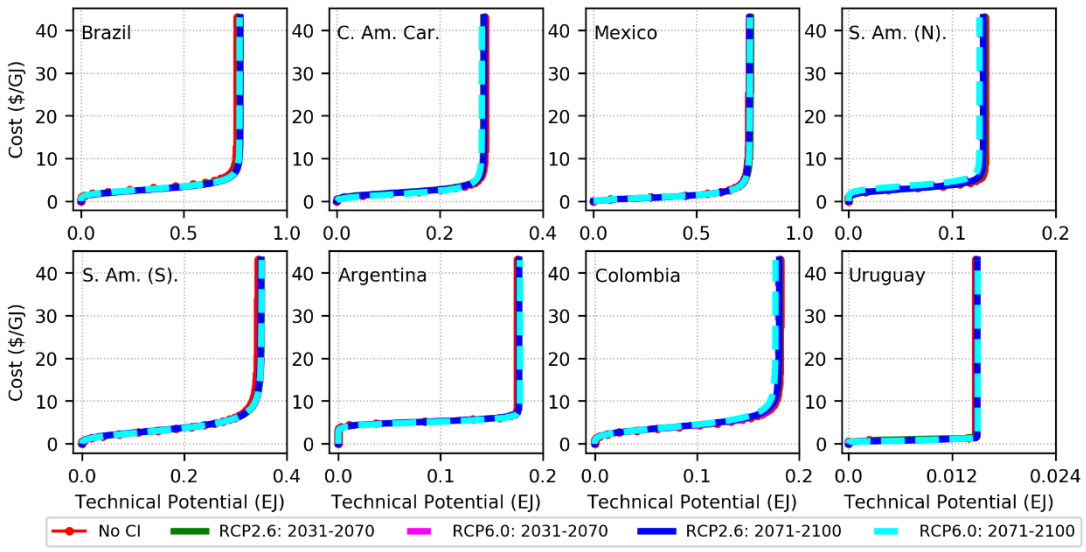

Figure B.7 Latin America and Caribbean cost-supply curves for solar (rooftop PV) energy using climate inputs from the GFDL-ESM2M model under RCPs 2.6 and 6.0. Cost-supply curves for three different periods were implemented in GCAM: two curves representing future climate states and one curve produced from data corresponding to the model historical period (labeled "No CI").

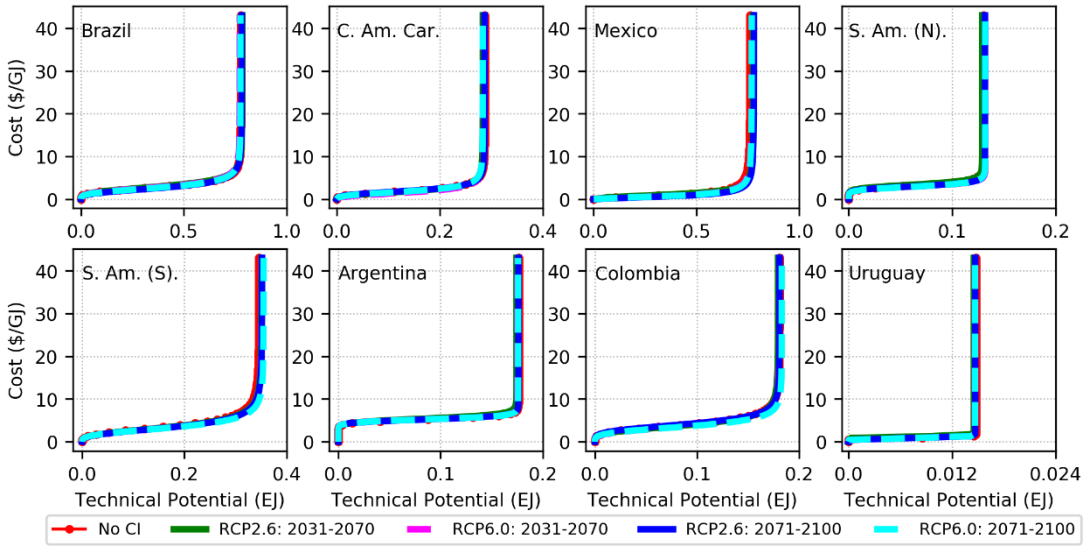

Figure B.8 As in Figure B.7 but using climate inputs from the HadGEM2-ES model.

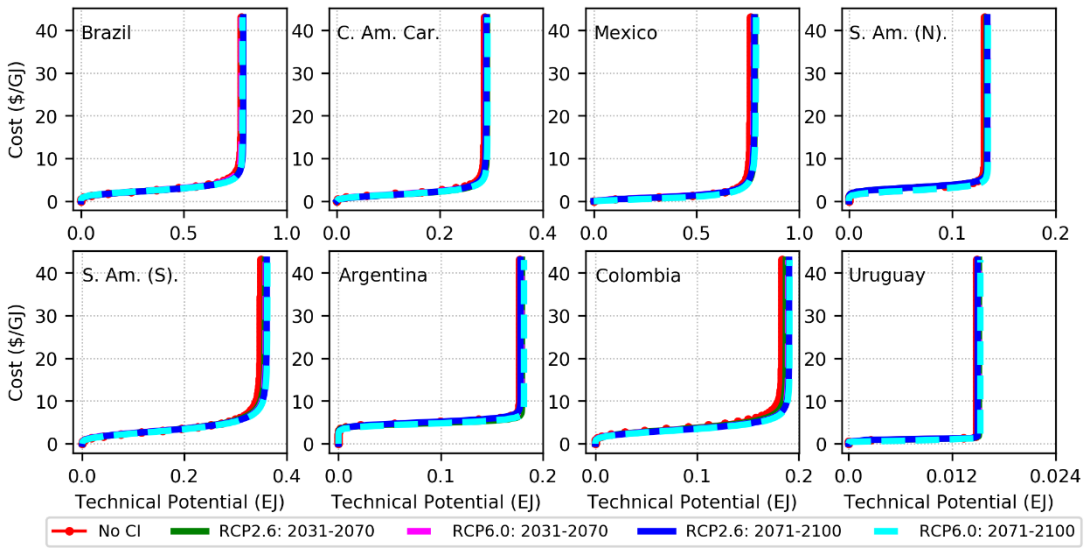

Figure B.9 As in Figure B.7 but using climate inputs from the IPSL-CM5A-LR model.

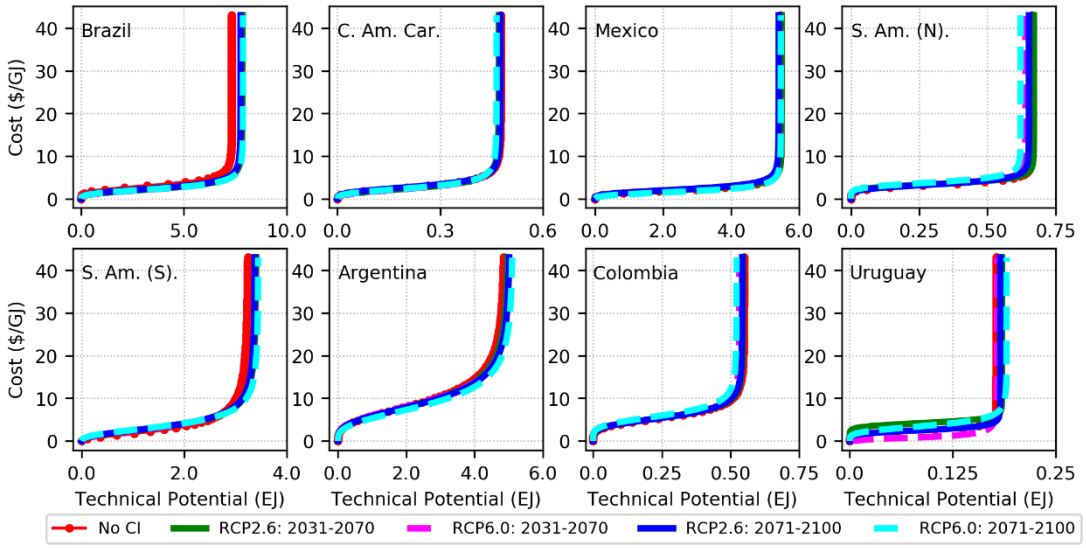

Figure B.10 Latin America and Caribbean cost-supply curves for solar (CSP) energy using climate inputs from the GFDL-ESM2M model under RCPs 2.6 and 6.0. Cost-supply curves for three different periods were implemented in GCAM: two curves representing future climate states and one curve produced from data corresponding to the model historical period (labeled "No CI").

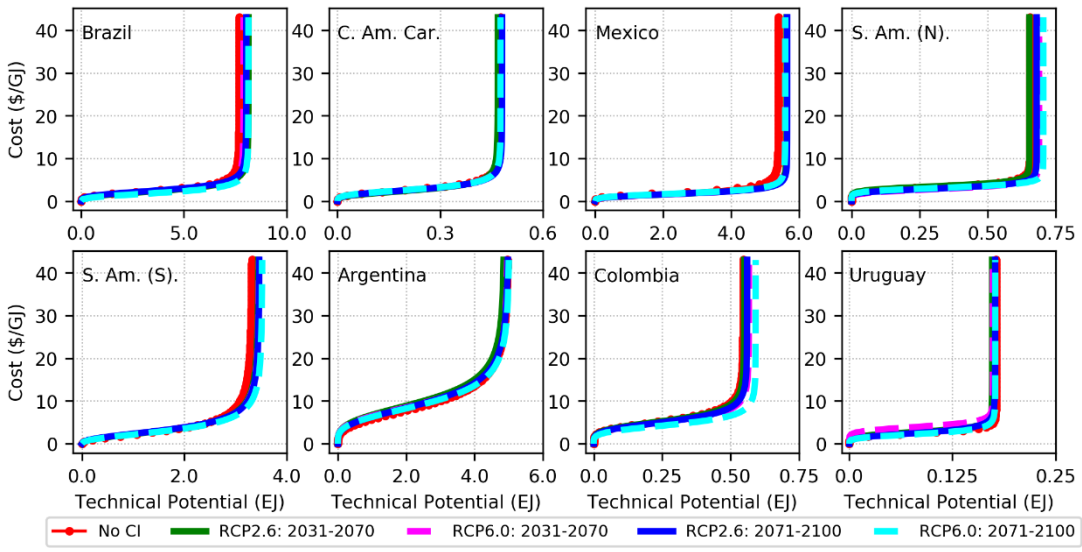

Figure B.11 As in Figure B.10 but using climate inputs from the HadGEM2-ES model.

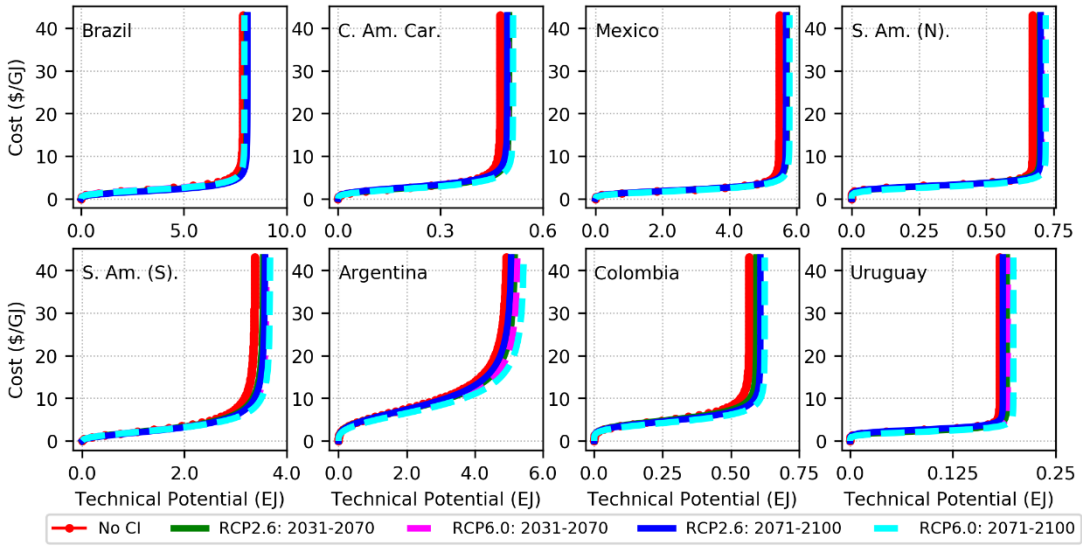

Figure B.12 As in Figure B.10 but using climate inputs from the IPSL-CM5A-LR model.

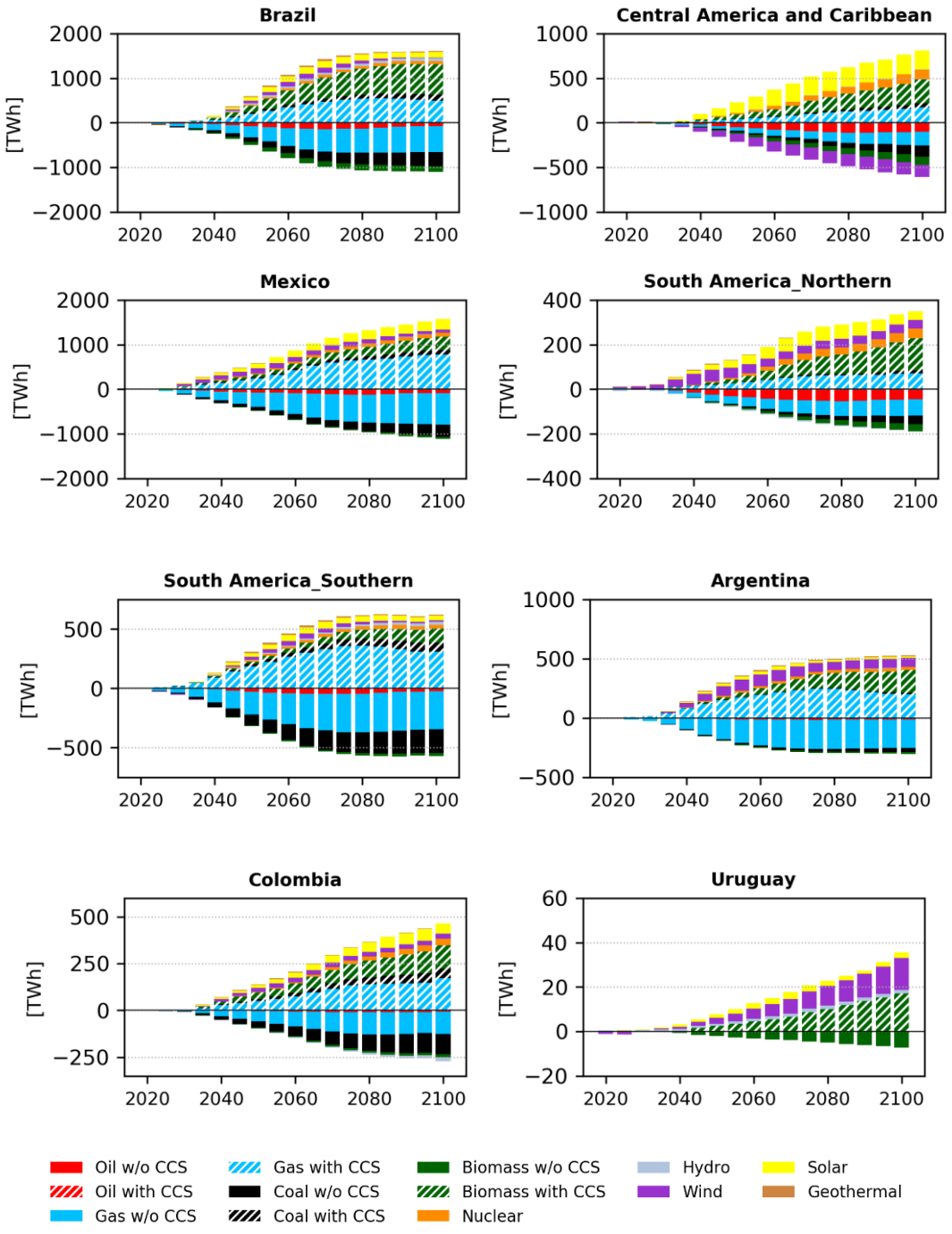

Figure B.13 Changes in electricity generation under the *RCP26_FullTech: Combined impacts* scenario relative to the GCAM *Baseline* scenario.

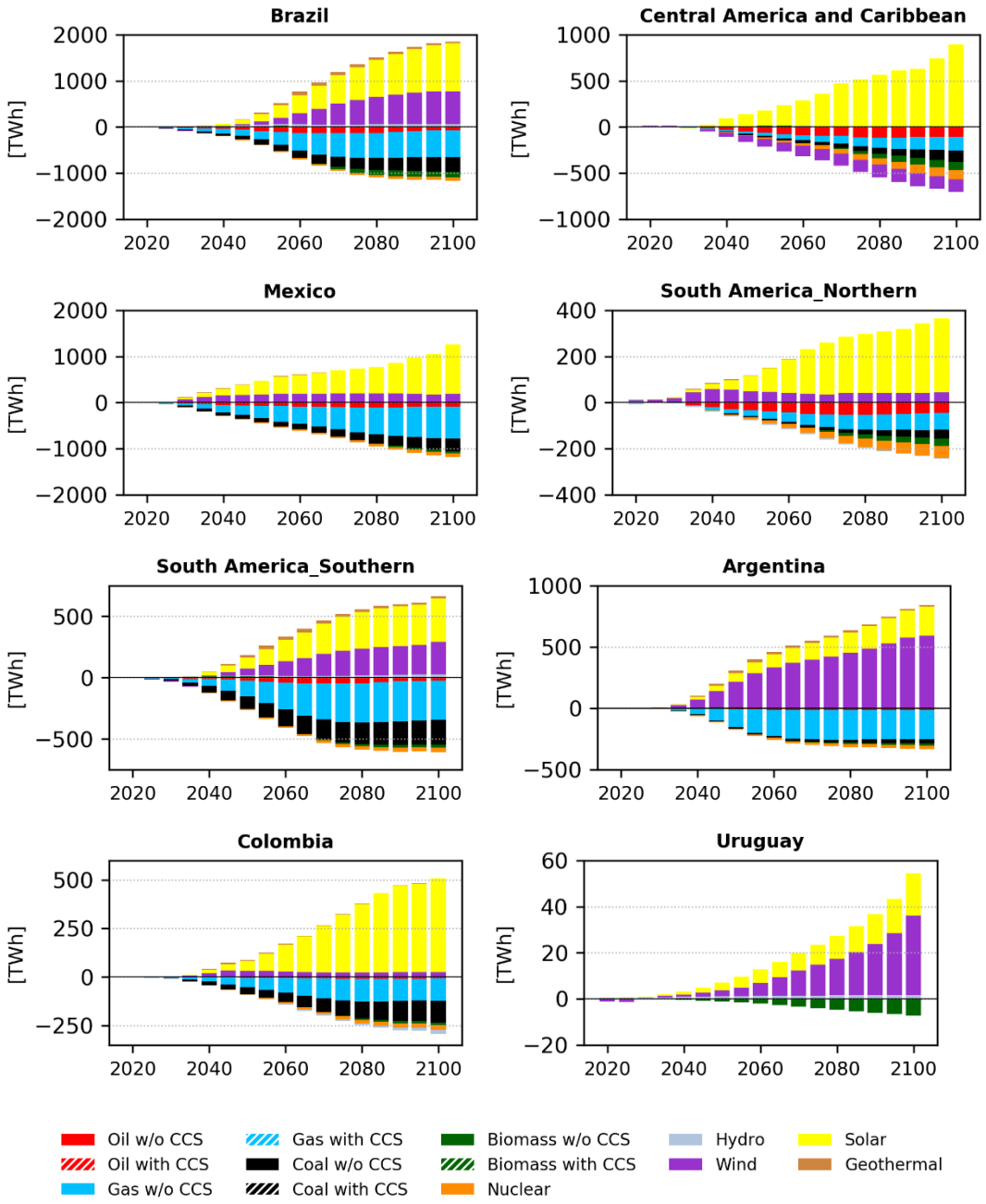

Figure B.14 Changes in electricity generation under the *RCP26_NoCCS & NoNewNuc: Combined impacts* scenario relative to the GCAM *Baseline* scenario.

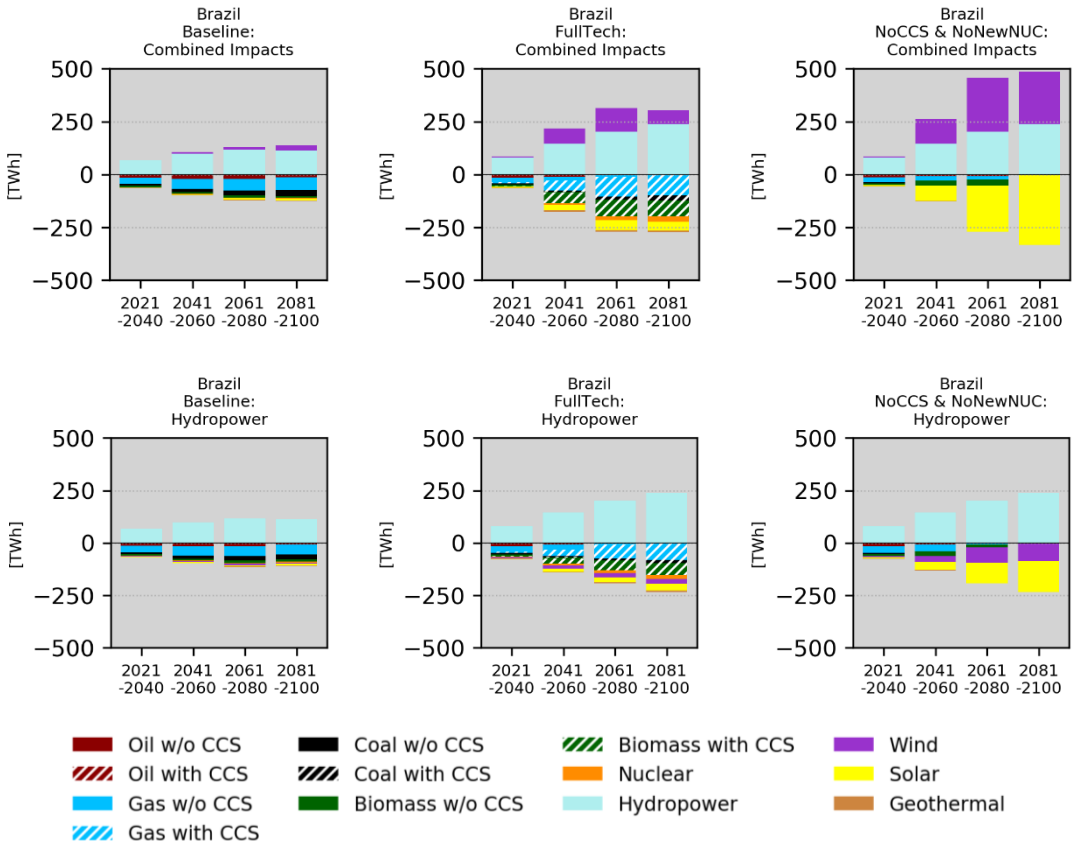

Figure B.15 Model mean differences in electricity production by technology in Brazil assuming climate change impacts on renewables for all climate-impact scenarios explored in this study. Differences are calculated by technology using cumulative generation changes by distinct periods (2021-2040, 2041-2060, 2061-2080, 2081-2100) and are relative to the corresponding *No-climate impacts* scenarios.

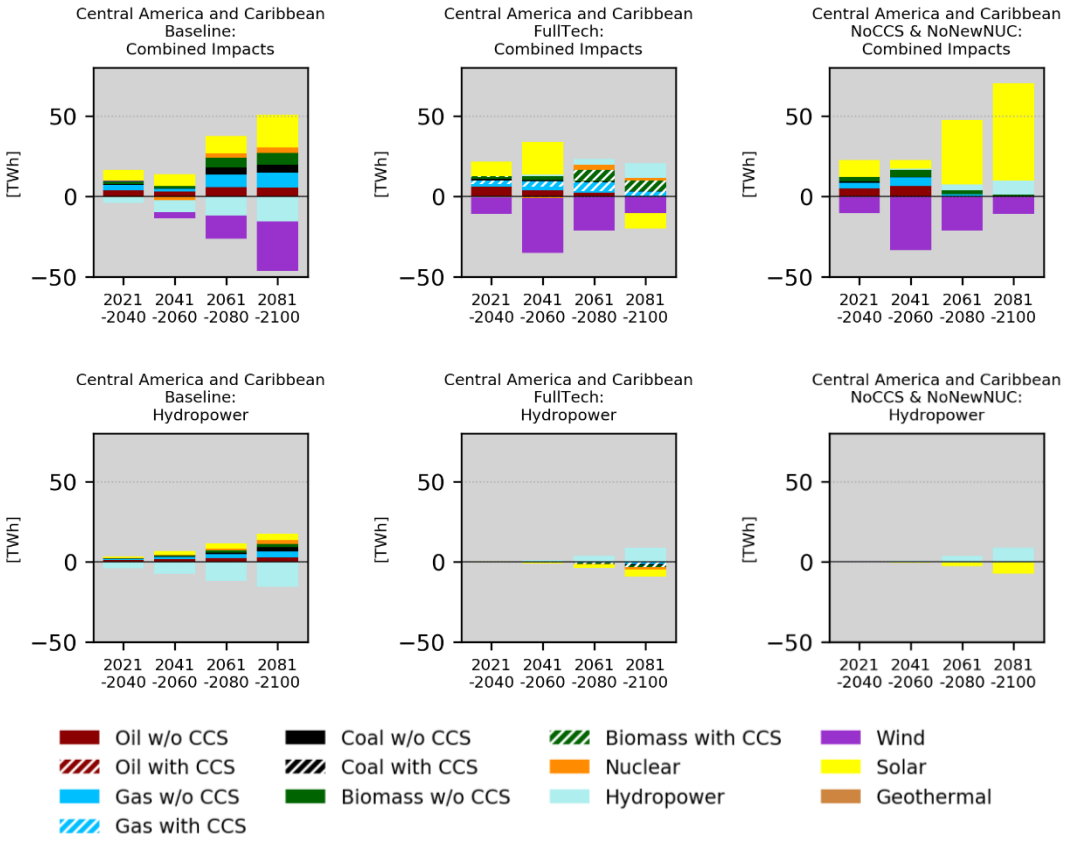

Figure B.16 As in Figure B.15 but for Central America and Caribbean.

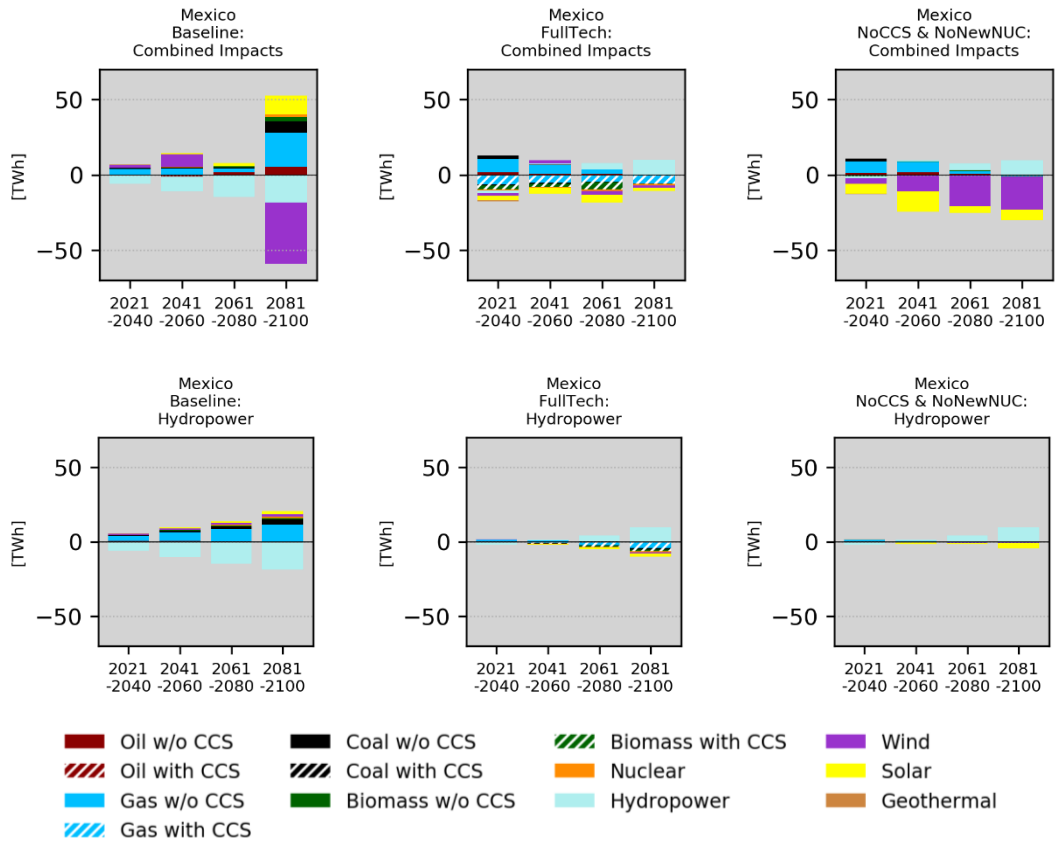

Figure B.17 As in Figure B.15 but for Mexico.

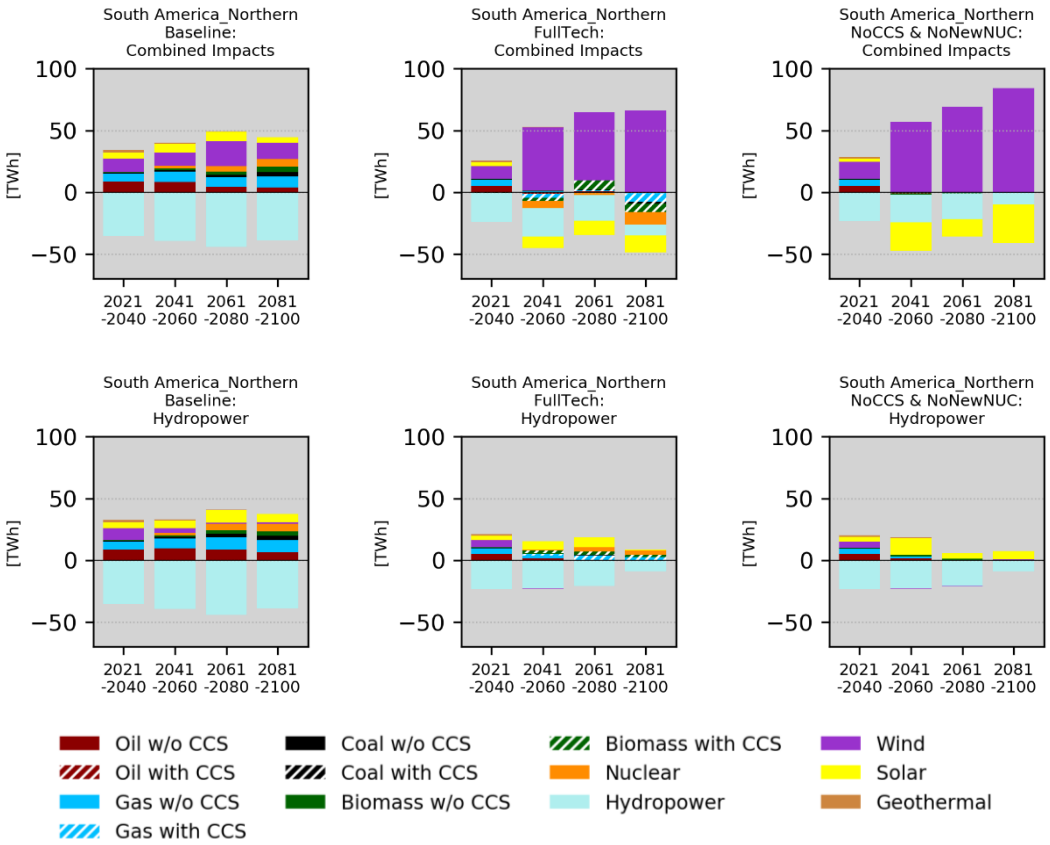

Figure B.18 As in Figure B.15 but for South America Northern.

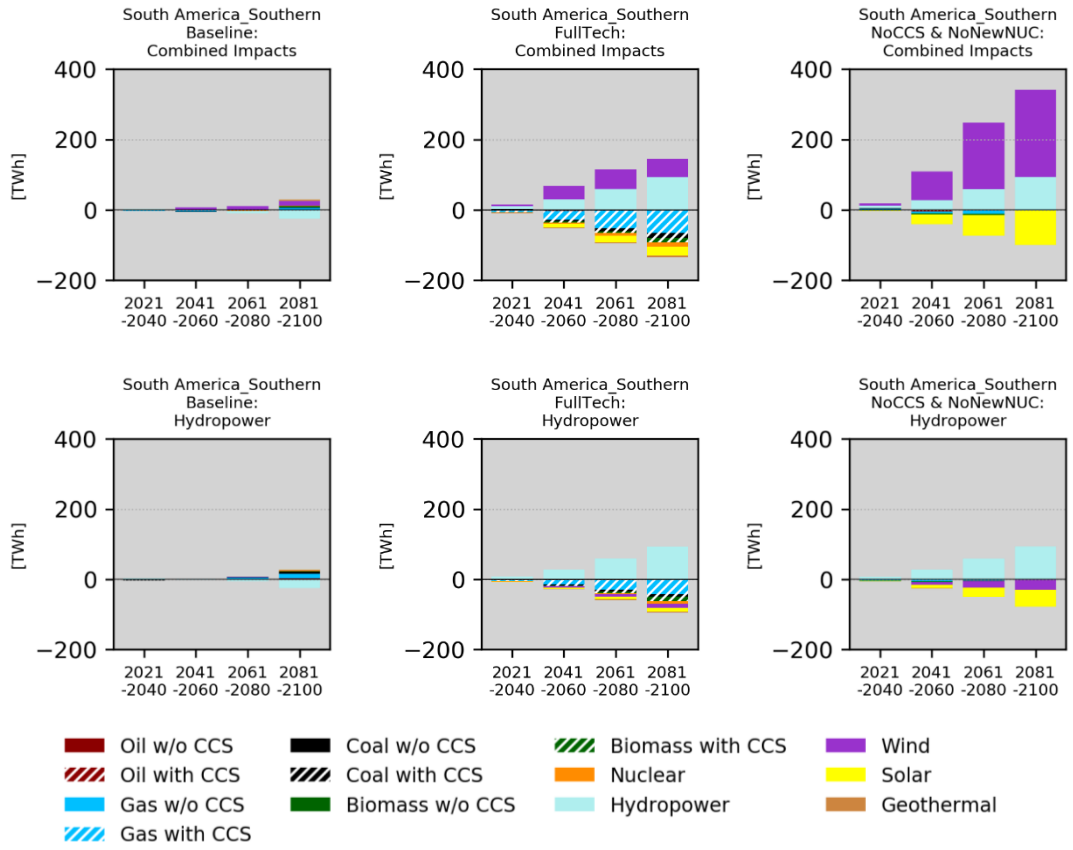

Figure B.19 As in Figure B.15 but for South America Southern.

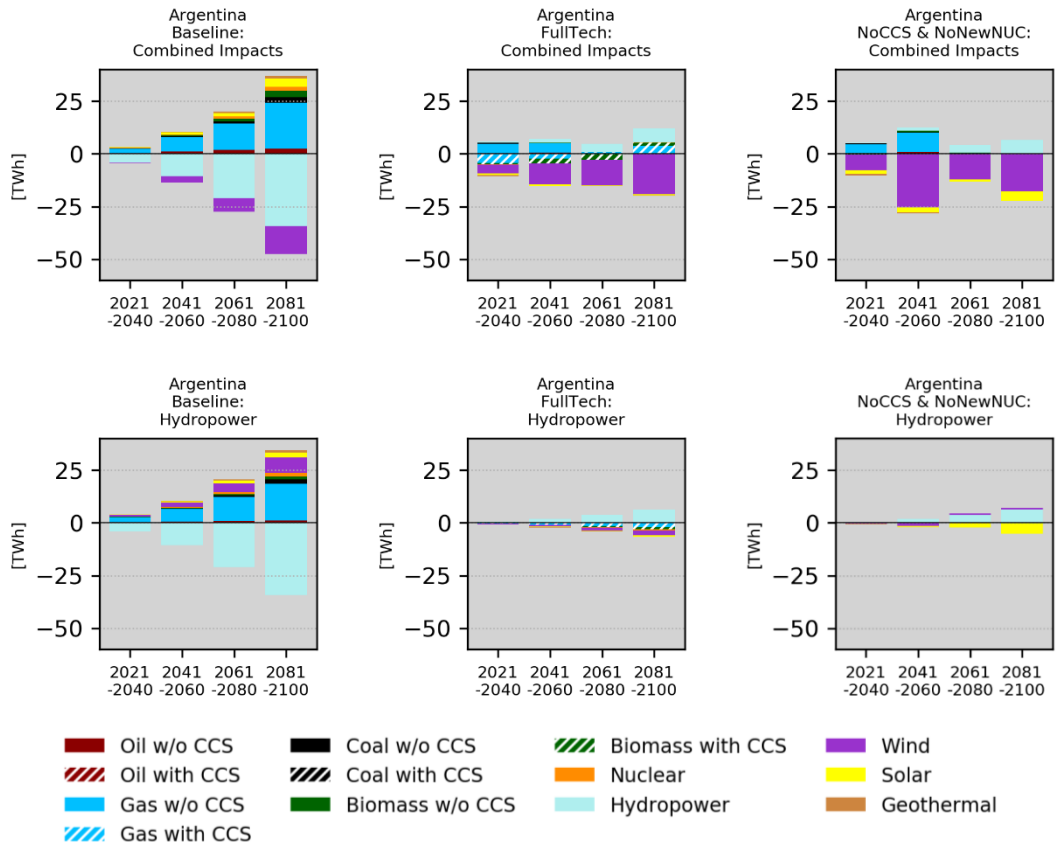

Figure B.20 As in Figure B.15 but for Argentina.

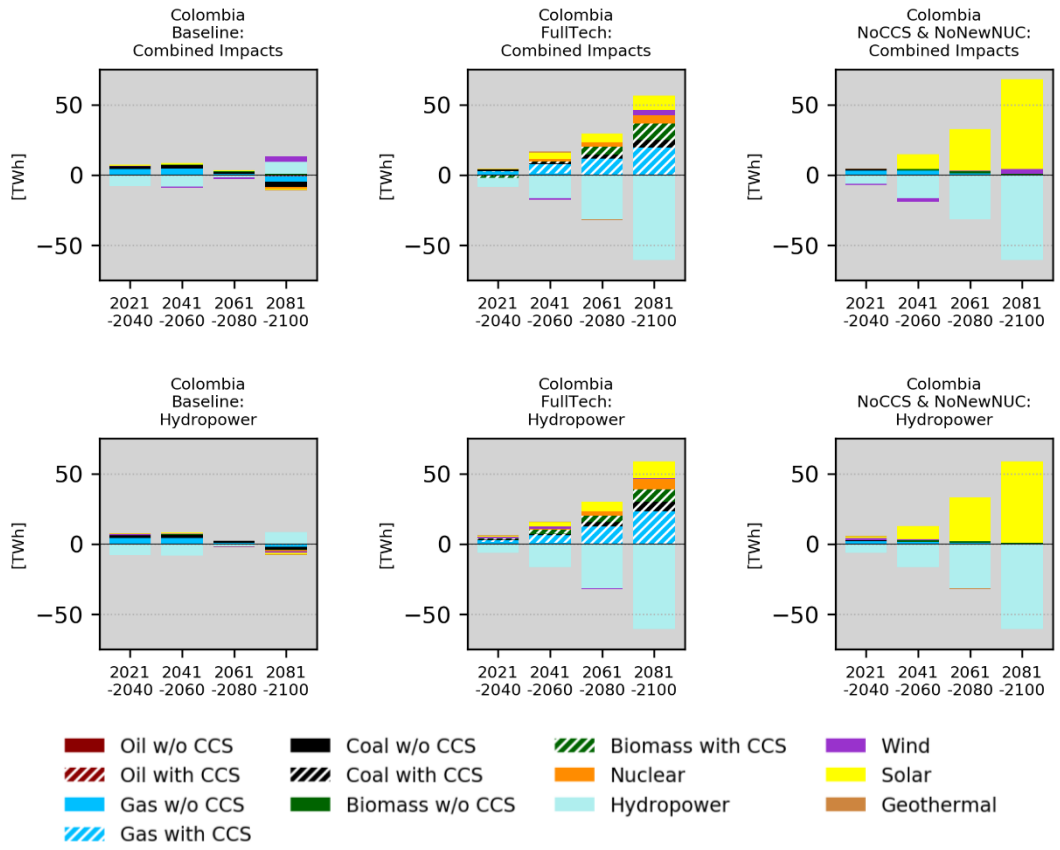

Figure B.21 As in Figure B.15 but for Colombia.

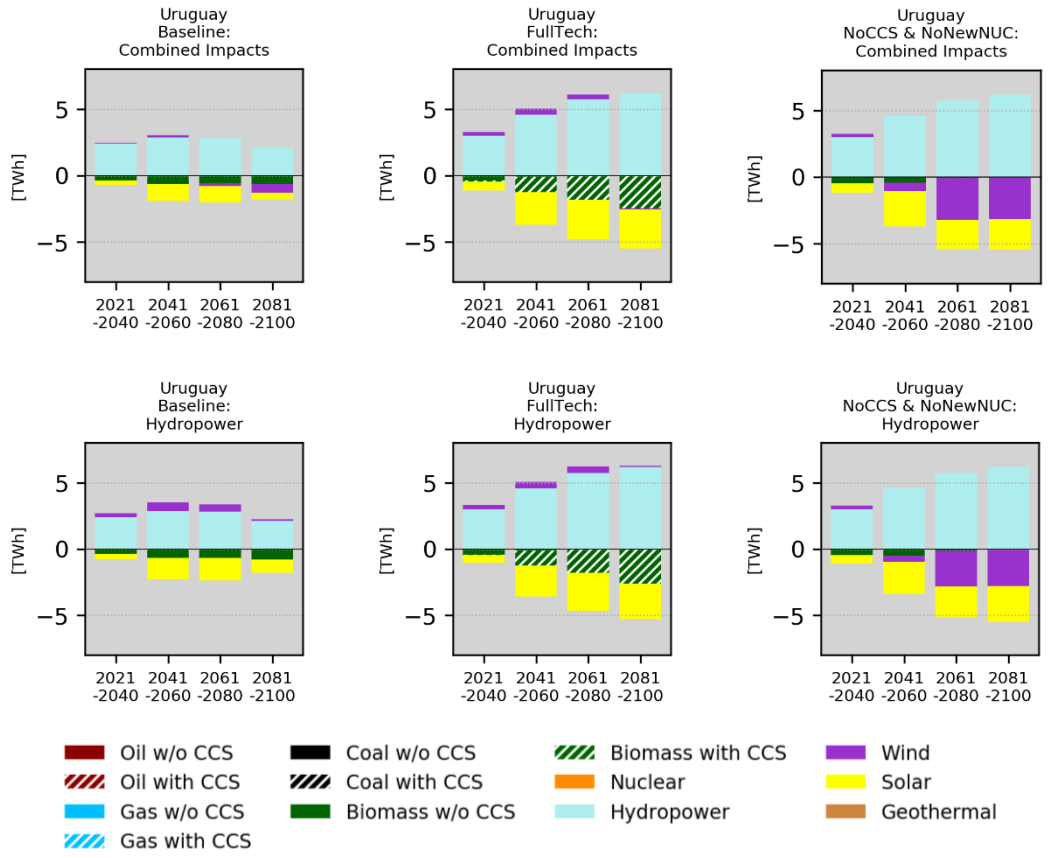

Figure B.22 As in Figure B.15 but for Uruguay.

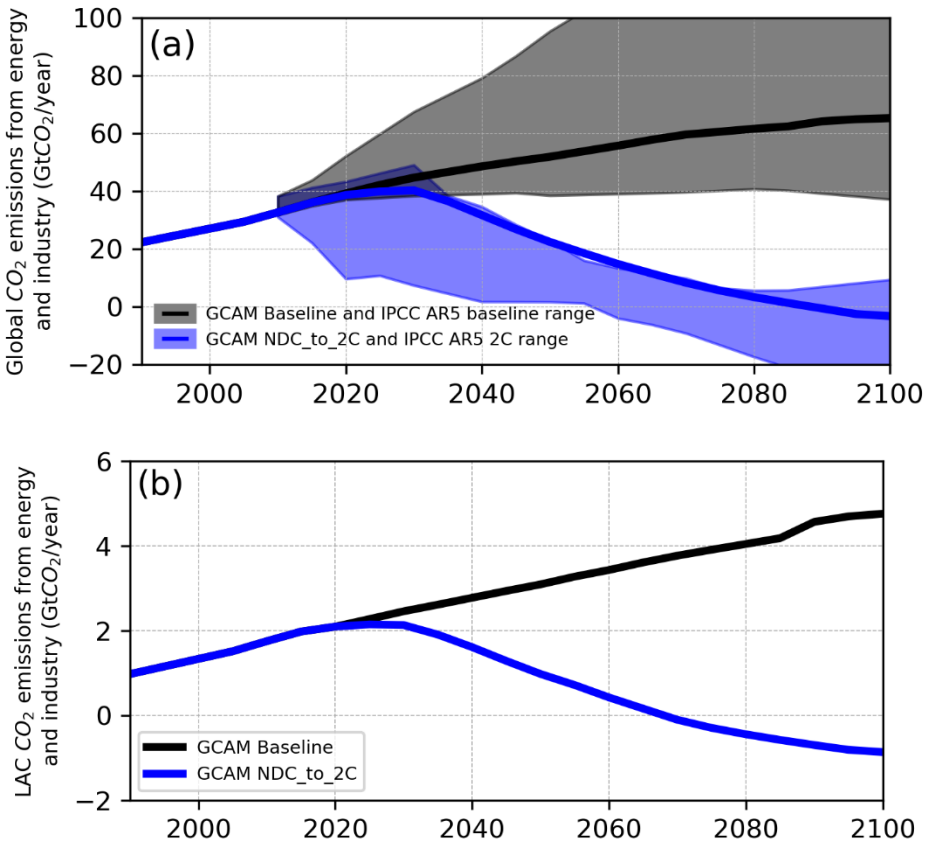

Figure B.23 Global (a) and LAC (b) CO_2 emissions from fossil fuel combustion and industrial processes in GCAM NDC_to_2C and Baseline scenarios (solid lines). Shaded areas in (a) represent scenarios included in the AR5 Scenario Database (available at https://secure.iiasa.ac.at/web-apps/ene/AR5DB/; documented in Krey et al. 2014), which maintains the long-term scenarios reviewed in the Fifth Assessment Report (AR5) by the Working Group III of the IPCC. The blue range comprises the subset of policy scenarios that fall within radiative forcing levels consistent with the RCP2.6, and limit global warming until 2100 to less than 2°C with at a least a 66% chance (IPCC 2014; Krey et al. 2014). The black range is formed by the baseline scenarios (i.e., scenarios that do not include any GHG mitigation policy throughout the century) associated with the mitigation scenarios in the blue range.

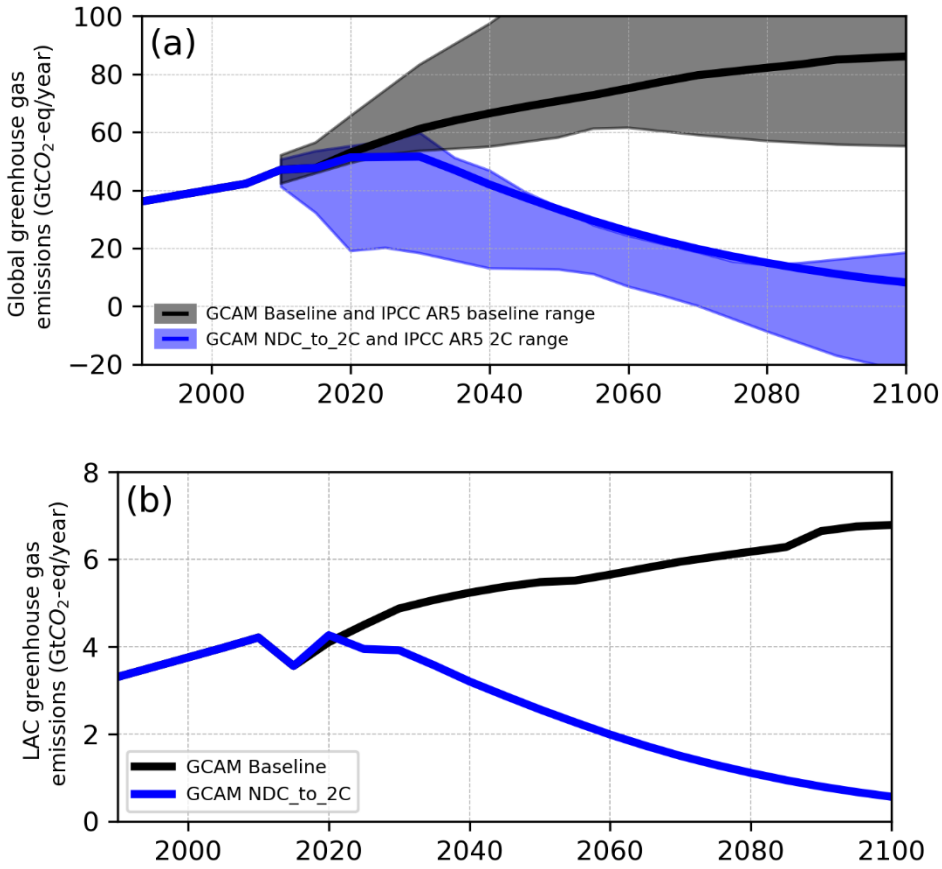

Figure B.24 Global (a) and LAC (b) greenhouse (GHG) gas emissions in GCAM NDC_to_2C and Baseline scenarios (solid lines). Shaded areas in (a) represent scenarios included in the AR5 Scenario Database (available at https://secure.iiasa.ac.at/web-apps/ene/AR5DB/; documented in Krey et al.(Krey et al. 2014)), which maintains the long-term scenarios reviewed in the Fifth Assessment Report (AR5) by the Working Group III of the Intergovernmental Panel on Climate Change (IPCC). The blue range comprises the subset of policy scenarios that fall within radiative forcing levels consistent with the RCP2.6, and limit global warming until 2100 to less than 2°C with at a least a 66% chance(IPCC 2014; Krey et al. 2014). The black range is formed by the baseline scenarios (i.e., scenarios that do not include any GHG mitigation policy throughout the century) associated with the mitigation scenarios in the blue range. [Note: CO_2-eq emissions include the basket of Kyoto gases (carbon dioxide (CO_2), methane (CH_4), nitrous oxide (N_2O) as well as fluorinated gases) aggregated using 100-year Global Warming Potential values from the IPCC Second Assessment Report.]

Supplementary Tables

Table B.1 Technology capacity factor assumptions

Technology	**Capacity Factor**
Biomass (conv)	0.85
Biomass (IGCC)	0.8
Biomass (conv CCS)	0.85
Biomass (IGCC CCS)	0.8
Coal (conv pul)	0.85
Coal (IGCC)	0.8
Coal (conv pul CCS)	0.8
Coal (IGCC CCS)	0.8
Gas (CC)	0.85
Gas (steam/CT)	0.8
Gas (CC CCS)	0.8
Refined liquids (steam/CT)	0.8
Refined liquids (CC)	0.85
Refined liquids (CC CCS)	0.8
Gen II LWR (Nuclear)	0.9
Gen III (Nuclear)	0.9
CSP	varies by region (Supplementary Table 9)
CSP with storage	varies by region (Supplementary Table 9)
PV	varies by region (Supplementary Table 9)
PV with storage	varies by region (Supplementary Table 9)
Wind	varies by region (Supplementary Table 9)
Wind with storage	varies by region (Supplementary Table 9)
Rooftop PV	varies by region (Supplementary Table 9)
Geothermal	0.9
Hydropower	0.54

Table B.2 Technology capacity factor assumptions in the LAC region

GCAM-LAC Region	Capacity Factor by Technology						
	CSP	**CSP with storage**	**PV**	**PV with storage**	**Wind**	**Wind with storage**	**Rooftop PV**
Argentina	0.25	0.65	0.23	0.23	0.37	0.37	0.23
Brazil	0.25	0.65	0.25	0.25	0.34	0.34	0.25
Central America and Caribbean	0.25	0.65	0.25	0.25	0.38	0.38	0.25
Colombia	0.25	0.65	0.22	0.22	0.32	0.32	0.22
Mexico	0.25	0.65	0.27	0.27	0.38	0.38	0.27
South America_Northern	0.25	0.65	0.24	0.24	0.35	0.35	0.24
South America_Southern	0.25	0.65	0.24	0.24	0.36	0.36	0.24
Uruguay	0.25	0.65	0.20	0.20	0.37	0.37	0.20

Table B.3 Electric power sector capital cost assumptions (2010$/kW)

	2020	**2030**	**2050**	**2100**
Biomass (conv)*	3951	3861	3703	3425
Biomass (IGCC)*	5746	5339	4819	4335
Biomass (conv CCS)*	7318	6766	6169	5665
Biomass (IGCC CCS)*	8338	7579	6721	6059
Coal (conv pul)*	2863	2799	2686	2482
Coal (IGCC)*	3832	3560	3215	2889
Coal (conv pul CCS)*	5504	5078	4619	4238
Coal (IGCC CCS)*	6195	5604	4945	4464
Gas (CC)*	1036	1014	972	901
Gas (steam/CT)*	742	723	694	642
Gas (CC CCS)*	1992	1837	1672	1533
Refined liquids (steam/CT)*	742	723	694	642
Refined liquids (CC)*	1036	1014	972	901
Refined liquids (CC CCS)*	2356	2153	1937	1775
Gen II LWR (Nuclear)*	5501	5501	5501	5501
Gen III (Nuclear)*	5433	5307	5094	4710
CSP*	4367	3770	3199	2905
CSP with storage*	7431	6617	5772	5216
PV	1788	1662	1501	1349
PV with storage	4213	3916	3535	3180
Wind	1914	1778	1608	1446
Wind with storage	5555	5162	4661	4190
Rooftop PV	4500	4183	3777	3396
Geothermal*	4348	4248	4074	3767
Hydropower	2600	2600	2600	2600

*For these generation technologies, the final overnight capital costs increase depending on the cooling technology deployed. The following cooling system options are available in GCAM: once through, seawater, recirculating, cooling pond and dry cooling. These cooling technologies can add between 19 (once through) and 200 (dry cooling) 2010$/KW to the final overnight capital costs of electricity generation technologies. However, the base costs presented in the table represent the major portion of the total overnight capital costs.

Table B.4 NDCs quantification in LAC*

GCAM Region	Country	2010 GHG emissions ($MtCO_2e$)	GHG percent change relative to 2010 levels	Emissions assumption in NDC ($MtCO_2e$)	Year
Argentina	Argentina	389.4	20%	467.3	2030
Brazil	Brazil	1285.0	-1%	1272.2	2025
Central America and Caribbean	Costa Rica	5.2	-28%	3.7	2030
	Dominican Republic	31.7	-25%	23.8	2030
	Grenada	1.8	-30%	1.3	2025
Colombia	Colombia	224.0	5%	235.2	2030
Mexico	Mexico	746.0	-5%	708.7	2030
South America Northern	Venezuela	200	36%	272.0	2030
South America Southern	Chile	84.9	11%	94.2	2030
	Peru	170.6	22%	208.1	2030

*Notes:

1. NDCs quantification based on Vrontisi et al. 2018.

2. Table only includes countries with quantifiable NDCs in terms of percent changes in emissions relative to 2010 levels. For this reason, Ecuador, which is listed in Vrontisi et al. 2018, is not represented.

3. When implemented in GCAM, it is assumed that NDCs cover GHGs from all sectors, including CO_2 emissions from land-use and land-cover change.

Table B.5 Summary of general assumptions for the NDC 2020-2030 period*

GCAM Region	Country	2020 GHG emissions	2025 GHG emissions	2030 GHG emissions
Argentina	Argentina	GHG emissions follow reference scenario	linear interpolation between 2020 and 2030 levels	Vrontisi *et al* (2018)
Brazil	Brazil		Vrontisi *et al* (2018)	Assumed 1200 $MtCO_2e$ as in Brazil's NDC[1]
Central America and Caribbean	Costa Rica		linear interpolation between 2020 and 2030 levels	Vrontisi *et al* (2018)
	Dominican Republic			
	Grenada		Vrontisi *et al* (2018)	GHG emissions follow reference scenario
Colombia	Colombia		linear interpolation between 2020 and 2030 levels	Vrontisi *et al* (2018)
Mexico[2]	Mexico			
South America Northern	Venezuela			
South America Southern	Chile			
	Peru			
Globe	–	52.71 $GtCO_2e$[3]	linear interpolation between 2020 and 2030 levels	53.7 $GtCO_2e$ (Vrontisi *et al* (2018))

*Notes:

1. Brazil's NDC submission available at: https://www4.unfccc.int/sites/submissions/INDC/Submission%20Pages/submissions.aspx

2. Following Vrontisi et al. 2018, Mexico is assumed not to achieve its Copenhagen pledge.

3. Average level between the "High" and "Low" global GHG emissions resulting from 2020 Copenhagen pledges (Riahi et al. 2015).

Supplementary Notes

Supplementary Note 1. Detailed description of the emissions reduction pathway and additional assumptions behind scenarios explored in this study

First, the emission reduction scenario, named *NDC_to_2C*, was devised to serve as the basis for all mitigation scenarios – with and without climate change impacts – in this study. In the *NDC_to_2C* scenario, 2020-2030 regional emissions pathways represent commitments made by United Nations Framework Convention on Climate Change's parties in the Paris Agreement. The quantification of the NDCs in Latin America and the Caribbean (LAC) within the 2020-2030 period follows Vrontisi et al. 2018 (Tables B.4 and B.5), which represents the conditional (high-ambition) NDCs by establishing 2025 or 2030 emissions changes relative to 2010 levels. Outside the LAC region, GHG emissions reductions are represented as single emissions constraints that are shared among the remainder of the world.

Beyond 2030 (period not covered by the current round of NDCs), it is assumed that all regions worldwide enhance their mitigation efforts resulting in the mean global surface temperature increase successfully limited to 2°C. This is achieved with all regions complying with annual rates of improvement in GHG emissions (excluding CO_2 emissions from land-use and land-cover change – LUC) per unit of GDP (i.e., GHG intensity) of 4.5%. Weaker GHG intensities were unable to meet the end-of-century 2°C climate goal. Note that CO_2 LUC emissions were not included in the GHG intensity computation due to the large uncertainty on the actual role of the land sector in future mitigation as discussed in the literature (Forsell et al. 2016; Grassi et al. 2017). In the GCAM framework, GHG emissions in the *NDC_to_2C* scenario are limited by

imposing economy-wide emissions constraints (computed from the GHG intensity values calculated above). This means that total GHG emissions are assigned to each GCAM region and the model internally calculates the carbon prices needed to achieve the emissions constraint. Following Binsted et al. 2020, medium mitigation efforts in the land-use sector globally are assumed by imposing that CO_2 emissions from LUC face a price that is 10% of the price per ton of carbon on fossil fuel and industrial emissions. Reductions in non-CO_2 emissions are achieved through equal marginal abatement costs across all sectors of the economy. It is important to acknowledge that actual climate policy approaches will significantly differ from the economy-wide carbon prices approach used herein, relying, for example, on a range of different sectoral measures. Hence, the resulting emissions pathway is meant to be illustrative. Indeed this scenario is only one of many possible scenarios that might reach the 2°C goal.

By designing a mitigation scenario in line with the 2°C climate goal, the goal is to keep consistency with the global warming level associated with the set of climate impact inputs developed under the RCP2.6. As noted in the main text, the RCP2.6 provides climate forcing levels consistent with the long-term goal of the Paris Agreement of keeping global warming likely below 2°C above pre-industrial temperatures (IPCC 2014). Figures B.23 and B.24 compare the *NDC_to_2C* scenario with a range of policy scenarios consistent with the RCP2.6 forcing levels explored by the scientific literature (for comparison, the GCAM baseline, i.e., “no policy” scenario is also shown; except for the climate policy, the GCAM baseline and *NDC_to_2C* scenarios share all other assumptions).

Global population and GDP assumptions in the *NDC_to_2C* derive from the GCAM implementation of the "Middle of the Road" Shared Socioeconomic Pathway (SSP) 2, which reflects a world in which social, economic and technological future trends do not differ markedly from historical patterns (Riahi et al. 2017). However, as noted in the Chapter 3, socioeconomic assumptions in LAC (specifically in Argentina, Colombia and Uruguay) were revised to align with LAC countries' future projections.

All mitigation scenarios explored in this study are based on the *NDC_to_2C* scenario. In other words, all *RCP26* scenarios presented in Table 3.1 share the same assumptions with the *NDC_to_2C* scenario, except for the climate impacts and technology availability components. Note that the *NDC_to_2C* and the *RCP26_FullTech: No-Climate impacts* scenarios share exactly the same assumptions since the *NDC_to_2C* scenario was constructed assuming that the full suite of power sector technologies represented by GCAM was available globally and under the assumption of no climate impacts on renewables.

Appendix C: Supplementary Material - Chapter 4

Supplementary Figures

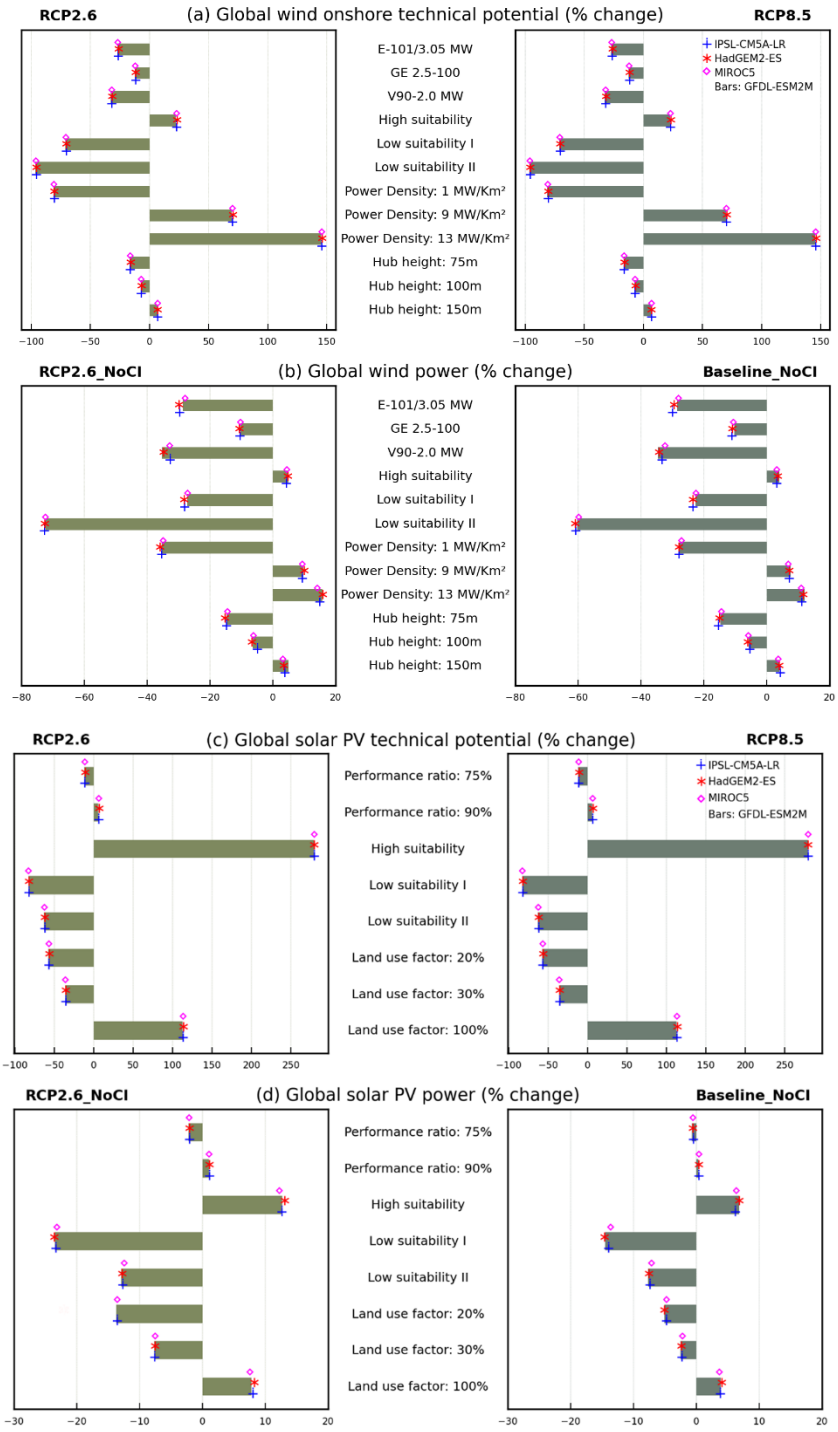

Figure C.1. (a) Changes in the global wind onshore technical potential relative to the *Central* case by sensitivity case and RCP. Technical potentials are computed for the 1971-2000 period.

(b) Changes in the global wind power generation by sensitivity case and scenario in 2100 (climate impact *"NoCI"* assumptions). Changes are relative to a GCAM simulation using supply curves produced from the *Central* technical potential case. (c) As in (a) but for the global solar PV technical potential. (d) As in (b) but for the global solar PV power. (Note: the case assuming land use factor of 20% has not solved for the RCP2.6_NoCI scenario using the HadGEM2-ES input data).

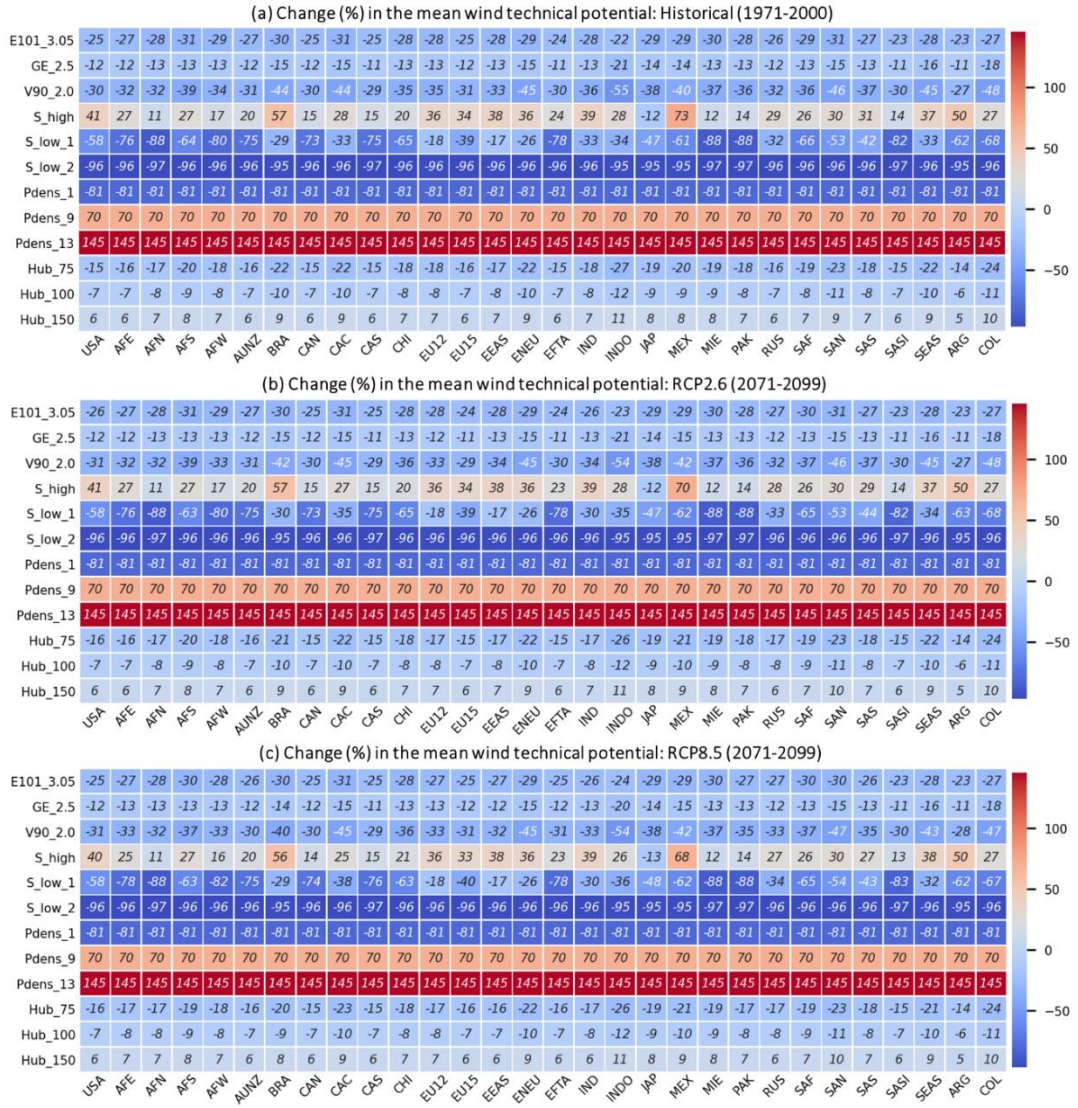

Figure C.2. (a) Relative changes in wind onshore technical potential from central assumption by sensitivity case and GCAM region (input data: GFDL-ESM2M model - 1971-2000). (b) As in (a) but using input data from the 2071-2100 under RCP2.6. (c) As in (b) but using input data from the 2071-2100 under RCP8.5.

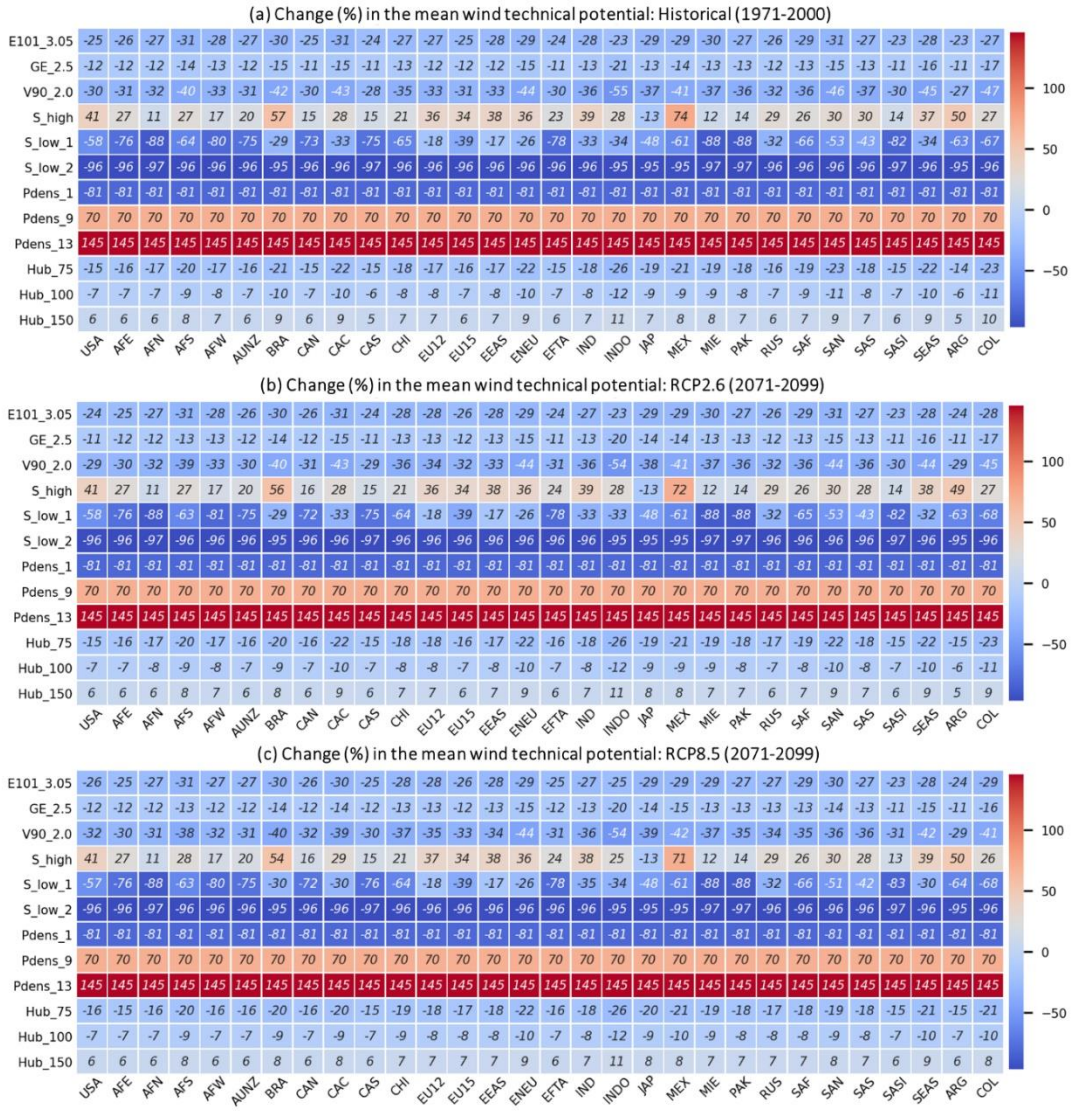

Figure C.3. (a) Relative changes in wind onshore technical potential from central assumption by sensitivity case and GCAM region (input data: HadGEM2-ES model - 1971-2000). (b) As in (a) but using input data from the 2071-2100 under RCP2.6. (c) As in (b) but using input data from the 2071-2100 under RCP8.5.

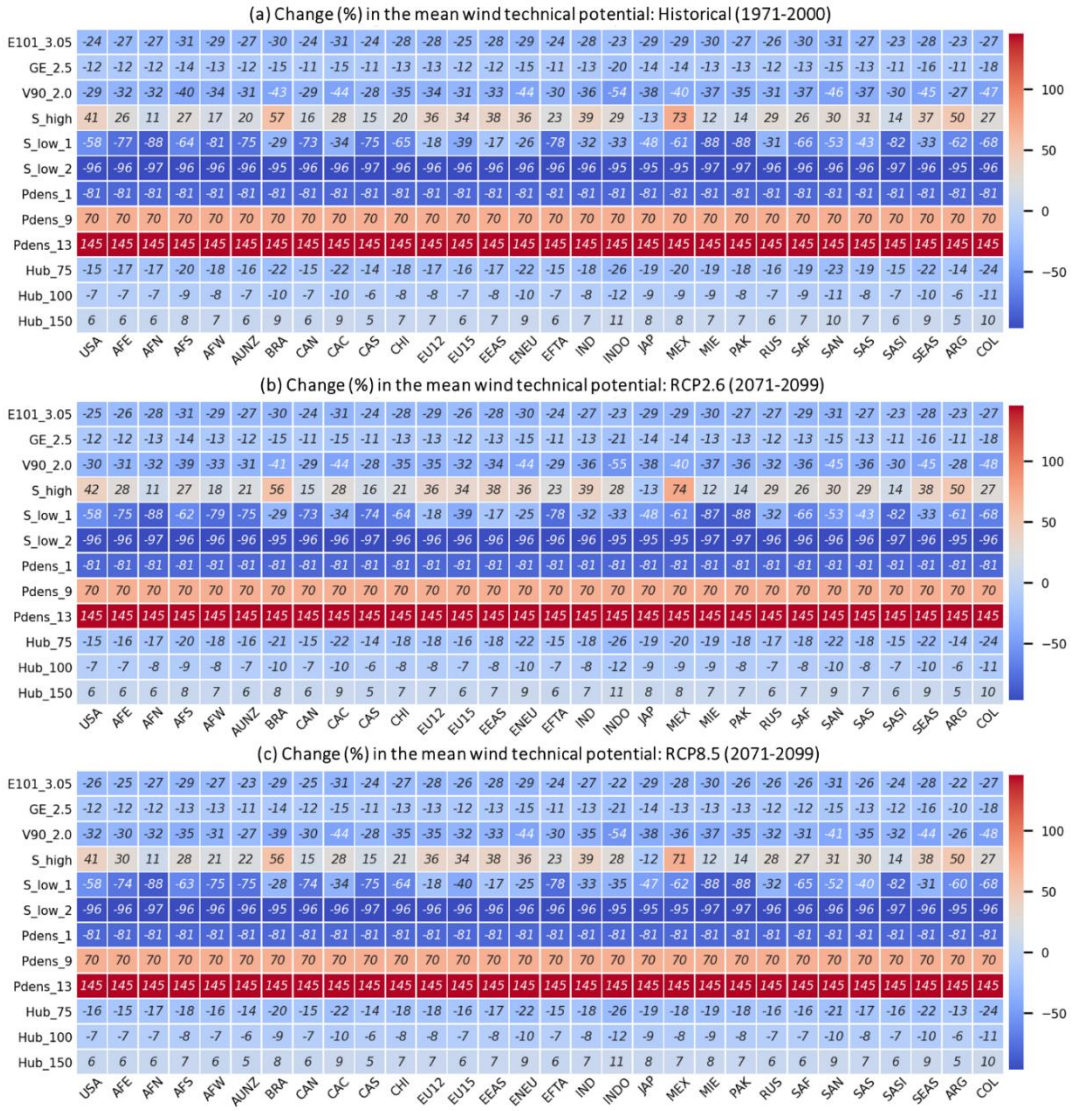

Figure C.4. (a) Relative changes in wind onshore technical potential from central assumption by sensitivity case and GCAM region (input data: IPSL-CM5A-LR model - 1971-2000). (b) As in (a) but using input data from the 2071-2100 under RCP2.6. (c) As in (b) but using input data from the 2071-2100 under RCP8.5.

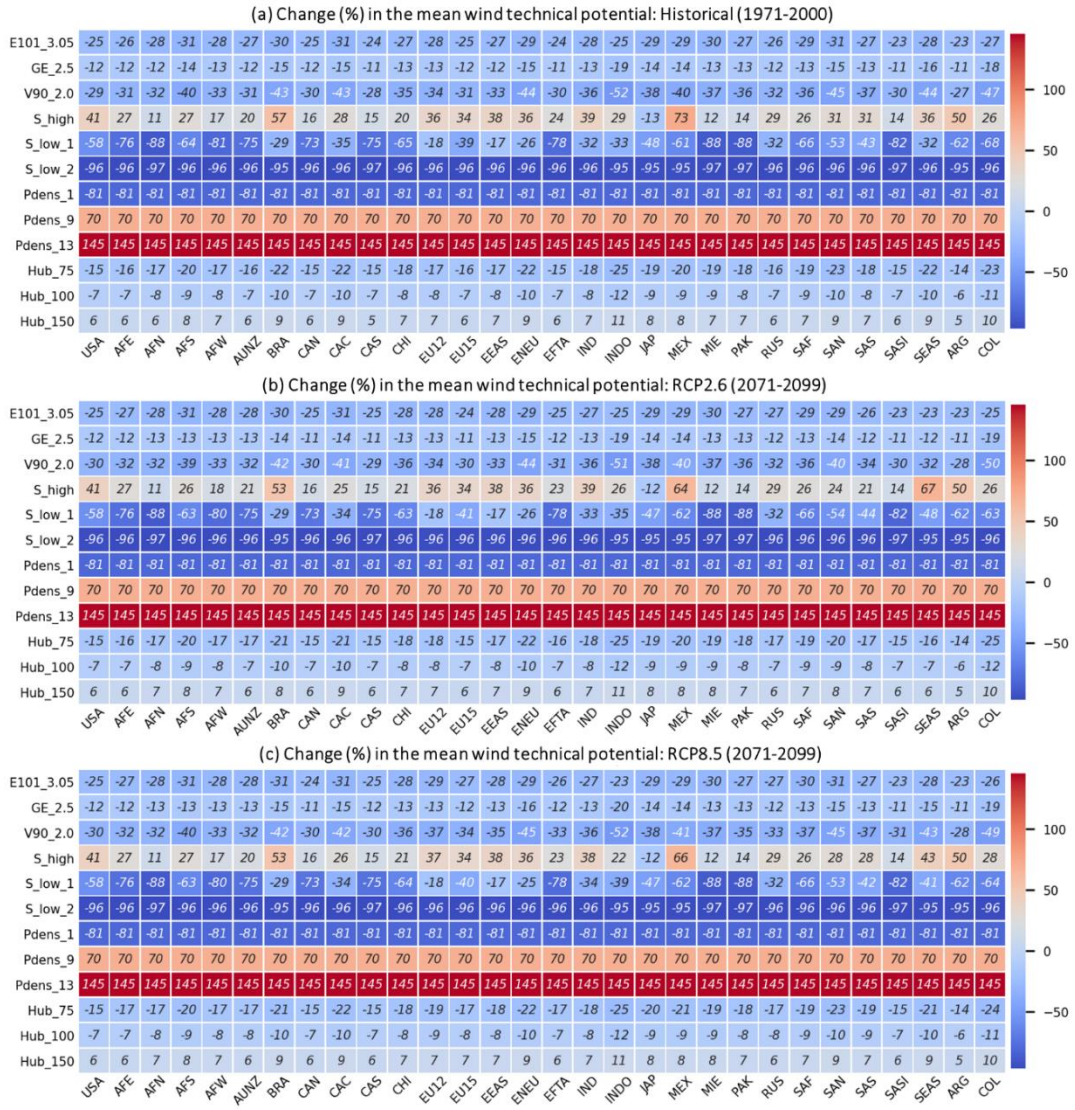

Figure C.5. (a) Relative changes in wind onshore technical potential from central assumption by sensitivity case and GCAM region (input data: MIROC5 model - 1971-2000). (b) As in (a) but using input data from the 2071-2100 under RCP2.6. (c) As in (b) but using input data from the 2071-2100 under RCP8.5.

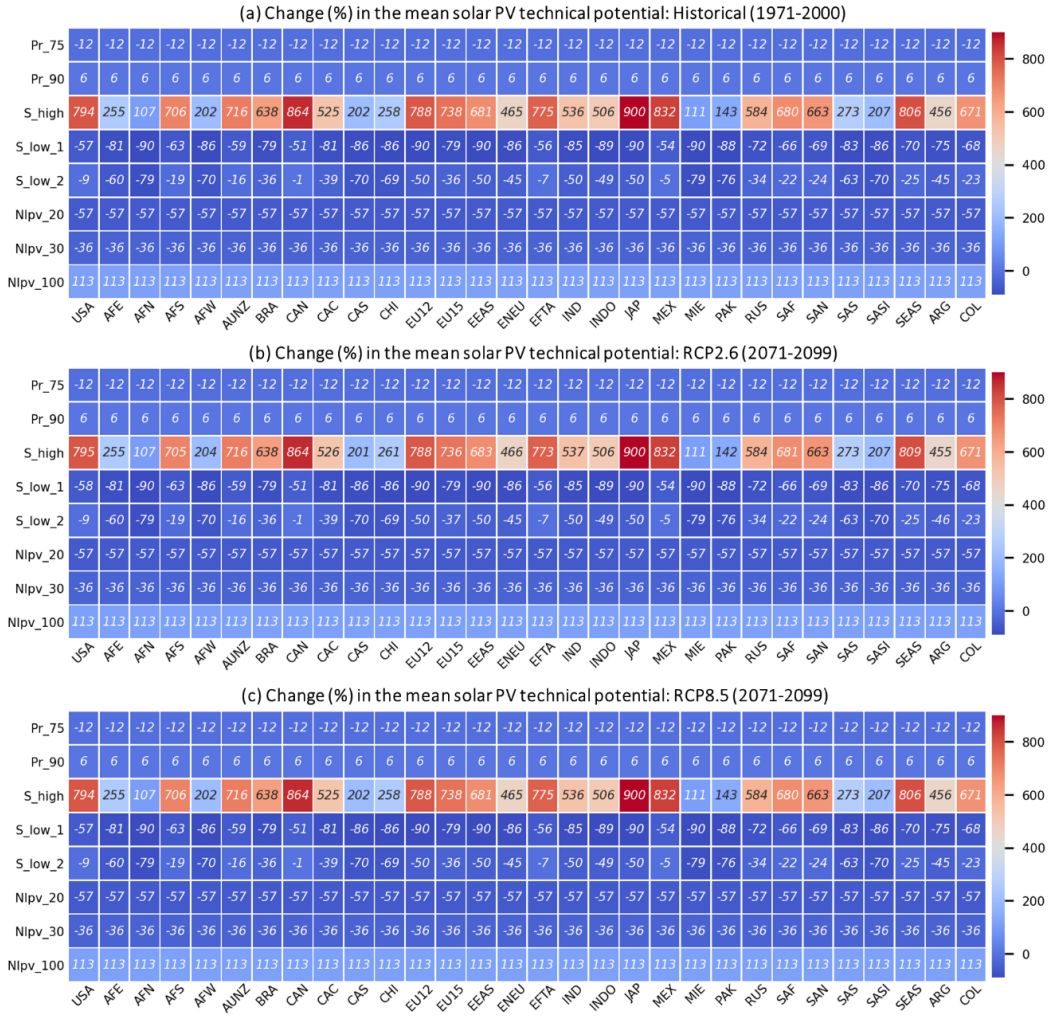

Figure C.6. (a) Relative changes in solar PV technical potential from central assumption by sensitivity case and GCAM region (input data: GFDL-ESM2M model - 1971-2000). (b) As in (a) but using input data from the 2071-2100 under RCP2.6. (c) As in (b) but using input data from the 2071-2100 under RCP8.5.

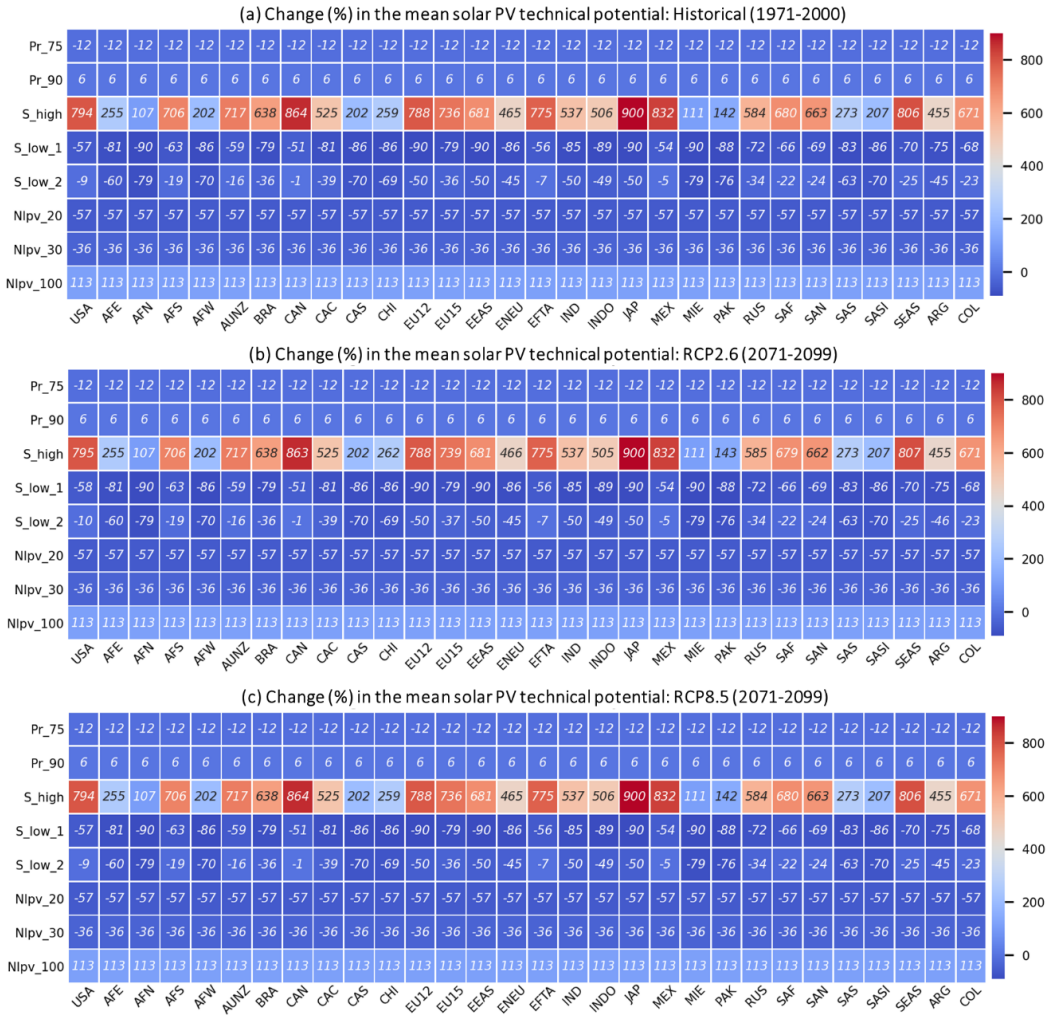

Figure C.7. (a) Relative changes in solar PV technical potential from central assumption by sensitivity case and GCAM region (input data: HadGEM2-ES model - 1971-2000). (b) As in (a) but using input data from the 2071-2100 under RCP2.6. (c) As in (b) but using input data from the 2071-2100 under RCP8.5.

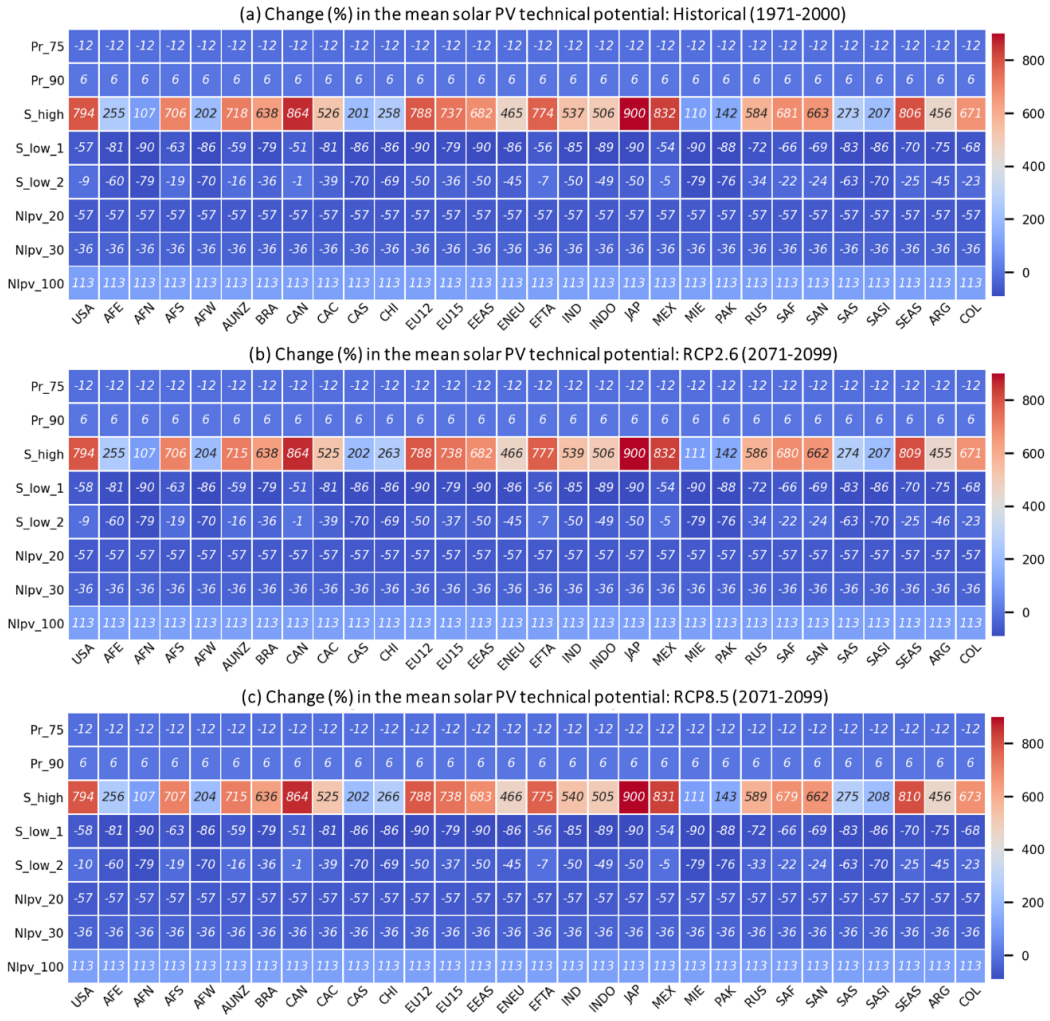

Figure C.8. (a) Relative changes in solar PV technical potential from central assumption by sensitivity case and GCAM region (input data: IPSL-CM5A-LR model - 1971-2000). (b) As in (a) but using input data from the 2071-2100 under RCP2.6. (c) As in (b) but using input data from the 2071-2100 under RCP8.5.

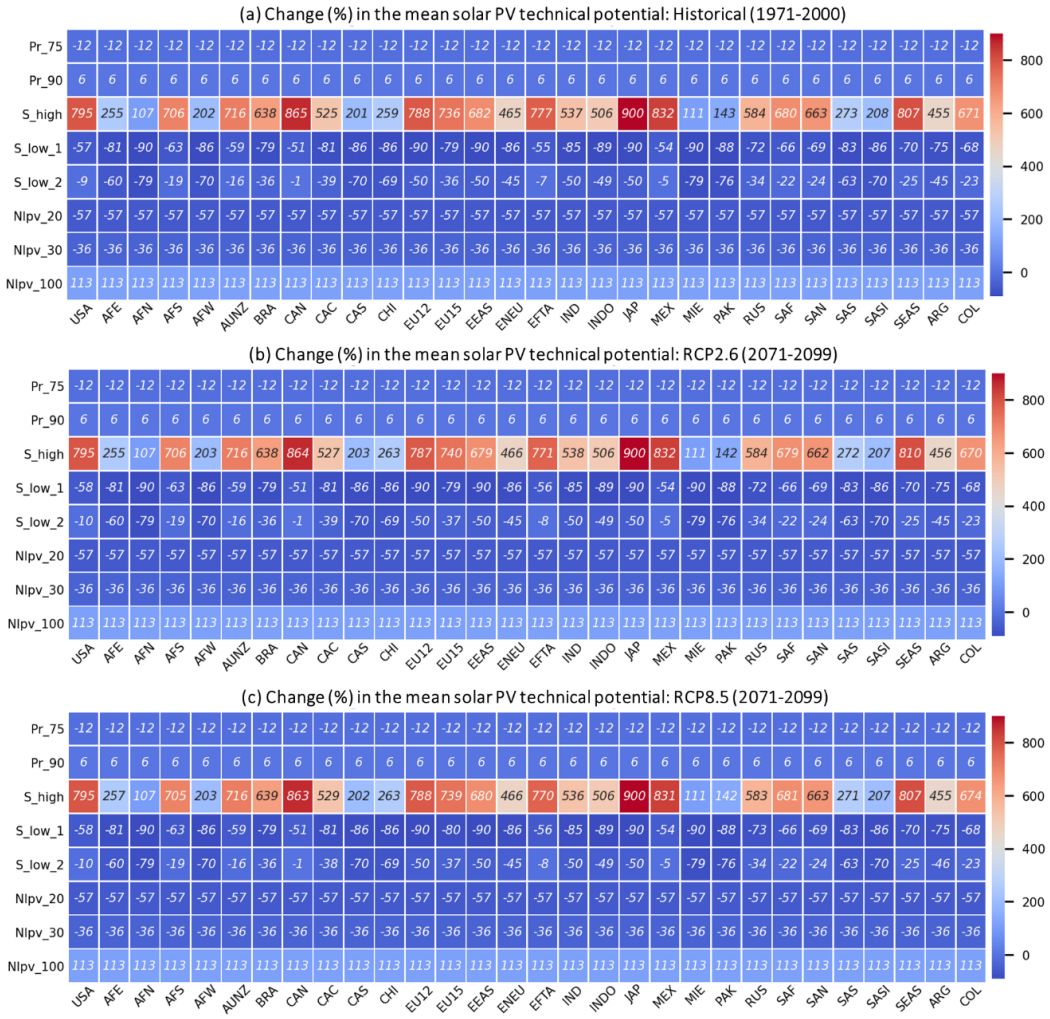

Figure C.9. (a) Relative changes in solar PV technical potential from central assumption by sensitivity case and GCAM region (input data: MIROC5 model - 1971-2000). (b) As in (a) but using input data from the 2071-2100 under RCP2.6. (c) As in (b) but using input data from the 2071-2100 under RCP8.5.

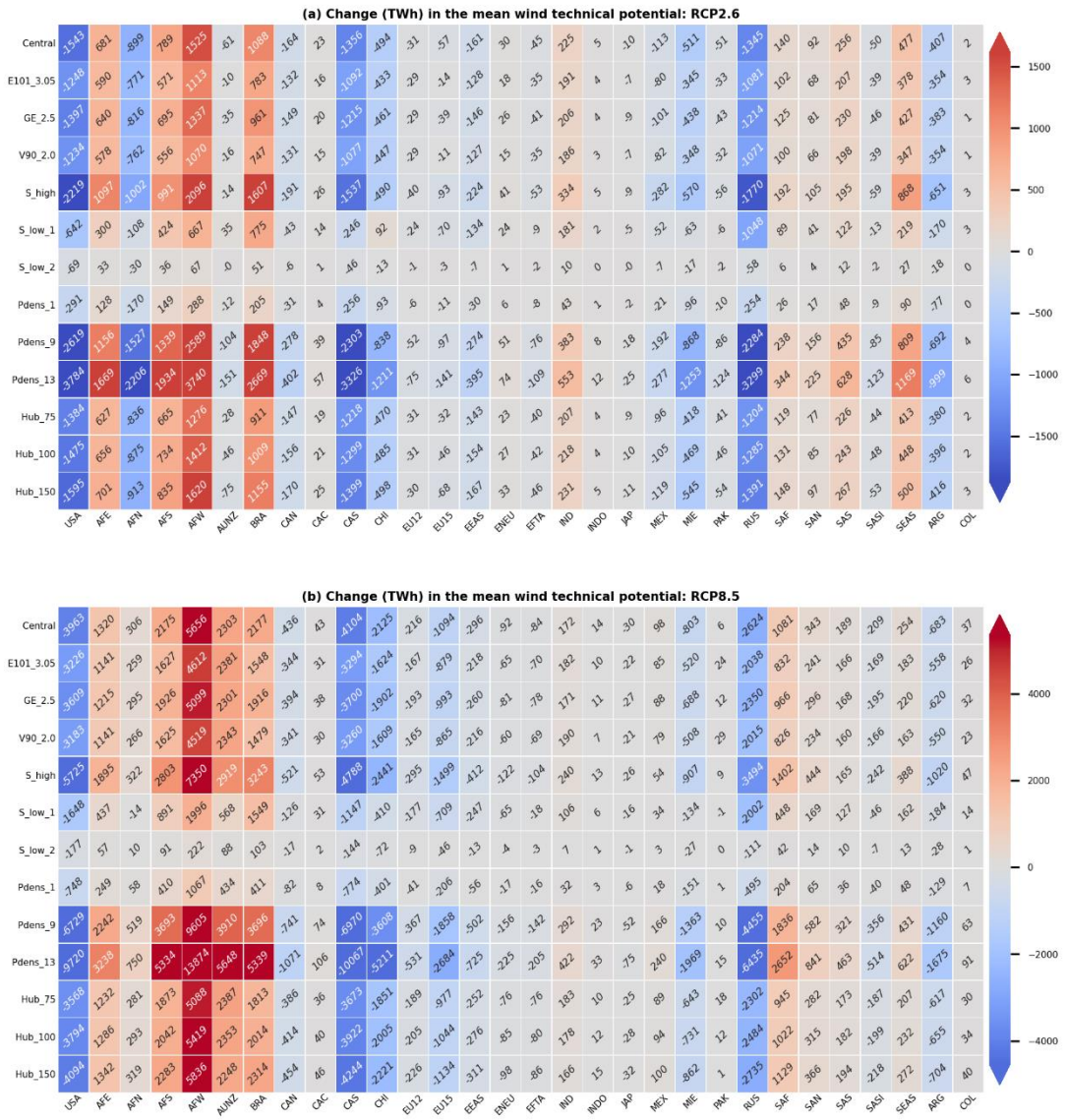

Figure C.10. Multi-model mean change in annual mean wind technical potential (TWh) in 2071-2099 relative to the historical period (1971-2000) from the four ISIMIP2b GCMs used in this study by forcing scenario.

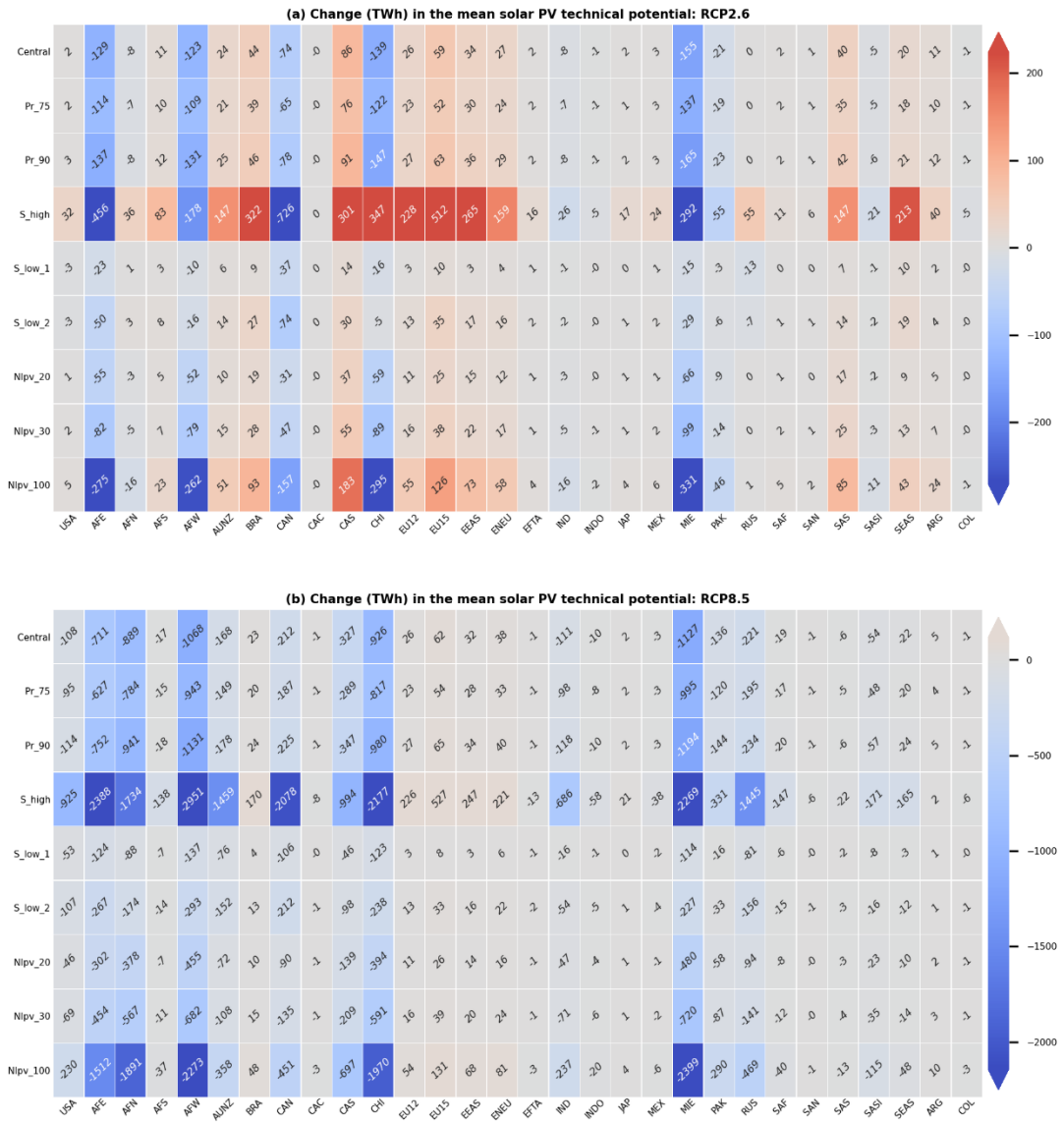

Figure C.11. Multi-model mean change in annual mean solar PV technical potential (TWh) in 2071-2099 relative to the historical period (1971-2000) from the four ISIMIP2b GCMs used in this study by forcing scenario.

Bibliography

Aide, T. M., and Coauthors, 2013: Deforestation and Reforestation of Latin America and the Caribbean (2001–2010). *Biotropica*, **45,** 262-271.

Albrecht, T. R., A. Crootof, and C. A. Scott, 2018: The Water-Energy-Food Nexus: A systematic review of methods for nexus assessment. *Environmental Research Letters*, **13,** 043002.

Almeida Prado, F., S. Athayde, J. Mossa, S. Bohlman, F. Leite, and A. Oliver-Smith, 2016: How much is enough? An integrated examination of energy security, economic growth and climate change related to hydropower expansion in Brazil. *Renewable and Sustainable Energy Reviews*, **53,** 1132-1136.

Amatulli, G., S. Domisch, M.-N. Tuanmu, B. Parmentier, A. Ranipeta, J. Malczyk, and W. Jetz, 2018: A suite of global, cross-scale topographic variables for environmental and biodiversity modeling. *Scientific Data*, **5,** 180040.

Arango-Aramburo, S., and Coauthors, 2019: Climate impacts on hydropower in Colombia: A multi-model assessment of power sector adaptation pathways. *Energy Policy*, **128,** 179-188.

Arent, D. J., and Coauthors, 2014: Key economic sectors and services. *Climate Change 2014: Impacts, Adaptation, and Vulnerability. Part A: Global and Sectoral Aspects. Contribution of Working Group II to the Fifth Assessment Report of the Intergovernmental Panel on Climate Change*, C. B. Field, V. R. Barros, D. J. Dokken, K. J. Mach, M. D. Mastrandrea, T. E. Bilir, and M. Chatterjee, Eds., Cambridge University Press, 659–708.

Bartos, M. D., and M. V. Chester, 2015: Impacts of climate change on electric power supply in the Western United States. *Nature Climate Change*, **5,** 748-752.

Bazilian, M., and Coauthors, 2011: Considering the energy, water and food nexus: Towards an integrated modelling approach. *Energy Policy*, **39,** 7896-7906.

Bellfield, H., 2015: Water, Energy and Food Security Nexus in Latin America and the Caribbean.

Bergin, M. H., C. Ghoroi, D. Dixit, J. J. Schauer, and D. T. Shindell, 2017: Large Reductions in Solar Energy Production Due to Dust and Particulate Air Pollution. *Environmental Science & Technology Letters*, **4,** 339-344.

Bertram, C., and Coauthors, 2018: Targeted policies can compensate most of the increased sustainability risks in 1.5 °C mitigation scenarios. *Environmental Research Letters*, **13,** 064038.

Binsted, M., and Coauthors, 2020: Stranded asset implications of the Paris Agreement in Latin America and the Caribbean. *Environmental Research Letters*, **15,** 044026.

Bontemps, S., P. Defourny, E. Van Bogaert, O. Arino, V. Kalogirou, and J. Ramos Perez, 2011: GLOBCOVER 2009 Products description and validation report.

Bosch, J., I. Staffell, and A. D. Hawkes, 2017: Temporally-explicit and spatially-resolved global onshore wind energy potentials. *Energy*, **131,** 207-217.

Bruinsma, J., 2009: The resource outlook to 2050: by how much do land, water, and crop yields need to
increase by 2050? Expert Meeting on How to Feed the World in 2050. Food and Agriculture Organization of the United Nations.

Bukhary, S., S. Ahmad, and J. Batista, 2018: Analyzing land and water requirements for solar deployment in the Southwestern United States. *Renewable and Sustainable Energy Reviews*, **82,** 3288-3305.
Calderón, S., and Coauthors, 2016: Achieving CO2 reductions in Colombia: Effects of carbon taxes and abatement targets. *Energy Economics*, **56,** 575-586.
Calvin and Bond-Lamberty, B., 2018: Integrated human-earth system modeling—state of the science and future directions. *Environmental Research Letters*, **13**.
Calvin, K., M. Wise, P. Kyle, P. Patel, L. Clarke, and J. Edmonds, 2014: Trade-offs of different land and bioenergy policies on the path to achieving climate targets. *Climatic Change*, **123,** 691-704.
Calvin, K., and Coauthors, 2019: GCAM v5. 1: representing the linkages between energy, water, land, climate, and economic systems. *Geoscientific Model Development*, **12,** 677-698.
——, 2017: The SSP4: A world of deepening inequality. *Global Environmental Change*, **42,** 284-296.
Calvin, K. V., R. Beach, A. Gurgel, M. Labriet, and A. M. Loboguerrero Rodriguez, 2016: Agriculture, forestry, and other land-use emissions in Latin America. *Energy Economics*, **56,** 615-624.
Carvajal, P. E., G. Anandarajah, Y. Mulugetta, and O. Dessens, 2017: Assessing uncertainty of climate change impacts on long-term hydropower generation using the CMIP5 ensemble—the case of Ecuador. *Climatic Change*, **144,** 611-624.
Carvajal, P. E., F. G. N. Li, R. Soria, J. Cronin, G. Anandarajah, and Y. Mulugetta, 2019: Large hydropower, decarbonisation and climate change uncertainty: Modelling power sector pathways for Ecuador. *Energy Strategy Reviews*, **23,** 86-99.
Carvalho, A. L. d., R. S. C. Menezes, R. S. Nóbrega, A. d. S. Pinto, J. P. H. B. Ometto, C. von Randow, and A. Giarolla, 2015: Impact of climate changes on potential sugarcane yield in Pernambuco, northeastern region of Brazil. *Renewable Energy*, **78,** 26-34.
Clarke and Edmonds, 1993: Modelling energy technologies in a competitive market. *Energy Economics*, **15,** 123-129.
Clarke, L., and Coauthors, 2018: Effects of long-term climate change on global building energy expenditures. *Energy Economics*, **72,** 667-677.
——, 2016: Long-term abatement potential and current policy trajectories in Latin American countries. *Energy Economics*, **56,** 513-525.
——, 2014: Assessing Transformation Pathways. *Climate Change 2014: Mitigation of Climate Change. Contribution of Working Group III to the Fifth Assessment Report of the Intergovernmental Panel on Climate Change*, O. Edenhofer, and Coauthors, Eds., Cambridge University Press.
Collins, M., R. Knutti, J. Arblaster, J.-L. Dufresne, T. Fichefet, P. Friedlingstein, and X. Gao, 2013: Long-term Climate Change: Projections, Commitments and Irreversibility. *Climate Change 2013: The Physical Science Basis. Contribution of Working Group I to the Fifth Assessment Report of the Intergovernmental Panel on Climate Change*, T. F. Stocker, D. Qin, G.-K. Plattner, M. Tignor, S. K. Allen, J. Boschung, and A. Nauels, Eds., Cambridge University Press.
Cronin, J., G. Anandarajah, and O. Dessens, 2018: Climate change impacts on the energy system: a review of trends and gaps. *Climatic Change*, **151,** 79-93.

Crook, J. A., L. A. Jones, P. M. Forster, and R. Crook, 2011: Climate change impacts on future photovoltaic and concentrated solar power energy output. *Energy & Environmental Science*, **4,** 3101-3109.
D'Odorico, P., and Coauthors, 2018: The Global Food-Energy-Water Nexus. *Reviews of Geophysics*, **56,** 456-531.
Dallemand, J., J. Hilbert, and F. Monforti, 2015: Bioenergy and Latin America: A Multi-Country Perspective (JRC Technical Report EUR 27185 EN).
Damassa, T., T. Fransen, B. Haya, M. Ge, K. Pjeczka, and K. Ross, 2015: Interpreting INDCs: Assessing Transparency of Post-2020 Greenhouse Gas Emissions Targets for 8 Top-Emitting Economies. World Resources Institute.
Davies, E. G. R., P. Kyle, and J. A. Edmonds, 2013: An integrated assessment of global and regional water demands for electricity generation to 2095. *Advances in Water Resources*, **52,** 296-313.
de Jong, P., T. B. Barreto, C. A. S. Tanajura, D. Kouloukoui, K. P. Oliveira-Esquerre, A. Kiperstok, and E. A. Torres, 2019: Estimating the impact of climate change on wind and solar energy in Brazil using a South American regional climate model. *Renewable Energy*, **141,** 390-401.
de Oliveira, A. S., R. Trezza, E. Holzapfel, I. Lorite, and V. P. S. Paz, 2009: Irrigation Water Management in Latin America. *Chilean journal of agricultural research*, **69,** 7-16.
De Souza Dias, V., M. Pereira da Luz, M. G. Medero, and D. Tarley Ferreira Nascimento, 2018: An Overview of Hydropower Reservoirs in Brazil: Current Situation, Future Perspectives and Impacts of Climate Change. *Water*, **10**.
de Vries, B. J. M., D. P. van Vuuren, and M. M. Hoogwijk, 2007: Renewable energy sources: Their global potential for the first-half of the 21st century at a global level: An integrated approach. *Energy Policy*, **35,** 2590-2610.
Deng, Y. Y., and Coauthors, 2015: Quantifying a realistic, worldwide wind and solar electricity supply. *Global Environmental Change*, **31,** 239-252.
Denholm, P., and R. Margolis, 2008: Supply Curves for Rooftop Solar PV-Generated Electricity for the United StatesNREL/TP-6A0-44073.
Dowling, P., 2013: The impact of climate change on the European energy system. *Energy Policy*, **60,** 406-417.
Dupont, E., R. Koppelaar, and H. Jeanmart, 2020: Global available solar energy under physical and energy return on investment constraints. *Applied Energy*, **257,** 113968.
Ebinger, J., and W. Vergara, 2011: Climate Impacts on Energy Systems: Key Issues for Energy Sector Adaptation.
ECLAC/FAO/IICA: The Outlook for Agriculture and Rural Development in the Americas: A Perspective on Latin America and the Caribbean. [Available online at http://www.fao.org/3/a-as167e.pdf.]
EIA, cited 2019: Independent Statistics & Analysis. [Available online at https://www.eia.gov/international/data/world.]
Elliott, J., and Coauthors, 2014: The parallel system for integrating impact models and sectors (pSIMS). *Environmental Modelling & Software*, **62,** 509-516.

Emodi, N. V., T. Chaiechi, and A. B. M. R. A. Beg, 2019: The impact of climate variability and change on the energy system: A systematic scoping review. *Science of The Total Environment*, **676,** 545-563.
EPE: Brazilian Energy Balance 2016. [Available online at https://ben.epe.gov.br/downloads/S%c3%adntese%20do%20Relat%c3%b3rio%20Final_2016_Web.pdf.]
Eurek, K., P. Sullivan, M. Gleason, D. Hettinger, D. Heimiller, and A. Lopez, 2017: An improved global wind resource estimate for integrated assessment models. *Energy Economics*, **64,** 552-567.
FAO, cited 2018: FAOSTAT Statistics Database. [Available online at fao.org/faostat/en/#data.]
——, cited 2018: AQUASTAT Main Database. [Available online at http://www.fao.org/nr/water/aquastat/main/index.stm.]
FAO/PAHO, 2017: Panorama of Food and Nutrition Security in Latin America and the Caribbean.
Fargione, J., J. Hill, D. Tilman, S. Polasky, and P. Hawthorne, 2008: Land Clearing and the Biofuel Carbon Debt. *Science*, **319,** 1235.
Fawcett, A. A., and Coauthors, 2015: Can Paris pledges avert severe climate change? *Science*, **350,** 1168.
Federative Republic of Brazil, cited 2020: Intended Nationally Determined Contribution towards achieving the objective of the United Nations Framework Convention on Climate Change. [Available online at https://www4.unfccc.int/sites/submissions/INDC/Published%20Documents/Brazil/1/BRAZIL%20iNDC%20english%20FINAL.pdf.]
Fisher-Vanden and Weyant, 2020: The Evolution of Integrated Assessment: Developing the Next Generation of Use-Inspired Integrated Assessment Tools. *Annual Review of Resource Economics*, **12,** 471-487.
Fisher-Vanden, K., and J. Weyant, 2020: The Evolution of Integrated Assessment: Developing the Next Generation of Use-Inspired Integrated Assessment Tools. *Annual Review of Resource Economics*, **12,** 471-487.
Forsell, N., O. Turkovska, M. Gusti, M. Obersteiner, M. d. Elzen, and P. Havlik, 2016: Assessing the INDCs' land use, land use change, and forest emission projections. *Carbon Balance and Management*, **11,** 26.
Frieler, K., and Coauthors, 2017: Assessing the impacts of 1.5 °C global warming – simulation protocol of the Inter-Sectoral Impact Model Intercomparison Project (ISIMIP2b). *Geosci. Model Dev.*, **10,** 4321-4345.
García, C. A., E. Riegelhaupt, A. Ghilardi, M. Skutsch, J. Islas, F. Manzini, and O. Masera, 2015: Sustainable bioenergy options for Mexico: GHG mitigation and costs. *Renewable and Sustainable Energy Reviews*, **43,** 545-552.
Gerbens-Leenes, W., A. Y. Hoekstra, and T. H. van der Meer, 2009: The water footprint of bioenergy. *Proceedings of the National Academy of Sciences*, **106,** 10219.
Gernaat, D. E. H. J., H. S. de Boer, V. Daioglou, S. G. Yalew, C. Müller, and D. P. van Vuuren, 2021: Climate change impacts on renewable energy supply. *Nature Climate Change*.

Graham, N. T., M. I. Hejazi, S. H. Kim, E. G. R. Davies, J. A. Edmonds, and F. Miralles-Wilhelm, 2020a: Future changes in the trading of virtual water. *Nature Communications*, **11,** 3632.
Graham, N. T., and Coauthors, 2020b: Humans drive future water scarcity changes across all Shared Socioeconomic Pathways. *Environmental Research Letters*, **15,** 014007.
Grassi, G., J. House, F. Dentener, S. Federici, M. den Elzen, and J. Penman, 2017: The key role of forests in meeting climate targets requires science for credible mitigation. *Nature Climate Change*, **7,** 220-226.
Gruber, S., 2012: Derivation and analysis of a high-resolution estimate of global permafrost zonation. *The Cryosphere*, **6,** 221-233.
Grubert, E., and S. Kitasei, 2010: How Energy Choices Affect Fresh Water Supplies: A Comparison of U.S. Coal and Natural Gas (Briefing Paper 2). *World Watch Institute*.
Hallegatte, S., 2009: Strategies to adapt to an uncertain climate change. *Global Environmental Change*, **19,** 240-247.
Hamududu, B., and A. Killingtveit, 2012: Assessing Climate Change Impacts on Global Hydropower. *Energies*, **5**.
Hartin, C. A., P. Patel, A. Schwarber, R. P. Link, and B. P. Bond-Lamberty, 2015: A simple object-oriented and open-source model for scientific and policy analyses of the global climate system – Hector v1.0. *Geosci. Model Dev.*, **8,** 939-955.
Haszeldine, R. S., 2009: Carbon Capture and Storage: How Green Can Black Be? *Science*, **325,** 1647.
Havlík, P., and Coauthors, 2011: Global land-use implications of first and second generation biofuel targets. *Energy Policy*, **39,** 5690-5702.
Hejazi, M., and Coauthors, 2014a: Long-term global water projections using six socioeconomic scenarios in an integrated assessment modeling framework. *Technological Forecasting and Social Change*, **81,** 205-226.
Hejazi, M. I., and Coauthors, 2014b: Integrated assessment of global water scarcity over the 21st century under multiple climate change mitigation policies. *Hydrol. Earth Syst. Sci.*, **18,** 2859-2883.
Hof, A. F., M. G. J. den Elzen, A. Admiraal, M. Roelfsema, D. E. H. J. Gernaat, and D. P. van Vuuren, 2017: Global and regional abatement costs of Nationally Determined Contributions (NDCs) and of enhanced action to levels well below 2°C and 1.5°C. *Environmental Science & Policy*, **71,** 30-40.
Hoff, H., 2011: Understanding the Nexus. *Background Paper for the Bonn 2011 Conference:* , Stockholm Environment Institute, 51.
Hoogwijk, M., 2004: On the global and regional potential of renewable energy sources. Ph.D. thesis, Utrecht University, 256 pp.
Hoogwijk, M., B. de Vries, and W. Turkenburg, 2004: Assessment of the global and regional geographical, technical and economic potential of onshore wind energy. *Energy Economics*, **26,** 889-919.
Howells, M., and Coauthors, 2013: Integrated analysis of climate change, land-use, energy and water strategies. *Nature Climate Change*, **3,** 621.
IEA, 2017: CO2 Emissions from Fuel Combustion Highlights (2017 edition).

——: Data and statistics. [Available online at https://www.iea.org/data-and-statistics.]
India, cited 2020: India's Intended Nationally Determined Contribution: working towards climate justice. [Available online at https://www4.unfccc.int/sites/submissions/INDC/Published%20Documents/India/1/INDIA%20INDC%20TO%20UNFCCC.pdf.]
IPCC, 2012: Special Report on Renewable Energy Sources and Climate Change Mitigation.
——, 2014: Climate Change 2014: Synthesis Report.
——, 2018: Summary for Policymakers. *Global Warming of 1.5°C. An IPCC Special Report on the impacts of global warming of 1.5 °C above pre-industrial levels and related global greenhouse gas emission pathways, in the context of strengthening the global response to the threat of climate change, sustainable development and efforts to eradicate poverty*, V. Masson-Delmotte, and Coauthors, Eds., *World Meteorological Organization*, 32.
IRENA, 2016: Renewable Energy Market Analysis: Latin America.
——, 2018: Renewable Energy Statistics 2018, 1 –348 pp.
Iyer, G., C. Ledna, L. Clarke, J. Edmonds, H. McJeon, P. Kyle, and J. H. Williams, 2017: Measuring progress from nationally determined contributions to mid-century strategies. *Nature Climate Change*, **7,** 871-874.
Iyer, G., and Coauthors, 2018: Implications of sustainable development considerations for comparability across nationally determined contributions. *Nature Climate Change*, **8,** 124-129.
Iyer, G. C., L. E. Clarke, J. A. Edmonds, B. P. Flannery, N. E. Hultman, H. C. McJeon, and D. G. Victor, 2015a: Improved representation of investment decisions in assessments of CO2 mitigation. *Nature Climate Change*, **5,** 436-440.
Iyer, G. C., and Coauthors, 2015b: The contribution of Paris to limit global warming to 2 °C. *Environmental Research Letters*, **10,** 125002.
Jerez, S., and Coauthors, 2015: The impact of climate change on photovoltaic power generation in Europe. *Nature communications*, **6,** 10014.
JGCRI, cited 2019: GCAM v5.1 Documentation. [Available online at http://jgcri.github.io/gcam-doc/v5.1/toc.html.]
Jones, J. W., and Coauthors, 2003: The DSSAT cropping system model. *European Journal of Agronomy*, **18,** 235-265.
Jägermeyr, J., D. Gerten, J. Heinke, S. Schaphoff, M. Kummu, and W. Lucht, 2015: Water savings potentials of irrigation systems: global simulation of processes and linkages. *Hydrol. Earth Syst. Sci.*, **19,** 3073-3091.
Karnauskas, K. B., J. K. Lundquist, and L. Zhang, 2018: Southward shift of the global wind energy resource under high carbon dioxide emissions. *Nature Geoscience*, **11,** 38-43.
Khan, Z., and Coauthors, 2020: Integrated energy-water-land nexus planning to guide national policy: an example from Uruguay. *Environmental Research Letters*.
Klapperich, R. J., and Coauthors, 2014: The Nexus of Water and CCS: A Regional Carbon Sequestration Partnership Perspective. *Energy Procedia*, **63,** 7162-7172.

Knutti, R., R. Furrer, C. Tebaldi, J. Cermak, and G. A. Meehl, 2010: Challenges in Combining Projections from Multiple Climate Models. *Journal of Climate*, **23,** 2739-2758.
Kober, T., J. Falzon, B. van der Zwaan, K. Calvin, A. Kanudia, A. Kitous, and M. Labriet, 2016: A multi-model study of energy supply investments in Latin America under climate control policy. *Energy Economics*, **56,** 543-551.
Korfiati, A., and Coauthors, 2016: Estimation of the Global Solar Energy Potential and Photovoltaic Cost with the use of Open Data. *International Journal of Sustainable Energy Planning and Management*, ***9,*** 17–30.
Krey, V., and Coauthors, 2014: Annex II: Metrics & Methodology. In: Climate Change 2014: Mitigation of Climate Change. Contribution of Working Group III to the Fifth Assessment Report of the Intergovernmental Panel on Climate Change.
Kundzewicz, Z. W., V. Krysanova, R. E. Benestad, Ø. Hov, M. Piniewski, and I. M. Otto, 2018: Uncertainty in climate change impacts on water resources. *Environmental Science & Policy*, **79,** 1-8.
Kyle, P., C. Müller, K. Calvin, and A. Thomson, 2014: Meeting the radiative forcing targets of the representative concentration pathways in a world with agricultural climate impacts. *Earth's Future*, **2,** 83-98.
Köberle, A. C., D. E. H. J. Gernaat, and D. P. van Vuuren, 2015: Assessing current and future techno-economic potential of concentrated solar power and photovoltaic electricity generation. *Energy*, **89,** 739-756.
Lamontagne, J. R., P. M. Reed, R. Link, K. V. Calvin, L. E. Clarke, and J. A. Edmonds, 2018: Large Ensemble Analytic Framework for Consequence-Driven Discovery of Climate Change Scenarios. *Earth's Future*, **6,** 488-504.
le Polain de Waroux, Y., R. D. Garrett, J. Graesser, C. Nolte, C. White, and E. F. Lambin, 2019: The Restructuring of South American Soy and Beef Production and Trade Under Changing Environmental Regulations. *World Development*, **121,** 188-202.
Lipponen, J., S. McCulloch, S. Keeling, T. Stanley, N. Berghout, and T. Berly, 2017: The Politics of Large-scale CCS Deployment. *Energy Procedia*, **114,** 7581-7595.
Lu, X., M. B. McElroy, and J. Kiviluoma, 2009: Global potential for wind-generated electricity. *Proceedings of the National Academy of Sciences*, **106,** 10933.
Lucena, A. F. P., and Coauthors, 2016: Climate policy scenarios in Brazil: A multi-model comparison for energy. *Energy Economics*, **56,** 564-574.
——, 2018: Interactions between climate change mitigation and adaptation: The case of hydropower in Brazil. *Energy*, **164,** 1161-1177.
Macknick, J., R. Newmark, G. Heath, and K. Hallett, 2011: A Review of Operational Water Consumption and Withdrawal Factors for Electricity Generating Technologies.
Magrin, G. O., J. A. Marengo, J.-P. Boulanger, M. S. Buckeridge, E. Castellanos, G. Poveda, and F. R. Scarano, 2014: Central and South America. *Climate Change 2014: Impacts, Adaptation, and Vulnerability. Part B: Regional Aspects. Contribution of Working Group II to the Fifth Assessment Report of the Intergovernmental Panel on Climate Change*, V. R. Barros, C. B. Field, D. J. Dokken, M. D. Mastrandrea, K. J. Mach, T. E. Bilir, and M. Chatterjee, Eds., Cambridge University Press.

Marin, F. R., J. W. Jones, A. Singels, F. Royce, E. D. Assad, G. Q. Pellegrino, and F. Justino, 2013: Climate change impacts on sugarcane attainable yield in southern Brazil. *Climatic Change*, **117,** 227-239.
Mathioudakis, V., P. W. Gerbens-Leenes, T. H. Van der Meer, and A. Y. Hoekstra, 2017: The water footprint of second-generation bioenergy: A comparison of biomass feedstocks and conversion techniques. *Journal of Cleaner Production*, **148,** 571-582.
Mavromatakis, F., G. Makrides, G. Georghiou, A. Pothrakis, Y. Franghiadakis, E. Drakakis, and E. Koudoumas, 2010: Modeling the photovoltaic potential of a site. *Renewable Energy*, **35,** 1387-1390.
Mekonnen, M. M., and A. Y. Hoekstra, 2016: Four billion people facing severe water scarcity. *Science Advances*, **2,** e1500323.
Miara, A., and Coauthors, 2019: Climate-Water Adaptation for Future US Electricity Infrastructure. *Environmental Science & Technology*, **53,** 14029-14040.
Miralles-Wilhelm, F., 2016: Development and application of integrative modeling tools in support of food-energy-water nexus planning—a research agenda. *Journal of Environmental Studies and Sciences*, **6,** 3-10.
Munoz Castillo, R., K. Feng, K. Hubacek, L. Sun, J. Guilhoto, and F. Miralles-Wilhelm, 2017: Uncovering the Green, Blue, and Grey Water Footprint and Virtual Water of Biofuel Production in Brazil: A Nexus Perspective. *Sustainability*, **9**.
Muratori, M., and Coauthors, 2017: Cost of power or power of cost: A U.S. modeling perspective. *Renewable and Sustainable Energy Reviews*, **77,** 861-874.
Nelson, G. C., and Coauthors, 2014: Climate change effects on agriculture: Economic responses to biophysical shocks. *Proceedings of the National Academy of Sciences*, **111,** 3274.
Nepstad, D., and Coauthors, 2014: Slowing Amazon deforestation through public policy and interventions in beef and soy supply chains. *Science*, **344,** 1118.
OECD/FAO, 2015: OECD-FAO Agricultural Outlook 2015. OECD Publishing.
Pereira de Lucena, A. F., A. S. Szklo, R. Schaeffer, and R. M. Dutra, 2010: The vulnerability of wind power to climate change in Brazil. *Renewable Energy*, **35,** 904-912.
Pereira, E. B., F. R. Martins, M. P. Pes, E. I. da Cruz Segundo, and A. d. A. Lyra, 2013: The impacts of global climate changes on the wind power density in Brazil. *Renewable Energy*, **49,** 107-110.
Peters, G. P., and Coauthors, 2017: Key indicators to track current progress and future ambition of the Paris Agreement. *Nature Climate Change*, **7,** 118-122.
Pietzcker, R. C., and Coauthors, 2017: System integration of wind and solar power in integrated assessment models: A cross-model evaluation of new approaches. *Energy Economics*, **64,** 583-599.
Popescu, I., L. Brandimarte, and M. Peviani, 2014: Effects of climate change over energy production in La Plata Basin. *International Journal of River Basin Management*, **12,** 319-327.
Popp, A., and Coauthors, 2014: Land-use protection for climate change mitigation. *Nature Climate Change*, **4,** 1095-1098.
Postic, S., S. Selosse, and N. Maïzi, 2017: Energy contribution to Latin American INDCs: Analyzing sub-regional trends with a TIMES model. *Energy Policy*, **101,** 170-184.

PRODES-INPE, cited 2018: Brazilian Amazon Satellite Monitoring Program. [Available online at http://www.obt.inpe.br/OBT/assuntos/programas/amazonia/prodes.]
Pryor, S. C., and R. J. Barthelmie, 2010: Climate change impacts on wind energy: A review. *Renewable and Sustainable Energy Reviews*, **14,** 430-437.
——, 2013: Assessing the vulnerability of wind energy to climate change and extreme events. *Climatic Change*, **121,** 79-91.
Ren, X., and Coauthors, 2018: Avoided economic impacts of climate change on agriculture: integrating a land surface model (CLM) with a global economic model (iPETS). *Climatic Change*, **146,** 517-531.
Riahi, K., and Coauthors, 2015: Locked into Copenhagen pledges — Implications of short-term emission targets for the cost and feasibility of long-term climate goals. *Technological Forecasting and Social Change*, **90,** 8-23.
——, 2017: The Shared Socioeconomic Pathways and their energy, land use, and greenhouse gas emissions implications: An overview. *Global Environmental Change*, **42,** 153-168.
Ringler, C., A. Bhaduri, and R. Lawford, 2013: The nexus across water, energy, land and food (WELF): potential for improved resource use efficiency? *Current Opinion in Environmental Sustainability*, **5,** 617-624.
Rinne, E., H. Holttinen, J. Kiviluoma, and S. Rissanen, 2018: Effects of turbine technology and land use on wind power resource potential. *Nature Energy*, **3,** 494-500.
Rogelj, J., G. Luderer, R. C. Pietzcker, E. Kriegler, M. Schaeffer, V. Krey, and K. Riahi, 2015: Energy system transformations for limiting end-of-century warming to below 1.5 °C. *Nature Climate Change*, **5,** 519.
Rogelj, J., and Coauthors, 2016: Paris Agreement climate proposals need a boost to keep warming well below 2 °C. *Nature*, **534,** 631.
Rolla, A. L., M. N. Nuñez, E. R. Guevara, S. G. Meira, G. R. Rodriguez, and M. I. Ortiz de Zárate, 2018: Climate impacts on crop yields in Central Argentina. Adaptation strategies. *Agricultural Systems*, **160,** 44-59.
Rosenzweig, C., and Coauthors, 2014: Assessing agricultural risks of climate change in the 21st century in a global gridded crop model intercomparison. *Proceedings of the National Academy of Sciences*, **111,** 3268.
Ruffato-Ferreira, V., R. da Costa Barreto, A. Oscar Júnior, W. L. Silva, D. de Berrêdo Viana, J. A. S. do Nascimento, and M. A. V. de Freitas, 2017: A foundation for the strategic long-term planning of the renewable energy sector in Brazil: Hydroelectricity and wind energy in the face of climate change scenarios. *Renewable and Sustainable Energy Reviews*, **72,** 1124-1137.
Santos da Silva, S. R., and Coauthors, 2021: Power sector investment implications of climate impacts on renewable resources in Latin America and the Caribbean. *Nature Communications*, **12,** 1276.
Santos Da Silva, S. R., and Coauthors, 2019: The Paris pledges and the energy-water-land nexus in Latin America: Exploring implications of greenhouse gas emission reductions. *PLOS ONE*, **14,** e0215013.
Savelsberg, J., M. Schillinger, I. Schlecht, and H. Weigt, 2018: The Impact of Climate Change on Swiss Hydropower. *Sustainability*, **10**.

Schaeffer, R., and Coauthors, 2012: Energy sector vulnerability to climate change: A review. *Energy*, **38,** 1-12.
SEMARNAT-INECC, cited 2020: Mexico's Climate Change Mid-Century Strategy. [Available online at https://unfccc.int/files/focus/long-term_strategies/application/pdf/mexico_mcs_final_cop22nov16_red.pdf.]
Snyder, A., K. V. Calvin, M. Phillips, and A. C. Ruane, 2019: A crop yield change emulator for use in GCAM and similar models: Persephone v1.0. *Geosci. Model Dev.*, **12,** 1319-1350.
Solaun and Cerdá 2019: Climate change impacts on renewable energy generation. A review of quantitative projections. *Renewable and Sustainable Energy Reviews*, **116,** 109415.
Solaun, K., and E. Cerdá, 2019: Climate change impacts on renewable energy generation. A review of quantitative projections. *Renewable and Sustainable Energy Reviews*, **116,** 109415.
Thomson, A. M., and Coauthors, 2011: RCP4.5: a pathway for stabilization of radiative forcing by 2100. *Climatic Change*, **109,** 77.
Tobin, I., and Coauthors, 2015: Assessing climate change impacts on European wind energy from ENSEMBLES high-resolution climate projections. *Climatic Change*, **128,** 99-112.
Tubiello, F. N., J.-F. Soussana, and S. M. Howden, 2007: Crop and pasture response to climate change. *Proceedings of the National Academy of Sciences*, **104,** 19686.
Turner, S. W. D., M. Hejazi, S. H. Kim, L. Clarke, and J. Edmonds, 2017: Climate impacts on hydropower and consequences for global electricity supply investment needs. *Energy*, **141,** 2081-2090.
UNEP-WCMC, 2019: User Manual for the World Database on Protected Areas and world database on other effective area-based conservation measures: 1.6.
UNFCCC, cited 2019: INDCs as Communicated by Parties. [Available online at https://www4.unfccc.int/sites/submissions/indc/Submission%20Pages/submissions.aspx.]
United Nations, 2015a: Paris Agreement, as contained in the report of the Conference of the Parties on its twenty-first session [Tech. Rep. FCCC/CP/2015/10/Add.1].
——, cited 2018 Transforming our world: The 2030 agenda for sustainable development [A/RES/70/1]. [Available online at http://www.un.org/en/development/desa/population/migration/generalassembly/docs/globalcompact/A_RES_70_1_E.pdf.]
van der Zwaan, B., and Coauthors, 2016: Energy technology roll-out for climate change mitigation: A multi-model study for Latin America. *Energy Economics*, **56,** 526-542.
van Ruijven, B. J., and Coauthors, 2016: Baseline projections for Latin America: base-year assumptions, key drivers and greenhouse emissions. *Energy Economics*, **56,** 499-512.
van Vliet, M. T. H., D. Wiberg, S. Leduc, and K. Riahi, 2016a: Power-generation system vulnerability and adaptation to changes in climate and water resources. *Nature Climate Change*, **6,** 375.
van Vliet, M. T. H., L. P. H. van Beek, S. Eisner, M. Flörke, Y. Wada, and M. F. P. Bierkens, 2016b: Multi-model assessment of global hydropower and cooling water

discharge potential under climate change. *Global Environmental Change*, **40,** 156-170.
van Vuuren, D. P., S. Deetman, J. van Vliet, M. van den Berg, B. J. van Ruijven, and B. Koelbl, 2013: The role of negative CO2 emissions for reaching 2 °C—insights from integrated assessment modelling. *Climatic Change*, **118,** 15-27.
van Vuuren, D. P., and Coauthors, 2011a: How well do integrated assessment models simulate climate change? *Climatic Change*, **104,** 255-285.
——, 2012: A comprehensive view on climate change: coupling of earth system and integrated assessment models. *Environmental Research Letters*, **7**.
——, 2010: What do near-term observations tell us about long-term developments in greenhouse gas emissions? *Climatic Change*, **103,** 635-642.
——, 2011b: The representative concentration pathways: an overview. *Climatic Change*, **109,** 5.
Vernon, C. R., M. I. Hejazi, S. W. D. Turner, Y. Liu, C. J. Braun, X. Li, and R. P. Link, 2019: A Global Hydrologic Framework to Accelerate Scientific Discovery. *Journal of Open Research Software*, **7**.
Vörösmarty, C. J., P. Green, J. Salisbury, and R. B. Lammers, 2000: Global Water Resources: Vulnerability from Climate Change and Population Growth. *Science*, **289,** 284.
Warszawski, L., K. Frieler, V. Huber, F. Piontek, O. Serdeczny, and J. Schewe, 2014: The Inter-Sectoral Impact Model Intercomparison Project (ISI–MIP): Project framework. *Proceedings of the National Academy of Sciences*, **111,** 3228.
Wild, M., D. Folini, and F. Henschel, 2017: Impact of climate change on future concentrated solar power (CSP) production. *AIP Conference Proceedings*, **1810,** 100007.
Wild, M., D. Folini, F. Henschel, N. Fischer, and B. Müller, 2015: Projections of long-term changes in solar radiation based on CMIP5 climate models and their influence on energy yields of photovoltaic systems. *Solar Energy*, **116,** 12-24.
Wise, M., P. Patel, Z. Khan, S. H. Kim, M. Hejazi, and G. Iyer, 2019: Representing power sector detail and flexibility in a multi-sector model. *Energy Strategy Reviews*, **26,** 100411.
Wise, M., and Coauthors, 2009: Implications of Limiting CO₂ Concentrations for Land Use and Energy. *Science*, **324,** 1183.
World Energy Council: 2010 Survey of Energy Resources. [Available online at worldenergy.org/publications/2010/survey-of-energy-resources-2010/.]
Yalew, S. G., and Coauthors, 2020: Impacts of climate change on energy systems in global and regional scenarios. *Nature Energy*.
Zhou, Q., N. Hanasaki, S. Fujimori, Y. Masaki, and Y. Hijioka, 2018: Economic consequences of global climate change and mitigation on future hydropower generation. *Climatic Change*, **147,** 77-90.
Zhou, Y., P. Luckow, S. J. Smith, and L. Clarke, 2012: Evaluation of Global Onshore Wind Energy Potential and Generation Costs. *Environmental Science & Technology*, **46,** 7857-7864.
Zou, L., L. Wang, J. Li, Y. Lu, W. Gong, and Y. Niu, 2019: Global surface solar radiation and photovoltaic power from Coupled Model Intercomparison Project Phase 5 climate models. *Journal of Cleaner Production*, **224,** 304-324.